Al-Mustansiriyah Journal of Science

ISSN 1814 - 635X

Vol. 23, No. 7, 2012

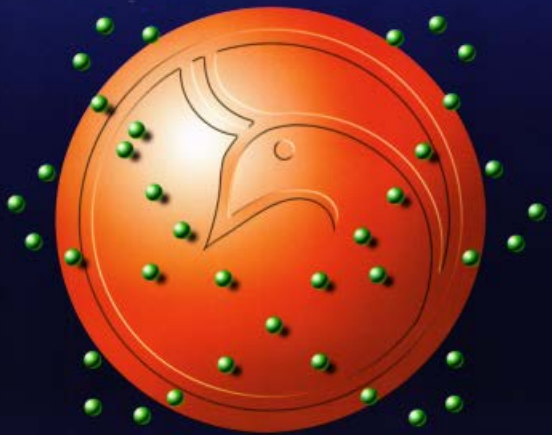

Issued by College of Science - Mustansiriyah University

Vol. 23
No. 7
2012

Al-Mustansiriyah Journal of Science

Issued by College of Science, Al-Mustansiriyah University, Baghdad, Iraq

Mobile: 07711184399
e-mail: mustjsci@yahoo.com

INSTRUCTION FOR AUTHORS

1. The journal accepts manuscripts in Arabic and English languages. Which had not been published before.
2. Author (s) has to introduce an application requesting publication of his manuscript in the journal. Four copies (one original) of the manuscript should be submitted. Should be printed by on the computer by laser printer and re produced on A4 white paper in three coppice with floppy disc should be also submitted.
3. The title of the manuscript together with the name and address of the author (s) should typed on a separate sheet in both Arabic and English. Only manuscripts title to be typed again with the manuscript.
4. For manuscripts written in English, full name (S) of author (s) and only first letters of the words (except prepositions and auxiliaries) forming title of the manuscript should be written in capital letters. Author (s) address (es) to be written in small letters.
5. Both Arabic and English abstracts are required for each manuscript. They should be typed on two separate sheets (not more then 250 words each).
6. References should be denoted by a number between two bracket on the same level of the line and directly at the end of the sentence. A list of references should be given on a separate sheet of paper, following the interactional style for names and abbreviations of journals.
7. Whenever possible, research papers should follow this pattem: INTRODUCTION, EXPERIMENTAL (MATERIALS AND METHODS), RESULTS AND DISCUSSION, and REFERENCES. All written in capital letters at the middle of the page. Without numbers or underneath lines.
8. The following pattern should be followed upon writing the references on the reference sheet: Sumame (s), intials of author (s), title of the paper, name or abbreviation of the journal, volume, number, pages and (Year). For books give the author(s) name(s), the title, edition, pages, publisher, place of publication and (Year).
9. A publication fees in the amount of ID. 50 thousand is charged upon a Receipt of the paper and 25 thousand upon the acceptance for publication for their ID. 75 thousand should be paid for the editorial board.

CONTENTS

Anatomical and histological study of stomach in adult local rabbits *Oryctolagus cuniculus*

Eman Mussa Khalel and Haider Dhahir Ghafi
University of Baghdad/ College of Veterinary Medicine

Received 1/12/2011 – Accepted 18/4/2012

الخلاصة

أجريت الدراسة الحالية لتحديد الشكل التشريحي والتركيب النسيجي لمعدة الأرنب المحلي البالغ (*Oryctolagus cuniculus*) استخدم في هذه الدراسة 16 أرنب بالغ محلي، قسمت إلى مجموعتين، ضمت المجموعة الأولى 8 ارانب بالغة (4 ذكور، 4 اناث) تضمنت الدراسة التشريحية دراسة التجهيز الدموي. ضمت المجموعة الثانية 8 أرانب (4 ذكور، 4اناث) استخدمت للدراسة النسيجية، استعملت نوعان من الصبغات، هما صبغة الهيماتوكسلين والايوسين والصبغة الخاصة (PAS). أظهرت نتائج الدراسة بشكل عام أنة لا توجد اختلافات معنوية من الناحية التشريحية والنسيجية للمعدة بين ذكور وإناث الأرانب. أظهرت نتائج الدراسة التشريحية إن التجهيز الدموي لمعدة الأرنب كان عن طريق الشريان الجوفي وفروعه الثلاثه

أظهرت نتائج الدراسة النسيجية في كلا الجنسين إن جدار المعدة يتكون من أربع طبقات، الطبقة المخاطية، الطبقة تحت المخاطية، الطبقة العضلية، الطبقة المصلية، لا توجد اختلافات معنوية في سمك الطبقات بين الذكور والإناث. جدار المعدة مبطن بالخلايا المبطنة السطحية والتي ظهرت بشكل ظهارة عمودية بسيطة طويلة والتي امتدت خلال الوهدات المعدية التي فتحت عندها الغدد المعدية. نسيجياً هناك ثلاث مناطق في المعدة اعتمادا على نوع الغدد الموجودة فيها فظهرت غدد نبيبية متفرعة، ملفوفة قصيرة في كل من منطقتي الغدد الفؤادية والغدد البوابية أما الغدد القاعية فظهرت بأنها غدد نبيبية متفرعة بسيطة وطويلة ومستقيمة وموازية لبعضها البعض ملتوية أو منحنية عند جزئها القاعدي.

ظهرت الغدد الفؤادية والبوابية بشكل رئيسي أنها غدد فارزة للمخاط مع وجود أعداد قليلة من الخلايا الجدارية ولكن لا توجد خلايا رئيسية في كلا النوعين من الغدد، بينما الغدد القاعية ظهرت بأنها مكونة من أنواع مختلفة من الخلايا ولكن النوعين الأساسين من الخلايا هما الخلايا الجدارية والخلايا الرئيسية.

لا يوجد اختلاف معنوي في إعداد الغدد في المناطق الثلاثة بين الذكور والإناث. إما ما يخص نوع الإفراز فقد أظهرت الخلايا المبطنة السطحية والوهدات والغدد في المنطقتين الفؤادية البوابية تفاعل ايجابي مع صبغة PAS بينما المنطقة القاعية أظهرت الخلايا المبطنة السطحية والوهدات فقط تفاعل ايجابي إما غددها فقد أظهرت نتيجة سالبة لهذه الصبغة.

ABSTRACT

The present study was conducted to determine the anatomical and histological structure of stomach in adult local rabbits 6-12 month (*Oryctolagus cuniculus*). This study was carried out on 16 adult local rabbits which were divided into two groups: the first group contained 8 adult rabbits (4 male and 4 female) used for anatomical study include study of blood supply. The second group included 8 rabbits (4 male and 4 female) used for histological study using two types of stains, the hematoxylin and eosin and the special stain (PAS). Anatomically the stomach in both sexes of adult local rabbits was supplied through the celiac artery and its three branches.

Histologically, in both sexes, the wall of the stomach consists of four tunics (tunica mucosa, tunica submucosa, tunica muscularis and tunica serosa). There was no significant difference in thickness of tunics between male and female. The stomach lined by a surface lining mucous cells appears as a tall simple columnar epithelium that extends through gastric pits, where the gastric glands are opened, three regions can be recognized in the mucosa of the stomach according to the types of glands that appear as branched, tubular, coiled, short glands in both cardiac and pyloric glands region, while the fundic glands in the fundic glands region appear as simple branched tubular long straight over most of their length parallel to each other and coiled or bent at the basal portion.

The cardiac and pyloric glands noted mainly mucous secreting cells and few numbers of parietal cells while the glands fundic region consist of different types of cells but the two main cells are the parietal and chief cells.

The number of glands in the three regions was not different significantly between the male and female. The surface lining cells, gastric pits in three regions of stomach, cardiac and pyloric glands gave a positive reaction with PAS while the fundic glands showed a negative reaction with PAS in both male and female rabbit stomach.

INTRODUCTION

Laboratory animals are extensively used for modern biomedical research including immunological studies, reproductive studies and other researches [1], also have been direct object of a great number of experiments that cannot be carried out *in vitro.* A number of authors paid attention to body structure and organ system [2]. Among the laboratory animals rabbits have been used an experimental model for research [1], it is a means of research in the field of biology, physiology, medicine, toxicology, pharmacology, surgery [3]. Rabbits have been used as an experimental animal in many diseases [4, 5] . Rabbits characterized by a unique anatomy of stomach [6]. It has a large simple stomach and contains food at all times. The aim of this work to study the normal histological observation of stomach and the normal blood supply of it in local rabbit's.

MATERIALS AND METHODS

Sixteen adult healthy male and female local rabbits (*Oryctolagus cuniculus*) including (8) male and (8) female, obtained from local supplier in Al- suwera city, Iraq in September, 2010. All these rabbits were used for anatomical and histological study.

Anatomical study include:-

Blood supply:-

After killing eight rabbits (4male and 4 female) by sacrificed, the skin of thoracic region of rabbits was removed, and then the thoracic region opened. The red colored gum-milk latex injected thought the aorta by blunt needle and syringe, to prevent any flow or loosing of latex from cutting small arteries, glacial acetic acid were used with cotton and pressed on the site of losing. The animal and all viscera were immersed in the fixative 10% formalin for two days [7], after that the stomach was dissected very carefully to study the distribution and branching of different arteries (using the digital photo camera 14.1 megapixel).

Histological study:-

In the current study, eight adult rabbit (4male and 4 female) were killed. Then the stomach immediately removed and opened along the

greater curvature, all the contents were removed and washed by normal saline. Then the tissue specimens were sectioned from three regions of the stomach: cardiac glands region, fundic glands region, and pyloric glands region [8] . The size of the specimens were taken about 1 cm^3 and then kept in 10% formalin for 48 hours. The samples were proceed with routine histological technique [9]. Two types stain were used in this work, the first is Harris Hematoxylin and eosin stain and the second is Periodic Acid Shiff (PAS). Different histological measurements done by light microscope under X40 by use of ocular micrometer [10], and the following incidences were used in this study:

-Highest of epithelial cells that lining the stomach.
-Thickness of different tunics of stomach wall.
-The appearance of glands.
-Number of mucosal glands.
-Numbers of parietal and chief cells in the mucosal glands.
-Nature of secretion of different type of secretory cells by using of special stain (PAS).

Statistical analysis

The values expressed as mean ± SE. The statistical analysis of data was performed to know the significant differences using analysis of T. test to show the important statistic, and significant differences limited on $p< 0.05$ of probability [11].

RESULTS AND DISCUTION

Anatomical Study / Blood Supply

This study revealed that the blood supply of adult local rabbit in both sexes through the celiac artery and its three branches, the splenic artery, left gastric artery and the hepatic artery (figure 1). The splenic artery, is the first branch of the celiac artery, it gives a short gastric to the fundus before and after entering the spleen, the left gastroepiploic courses distally along the greater curvature to anastomoses with the right gastroepiploic (figure 1).The left gastric artery is the second and shortest branch of the celiac artery, it distributed to supply the lesser curvature and gives off to the fundus (figure 1) and the cardiac region by the right and left gastric branches (figure 2). The last branch of the celiac artery is the hepatic artery that gives rise to first branch (right gastric) before the gastroduodenal artery where the right gastroepiploic artery arises to course proximately along the greater curvature and anastomoses with the left gastroepiploic artery (figure1),the right gastric arteries the second branch that arise at the pylorus and courses proximally in the lesser curvature to join the left gastric artery, finally the hepatic artery gives off its hepatic branches (figure 1).

Histological Study / Morphometric measurement

This study showed the histological structure of stomach of rabbit in both male and female are similar but the morphometric measurements are different between them. The entire surface of gastric mucosa was lined by a simple tall columnar epithelium with a lightly stained cytoplasm which form the surface mucous lining cells that invaginate into varying depth into the lamina propria according to the regions of stomach in rabbit forming the gastric pits that lined by the same surface epithelium and where the glands are opened in the base of it (figure 3). The mucosa of stomach in rabbits in both sexes appear as divided into three regions according to the types of glands which is contains, the cardiac, fundic and pyloric glands region. The wall of stomach in cardiac, fundic and pylorus regions has the same four tunics; the Tunica mucosa, Tunica submucosa, Tunica muscularis, and Tunica serosa. The Tunica mucosa and submucosa in contracted stomach of rabbit are folded into longitudinal folds or rugae which are numerous in the fundic and pyloric glands region (figure 4, 5) while in distended rabbit stomach, these folds become flattened.

Cardiac glands region

Hight of epithelium, thickness of tunics and appearance of glands

This study showed that the mean thickness of all tunics of this reagion of stomach local rabbit was shown on Table 1. Cardiac region appear as a narrow area at the gastro esophageal junction. The Tunica mucosa appear as consist of surface lining cells that appear as tall columnar cells mucus secreting that extend in relatively the long gastric pits (figure 3). The mean thickness of all tunics of the three region of stomach local rabbit. The second component of mucosa is the lamina propria that appear as connective tissue restricted to the area underneath the surface epithelium to the muscularis mucosa and occupied by the cardiac glands (figure 5). The cardiac glands that occupied the lamina propria appear as a short branched tubular, coiled gland, opened into bottom of relatively long pits (figure 5, 6). The other component of mucosa is the muscularis mucosa that appears as a several layers of smooth muscle fibers arranged in longitudinal and circular layers that separate the tunica mucosa from the tunica submucosa (figure 5). The second tunica in the wall of stomach in rabbit is Tunica submucosa that appears as a connective tissue containing fat cell, and contains a numerous large blood and lymphatic vessels. Under the tunica submucosa is the tunica muscularis externa that appear as consist of two layers of smooth muscle fibers, the inner is circular and the outer is longitudinal layer (figure 7).The outer most layer is the tunica serosa

which attached to the muscularis externa and appear as a thin layer of loose connective tissue covered with mesothelium (figure7).

Fundic glands region

Hight of epithelium, thickness of tunics and appearance of glands.

The gastric mucosa of stomach in rabbit in fundic glands region is thrown into prominent longitudinal folds or rugae that protruded into the lumen of contracted stomach, the core of these folds consist of submucosa (figure 8). The epithelial surface cells are simple tall columnar epithelium which extend and lined the short gastric pits (figure 3).The mean thickness of tunics of this region as in Table (2). The lamina propria is a fine connective tissue and quite difficult to differentiate between the fundic glands numerous simple branched tubular glands that are arranged almost parallel to one another and are perpendicular to the surface of mucosa they are appear as a very long straight over most of their length extend through the lamina propria to reach the muscularis mucosa where these glands are bent or coiled (figure 9). In the fundic glands region the muscularis mucosa appear as a layer of smooth muscle fibers oriented both longitudinally and circularly underlying the mucosa (figure 8). The tunica submucosa revealed as a highly vascularized supporting connective tissue and also contains lymphatic vessels, the tunica submucosa participates in forming the rugae (figure 8). The tunica muscularis was composed of smooth muscle fibers arranged in a relatively thick inner circular layer and a thin outer longitudinal layer. Between these muscularis layers Auerbach's plexus is present (figure10). The outer most tunica is the tunica serosa that appear as a thin layer of a loose connective tissue covered by mesothelium (figure 10).

Pyloric glands region

Hight of epithelium, thickness of tunics and appearance of glands.

The hight of epithelium thickness of tunics showed in Table 3.The lining epithelium appear as in cardiac and fundic glands region. The lamina propria showed as loose connective tissue more than in fundic glands region, occupied by loosely packed the pyloric glands (figure11). The pyloric glands appear as short tubular branched and coiled open at the base of long pits (figure12). The muscularis mucosa appears as layers of smooth muscle fibers separating the mucosa from the submucosa (figure12). The Tunica submucosa in the pyloric glands region similar to that of the cardiac and fundic glands region of the stomach, it consist of a loose connective tissue contain a large blood vessels (figure 13). The Tunica muscularis appear as consist of two layers of smooth muscle, the thickest one is the inner most layer, circularly arranged and the outer is a thin and longitudinal arrangement

(figure14). The outer most layer of the wall stomach in rabbits is the tunica serosa, appear similar to that in the cardiac and fundic regions as consist of loose connective tissue covered by one layer of simple squamous epithelium or mesothelium (figure 14).

Numbers of Glands, Parietal and Chief Cells:

Cardiac glands Region

The number of glands in cardiac glands region in the stomach of male and female rabbit was showed in Table 4. The cardiac glands are predominantly mucous secreting glands consist of mucous secreting cells which appear as a tall columnar, pyramidal cells lightly stained cytoplasm with oval or flattened basally located nuclei and a few numbers of parietal cells are present in the mucous glands, and there is no chief cells are present. The parietal cells which present appear as large, round cells with centrally located nuclei and eosinophilic cytoplasm (figure 6).The number of parietal cells in the cardiac glands as in Table 4 . There are no chief cells in the cardiac glands Table 4.

Fundic glands Region

The number of glands in the fundic glands region showed in Table 4. There were different types of fundic gland cells, but the two main type cells are parietal cells and chief cells, the parietal cells are scattered along the length of the glands but are more numerous in the upper half of the tubular glands than in the lower half (figure 15). They appear as a large, rounded, some are pyramidal shaped and are bulges out ward in to the surrounding basement membrane of the gland, the nucleus is round and centrally placed with eosinophilic granulated cytoplasm (figure 15).The chief cells are the second main type cells of the fundic glands, they are scattered and squeezed between the parietal cells but occur principally in the lower half of fundic glands they are much smaller than the parietal cells, they appear as a pyramidal or cuboidal shape with basally located round nucleus and a basophilic cytoplasm (figure15). The numbers of parietal cells and chief cells showed in Table 4.

Pyloric glands Region

The current study observed that the numbers of pyloric glands showed in Table 4. The pyloric glands are lined mostly with a large of tall columnar epithelium with clear basophilic cytoplasm and flattened basally located nuclei, some parietal cells are present (figure 16). The number of parietal cells showed in Table 4 .

Special Stains / PAS Stain

The PAS stain has been used to high light the mucus-secreting cells of the gastric mucosa. The surface lining cells of entire mucosa of rabbit stomach in both sexes that extends into gastric pits. That gave a strong

reactivity with PAS, which appear as pink or magenta color and they were considered as mucus producing cells (figure 17). Also The cardiac glands are confirmed the histological study of number of parietal and chief cells composed mainly from mucous secreting cells are gave a positive reaction with PAS and appear as a pink color, some glands composed entirely from mucous secreting cells and others contain a very few of parietal cells which appear as a clear cells (figure18). The fundic glands gave position reactivity in a surface lining cells and gastric pits but the fundic glands gave a negative reaction with PAS (figure17). While the main cells of fundic gland are parietal and chief cells which gave a negative reaction with PAS. In pyloric glands region of both sexes, the pyloric glands gave a position reaction with PAS and appear as pink color (figure18). The predominant cells in the pyloric glands are mucous secreting cells, some glands contain a very few number of parietal cells.

Table-1 :the thickness of tunics in the cardiac glands region of stomach in the male and female rabbit (micrometer).

sex	Tunica mucosa			Tunica submucosa Mean ±SE	Tunica muscularis externa Mean ±SE	Tunica serosa Mean ±SE
	Hight of epithelium Mean ±SE	Hight of lamina propria Mean ±SE	Hight of muscularis mucosa Mean ±SE			
Male	22.25 ± 1.083	383.00 ± 16.392	48.25 ± 3.594	85.50 ± 8.256	535.10 ± 15.767	28.50 ± 1.979
Female	22.25 ± 0.786	405.75 ± 18.480	52.00 ± 3.370	91.50 ± 3.894	529.75 ± 14.908	29.25 ± 1.750

NS = NO significant differences at ($p<0.05$).

Table-2:The thickness of tunics in the fundic glands region of stomach in the male and female rabbit (micrometer).

Sex	Tunica mucosa			Tunica submucosa Mean ±SE	Tunica muscularis externa Mean ±SE	Tunica serosa Mean ±SE
	Hight of epithelium Mean ±SE	Hight of lamina propria Mean ±SE	Hight of muscularis mucosa Mean ±SE			
Male	22.50 ± 0.645	640.50 ± 26.370	31.50 ± 2.142	195.00 ± 6.476	510.25 ± 14.250	22.75 ± 1.314
Female	22.25 ± 0.786	639.25 ± 29.919	35.75 ± 2.142	197.75 ± 7.568	515.00 ± 13.885	17.50 ± 1.343

NS = NO significant differences at ($p<0.05$).

Table-3:The thickness of tunics in the pyloric glands region of stomach in the male and female rabbit (micrometer)

sex	Tunica mucosa			Tunica submucosa Mean ±SE	Tunica muscularis externa Mean ±SE	Tunica serosa Mean ±SE
	Hight of epithelium Mean ±SE	Hight of lamina propria Mean ±SE	Hight of muscularis mucosa Mean ±SE			
Male	22.27 ± 1.021	334.75 ± 15.795	42.25 ± 2.873	158.00 ± 8.788	591.25 ± 12.819	21.50 ± 1.190
Female	22.30 ± 1.083	339.00 ± 17.552	47.00 ± 2.198	177.75 ± 8.735	585.75 ± 12.819	22.25 ± 0.946

NS = NO significant differences at ($p<0.05$).

Table-4:the number of mucosal glands, parietal and chief cells in the three regions of stomach in the male and female rabbit.

sex	Cardic region			Fundic region			Pyloric region		
	Number of glands Mean ±SE	Number of Parietal cells Mean ±SE	Number of chief cells Mean ±SE	Number of glands Mean ±SE	Number of parietal cells Mean ±SE	Number of chief cells Mean ±SE	Number of glands Mean ±SE	Number of parietal cells Mean ±SE	Number of chief cells Mean ±SE
Male	9.10 ± 0.861	0.73 ± 0.248	nil	20.10 ± 0.612	3.92 ± 0.122	8.42 ± 0.285	15.60 ± 0.642	0.46 ± 0.257	nil
Female	18.05 ± 0.875	0.62 ± 0.251	nil	20.35 ± 0.563	3.87 ± 0.164	8.58 ± 0.360	17.15 ± 0.512	0.59 ± 0.246	nil

NS = NO significant differences at ($p<0.05$).

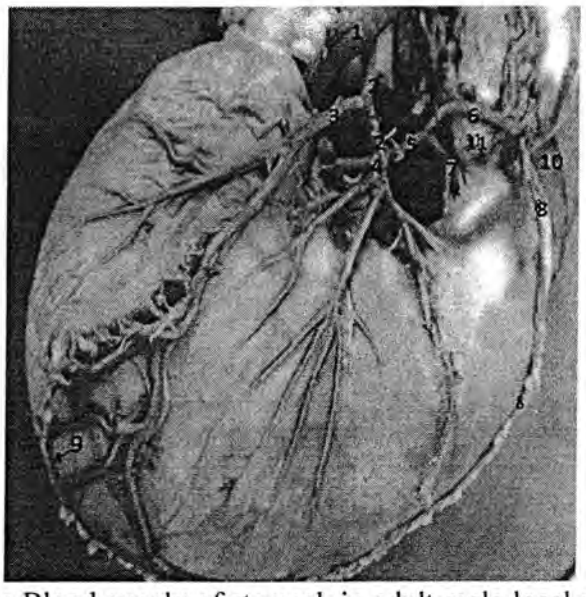

Figure-1: Show the Blood supply of stomach in adult male local rabbit: 1–Aorta 2-Celiac artery 3-Splenic artery 4–Left gastric artery 5-Hepatic artery 6–Gastro duodenal 7–Right gastric 8–Right gastroepiploic 9–Left gastroepiploic 10–Liver 11–Duodenum 12-Spleen

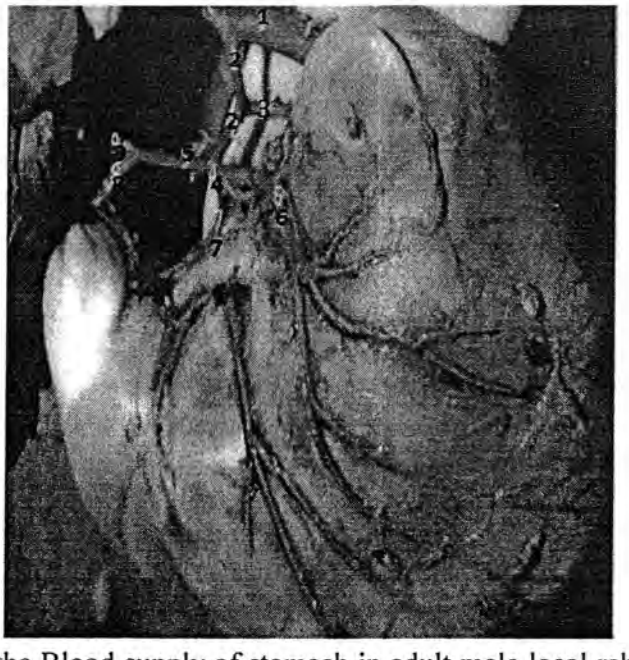

Figure-2: Show the Blood supply of stomach in adult male local rabbit showing: 1-Aorta 2–Celiac artery 3- Splenic artery 4 – Left gastric artery 5– Hepatic artery 6-Left gastric branch 7-Right gastric branch 8–Right gastric artery 9–Gastro duodenal

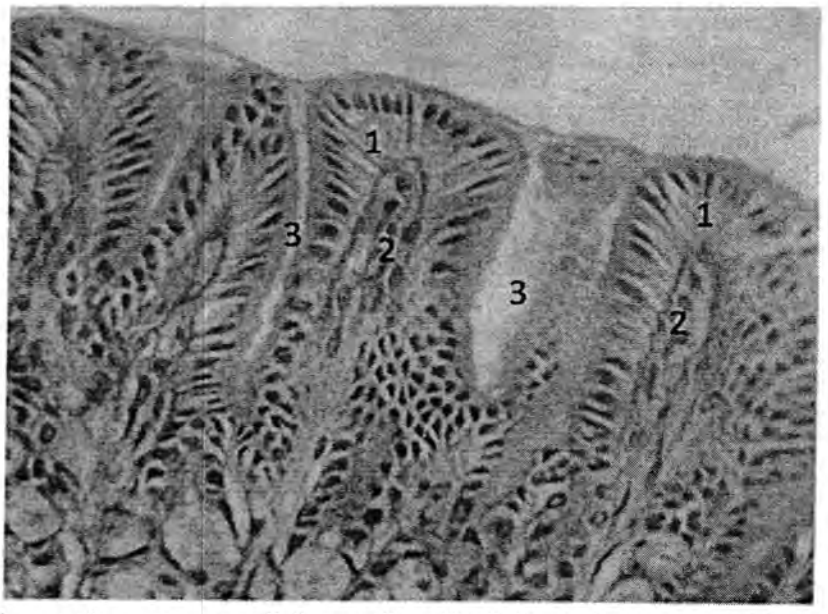

Figure-3:Show the surface mucous lining cells of adult male local rabbit: 1-Simple columnar epithelium 2- Lamina propria 3-Gastric pits H&EX 400

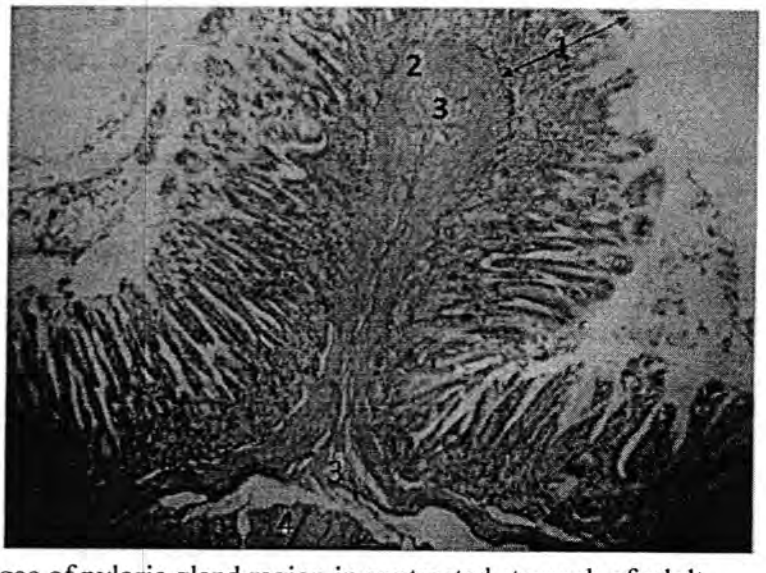

Figure -4: show the rugae of pyloric gland region in contracted stomach of adult male local rabbit: 1-Tunica mucosa 2-Muscularis mucosa 3-Tunica submucosa 4-Tunica muscularis H&E X 300

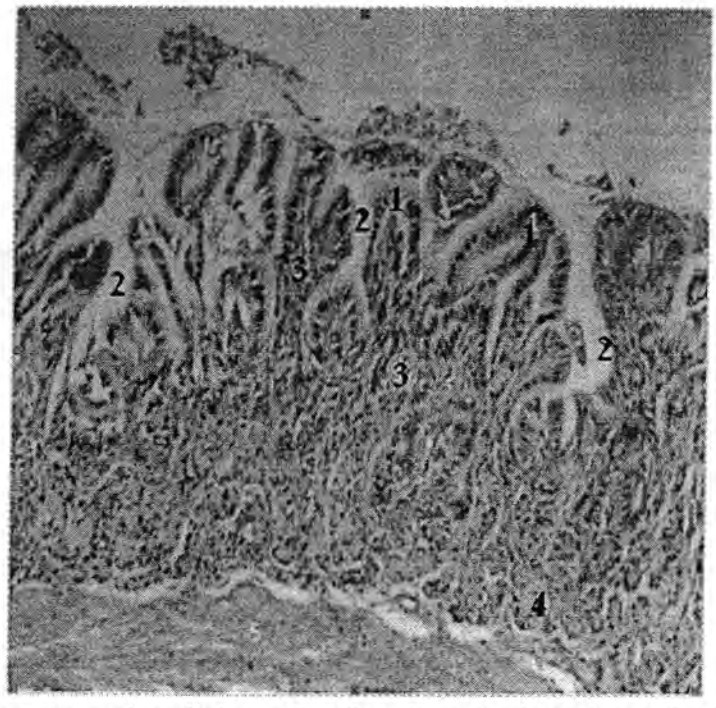

Figure-5: Show the surface lining cells of cardiac glands region and relatively long gastric pits in the stomach of adult female local rabbit: 1-Simple columnar epithelium 2-Gastric pits 3-Lamina propria 4- Cardiac glands 5-Muscularis mucosa H&E X 34

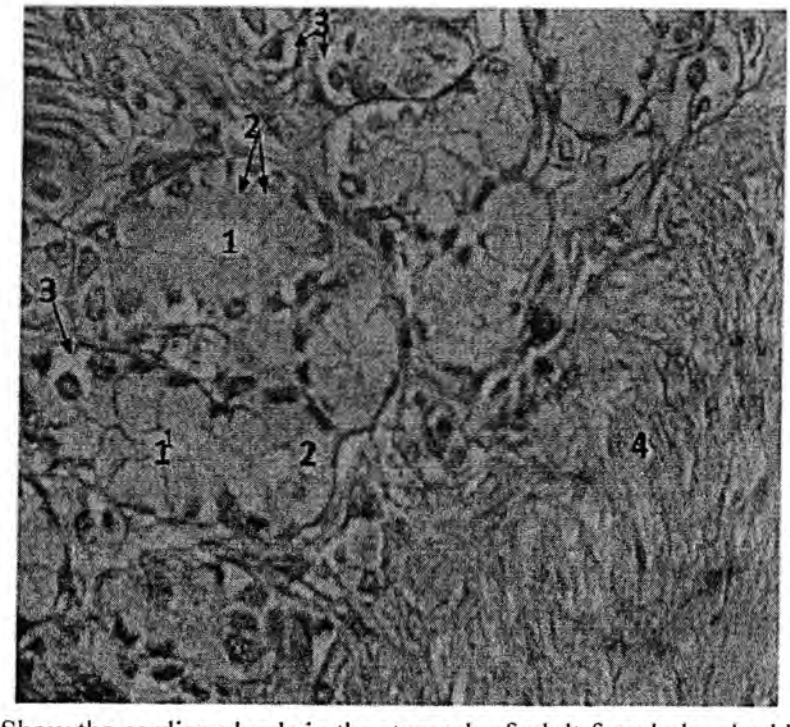

Figure-6: Show the cardiac glands in the stomach of adult female local rabbit: 1-Cardiac glands 2-Mucous secreting cells 3-Parietal cells 4- muscularis H&E X 540

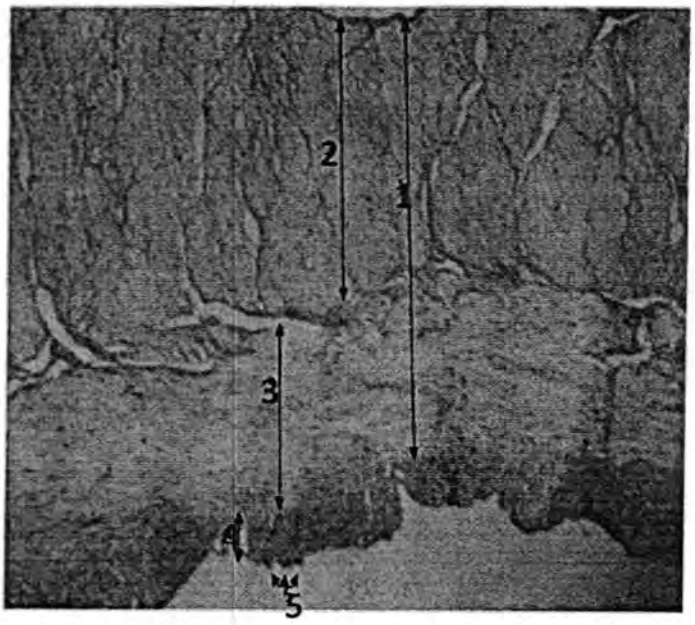

Figure-7: Show the tunica muscularis externa in the cardiac region in stomach adult female local rabbit: 1-Tunica muscularis 2-Inner layer 3-Outer layer 4-Tunica serosa 5-Mesothelium H&E X 300

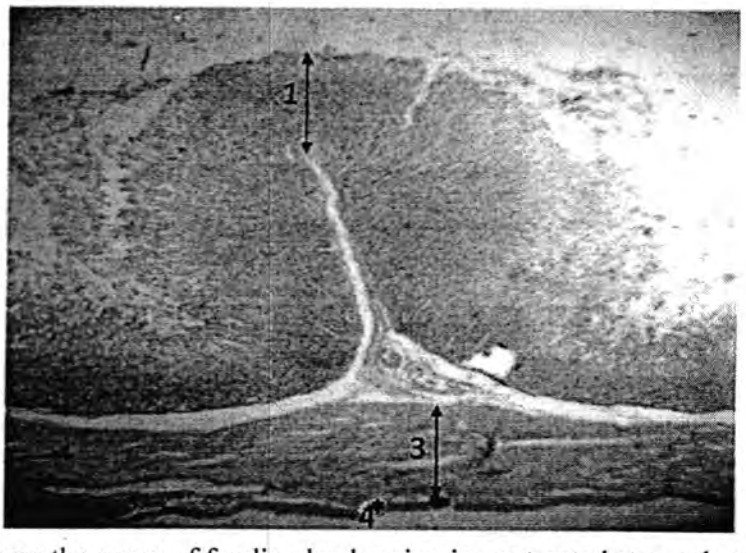

Figure-8: Show the rugae of fundic gland region in contracted stomach of adult male local rabbit: 1-Tunica mucosa 2-Tunica submucosa 3-Tunica muscularis 4-Tunica serosa H&E X 240

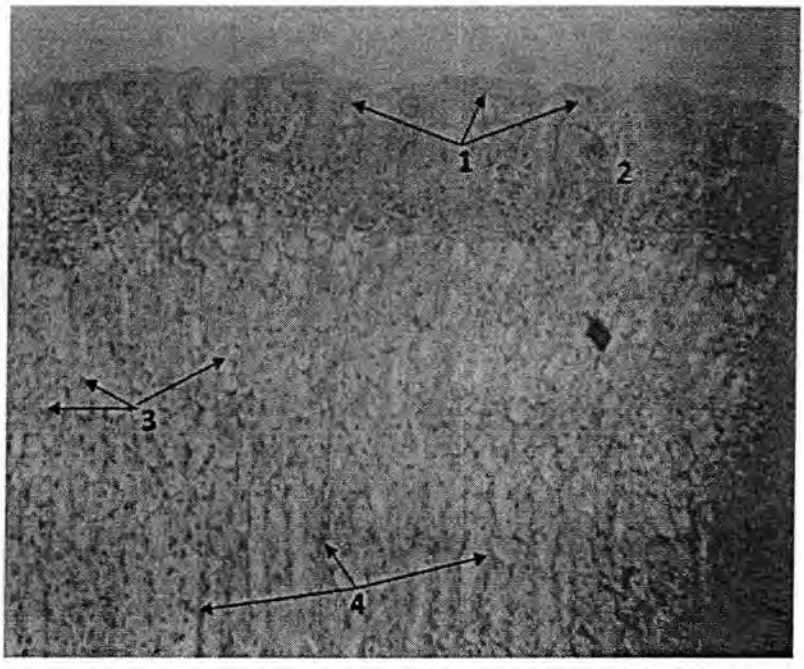

Figure- 9: Show the tunica mucosa of fundic glands region in stomach of adult male local rabbit: 1- Simple columnar epithelium 2-Gastric pits 3-Fundic glands 4-Lamina propria H&E X 300

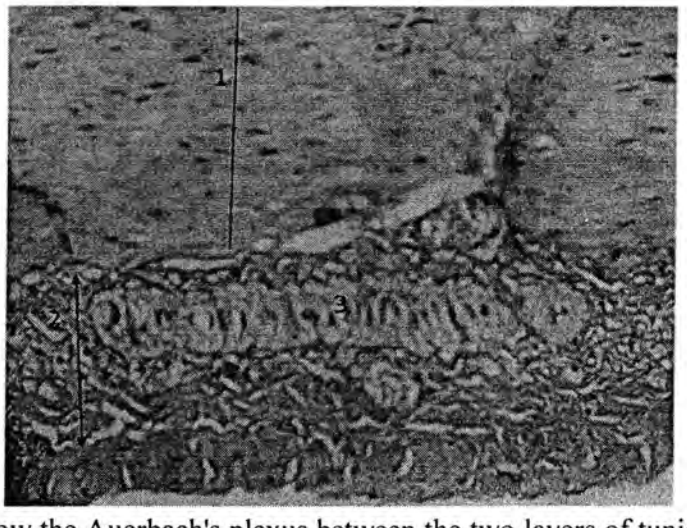

Figure-10: Show the Auerbach's plexus between the two layers of tunica muscularis in the fundic glands region in stomach of male local rabbit: 1-Inner layer 2-Outer layer 3- Auerbach's plexus H&E X 340

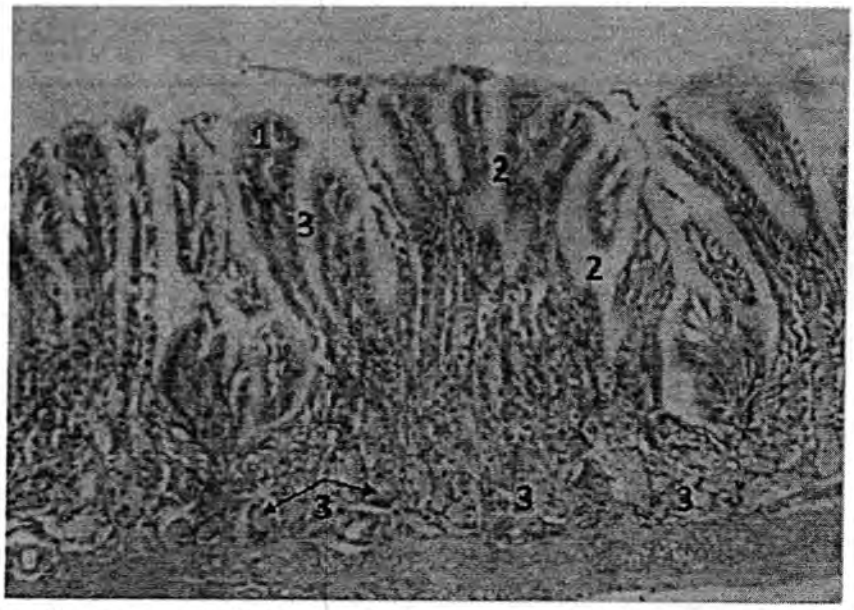

Figure-11: Show the pyloric mucosa in the stomach of adult male local rabbit: 1-Simple columnar epithelial cells 2-Gastric pits 3-Pyloric glands H&E X 300

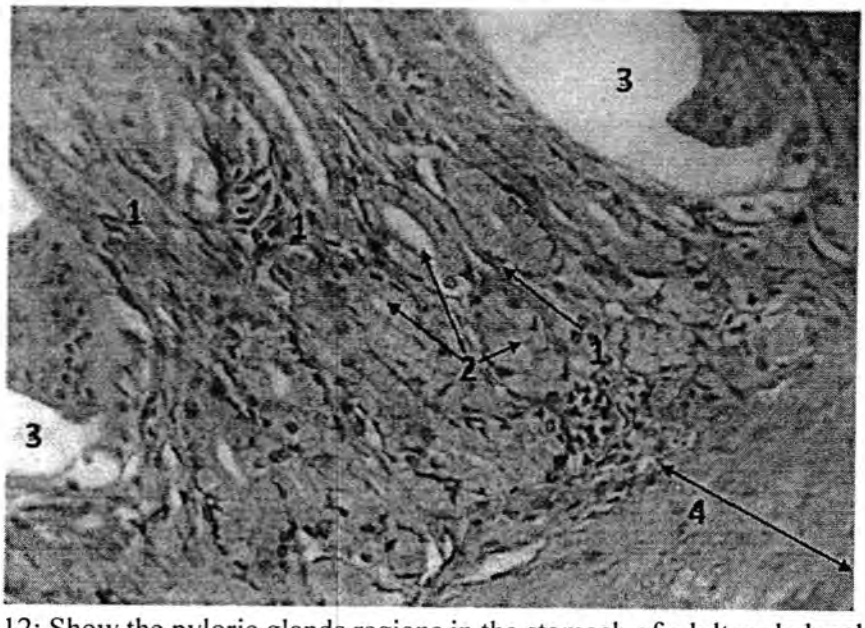

Figure-12: Show the pyloric glands regions in the stomach of adult male local rabbit: 1-Lamina propria 2- Pyloric glands 3-Gastric pits 4-Muscularis mucosa H&E X 340

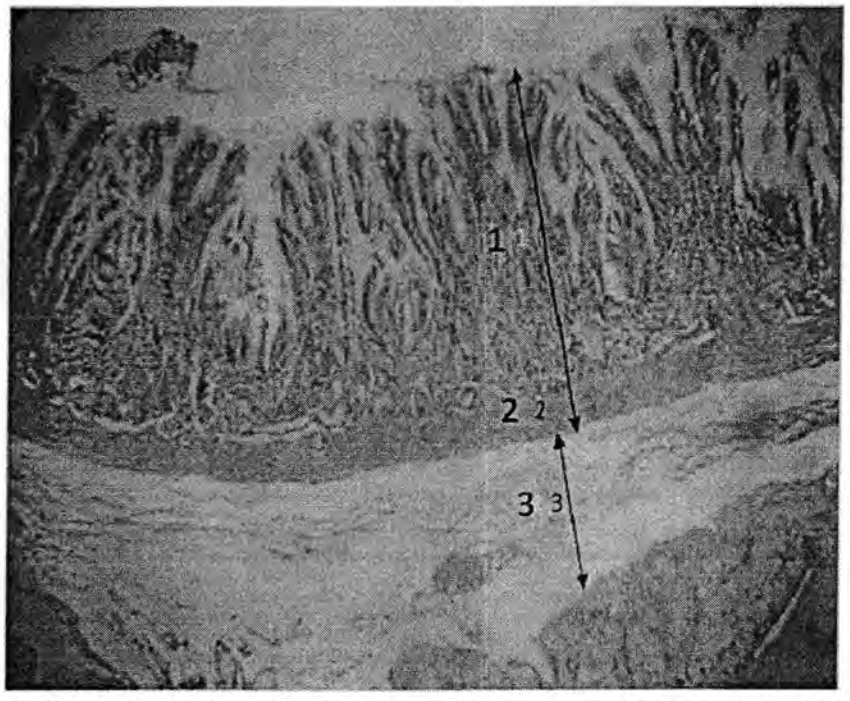

Figure-13: Show the muscularis mucosa of the pyloric glands region in the stomach of adult male local rabbit: 1-Tunica mucosa 2-Muscularis mucosa 3-Tunicasubmucosa H&E X 240

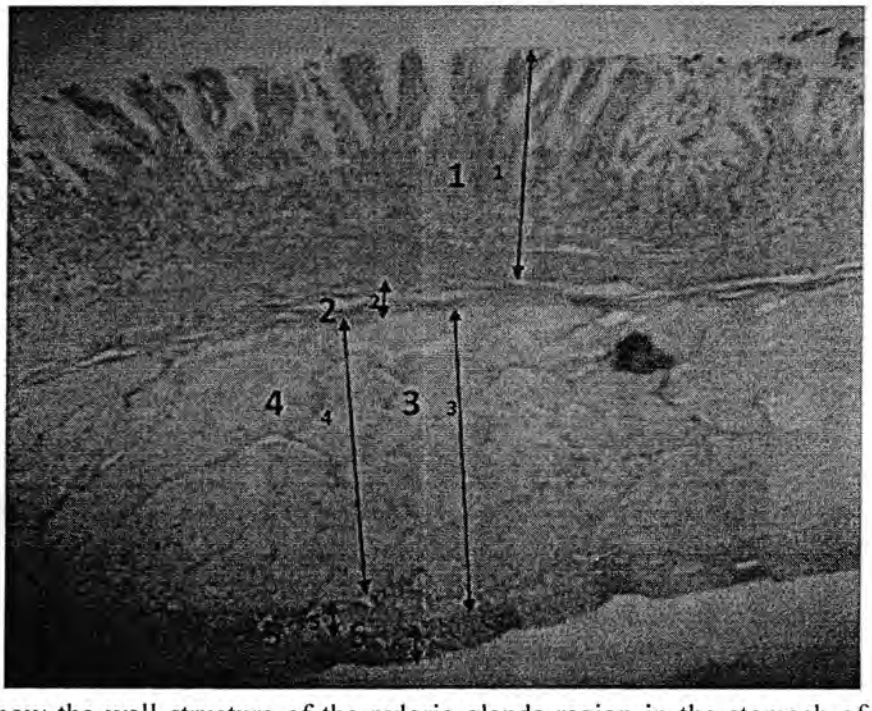

Figure-14: Show the wall structure of the pyloric glands region in the stomach of adult male local rabbit: 1-Tunica mucosa 2-Tunica submucosa 3-Tunica muscularis 4-Inner circular 5-Outer longitudinal 6-Tunica serosa H&E X 240

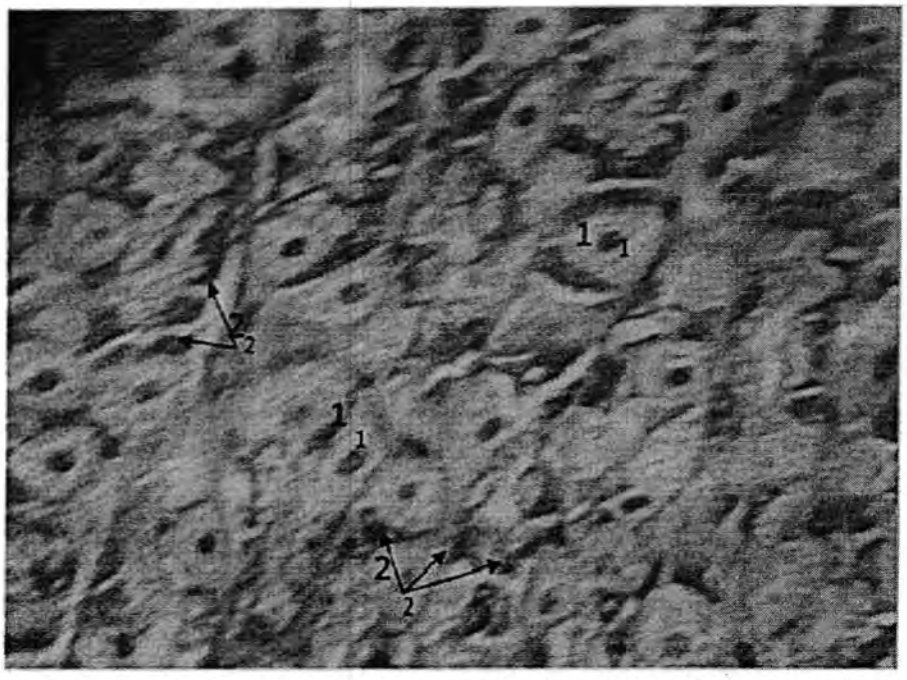

Fig-15: show the fundic glands in the stomach of adult female local rabbit: 1-pyloric glands 2-mucous secreting cells 3-Parietal cell H & E X 340

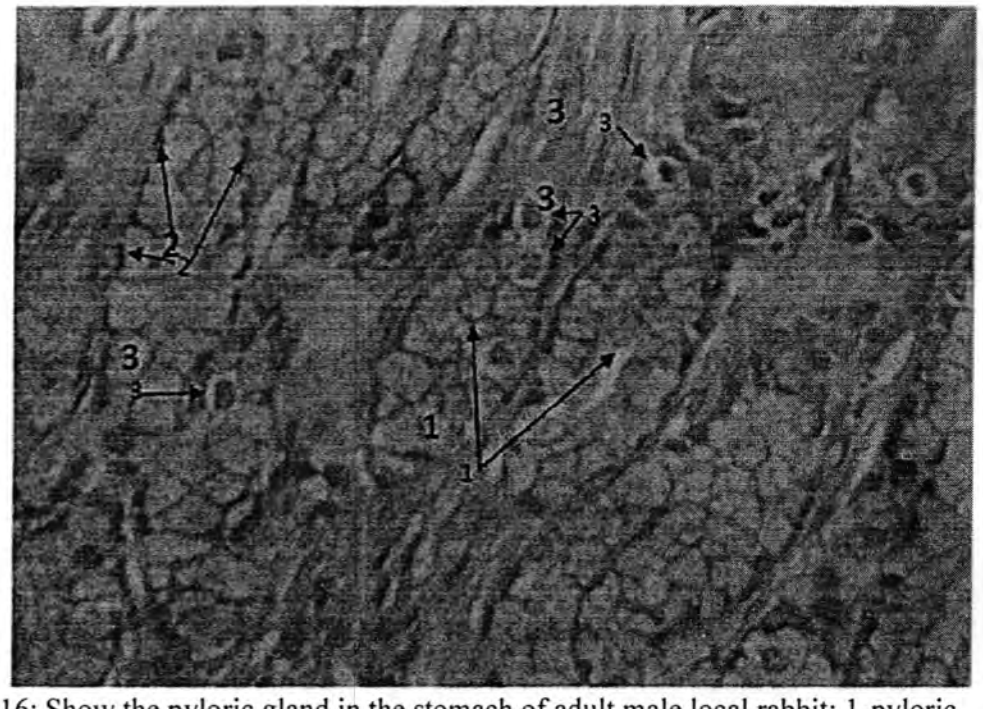

Fig- 16: Show the pyloric gland in the stomach of adult male local rabbit: 1-pyloric glands 2-mucous secreting cells 3-Parietal cell H & E X 340

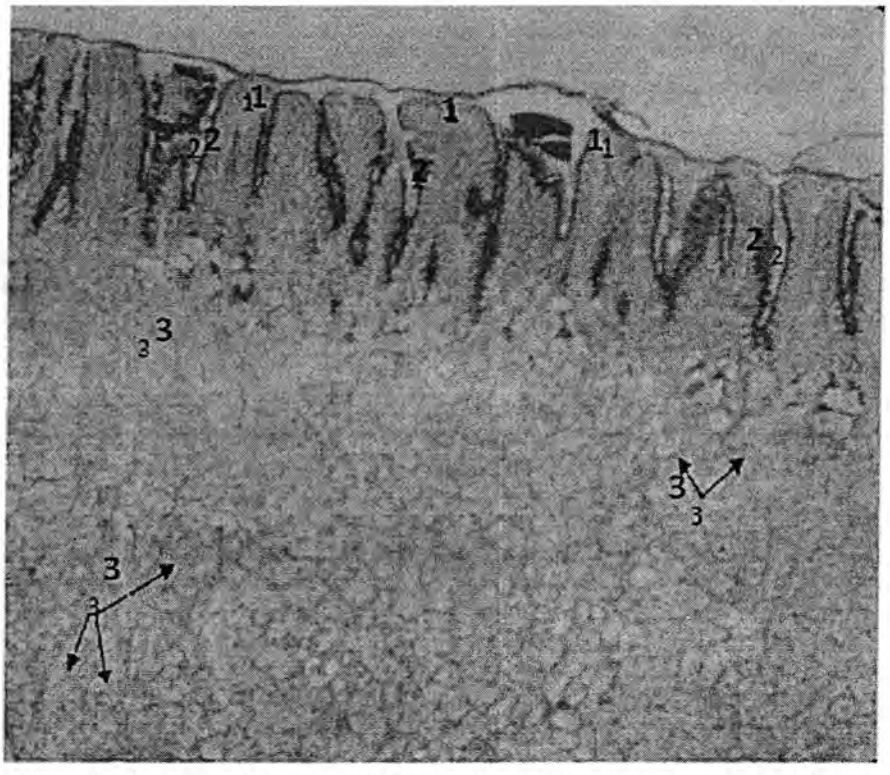

Fig-17:show 1-simple columnar epithlium 2-gastric pits gave a positive reaction with PAS 3-the fundic glands gave a negative reaction with PAS X300

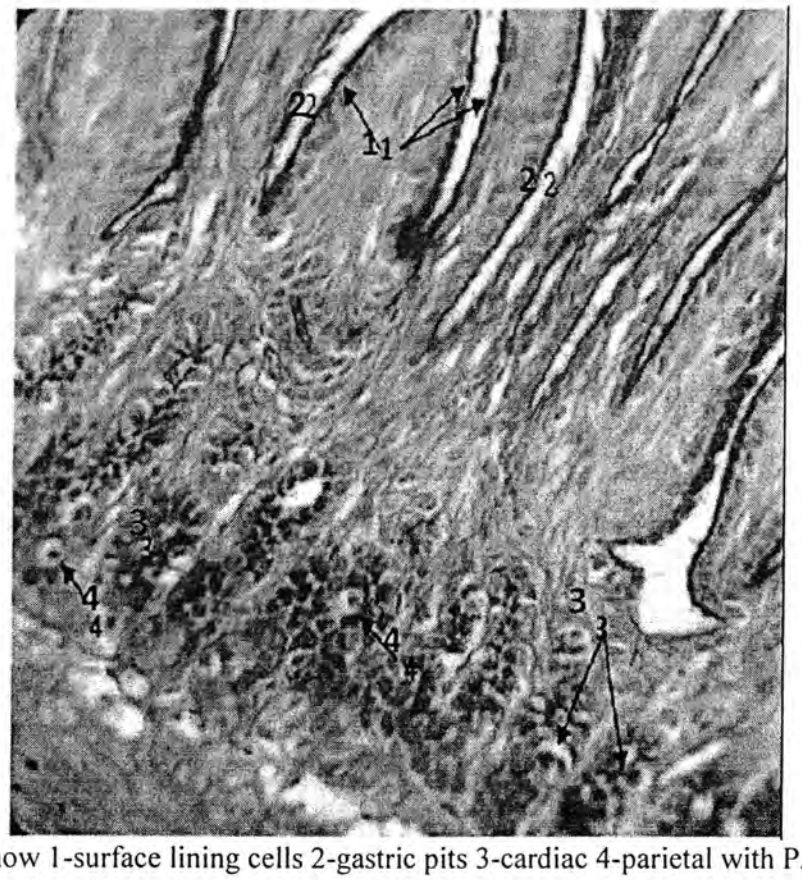

Fig-18: show 1-surface lining cells 2-gastric pits 3-cardiac 4-parietal with PAS stain X340

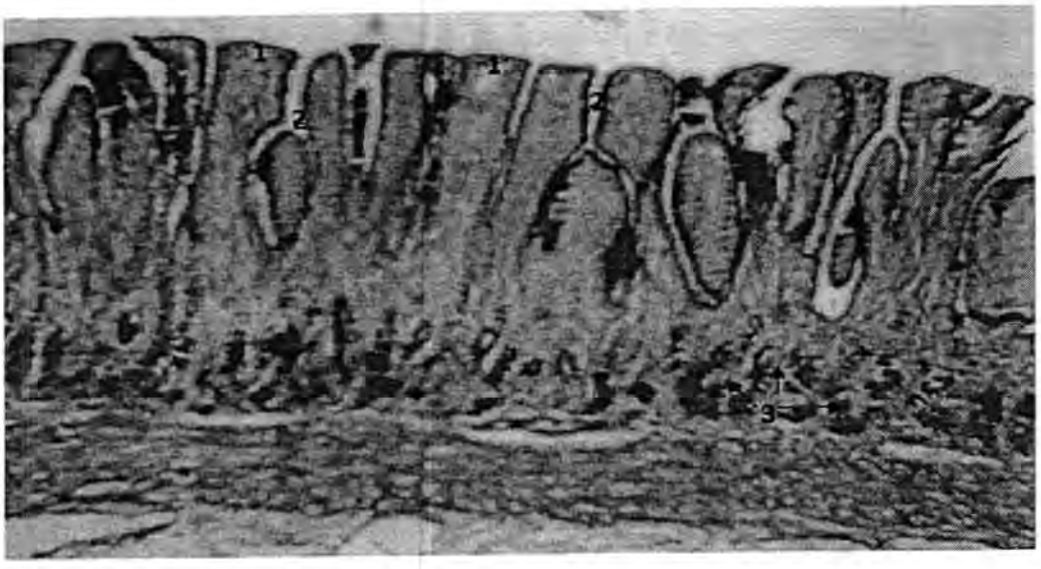

Fig-19: show the 1-surface lining cells 2-gastric pits 3-pyloric glands gave a positive reaction with PAS stain X300

Blood Supply

The present study revealed that the blood supply of stomach in adult local rabbit is similar to that described in the basic simple stomached mammalian pattern and varanus niloticus that the celiac artery and its three major branches , splenic, left gastric and the hepatic artery were basically responsible for supplying the stomach described by [12] in addition to two branches the left and right gastric branches, short gastric branch which found in this study, this result may be due to that the stomach of rabbit has more endocrine cells that secret its secretory hormone in the blood. The general wall structure of entire stomach in rabbit was similar to that previously described in monogastric animals reported by [1] and in some mammalian stomach [13]. But differ from the stomach of ruminant that have a permanent spiral folds [14], that increase the secreting surface area of mucous membrane and receive large amount of food [15]. The appearance of cardiac glands similar to that in feline stomach by [16]. There is no difference between the histological structure of the fundic glands in rabbit stomach from the histological structure of the fundic glands in the simple stomach in domestic mammals described by [17]. The number of glands in the three glands regions in the stomach of male and female rabbit were differ from the number of mucosal gland of ruminant,this may be duo to difference in the species .The cardiac glands are predominantly mucous secreting glands consist of mucous secreting cells and few numbers of parietal cells and there are no chief cells a present.

The histological results were confirmed by using the PAS.The appearance of mucous secreating cells and parietal cells as in simple stomach described by [8]. The composition of fundic glands in rabbit stomach confirmed with [1,18] in monogastric animals, and the parietal cells have the same histological characteristic in the stomach of human, monogastric animals and ruminant as reported by [19].

The eosinophilic granulated cytoplasm of parietal cells is due to that it contains numerous packed mitochondria which reflects a high metabolic activity utilized in the production and secretion of components of gastric juices [9]. The chief cells are the second main type cells of the fundic glands, they are scattered and squeezed between the parietal cells , similar histological description by [20] in simple stomach and [1] in monogastric animals that suggest the strongly basophilic granular cytoplasm is due to reflects their huge contact of rough endoplasmic reticulum [21] ribosome's and agree with [1] in mouse. The appearance of pyloric glands is similar to the description of [20]. The pyloric glands have predominantly mucous cells with few parietal cells, this finding agrees with [22] and they defined the pyloric glands region near the pylorus containing only mucous cells and they pointed out that between the fundic glands and the pyloric glands there is a transition zone in addition to mucous cells, parietal cells are present but the peptic cells are absent. The mucous cell is the most common cell type observed in the pyloric gland region of human stomach .This study disagrees with (19], who showed that the pyloric glands consist of mucous secreting cells only and abrupt disappearance of parietal and chief cells marks the boundary between pyloric and fundic glands.The PAS stain has been used to highlight the mucus-secreting cells of the gastric mucosa. This study noted that the surface lining cells of entire mucosa of rabbit stomach in both sexes that extend into gastric pits gave a strong reactivity with PAS, which appear as pink or magenta color and they are considered as mucus producing cells.The mucous is positive for PAS because it is a polysaccharide[12]. The mucus cells protect the epithelium from auto digestion [23]. The mucopolysaccharide represent as buffer system protection against acidic substance and may be important for lubrication of mucosa [12]. The current study consistence with [24]in simple stomach, [20] in human stomach and [25]in rodent. Also the PAS of cardiac glands are confirmed the histological study of number of parietal and chief cells are gave a positive reaction with PAS and appear as a pink color, some glands composed entirely from mucous secreting cells and others contain a very few of parietal cells which appear as a clear cells . The fundic glands gave a negative reaction with PAS due to the main cells of fundic gland are parietal and chief cells which gave a negative

reaction with PAS due to its function in manufacture and secretion of hydrochloric acid and gastric proenzyme respectively [26], the finding of this study agrees with [27] in rat, [28] in rabbits, [29] in toad, [30] in buffalo, [24] in human and [31] in man and laboratory animals .In pyloric glands region the pyloric glands gave a positive reaction with PAS since the predominant cells in the pyloric glands are mucous secreting cells, some glands contain a very few number of parietal cells. This result is agree with [31] in human [12] in reptile. The difference in the reactivity of the gastric glands of rabbit with PAS may by a reflection of different functions of these glands in stomach of rabbit.

CONCLUSION

1. The gross morphology, anatomy of stomach was similar between male and female
2. The blood supply do not changes between the male and female and was through the branches of celiac artery.
3. Histologically the wall of rabbit stomach in both sexes consists of four tunics, tunica mucosa, tunica submucosa, tunica muscularis and tunica serosa.
4. The thickness of tunics in both cardiac and pyloric glands region was higher than that in the fundic glands region in both sexes.
5. With special stain PAS the surface lining cell, gastric pits, cardiac and pyloric glands were gave a positive reaction and appear as pink color due to the their mucous secreting cells while the fundic glands gave a negative reaction with PAS .

REFERANCES

1. Ghoshal, N. G. and Bal, H. S. Comoarative morphology of the stomach of some laboratory mammals laboratory animals. Vol 23. Pp 21-29. (1989).
2. Smallwood, J. E. A guided Tournto of veterinary anatomy. W. B. Saunders Company. Pp. 74-84. USA. (1992).
3. Abidu- figueiredo, M., Xavier-silva, B., Cardinot, M., Babinski, M. and Chagas, M. Celiac artery in New Zealand Rabbit: anatomical study of its origin and arrangement for experimental research and surgical practice. Pesq. Vet. Bars. Vol. 28, No. 5. (2008).
4. Maia, R. S., Babinski, M. A., Abdu-figueiredo, M., Chagas, M. A., Costa, W. S. and Sampaio, F. J. B. Concentration of elastic system fibers in the *Corpus cavernosum*, *Corpus spongiosum*, and Tunica albuginea in the rabbit penis. Int. J. Impot. Res. 18(2): 121-125. (2006).

5. Kang, C. H. and Kim, W. G. The effect of vasopressin on organ blood flow in an endotoxin-induced rabbit shock model. J. Invest. Surg. 19(6): 361-369. (2006).
6. Alexander, F. and Chowdhury, A. Digestion in the rabbits stomach. British Journal of nutrition. Vol. 12. No. 1. P 65-73. (1958).
7. Tompsset, D. H. Anatomical Techniques 2nd ed. Longman group limited. (1970).
8. Samuelson, D. A. Textbook of veterinary histology. ISBN- 31: 978-0-7216-8174-0. Printed in China. (2007).
9. Luna, I. G. Manual of histology staining methods of the armed force institute of pathology. 3rd ed. McGraw-Hill book Company. New York. (1968).
10. Galigheer, A., and Kozloff. Essential practical microtechnique. Lee and Fabiger. Philadelphia. USA. (1964).
11. Al-Mohammed, N. T., Al-Rawi, K. M., Younis, M. A. and Al-Morani, W. K. Principle of statistics. J. Al Mousl University. (1986).
12. Ahmed, Y. A., El-hafez, A. A. E. and Zayed, A. E. Hitological and Histochemical Studies on the esophagus, stomach and small intestine of varanus niloticus. Vol 2. No. 1, pp. 35-48. (2009).
13. Mescher, A. L. Junqueira's Basic Histology. Text Atlas. 12th edn. Mc Graw Hill, Pp. 260-266. (2010).
14. Agungpriyono, S., Yamamoto, Y., Kitamura, N. Yamada, J., Sigit, K., and Yamashita, T. Morphological study on the stomach of the lesser mouse deer (*Tragulus javanicus*) with special references to the internal surface. J. Vet. Med. Sci54 (6): 1063-9. (1992).
15. Umphrey, J. E. and Staples, C. R. General anatomy of the ruminant digestive system http://edis.ifas.ufl. edu/index.html. (1992).
16. Al-Tikriti, M., Al-Baghdadi, F. K., Henry, R. W., Hoskins, H. and Titkemeyer, C. Correlative Light and Scanning Electron-Microscopic Study of Feline Gastric Mucosa: The Cardiac Region (*Pars cardiac*). Acta anat. 128:281-285. (1987).
17. Dellmann, H. Textbook of veterinary histology. 4th edn, Philadelphia. States of America. P. 167-171. (1993).
18. Bacha, W. J. and Bacha, L. M. Color Atlas of veterinary histology. 2nd edn. Lippin coot Williams and wilkins pp. 153-160. (2000).
19. Al-Neamy, E. M. K. A of Anatomical, histological and ultrastructural study of Abomasum and its glands development in Iraqi male goat, PH. D thesis Baghdad university Coll. Vet. Med. (2007).
20. Wheater, P. R., Burkitt, H. G. and Daniels, V. G. Functional history. 2nd ed. Churchill livingstone. pp. 208-214. (1987).

21. Elias, H., Pauly, J. E. and Burns, E. R. Histology and Human Microanatomy. 4th edn. New York, pp. 296-309. (1978).
22. Moraes, P. T., Pacheco, M. R., de-souza, W. M., da-silva, R. A., Neto, P. B., Barreto, C. S., and Ribeiro, A. A. Morphological aspects of the capybara stomach *(Hydrochaeris hydroichaeris)* : gross and microscopic structure. Anat. Histol. Embryol. 31(6): 362-6. (2002).
23. Young, B. and Health, J. W. Functional histology. A Cormack. D. H. (1984). Introduction to histology. J. B. libincott Company, Sydney. Pp. 295-303. text and colour atlas. 3rd ed. Pp. 249-259. (2000).
24. Cormack. D. H. Introduction to histology. J. B. libincott Company, Sydney. Pp. 295-303. (1984).
25. Kantani, A., Matsumoto, A. and Kataoka, K. A carbohydrate histochemical study on surface mucous cells, mucous neck cells and chief cells in the gastric mucosa of developing mice. Arch. Histol. Cytol. 52(1): 37-50. (1989).
26. Raven, P. H. and Johnson, G. B. Understanding biology. 3 rd ed. McGraw-Hill Company. New York. Pp. 726-729. (1995).
27. Leblond, C. P. and Stevens, C. E. The constant renewal of the intestinal epitlelium in the albino rat. Anat. Rec. 100:357. (1948).
28. Menzien, G. Observations on the development of certain cell types in the fundic region of the rabbits stomach.499-453. (1964).
29. Loo, S. K. and Wong, W.C. Histochemical observations on the mucins of the gastrointestinal tract in the toad *(Bufa melanostictus)*. Acta. Anat. 91: 97-103. (1975).
30. Mouly, K. N. and Rao, K. T. Histology and mucopolysaccharide content of the surface epithelial chief and parietal cells of the fundic glands of buffalo. Indian. J. Anim. Sci. 54(1): 50-54. (1984).
31. Sheahan, D. G. and Jervis, H. R. Comparative histochemistry of gastrointestinal mucosubstaces. Am. J. Anat. 146.103-132. (1976).

Phenotypic and Genotypic Detection of Methecillin Resistance in Locally Isolated *Staphylococcus aureus*

Shaimaa A.Al-Oubaidy[1] and Sawsan S. Al-Jubori [2]
[1]College of medicine /Babylon University.
[2]Department of Biology -College of Science/ Al-Mustansiriyah University
E-mail: sawsam_sajid_ma2000@yahoo.com

Received 29/2/2012 – Accepted 18/4/2012

الخلاصة

تم الحصول على 150عزلة من المكورات العنقودية من اصابات سريرية متنوعة ,توزعت العينات ما بين 41 عزلة من الادرار، 59 من خمجات جروح و 50 عزلة من مسحات الأذن . شخصت هذه العزلات اعتمادا على عدد من الفحوص المورفولوجية والكيموحيوية المتبوعة بالتشخيص بعدتي api staph و Mast staph .من مجموع 150 عزلة كان بينها (58%) عزلة، شخصت على انها مكورات عنقودية ذهبية *Staphylococcus aureus*.بينت نتائج المسح الاولي لمقاومة المثسلين باستخدام طريقة انتشار الاقراص(Kerby bauer method)بان هنالك 84 عزلة مقاومة للمثسلين (MRSA) من مجموع (96.5%) عزلة .انتخبت 25 عزلة لغرض اجراء الدراسة الوراثية باستخدام طريقة التفاعل التضاعفي لسلسة الدنا (PCR) للتحري عن جين مقاومة المثسلين (*mec* A)، واختيرفي الدراسة الحالية تسلسلين لجين مقاومة المثسلين يمثل الاول قطعة الجين بالكامل (1339زوج قاعدة) كون ان البادئ الامامي والعكسي قد حددت من منطقتي اعلى التيار واسفل التيار على التوالي اما القطعة المضاعفة الثانية فانها تمثل جزء من الجين (314زوج قاعدة). استخدم الدنا الجينومي الكامل كقالب ،وحضر اما بطريقة المستعمرة المباشرة اوبطريقة الغليان باستخدام الماء المقطراوداري TE.اظهرت النتائج ان 25 عزلة المنتخبة تملك جين *mec* A اعتمادا على ظهور حزم واضحة بحجم 1339bp و 314 bp في 1% هلام الاجاروز ومقارنتها مع الدلائل الحجمية .لقد كانت طريقة المستعمرة المباشرة هل الافضل في تحضير الدنا القالب مقارنة مع طريقة الغليان التي اعطت نتيجة سالبة مع قطعتي الجين المضاعفة .

ABSTRACT

Total (150) isolates of Staphylococci species were isolated from different clinical samples. They were distributed as (41) isolates from urine, (59) isolates from wound infections and (50) isolates from ear swabs. These isolates were diagnosed using different morphological and biochemical test followed by the complementary api 20E test and mast staph kit. Out of 150 isolates, (58%) were *Staphylococcus aureus*. Results of primary screening test for methicillin resistance using disk diffusion method revealed that 84 isolates(96.5%) were proved to be methicillin resistant *Staphylococcus aureus*(MRSA). Twenty five isolates were selected for the genotypic study to detect methicillin resistance gene (*mec*A)using the polymerase chain reaction (PCR) . Two target sequences related to this gene were chosen in the current study ,the first represent the total gene segment (1339 bp) since the forward and the reverse primers were picked up from the upstream and the downstream region from the original gene while the other amplified segment represent part of the gene (314 bp) . Total genomic DNA was used as a Template and it was prepared either by direct colony or by boiling method using distilled water or TE buffer. Results showed that all the selected 25 isolates (100%) were harboring *mec* A gene based on the presence of 314 bp or 1339bp clear bands in 1% agarose gel as compared with DNA ladder .Direct colony was better in preparing the template DNA compared with the boiling method which gave a negative results with the two amplified segments.

INTRODUCTION

Methicillin resistant *Staphylococcus aureus* (MRSA) is a significant pathogen causing both nosocomial, community acquired infections, and its high prevalence in hospitals has been reported from many Countries[1]. Since most of these bacteria carry multiple resistance genes against commonly used antibiotics, they show multiple antibiotic resistance patterns thus causing important treatment problems[2].MRSA has the ability to resistance β-lactam antibiotics either by production β-lactamase enzyme which binds specifically to β-lactam ring in the β-lactam antibiotics rendering them inactivate[3] beside that ,resistance could be due to altering or modification target site represent by penicillin binding proteins((PBPs) ,once the organism alters the PBPs, the β-lactam antibiotics significantly decreases its affinity for their substrate that is to say to PBPs [4] The low-affinity to (PBP2a) is encoded by mec A gene which represent the main factor responsible for methicillin resistance in *Staphylococcus* [5] The mec A gene have never been found in methicillin-susceptible *Staphylococcus aureus*(MSSA) , while they have been detected in almost all MRSA isolates[6] . The mecA gene becomes a useful molecular tool for identification of MRSA since molecular techniques(mostly based on polymerase chain reaction) had been used for the rapid detection of MRSA [7] .The aims of this study are to isolate *S,aureus* from different infections then to detect MRSA using primary screening test followed by genotypic detection for mecA gene using PCR technique using DNA template prepared by different methods .

MATERIALS AND METHODS

Specimen's collections and Diagnosis:

Total of (150) clinical isolates primary identify as *Staphylococcus species* were obtained from hospitalized and non hospitalized patients from two hospitals: Al-habibia and Noaman hospital in Baghdad city during the period from January to April 2011. Types and the numbers of these clinical samples were distributed as (41) isolates from urine, wounds include (59) isolates from wound infections and (50) isolates from ear swabs. Bacterial diagnosis including morphological and biochemical tests were done according to [8] which involve coagulase test and the culturing on specific media like mannitol salt agar ,staph 110 and Baird parker agar .The diagnosis was followed by the complementary api 20E test and mast staph kit for *S. aureus* and the latter was done according to (BioMérieux /France)and (MastGroup Ltd., Bootle, Mersegside, / U.K)

Phenotypic detection of Methicillin resistant

All isolates were tested for primary screening test of antimicrobial susceptibility depending on the [9] .Disk diffusion tests was done by placing 5µg/disc of methecillin on Mueller-Hinton agar cultured with the bacterial isolate.The zone of inhibition was measured after 24 hours of incubation at 37°C and the results were compared with the negative control represent by the standard strain ATCC 25923.

PCR amplification:

The selected resistance isolates with positive phenotypic tests were subjected to molecular

Screening study using PCR amplification technique according to following steps:

DNA template preparation

The preparation of DNA template was conducted by two ways:

1-direct colony: It was performed according to [10] in which a sterile wooden stick was simply attached with a single isolated bacterial colony then it was carefully suspended in the wall of Eppendrof tube containing the PCR mixture, then it was mixed by vortex to get fully dissolved mixture .

2-Boiling method

TE buffer method: Template DNA was prepared by dissolving 1µl of bacteria in 1ml of TE buffer, centrifuged at 5000 rpm for 5 min, and the pellet resuspended in 100µl of TE buffer. The suspension was boiled at 100c° for 10 min before centrifugation at 5000 rpm for 5 min. The supernatant served as PCR template [11]

Distilled water method: It was prepared according to Ruppé *et al* .[12] Briefly, 5 isolated colonies of overnight growth bacteria were suspended thoroughly in 1 mL distilled water and boiled in a water bath for 10 min. After centrifugation, supernatant was used as template DNA for the PCR.

Primers used for PCR: Oligonucleotide primers specific for the methecillin resistant genes(*mec* A) were chosen in this study to get two amplified segment ,one of them represent the total gene sequence since it was picked from the upstream and the downstream region and the amplified size was 1339bp,the other represent part of the gene with amplified size 314bp[14].Table 1 shows the details of these two primers .

Table-1 :The primers used in the current study for PCR amplification .

Target Gene	Primer name	Nucleotide sequences and direction 5`——→3`	MW µg/µmol	Product size (bp)	Reference
*mec*A	*mec*A1 (F) *mec*A1 (R)	CCTAGTAAAGCTCCGGAA CTAGTCCATTCGGTCCA	1024 732	314	[14]
*mec*A	*mec*A2 (F) *mec*A2 (R)	GTGGAATTGGCCAATACAG TGAGTTCTGCAGTACCGGAT	6206 6148	1339	[13]

PCR amplification procedure: Twenty five selected isolates were submitted to genotypic study using PCR. The oligonucleotide primers specific for the *mec*A genes (table1) were diluted using nuclease free water according to the manufacture company information (alpha Canada) to get primary concentration equal to 100 pmol . The amplification was performed in a TECHNE (TC-3OOO) thermal cycler and the reaction mixture was prepared according to the procedure that suggested by the manufacture company (Promega, USA). PCR mixture was composed from 12.5 µl of GoTaq®Green Master Mix(2x), 1.5 µl (10 pmol) from each forward and reverse primers ,5 µl of DNA template(prepared by boiling method) and 4.5 µl of nuclease free water to get final volume of 25 µl. In case of using direct colony method ,the volume of the DNA template was considered zero and the volume of the PCR mixture was completed with nuclease free water(9.5 µl instead of 4.5 µl) to get final volume of 25 µl. PCR mixture without DNA template was used as a negative control. Table 2 represent Conditions for PCR amplification which were set according to this study for the two primers and was started with predenaturation step at 95°C for 5 min followed by 30 repeated cycles of denaturation at 95°C for 45 sec ,annealing step at 56°C for 45 sec (annealing temperature was increased to 60 °C for 1min for mecA2)and an extension step at 72°C for 45 sec for mecA1 (72°C for 1 min for mecA2), finally one extension step at 72°C for 7 min. The amplified PCR product were analyzed by agarose gel electrophoresis according to [13] using 1% agarose supplied with 0.5 µg/mL ethidium bromide for 1 hour and a half (7 Volts/ cm^2) . DNA ladder (100bp and 1000bp) were used to assess PCR product size, then PCR products were visualized by UV light at 336 nm, and photographs were taken using digital camera.

Table-2: PCR programs applied in this study.

PCR	Initial Denaturation	Cycles No.	Denaturation	Primer annealing	Elongation	Final elongation
mecA1	95c°/5 min	30	94c° / 45 sec	58c°/45sec	72c°/45 sec	72c°/7 min
mecA2	95c°/5 min	30	94°C / 45 sec	60 c°/1min	72c°/1 min	72c°/ 7 min

RESULTS AND DISCUSSION

Spread of methicillin-resistant *Staphylococcus aureus* (MRSA) and coagulase-negative Staphylococci (CNS) is an important concern in hospitals and other health care settings[15]. In the current study, a total of 150 specimens showed significant growth as *Staphylococcus* species. To distinguish *S.aureus* from others ,the isolates were submitted to different biochemical test including culturing on mannitol salt agar and here *S.aureus* isolates were able to grow on this media converting the

red color to yellow due to mannitol fermentation [16]while growing on Baird-Parker agar, the colonies of this species appeared black, shiny, circular and convex, surrounded by a clear zone[17]Coagulase test also was performed since it considered a remarkable diagnostic test and only *S.aureus* has the ability to give positive result [18]Another important diagnostic test was performed using specific kit known as Mast staph which is a agglutination test specific for detecting protein A in this species .Positive results appeared as a clear agglutination after a few seconds from the addition of one drop mast staph solution, while the negative result appears transparent (clear) without any agglutination according to (Mastgroup ltd., Bootle, Mersegside, /U.K)catalog.figure 1 represent a positive and negative results .

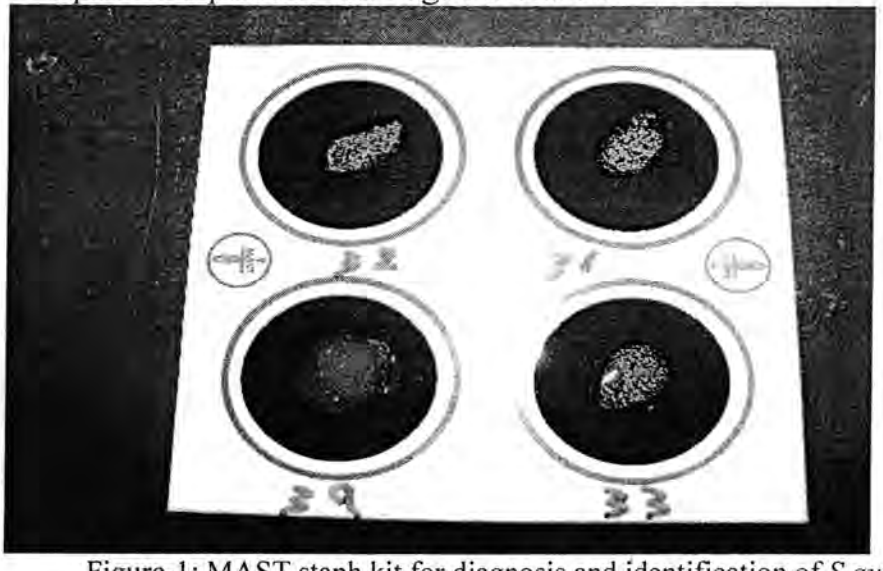

Figure-1: MAST staph kit for diagnosis and identification of *S.aureus*, positive results for the isolates (32,36,33)

Out of 150 isolates, 87(58%) diagnosed as *S. aureus* and 63 (42%) isolates include other *Staphylococcus* spp. This result is comparable to Rallapalli [19]who reported that out of 150 Staphylococcal clinical isolates only 95 isolates were *S. aureus* (63.33%), while results of Farzana and Hameed [20] illustrated that out of 2580 Gram-positive cocci ,1688 isolates were *S. aureus*(65.5%). This percentage may be differ from time to time according to source of the isolates , nature and size of the samples , the type of study and the geographic location that samples were taken from . By using disk diffusion method to detect methicillin resistance , 84 MRSA were identified out of 150 isolates (96.5%) while the remaining 3 isolates (3.5%) showed their susceptibility for methecillin(MSSA). Kader *et al.* [21] reported that (88.24%) isolates were resistant to methicillin and Oxacillin, while Odonkora and Addob[22]reported that methicillin disc diffusion test detected 54(21.6%) representing MRSA while 196 (78.4%)

representing MSSA and this result is less than the result of the current study and other studies. Disc diffusion test or the phenotypic method in some cases has low specificity and sensitivity for the detection of MRSA and other type of resistance since the phenotypic expression is influenced by many factors such as inoculums size, incubation time , temperature, pH and salt concentration of the medium[23]Twenty five isolates of MRSA which gave positive results in phenotypic detection were selected for the genotypic study by PCR technique using two different gene sequence ,the first one represent the total genomic segment since the forward and reverse primers were picked up from the upstream and downstream region of the original gene sequence with amplified size equal to 1339bp [13].The second represent part of the gene and the amplified size was314 bp[14].To perform the test, two process was used for template DNA preparation. The results revealed that using the direct colony was more efficient in expressing the results as compared with the boiling method whether distilled water or TE buffer was employed in spite of repeating the experiments for several time, hens that the first method was followed. The results of PCR experiment revealed that all selected isolates demonstrating resistance to methicillin and expressing of *mecA* gene .Figur 2 illustrates number of isolates harboring *mec* A based on the presence of 1339 bp bands (as compared with the ladder DNA ladder) on 1%agarose gel .

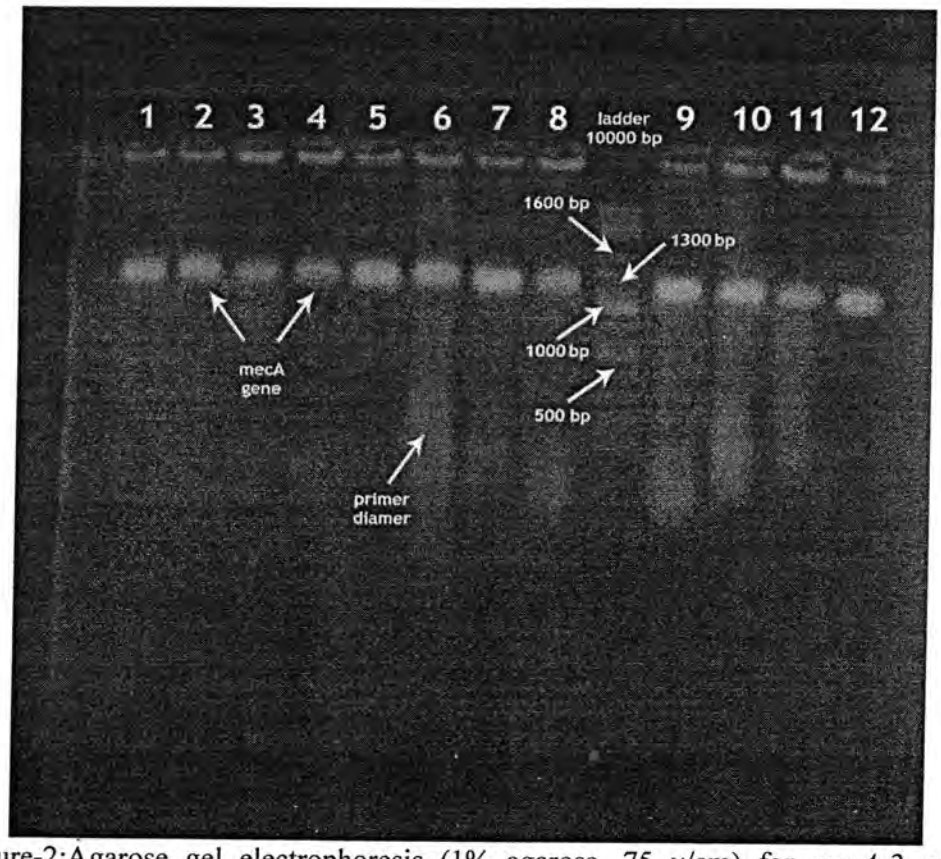

Figure-2:Agarose gel electrophoresis (1% agarose, 75 v/cm) for *mecA-2* gene (amplified size 1339bp as compared with 1000bp DNA ladder) using template DNA prepared by direct colony. Line 1-12 represents positive results.

This result is close to the result of Rallapalli (19)who showed that all the 40 isolates determined as MRSA by phenotypic methods, gave positive results using PCR. Also Kader *et al.* [21]reported that all the 34 strains were harboring *mecA* gene. The same result was obtained in the current study when another amplified sequence was used and all the selected isolates gave positive results for *mecA* gene.Figur (3)shows number of isolates harboring *mec* A based on the presence of 314 bp bands (as compared with 100bp DNA ladder) on 1% agarose gel

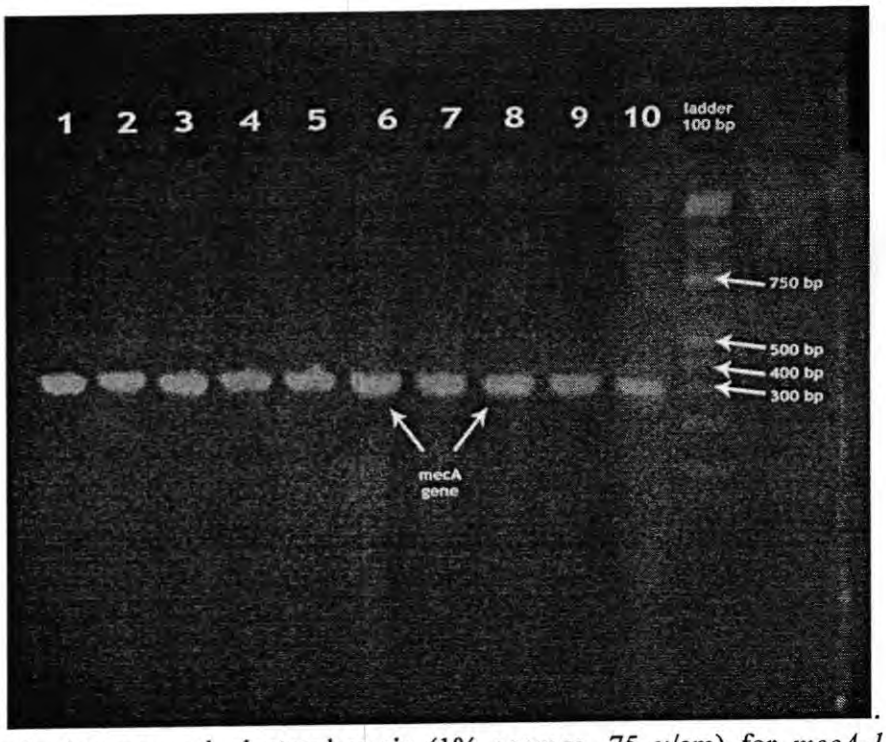

Figure-3: Agarose gel electrophoresis (1% agarose, 75 v/cm) for *mecA-1* gene (amplified size 314bp as compared with 100bp DNA ladder) using template DNA prepared by direct colony . Positive results in lines 1-10.

Usually those isolates possessing an altered PBP2 are resistant to methicillin, oxacillin, and probably to all other currently available β-lactam antibiotics and such isolates which responsible for serious nosocomial infections will require administration of non ß-lactam antimicrobial therapy[23]. Rapid and accurate detection of methicillin resistance in *S. aureus* is important for using other appropriate antimicrobial therapy beside controlling nosocomial spread of MRSA strains[24]. Identification of the *mecA* gene remains the most reliable method of detecting MRSA isolates since there is no optimal phenotypic method for detecting methicillin resistance in *S. aureus* , however not all laboratories can include molecular biology techniques in their routine clinical practice. In conclusion, molecular techniques remain the most sensitive method in detecting *S. aureus* at both genus and species level and with 100% accuracy in detecting MRSA, as compared with the classical identification method.

REFERENCES

1. Kaya,E. G.; Karakoç, E.; Yagci, S. & Yücel, M. Evaluation of phenotypic and genotypic methods for detection of methicillin resistance in *Staphylococcus aureus. J. Afri. Microbiol. Res.* 3(12): 925-929. (2009).

2. Karami, S.; Rahbar, M. & Yousefi, J.V. Evaluation of Five Phenotypic Methods for Detection of Methicillin Resistant *Staphylococcus aureus* (MRSA). *Iran.J. Path.* 6 (1):27- 31. (2011).
3. Baddour, M. M.; Abu El-Kheir, M. M. & Fatani, A. J. Comparison of *mecA* Polymerase Chain Reaction With Phenotypic Methods for the Detection of Methicillin-Resistant *Staphylococcus aureus.J.Curr. Microbiol.* 55:473–479. (2007).
4. Ekrami, A.; Samarbafzadeh, A.; Alavi, M., Kalantar, E. & Farhad, H. Prevalence of methicillin resistant *Staphylococcus* species isolated from burn patients in a burn center, Ahvaz, Iran. *Jund. J. Microbiol.* 3(2): 84-91. (2010).
5. Chambers H,F. Methicillin Resistance in Staphylococci: Molecular and Biochemical Basis and Clinical Implications. Review. Clin Micro. 4(10): 781–791. (1997).
6. Enright, M.C.; Robinson D.C.; Randle G.; Feil E.J.; Grundmann H.; and Spratt G.E. The evolutionary history of methicillin-resistant *Staphylococcus aureus* (MRSA). PNAS. 99(11):7687-7692. (2002).
7. *Unal*,S.; Hoskins,J.; Flokowitsch,JE.; Wu,C.; Preston, D.A. and Skatrud P.L.Detection of methicillin-resistant staphylococci by using the polymerase chain reaction. Jour.Clin.Micro.30(7):1685-1691 .(1992).
8. Atlas, R.M.; Brown, A.E.; and Parks, L.C. Laboratory manual of experimtal microbiology. 1st ed .Mosby,st.Louis U.S.A. (1995).
9. CLSI. Performance standard for antimicrobial susceptibility testing;Twenty-First informational supplement. M100-S21.vol.31 No.(1). (2011).
10. Al-Kaabi ,M, H. Detection of bla TEM,*bla* SHV, CTX-M-I and CTX-M-III genes by using polymerase chain reaction technique from some Gram negative bacteria. Thesis. Al-Mustansiriyah university- College of Science .(2011).
11. Klingenberg,C; Sundsfjord,A; Rønnestad,A; Mikalsen, J; Gaustad,P & Flaegstad,T. Phenotypic and genotypic aminoglycoside resistance in blood culture isolates of coagulase-negative staphylococci from a single neonatal intensive care unit, 1989–2000.*J. Antimicrob.Chemother.* 54: 889–896. (2004).
12. Ruppé, E.; Hem, S.; Lath, S.; Gautier, V.; Ariey, F.; Sarthou, J.L.;Monchy, D. and Arlet, G. CTX-M β-Lactamases in *Escherichia coli* from Community-acquired Urinary Tract Infections, Cambodia. *Emerg Infect Dis.* 15(5):741-748. (2009).
13. Moussa,I,M& Shibl, A,M .Molecular characterization of methicillin-resistant *staphylococcus aureus* recovered from outpatient clinics in riyadh, saudi arabia. *Saudi. Med. J* . 30 (5):612-617. .(2009).

14. Choi,S,M; Kim,S,H; Kim, H-J; Lee,D-G; Choi, J-H; Yoo,J-H; Kang,J-H, Shin,W-SH& Kang,M-W .Multiplex PCR for the detection of genes encoding aminoglycoside modifying enzymes and methicillin resistance among Staphylococcus species. *J. Korean. Med .Sci.* 18: 631-636.(2003).
15. Wallet, F.; Roussd-Delvallez , M. & Courcol, R. J. Choice of a routine method for detecting methicillin-resistance in staphylococci. *J. Antimicrob. Chemother.* 37: 901-909. (1996).
16. Heuck,C.C;Piot,P.& Engback,K .Basic Laboratory Procedures in Clinical Bacterology.WHO library Cataloguing in Publication. pp. 69-70 (1991).
17. Antony,A.Study of Biofilm forming capacity of pathogens involved in Chronic Rhinosinusitis. Thesis. Auckland University. (2011).
18. Caiazza, N.C.; and G.A. O'Toole.Alpha-Toxin Is Required for Biofilm Formation by *Staphylococcus aureus*. J. Bacteriol.**185**(10): 3214-3217.(2003).
19. Rallapalli ,S., Verghese, S .andVerma, RS. validation of multiplex pcr strategy for simultaneous detection and identification of methicillin resistant *staphylococcus aureus. India. J. Med.Microbio, 26(4): 361-4. (2008).*
20. Farzana,K.& Abdul Hameed .Resistance pattern of clinical isolates of *staphylococcus aureus* against five groups of antibiotics. *J. Rese.* 17(1): 19-26.(2006).
21. Kader ,O; Ebid ,S, Mostafa ,N; El Sayed ,SH& Ghazal ,A .Detection of community acquired methicillin resistance *Staphylococcus aureus* among *staphylococcus aureus* isolates. J. Americ. Scie.,7(1).(2011).
22. Odonkora,S,T and Addob,K,K. Evaluation of three methods for detection of methicillin resistant staphylococcus aureus (MRSA).. Int. J. Biol. Med .Res. 2(4): 1031 – 1034 (2011).
23. DeGiusti,M;Pacifico,L;Tufi,D;Panero,A;Boccia,A.&Chiesa,C.Phen otyoeic detection of nosocomial mecA-positive coagulase-negative staphylococci from neonates.*J.Antimicrob,Chemo*. 44:351-358 (1999).
24. Kolář, M.; J. Bardoň; V. Hanulík; P. Sauer; V. Babák; and J. Schlegelová. Resistance to Methicillin in Coagulase-negative Staphylococci and Its Detection. Acta Vet. Brno.79:261-267. (2010).

Induce Resistance of Alfafa Plant against the Fungus *Verticillium albo-atrum* that Causing Vascular Wilt by Avirulant Strains of the Fungus *Verticillium albo-atrum*

Abdulazeez M. Nokhalan
Al-Mustansyraih University, College of Science, Department of Biology
Received 29/11/2011 – Accepted 18/4/2012

الخلاصة

لغرض إيجاد مقاومه بيولوجيه مقنعه ضد الإمراض النباتية التي تسببها الفطريات من خلال تحفيز مقاومة النباتات الذاتيه باستعمال ضروب من الفطريات التى لاتسبب امراض نباتيه تم اختيار الفطر *Verticillium albo-atrum* الذى يسبب الذبول الوعائى لمجموعه كبيره من النباتات منها نباتاتAlfalfa الجت العراقي (*Medicago sativa*) كمثال لتجارب مستقبليه فى هذا المجال. اجريت تجارب اوليه لتحديد قابلية ضربين من الجت هما Euver & Vela cultivar للاصابة بضربين من الفطر *Verticillium albo-atrum* احدهما عزل من الجت (V1) والاخر عزل من الطماطه(V2). اثبتت النتائج ان الضربين احدهما cultivar Vela حساس للضربV1 ومقاوم للضرب V2 و الثانى Euver cultivar مقاوم للضربين ولغرض تحفيز مقاومة النباتات الذاتيه استعمل ضرب V2 لمقاومة المرض الذى يسببه الضربV1 فى الجت العراق الذى يشكل مشكله حقيقيه فى العراق وقد بينت النتائج ان الضرب V2 الذى لايسبب المرض حفز مقاومة نباتات ضد الضرب V1 الذى يسبب المرض ولكن لم يمنعها تماما.

ABSTRACT

To identify a conventional biological method to control plants diseases which caused by Fungi we used AVirulent isolate of the fungus *Verticillium albo- atrum* (V2) which was isolated from Tomato to induce resistance against the Virulent fungus *Verticillium albo-atrum* (Isolate V1) which was isolated from Alfalfa plants. Two cultivars of Alfalfa plants cultivar Euver & Vela were used in the experiments. The results showed that Avirulent (*Verticillium albo-atrum*(isolate V2) increased resistance against the Virulent fungus *Verticillium albo-atrum* (Isolate V1) in both cultivors but could not prevent or stop the disease entirely.

INTRODUCTION

The wilt disease which caused by *Verticillium* species has been a destructive disease and a major limiting factor in Alfalfa plants production [1]. Therefore it became urgent and very important to establish an effective method to control this disease. Cross protection or induced resistance can be defined as a type of biological control in which inoculation the plants with avirulent pathogen (inducer) causes a reduction in severity of the symptoms or delays disease development which is caused by a virulent pathogen. This definition is a modification of the original concept in which the phenomenon is known to occur in interactions with plant viruses [2].

The mechanism by which the cross-protection phenomenon is expressed is still poorly understood, although a number of explanations have been suggested to explain this phenomenon [2]. Inspite of this criticism and difficulties, there are many workers who have got good results from cross protection experiments, for example, [3] protected green -house grown tomato against vascular wilt caused by *Verticillium albo-atrum*, by dipping roots of the seedlings in a spore suspension of a virulent

isolates of *Verticillium albo-atrum*. [4] reduced the severity of symptoms of wilt disease in sunflower caused by *Verticillium dahliae*, by inoculating plants with a non-pathogenic isolate of *Verticillium dahliae*, They reported that antagonism between the two strains must be considered but they did not observe any antagonism between the isolates in culture In present study we used A virulent isolate of *V albo-atrum* to induce resistance in Alfalfa plants against the virulent isolates of *V albo-atrum* and we test the effect of time interval between inoculation with inducer and challenger.

MATERIALS AND METHODS

Fungi & Plants: Two isolates of *Verticillium albo-atrum* were used. One (designated V1) was isolated from Alfalf plants grown in the field (V2), which had been isolated from tomato, cultivar Ailsa Craig. The isolates were maintained on Potato Dextrose Agar (PDA) at 23 C° in the dark. The cultures were renewed by sub-culturing monthly.

Two cultivars of Alfalfa namely, Euver, Vela, and one cultivar of tomato, Ailsa Craig, were used in experiments. Cultivar Euver was reported to be susceptible to *Verticillium* wilt,. Cultivar Vela also was known to be resistant to wilt disease that caused by *V. albo-atrum,* The tomato cultivar, Ailsa Craig was known to be susceptible to wilt disease which cause by *Verticillium* species, [5].

Preparation of inoculum Spores suspensions of fungi were prepared from 12 day old cultures, grown on Potato dextrose agar plates (9.5 cm, diameter. 1.5 cm, depth) at 23 C ° in the dark. Cultures were flooded with sterile distilled water (10 ml per plate) and the surface of the culture was scraped gently with a sterile glass rod to free the spores. The spores suspensions were collected and filtered through a double layer of muslin cloth. The concentration of spores was measured using a haemocytometer and sterile distilled water added to adjust to the required concentration.

Method of inoculation A root-dip inoculation method was used to inoculate the plants in all experiments. 5-6 week-old plants were carefully uprooted from the pots and the roots were washed with distilled water to remove the soil. The roots were then dipped in a beaker containing a spores suspension (100 ml of 10^7 spore ml-1) of the fungus, for 10 minutes. Control plants were dipped into sterile distilled water for the same length of time. Inoculated plants were replanted either directly in a field plot in the Botanical garden, Swansea University, or into plastic pots (15 cm diameter) containing unsterilized "all purpose compost" (Arthur Bowers) and maintained in the greenhouse at 23 C ° with a photo-period of 16 hr and light intensity of 9000 Lux.

Pathogenicity of *V. albo_atrum* isolates V1, V2 to Alfalfa and tomato cultivar:

5-6 week-old seedlings of two cultivars of Alfalfa namely, Euver, Vela, and one cultivar of tomato plants cultivar Ailsa Craig were inoculated by roots dipping for 10 minutes in spores suspensions (10^7 spore ml-1) of one of two isolates of *V. albo-atrum,* V1 (Alfalfa-isolate) or V2 (tomato-isolate). Control plants were dipped in sterile distilled water for the same period of time. The inoculated plants were replanted either in the experimental plots or in plastic pots (15 cm diameter) containing unsterilised "all purpose compost" (Arthur Bowers). Plants maintained in the greenhouse. Five plants were used for each treatment. Measurement of height of the main stem of the plants and recordings of the development of wilt symptoms were made at weekly intervals over an 10-week period following inoculation. Longitudinal sections from the basal part of the stems of test plants, and reisolation of the fungus were made from the test plants.

Induced resistance in the Alfalfa cultivars: 5-6 week-old plants of two cultivarsof Alfalfa, cultivar Euver, susceptible to *V. albo-atrum,* isolate V1 and resistant to V2 and cultivar Vela, with a degree of resistant to both isolates, V1 & V2, (the result of pathogenicity experiment) were inoculated simultaneously by the root dipping method (Materials and Methods) for 10 minutes in spore suspensions (107 spore ml-1), as follow;

Treatment I. V1 alone. Treatment II. V2 alone. Treatment III. V1 + V2 and treatment IV. sterile distilled water as control. Six replicates were used for each treatment. Inoculated plants were replanted in plastic pots (15 cm diameter) containing unsterilized "all purpose compost" (Arthur Bowers) and maintained in the greenhouse.

Measurement of the height of the main stem of the plants and recordings of the development of wilt disease symptoms were made at weekly intervals over an 8-week period following inoculation.

Assessment of wilt disease symptoms:

Progress of the severity of wilt disease as determined by visual assessment.

Plants were scored individually by observing growth (measuring the height of the main stem) and recording development of wilt disease symptoms at weekly intervals over a 10-week period following inoculation. The following rating, adapted from [5] and used by [7] and [8].

The keys were:

0 = The plants healthy, no wilt symptoms appeared.

1 = The lower leaves lost turgar and showed yellowing.

2 = Less than a quarter of the plant showed wilt symptoms.

3 = Less than half of the plant showed wilt symptoms

4 = Less than three quarters of the plant showed wilt symptoms such as, lost of turgar and yellowing in leaves, necrosis, desiccation, eipnasty or leaves defoliated .

5 = The plants were dying or dead.

The following equation that was used by [8] was used to obtain the disease symptom index.

$$\%Disease\ Symptom\ Index = \frac{^{*}Sum\ of\ Individual\ Rating\ X\ 100}{^{**}5X\ the\ number\ of\ plants\ assessed}$$

* Sum of each plant multiple by the particular value.

** The maximum value of the symptoms.

RESULTS AND DISCUSSION

Pathogenicity of *V. albo-atrum* isolates V1,V2 to Alfalfa and tomato cultivars

Alfalfa Cultivars: In order to investigate the pathogenicity of *Verticillium albo-atrum* isolates V1 (Alfalfa-isolate) & V2 (tomato-isolate) towards cultivars of Alfalfa and in order to monitor development of the severity of wilt disease in greenhouse grown plants the experiment were carried out.

The results are shown in table 1. They show that inoculated plants grown in the greenhouse showed no symptoms of wilt disease in response to inoculation with *V. albo-atrum* isolate V2. This was true for all the cultivars as well as the control plants, (plants which were inoculated with sterile distilled water). These results lead to the conclusion that all the Alfalfa cultivars which were used in this experiment were resistant to *V. albo-atrum* isolate V2 the isolate which had been originally isolated from wilt infected-tomato plants.

The reactions of greenhouse grown alfalfa cultivars which were inoculated with *V. albo-atrum* isolate V1 can be divided into two categories. In one group, which contained cv. Vela, plants showed stunting in growth of the plants but no symptoms of wilt disease were observed.

The second category contains cv. Euver, cv. which was susceptible to isolate V1. A reaction appeared in the plants 3 weeks after inoculation resulting in wilt symptoms such as, loss of leaf turgid, followed by yellowing and browning necrosis of the leaves. In the later stages the leaves were desiccated and branches were died. The infection also caused stunting of the plants, table1.

Table-1: The mean heights & disease symptom index of Alfalfa cultivars inoculated with two isolates of *V albo-atrum* V1 & V2 separately

W	Cultivar Euver						Cultivar Vela					
	C		V1		V2		V1		V2		C	
	S.I	H	S.I	H	S.I	H	S.I	H	S.I	H	S.I	H
1	0	0.8	0	0.8	0	0.8	0	0.8	0	0.8	0	0.8
2	0	12.1	0	9.2	0	11.5	0	11.2	0	10.4	0	11.5
3	0	17.2	5	10.0	0	15.5	0	15.5	0	13.2	0	14.1
4	0	22.3	10	12.4	0	21.5	0	20.3	0	17.8	0	18.4
5	0	27.8	25	14.5	0	26.6	0	25.6	0	24.2	0	24.4
6	0	33.2	35	17.3	0	31.4	0	31.3	0	29.3	0	29.4
7	0	39.2	55	19.7	0	38.3	0	39.3	0	33.3	0	36.7
8	0	44.3	65	21.4	0	42.3	0	45.6	0	38.2	0	45.5

The Key:
H Heights were measured in Cm, the means of 5 plants
W Weeks following the inoculation
Si Diseases symptoms index
C Control
V1 *V. albo-atrum* isolated from Alfalfa
V2 *V. albo-atrum* isolated from Tomato.

Tomato cultivar: The results are summarized in table 2. Symptoms of wilt disease appeared on the lower older leaves of all the plants 4 weeks after inoculation with isolate V2 (plate 2). In contrast all the tomato plants that were inoculated with isolate V1 remained as healthy as the control.

Table-2: The mean of the heights & disease symptom index, of Tomato, cv. Ailsa Craig inoculated with *V. albo-atrum*, isolates V1 or V2, in the greenhouse

Treatment	C		V1		V2	
Week	S.I	H	S.I	H	S.I	H
1	0	16.0(±0.0)	0	16.0(±0.0)	0	16.0(±0.0)
2	0	18.2(±1.6)	0	17.2(±3.3)	0	17.4(±4.4)
3	0	21.2 (±8.0)	0	20.1(±9.0)	0	18.4(±3.4)
4	0	30.5(±6.0)	0	28.9(±8.8)	15	20.2(±6.6)
5	0	38.9(±8.0)	0	37.8(±1.5)	15	21.1(±7.8)
6	0	46.7(±2.4)	0	45.5(±4.5)	25	23.3(±4.6)
7	0	55.5(±5.6)	0	55.4(±8.0)	45	25.6(±2.2)
8	0	70.0(±1.3)	0	68.9(±6.2)	60	27.8(±2.3)
9	0	80.1(±2.4)	0	77.8(±5.5)	75	30.5(±9.0)
10	0	90.0(±3.3)	0	86.7(±2.2)	75	32.5(±3.3)

Figure in brackets represent the standard deviation.
The Key
H Heights were measured in cm, the means of 5 plants.
W Weeks following the inoculation.
S.I Disease symptoms index.
C Control.
V1 *V. albo-atrum*, isolated from Alfalfa.
V2 *V. albo-atrum*, isolated from tomato.

Induced resistance in Alfalfa: In order to investigate the occurrence of induced resistance in the interaction between two isolates of *Verticillium albo-atrum,* isolate V1 (pathogenic toAlfalfa) & V2 (non-pathogenic toAlfalfa), and the cultivars of Alfalf the following experiment was conducted.

Two cultivars ofAlfalfa, Euver, (susceptible to *V. albo-atrum,* isolate V1 and resistant to isolate V2) and Vela, (with a degree of resistant to both isolates V1 & V2), were inoculated by the root dipping method either separately or

simultaneously (Materials & Methods page), 10 minutes with spores suspension (107 spore ml-1) of two isolates of *V. albo-atrum,* V1 and V2 as follows:

Treatment I. V1 alone; Treatment II. V2 alone; Treatment III. V1 + V2 and Treatment IV. Sterile distilled water as control. Inoculated plants were maintained in the greenhouse. Observation of the growth of the plants and development of wilt disease symptoms were made at weekly intervals over an 8-week period following inoculation.

Euver the susceptible cultivar: The results (table 3 and 4) demonstrate that the simultaneous inoculation of susceptible cultivar of Alfalfa with two isolates of *V. albo-atrum,* V1 and V2 increased their resistance to wilt disease caused by *V. albo-atrum* isolate V1. The severity of the wilt disease was reduced and the growth of susceptible plants was comparable to the resistant cultivar.

The reaction of the cv. Vela (resistant) to inoculation with *V. albo-atrum,* isolates V1 & V2 simultaneously shown in table 3 and 4). It demonstrates that there is no large difference in growth or severity of wilt symptoms between the plants which were inoculated with V1 or V2 alone or with V1 + V2.

Table-3: The mean heights of Alfalfa cultivars inoculated with *V. albo-atrum,* isolate V2 as resistance inducer against V1 as the challenger

W	Cultivar Euver				Cultivar Vela			
	C	V1	V2	V1+V2	C	V1	V2	V1+V2
1	0.8(±0.0)	0.8(±0.0)	0.8(±0.0)	8.0(±0.0)	0.8(±0.0)	0.8(±0.0)	0.8(±0.0)	8.0(±0.0)
2	12.1(±2.0)	9.2(±2.2)	11.5(±3.0)	10.1(±5.2)	11.2(±3.2)	10.4(±6.4)	11.0(±9.0)	12.0(±1.2)
3	17.2(±2.0)	10.0(±0.0)	15.6(±0.5)	14.2(±2.7)	15.5(±9.0)	13.2(±4.0)	14.1(±4.0)	14.2(±1.5)
4	22.3(±2.0)	12.4(±4.3)	21.5(±2.3)	18.3(±9.1)	20.3(±4.2)	17.8(±2.6)	18.9(±4.5)	18.9(±2.2)
5	27.8(±3.5)	14.5(±5.0)	25.6(±1.5)	21.1(±4.0)	25.6(±2.3)	24.2(±3.3)	24.4(±2.5)	25.0(±1.4)
6	33.2(±4.5)	17.3(±3.0)	31.4(±2.5)	25.3(±1.0)	31.3(±3.4)	29.3(±2.2)	29.4(±0.8)	28.1(±6.0)
7	39.2(±5.5)	19.7(±5.4)	38.3(±2.3)	28.2(±8.9)	39.3(±7.1)	33.3(±1.9)	36.7(±6.5)	35.2(±3.5)
8	44.3(±7.5)	21.4(±3.0)	42.3(±0.3)	31.0(±0.9)	45.6(±7.0)	38.2(±9.0)	45.5(±7.3)	40.1(±6.8)

Figures in the brackets represent the standard deviation.

The Key:

W Weeks following inoculation.
C Control plants.
V1 *V. albo-atrum*, isolated from Alfaalf.
V2 *V. albo-atrum*, isolated from tomato.

Table-4: The disease symptoms index, of the cv of Alfalfa inoculated with *V. albo-atrum* isolates, V2 as resistance Alfalfa against V1 as challenger

W	Cultivar Euver				Cultivar Vela			
	C	V1	V2	V1+V2	C	V1	V2	V1+V2
1	0	0	0	0	0	0	0	0
2	0	0	0	0	0	0	0	0
3	0	5	0	5	0	0	0	0
4	0	20	0	10	0	0	0	0
5	0	35	0	15	0	0	0	0
6	0	45	0	25	0	0	0	0
7	0	55	0	35	0	0	0	0
8	0	75	0	50	0	0	0	0

V1 *V. albo-atrum Alfalfa* isolate.
V2 *V. albo-atrum*, tomato isolate.

Biological control is considered to be the best alternative to chemical methods of controlling *Verticillium* wilt diseaseof Alfalfa. Biological method comprises many aspects, such as, breeding of resistant cultivar to the diseases, and cross-protection.

Cross-protection, disease control method, by using an avirulent pathogen to the plant to induce resistant against a virulent pathogen is another method to tackle the problem. To use the cross-protection method to control wilt disease there are many problems. For example, [9] in his review about cross-protection mentioned the difficulties that faces the workers in cross-protection and the complexity of wilt pathogenesis made the research on cross-protection with the vascular wilt diseases mach less handy. [10] reported that an economical biological control will require extensive research. Despite this criticisms there are many workers who have studied cross protection as a biological method of control and the results they have found have proved to be very interesting, for example; [11], [12] and [13].

In order to investigate cross protection or induced resistance as a tool for biological control, or to find a new fungal product that will act to stimulate a natural disease-resistance mechanism. V2, the isolate of *V. albo-atrum,* non-pathogenic to the cultivars of Alfalfa was used in this study to induce resistance (The inducer), against isolate V1 (virulent to Alfalfa), (The challenger). To allow as comparison resistance induced in resistant and susceptible cultivars, two cultivars of Alfalfa were used, Euver (susceptible to isolate V1, resistant to isolate V2) and Vela (resistant to both isolates of *V. albo-atrum*). Both were inoculated simultaneously (Materials and Methods) with the two isolates of *V. albo-atrum,* V1 & V2, while control plants were inoculated with sterile distilled water. Inoculated plants were maintained in the greenhouse.

The results, show that the effect of simultaneous inoculation of the susceptible cultivar with the two isolates of V1 & V2 was increased resistance against V1. Growth of the inoculated- Alfalfa plants was increased compared to plants inoculated only with V1 and the severity of the wilt disease was reduced. There were no effects of simultaneous inoculation with the isolates on the resistant cultivar. These results are in agreement with those, [11], [14], [3], [4] and [15].

The results from the previous experiments confirmed the occurrence of induced resistance in Alfalf induced by V2 against V1. However, isolate V2 did not totally prevent isolate V1 from causing wilt disease in Alfalfa. Nor isolate V1 did totally prevent isolate V2 from causing wilt disease in tomato. From this it may be concluded that cross protection results from interaction or antagonisms at root surface and involve localized rather than systematically induced host responses, and this agree with [16]. This subject is need more study and work to prove and use the induce resistance as biological method to control plant pathogen.

REFERENCES

1. Page M. S., Gray F. A., Legg D. E. and Keral W. G., Economic impact and management of *Verticillium* wilt. Biol Abstr, 9795(1994).
2. Hillocks R. J., Cross-protection between strains of *Fusarium oxysporium*. F. sp. and its effect on vascular resistance mechanism *J. Phytopathology 117*: 216-225, (1986).
3. Matta A. and Garibaldi A., Control of *Verticillium* wilt in tomato by preinoculation with a virulent fungi.Nett j plant pathology 83(supp1), 457-462, (1977).
4. Price D. and Sackston W. E., Cross-protection against *Verticillium* in sunflower. *phytopathology 73*: 372-373, (1983).
5. Flood J., The role of phytoalexins in *Verticillium* wilt of lucerne. Ph.D thesis, Uni of Wales, (1980).
6. Dixon G. R. and Doodson J. K., Assessment keys for some disease of vegetable, fodder and herbage crops. *Journal of the National institute of Agricultural Botany. 12*: 299-307, (1971).
7. Latunde-Dada A. O. and Lucas J. A., Variation in resistance to *Verticillium* wilt with in seedling population of some varieties of lucerne *(Medicago sativa* L. *PLant pathology 31*: 179-186, (1982).
8. Esyanti R. R., A study of the factors affecting phytoalexin production in tissue of lucerne (*Medicago sativa* L.). Ph.d thesis to University of Wales, (1993).
9. Matta A., Induced resistance to *Fusarium* wilt disease NATO SAI series Vol 28, 175-195, (1989).
10. Adams P.B., The potential of Mycoparasites for biological control of plant diseases. *Annu. Rev. phytopathology 28*: 59-72, (1990).
11. Davis, D., Cross-protection in *Fusairum* wilt disease. *Phytopathology 57*: 311-314, (1967).
12. Davis D., Partial control of *Fusarum* wilt of tomato by formae *Fusarum oxysporium*. *Phytopathology 58*: 121-122, (1968).
13. Jorge P.E., Green J., and Chaney R., Inoculation with *Fusarium* and *Verticillium* to increase resistance in *Fusarium*-resistance Tomato *Plant disease 76*: 340-343, (1992)
14. Schnathorst W. C and Mathre D. E., Cross protection in cotton with strain of *Verticillium albo-atrum. Phytopatholgy. 56*: 1204-1208, (1966).
15. Price D. and Sackston W. E., Cross-protection among strains of *Verticillium dahliae* on sunflower. NATO ASI series Vol.H28, (1989).
16. Jorge P. E., Resistance induce in herbaceous and hardwood plant species by vascular wilt fungi. Ph.D thesis Faculty of Purdue University, (1990).
17. Hastie A. C. and Heale J. B., Genetic of *Verticillium* sp. *Phytopathology Medit 23*: 130-162, (1984).

Treatment of Tinea Capitis by *Calvatia Craniformis* Mushroom Powder

Ghassan H. Jameel
Dyala University, College od Education, Department of Biology

Received 20/2/2012 – Accepted 6/11/2012

الخلاصة

يعد داء القرع في فروة الرأس Tinea capitis أو داء السعفة من الأمراض الفطرية السطحية التي تتسبب بجنسين من الفطور *Trichophyton* و *Microsporum* ،إذ ينتقل المرض بواسطة الأشخاص المصابين والحيوانات والأدوات الملوثة التي تأوي الفطر المسبب. يتسبب هذان الجنسان بأحداث حكة شديدة في فروة الرأس مع قشور وبقع صلع وذلك لأن للفطر القدرة على اختراق الجلد.

أستخدم مسحوق احد فطور التربة النوع *Calvatia craniformis* بعد خلطه مع الفازلين في علاج داء السعفة التي تصيب الإنسان إذ أظهرت المركبات الكيماوية المتواجدة في هذا الفطر كفاءة عالية في القضاء على المسبب المرضي وكان واضحاً عند شفاء الآفة المرضية في وقت مقارب للفترة الزمنية لشفاء المرضى في مجموعة السيطرة.

ABSTRACT

Tinea capitis or scalp ringworm is a superficial fungal infection caused by *Trichophyton* and *Microsporum* genera . It is transmitted by humans, animals , or objects that harbor the fungus . The pathogenic fungus has rooted itself in the skin result in severe itching of the scalp , dandruff , and bald patches.

Powder of some soil fungi named *Calvatia craniformis* mushroom is used after mixing with Vaseline in treatment of tinea capitis in human being , so the chemical compounds which present in this mushroom reveals high efficiency in killing the causative agent of the disease. Both concentrations were showed excellent activity against the isolates and reveals clear improvement compared to control group.

Key words : tinea capitis , *Calvatia craniformis*.

INTRODUCTION

Tinea capitis or scalp ringworm is a superficial fungal infection (dermatophytosis) of the scalp. The disease is primarily caused by dermatophytes include *Trichophyton* and *Microsporum* genera that invade hair and skin [1] . The disease is infectious and can be transmitted by humans , animals , or objects that harbor the fungus [2].Disease manifestations range from small , scaling patches , to involvement of the entire scalp with extensive hair loss . The hair shafts can become invaded by *Microsporum* hyphae [3] . Common symptoms are severe itching of the scalp, dandruff, and bald patches where the fungus has rooted itself in the skin [4,5].There are three types of tinea capitis , microsporosis occurred by *Microsporum audouinii* , *M. canis*. The source of this fungus is typically sick cats and kittens . Trichophytosis is usually caused by *Trichophyton tonsurans* , *T.violaceum* . The third type called Favus , caused by *Trichophyton schoenlenii* [6,7].Abdel –Rahman etal.,[7] were be isolate the *Trichophyton rubrum* from tinea capitis lesion. *Trichophyton rubrum* is the main cause of tinea corporis or ringworm of trunk and extremities in human , transmitted by direct contact with infected animals and

humans or by indirect contact through contaminated instruments by the fungus [8] . The treatment of choice by dermatologist is a safe and inexpensive oral medication ,griseofulvin, a secondary metabolite of the fungus *Penicillium griseofulvin*. Other oral antifungal treatment for tinea capitis also frequently reported in literatures include terbinafine, itraconazole, and fluconazole; these drugs have the advantage of shorter treatment durations than griseofulvin [9] .

The mushroom used in this study is puffball mushroom, belongs to Basidiomycota division, Lycoperdaceae Family, *Calvatia* genus, *craniformis* species figure -(1),[10] .

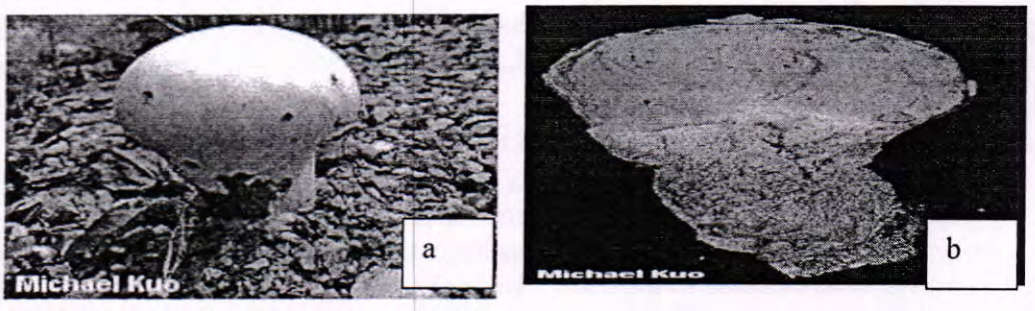

Figure-1:a: represent the mushroom in the world.
b : represent the longitudinal section .

The study aims to evaluate the efficiency of the ointment prepared from *Calvatia craniformis* mushroom powder in treatment of tinea capitis in topical using.

MATERIALS AND METHODS

1. Preparation of a topical antifungal agent .

a. Fruiting body is dried completely and crushed in sterile Petri dish to obtain a yellow-brown powder .

b. By using a balance Weight , two weights (1,2 gm) each one singly alone .

c. Each weight is completed to 100 gm of Vaseline to reach 1% and 2% concentration .

2.The patients:

The diagnosis of the disease depends upon the clinical symptoms which is include the shape and position of the lesion , and confirmed by microscopic examination using 10% KOH examination .The number of patients is forty, their ages are from (6-30) years, but the most are between (6-10) years, the infection is more common in males than females. All cases were admitted dermatology clinic in Baquba city during the period between June 2010 to June 2011.

The patients are divided into two groups ; the first is treatment group includes twenty patients , is divided to two subgroup, in each subgroup

10 patients. The first subgroup are treated by 1% concentration, and second subgroup are treated by 2% concentration topically once daily with cleaning the infected patches by soapy water after 24 hours and before the last treatment ; the duration of therapy is two months. While the control group which is include twenty patients treated by oral administration of griseofulvin at a dose10 mg/kg. Bwt. daily for two months for pediatrics and 20 mg /kg.Bwt. daily for adult .

Figure (2) represents the discovered mushroom in Jadidat Al-Shat Village in Hibhib city and Bany Saad city-Diyala province for first time in Iraq according to the diagnosis of laboratory of fungus researches and plant diseases in the college of Agriculture-Baghdad University with certification of professor Kamil Salman Jabor as a taxonomist.

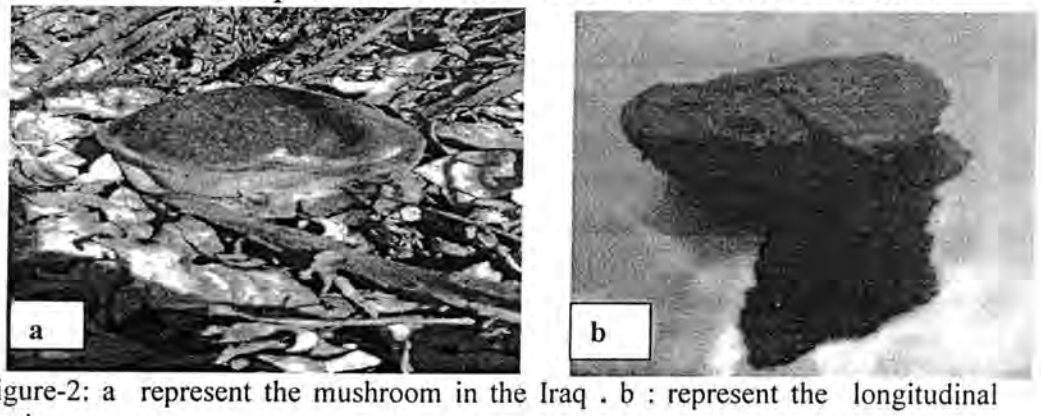

Figure-2: a represent the mushroom in the Iraq . b : represent the longitudinal section .

The Statistical analysis

The differences were compared by using (F- test) at $p< 0.05$ [10] .

RESULTS AND DISCUSSION

Sixteen patients are responses to ointment but in different period of time between (38-50) days ; less time of clearance was be in adult and the long time was be in children mostly and, this is due to the weakness of their immune system which is in development stage[11] . The hair growth occurs after thirty days from treatment start , and the figure (3) represent the treated child by our preparation.

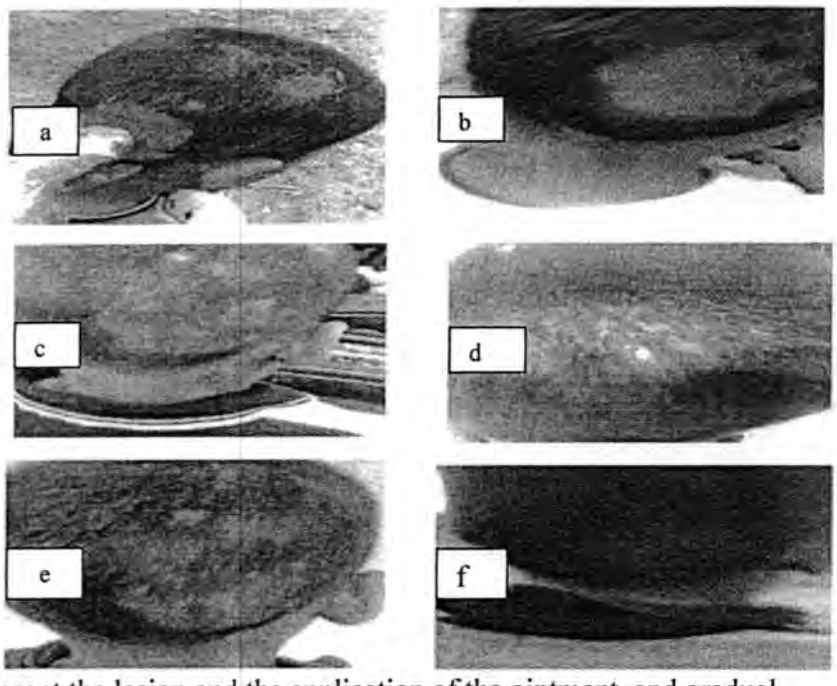

Figure-3: Represent the lesion and the application of the ointment ,and gradual improvement of the lesion.

Four patients are dropped from the study for unknown reasons , while the control group fourteen patients were completed the treatment course and six patients are considered as defaulter .

Table-1: Represent the response of the patients to different concentrations of the ointment .

Patients group	The number of real treated	Ointment concentration %	Period of clearance
Treated -10	7	1	49 days
Treated -10	9	2	38 days
Control -20	14	Oral administration of griseofulvin	40 days

($p < 0.05$)

These result are reflects the medical importance of the *Calvatia craniformis* mushroom powder after dissolving it's components by Vaseline for first time to make it ointment. Gupta and Cooper ,[12] illustrates the action of topical antifungal infection by , the method allows the drug to penetrate the hair shaft where the fungus lives. This illustration didn't identify with Grace , [13] who is mention about the topical treatment of tinea capitis alone is ineffective and is not recommended , but he is prefer using of selenium sulfide shampoo to reduce the risk of spreading the infection early in the course of

griseofulvin therapy by reducing the number of viable spores that are shed ,and this already consider as topical treatment.

The medical analysis of the powder of mushroom proved the presence of three components; the first is calvatic acid which has chemical formation P-carboxyphenyl-azoxycarbonitrile [14]. This calvatic acid reveals strong action against the yeast and fungi like *Saccharomyces cerevisiae* and some *Candida* species and *Trichophyton asteroids* [15] .

The second components from chemical analysis and spectroscopic means of the mushroom powder is hydroxyphenylazoformamide derivatives which has three chemical compounds, 4-hydroxyphenyl-1azoformamid, 4-hydroxyphenyl-ONN-azoformamid and 2-methylsulfonyl-4-hydroxy-6-methylthiophenyl-1-azoformamid, it is known craniformin (phenolic tautomer of rubroflavin), and also three components are known steroids, ergosta-4,6,8 (14), 22-tetraene- 3-one, ergosta-7,22-diene-3-01 and ergosterol peroxide [16] .

The hydroxyphenylazoformamide derivatives or craniformin have phenolics in its formation which are endowed with interesting biological activities as a broad spectrum bactericidal and fungicidal effect represented by *Candida albicans, Aspergillus niger* [17]. Also the craniformin has azol compound which inhibit the synthesis of ergosterol by blocking the action of 14-alpha-demethylase and stop proliferation of the fungus [18] . The action of azol compounds reveals inhibition fungal mRNA transcription [19].While steroid compounds, and these are lipophilic and facilitates entry into the cells, also the specific binding proteins which are present in any animal cells may facilitate steroids entry into target tissues [20].

Also the chemical analysis of mushroom powder which is done in White Fields Company for Chemical and Engineering Studies and Consultations in Baghdad – Iraq proved the presence of different materials as β-glucans, ergothioneine and gallic acid. β- glucans are polymers of β- (1,3)-D -glucose (with or without β-(1,6)-D-glucose side chains) found in the cell walls of many bacteria ,plants and yeasts [21] .β- glucan bind to glucan receptors on phagocytic cells [22] ,and cause these cells to become "activated " [23] .Other material is ergothioneine (ET) which is an unusual sulfur-containing derivative of the amino acid, histidine. It may be represent a new vitamin whose physiologic roles include antioxidant cytoprotectant [24] .

The last material termed gallic acid ; it is a trihydroxybenzoic acid, a type of phenolic acid. Gallic acid is found both free and as part of tannins . Gallic acid seems to have anti-fungal and anti-viral properties. Gallic acid act as an antioxidant and help to protect human cells against oxidative damage [25] .

β-glucans ,ergothioneine and gallic acid are displaying immunological , antimicrobial and physiologic cytoprotection effect respectively. These effects may be led to enhance the immunity of patients especially a young ,and improve the infected tissue status. The results are coming in agreement with Ghosh [26], who is elicits many essential amino acids and vitamins like A,D,C,K and B-complex from *Calvatia craniformis* mushroom.

These objectives are essential to the repair or healing of infected epidermis and the disappearance of the lesion , for example the figure (4) represents my published research in treatment ringworm in cattle by same preparation in
different concentration and was gave good results.

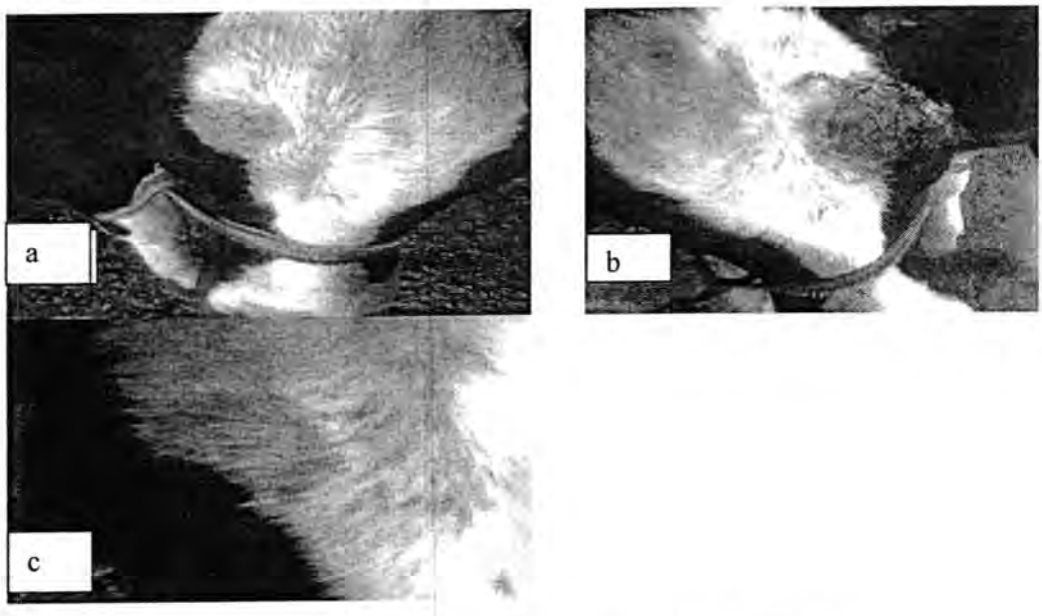

Figure-4: a: represent the lesion before the application of the ointment.
b:represent the lesion and the application of the ointment.
c:represent the clearance of the lesion and hair growth.

REFERENCES

a. James, W.D; Berger, T.G and Odom, R.B. Andrew's Disease of the skin : Clinical Dermatology. Saunders Elsevier. ISBN: 7216 – 2921,(2006).
2. Freedberg, I.M and Fitzpatrick, T.B. Fitzpatrick's Dermatology in General Medicine. New York : Mc Graw - Hill , Medical Pub. Division. p.645. ISBN, 0 -07.138076,(2003).
3. Weller, R.; Hunter, J. ; Savin, J. and Dahh, M. Clinical Dermatology. 4th. ed . Blackwell science . for Ruth . Patricia and Arlene,(2008) .

4. Degreef, H. "Clinical forms of dermatophytosis (ringworm infection)" . *Mycopathologia 166(5-6) : 257-265,* (2008) .
5. Hunter, J.A. ; Savin, J.A. and Dahi, .M.V.Clinical Dermatology. 3rd. ed. Blackwell Science .for Ruth .Patricia and Arlene,(2002).
6. Ali, S.; Graham, T.A. and Forgie, S.E. " The assessment and management of tinea capitis in children " . *Pediatric Emergency care 23 (9) :662 –665,*(2007).
7. Harvey, R.A.; Champe, P.C and Fisher, B.D. Cutaneous Mycosis . Tinea capitis (Scalp ringworm): Lippincott's Illustrated Reviews Microbiology . 2nd. ed . pp :206-207 ,(2007).
8. Abdel -Rahman, S.M; Penny, J. and Alaxnder, S.W. *Trichophyton rubrum* ,tinea capitis in a young child .*Pediatr. Dermatol; 21(1) :63- 65,*(2004) .
9. Gupta, A.K and Summerbell, R.C."Tinea capitis" Medical Mycology :Official Publication of the international Society for Human and Animal Mycology 38(4):255-87,(2000).
10. Zar, J.H. Biostatistical analysis, 2nd. ed., prentice Hall Inc., Englewood, N.J. ,(2000).
11. Kezeer, E. G. Incidence of dermatophytosis among children. *Journal of AL -buhooth AL- tachanyia , Baghdad , (3);40 – 44,*(2002).
12. Gupta, A.K and Cooper, E.A. Update in antifungal therapy of dermatophytosis . *Mycopathologia 166(5-6)-67,* (2008).
13. Grace, F.K. Tinea Capitis Treatment and Management. American Academy of Dermatology. Veterans Affairs Maryland Healthcare System, Baltimore, (2009).
14. Okuda, T and Fujiwara, A. Calvatic acid and product by the Lycoperdeceae 2. Distribution among the Gasteromycetes *Trans. mycol.Soc .Jpn-23.235-239* , (1982).
15. Hamao, U.; Tomio, T. Hironobu, L. and Osamu, T. Production of a new antibiotic, calvatic acid . Assignee: Zaidan, Hojin Biseibutsu Kagaku Kenkya Kai (Tokyo, JA),(1976).
16. Takaishi ,Y., M. Murakami , T. Uda , M. Ohashi, K. Hamamura , and S .Kadota. Hydroxyphenylazoformamide derivates From *Calvatia craniformis* .Faculty of pharmaceutical Sciences , University of Tokushima , 1-78 Shomachi , Tokushima, 770,Japan, (1998).
17. Bouaziz, M.; Lassoued, S.; Bouallagui, Z.; Smaoui, S.; Gargoubi, A.; Dhouib, A. and Sayadi, S. Synthesis recovery of high bioactive phenolics from table- olive brine process wastewater. *Bioorg . Med .Chem.; 1,(20):9238-46,* (2008).
18. Lewis, R.E. Managing drug interactions in the patients with aspergillosis. Medical Mycology. 4, (1); PP- 349-356,(2006).

19. Wobbe, R.C.; Bradley, J.D. and Li, Z. Antifungal agents-United States Patent 6165998. Scriptgen Pharmaceuticals, Inc. (Waltham, MA), (2000).
20. Jhonson, M. and Eviritt, B. Essential Reproduction of Fungi. Blackwell Publications, Oxford,(1980).
21. Hunter, K.W.; Gault, R.A. and Berner, M.D..Preparation of microparticulate β-glucan from *Saccharomyces cerevisiae* for use in immune potentiating. Letters in Applied Microbiology 35,267-271, 2002). (
22. Brown, G.D and Gordon, S. A new receptor for β-glucans. *Nature, 413:36-37,PP,* (2001).
23. Diluzio, N.R. Immunopharmacology of glucan: a broad spectrum enhancer of host defense mechanisms. Trends in pharmacological science 4,344-25,(1983).
24. Paul, B.D. and Snyder, S.H. The unusual amino acid L-ergothioneine is a physiologic cytoprotectant . *Cell Death and Differentiation 17,1134-1140,* (2010).
25. Jeremy, D.K. and Nuansri, R. Antimicrobial gallic acid from *Caesalpinia mimosoides* Lamk. *Food Chemistry, V(100) ,Issue 3:1044-1048, P,P,*(2007).
26. Ghosh, D.2004. Algae and fungi as food. *Resonance, 9(4). 2004.*

Bacteriological study of Septicemia in Neonate at Baghdad pediatric hospitals

Waseem Faeq Mohammed[1], Rajwa H. Essa[2], Rabab Q. AL-segar[2]
[1,2]Department of Biology -College of Science/ Al-Mustansiriyah University.
[3]Department of Bacteriology /Central Public Health Laboratory.

Received 22/3/2012 – Accepted 20/6/2012

الخلاصة

جمعت عينات الدم من مائة مريض بعمر (1- 28) يـوم بعد ان شخصت حالة المرضى سريرياً من قبل أطباء الاطفال فـي مستشفيات بغداد للأطفال (مستشفى الطفل المركزي التعليمي، م. ابن البلدي للاطفال، م. العلوية التعليمي للاطفال، مستشفى حماية الطفل التعليمي) للفترة من تشرين الاول 2010 الى اب 2011. أظهرت النتائج 34٪ مـن الحالات ذات نتيجة موجبة لزرع الدم بينما 66٪ كانت سلبية (لم تعطي اي نمو بكتيري) اما من ناحية الجنس فكانت النسبة 61.76٪ مـن الذكور و 38.24٪ من الإناث من بين الحالات الايجابية اي ان نسبة الذكور هي الاعلى. توزعت الحالات الـى الإنتان المتأخر لحديثي الولادة Late onset neonatal sepsis (LONS) وكانت النسبة 70.59٪ بينما الحالة الاخرى هيه الإنتان المبكر لحديثي الولادة Early onset neonatal sepsis (EONS) وكانت النسبة 29.41٪ وبـذلك كانت نسبة الإنتان المتأخر لحديثي الولادة اعلى مـن نسبة الإنتان المبكر لحديثي الولادة. لوحظ مـن النتائج ذات النتيجة الموجبة لزرع الدم بان 58.82٪ مـن الحالات كانت تعود الـى أطفال حديثي الولادة ذوي الوزن الواطئ و 41.18٪ تعود الى أطفال حديثي الولادة ذوي الوزن الطبيعي لذلك تكون نسبة تجرثم الدم في أطفال حديثي الولادة ذوي الاوزان الواطئ اعلى مـن نسبتها في الاوزان الطبيعية. كـذلك لـوحظ ان نسبة الاصابة فـي الاطفال حديثي الولادة في حالة مدة الحمل غير الكاملة (اقل من 36 اسبوع) و هي 64.70٪ اكثر من نسبة الاصابة فـي الاطفال حديثي الولادة في حالة مدة الحمل الكاملة 35،30٪. عـزلت البكتريا وشخصت باستعمال الاوساط الزرعية وبعض الاختبارات فضلاً عن تأكيد التشخيص باستعمال نظام API. عزلات البكتريا الموجبة لكرام كـانت بـالنسب التالية *Staphylococcus aureus* (17.64%) *Staphylococcus epidermidis* (14.71%), *Staphylococcus capitis* (11.76%) , *Staphylococcus hominis* (5.88%), *Staphylococcus xylosus* (2.94%), بينما كانت البكتريا السالبة لكرام بالنسب :

Escherichia coli (11.76%), *Enterobacter cloacae* (8.82%) *Klebsiella pneumoniae* (8.82%), *Pseudomonas aeruginosa* (5.88%), *Pasteurella* spp (5.88%), *Burkholderia cepacia* (2.95%), *Serratia marcescens* (2.95%). تم عزل بكتريا *Burkholderia cepacia* لاول مرة في اطفال حديثي الولادة مصابين بتجرثم الدم في بغداد حسب معلوماتنا عن الموضوع. وتم التحري عن حساسية المضادات الحيوية وفق طـريقة Kirby-Bauer ومن ثم تم تحديد مناطق التثبيط حسب CLSI (2011) حيث كـانت مقاومة *Staphylococcus spp* للاوكساسيلين أعلى من أنواع أخرى مـن المضادات الحيوية مثـل جنتاميسين في حين ان كل العزلات كانت حساسة للفانكومايسين. و العائلة المعوية (*E coli, Enterobacter cloacae, Klebsiella pneumonia Serratia marcescens*) اظهرت مقاومة للأمبيسيلين و سفازولين و سيفو تاكسيم ولم تبدي اي مقـاومة الى اميبينم والاميكاسين. وكانت *Pasteurella spp* حساسية لمعظم المضادات الحيوية ما عدا بيبيراسيلين و بيبيراسلين / تازوبكتام اما بكتريا *Pseudomonas aeruginosa* كانت حساسة للسيفتازيديم و اميبينم والاميكاسين بينما نصف عزلاتها مقاومة للبيبيراسيلين، بيبيراسلين / تازوبكتام و جنتاميسين وسيبروفلوكساسين. امـا بكتريا *Burkholderia cepacia* فكانت حساسة للسيفتازيديم واميبينم و مقاومة للتريميثوبريم، سلفاميثوكسازول، جنتاميسين، كلورامفنيكول.

ABSTRACT

A total of hundred patients of neonate below twenty eight days which Suspected have septicemia, clinically diagnosed by pediatric physicians in Baghdad pediatric hospitals from Oct 2010 to Aug 2011. The results have revealed that 34 % gave blood culture positive whereas 66 % gave no growth. among 34 positive blood culture cases 61.76% were males and 38.24% were females so males were higher number in compared to females, 70.59% belonged to late onset neonatal sepsis (LONS) and 29.41% belonged to early onset neonatal sepsis (EONS). So the incidence was higher in LONS than EONS. 58.82% were of low birth weight (LBW) and 41.18% were of normal birth weight (NBW) so the incidence of neonatal septicemia was higher in LBW neonates compared to NBW. 64.70% preterm and 35.30%

were term. The incidence of preterm neonates was higher compared with term neonates. Bacteria were isolated and diagnosed by using culture media some biochemical tests then identified by Analytic Profile Index (API) system. The Gram positive isolates were *Staphylococcus aureus* (17.64%), *Staphylococcus epidermidis* (14.71%), *Staphylococcus capitis* (11.76%), *Staphylococcus hominis* (5.88%) and *Staphylococcus xylosus* (2.94%). While Gram-negative bacteria were *Escherichia coli* (11.76%), *Enterobacter cloacae* (8.82%), *Klebsiella pneumoniae* (8.82%), *Pseudomonas aeruginosa* (5.88%), *Pasteurella spp* (5.88%), *Burkholderia cepacia* (2.95%), *Serratia marcescens* (2.95%). *Burkholderia cepacia* is isolated from NNS for the first time in Baghdad accordingly to our information subject. Antibiotic sensitivity was detected by using Kirby-Bauer Method and the zones of inhibition determined by CLSI 2011.). *Staphylococcus spp.* resist to Oxacillin were higher than Gentamicin. While all strain were sensitive to Vancomycin. Enterobacteriaceae (*Escherichia coli, Enterobacter cloacae, Klebsiella pneumonia* and *Serratia marcescens*) showed remarkable resistancy to Ampicillin (AMP), Cefazolin (CZ) and Cefotaxime (CTX) while no resistancy to Imipenem (IMP) and Amikacin(AK). *Pasteurella spp* were sensitive to most antibiotics. *Pseudomonas aeruginosa* were sensitive to CAZ, IMP and AK while half of isolate resist Piperacillin, PIT, GEN and CIP. *Burkholderia cepacia* were sensitive to CAZ, IMP and resist to Trimethoprim-sulfamethoxazole, GEN and Chloramphinicol.

Key words septicemia, neonates, Neonatal sepsis NNS, late onset neonatal sepsis (LONS) early onset neonatal sepsis (EONS).

INTRODUCTION

The term neonatal septicemia refers to circulation and multiplication of infecting bacteria with their toxic products in new born within twenty-eight days of birth, the term neonatal septicemia is synonymous with neonatal sepsis [1]. Neonatal sepsis can be categorized as early and late onset. Early onset neonatal sepsis (EONS) presents within the first 72 hours of new born acquisition from the mother via transplacental infection or an ascending infection and Late onset neonatal sepsis (LONS) occurs at 4-28 days of life and is acquired from the care unit [2]. In Baghdad Central Teaching Hospital for Children in Baghdad in 1998-1999 the EONS were *Klebsiella* (33%), *Escherichia coli* (22%), GBS (33.3%), *Staphylococcus aureus* (11.1%), and none of *Staphylococcus epidermidis* or *Enterobacter* . while LONS were *Klebsiella Pneumonia* (28.5%), *E. coli* (19.1%), *Staphylococcus aureus* (19.1%), *Enterobacter* (19.1%), *Staphylococcus epidermidis* (9.4%) and GBS (4.7%) [3]. In Mosul from 2004-2005 Coagulase negative staphylococcal 50%, *Staphylococcus aureus* 18%, *Enterobacter Cloacae* 8%, *Klebsiella Pneumonia* 7%, *E. coli* 6%, *Pseudomonas aeruginosa* 5%, *Pasteurella haemolytica* 1%, *serratia marcescens* 1% [4].

In the United States and Canada the current approach to the treatment of early-onset neonatal sepsis syndrome includes combined intravenous aminoglycoside and expanded-spectrum penicillin antibiotic therapy. This provides coverage for gram-positive and gram-negative bacteria [5]. If an infection appears to be nosocomial (late-onset sepsis) the antibiotic coverage should be directed at microorganisms implicated in hospital-acquired infections including *Staphylococcus aureus, S epidermidis, and Pseudomonas* species. Strains of *S aureus* which resistant to most β-lactam antibiotics

(penicillin G, ampicillin, carbenicillin, ticarcillin and oxacillin), Vancomycin has been favored for this coverage, concern exists that over use of this drug may lead to vancomycin-resistant microorganisms; treat eliminating the best response to these resistant microorganisms. Oxacillin therapy is preferred by some clinicians because of this [6].

MATERIALS AND METHODS

Collection of specimens had been taken from hundred patients of neonate below twenty eight days which Suspected have septicemia, clinically diagnosed by pediatric physicians in Baghdad pediatric hospitals before antibiotic therapy at a period from Oct 2010 to Aug 2011. Isolation and identification of common Gram-positive and Gram-negative aerobic bacteria of the causative neonatal septicemia diagnostic procedures are used which recommended by [7-8].

Specimens of The blood sample inoculated into sterilized Brain heart infusion broth (BHIB) bottle (20ml) then putted in incubator for 24 hours at 37°C which used as enrich media for aerobic culture then pull 0.5 ml from BHIB by used syringe through rubber cap then a few drops putted on blood agar plate, chocolate agar plate and MacConkey agar plate. All plates were make isolated streaking then incubated for 24 hours at 37°C after that studied the colonial morphology and examined of microscopically by using Gram's stain technique for the different colonies then made some biochemical tests (Catalase test used for Gram-positive bacteria, Oxidase test used for Gram-negative bacteria, Coagulase test used for *staphylococcus spp*). Confirm identification by using analytic profile index (API) system as follows: API Staph is a standardized system for the identification of the genera *Stphylococcus spp.* API 20 E is a standardized identification system for Enterobacteriaceae (*Escherichia coli, Enterobacter cloacae, Klebsiella pneumonia and Serratia marcescens*). API 20 NE is a standardized system for the identification of non-fastidious, non-enteric, Gram-negative rods (*Pseudomonas aeruginosa, Burkholderia cepacia, Pasteurella spp*). Antibiotic sensitivity was detected by using Kirby-Bauer Method [9] and the zones of inhibition determined by CLSI (2011).

RESULTS AND DISCUSSION

Neonatal septicemia were constituted 34 from a total of 100 patients. 61.76% were males and 38.24% were females so males were higher in number compared to females, these findings are in agreement with Mosayebi *et al.*, (2003) . The usual male predominance in neonatal septicemia has suggested the possibility of a sex-linked factor in host susceptibility, a gene located in X chromosome and involved with function of the thymus or with synthesis of immunoglobulins has been postured so the female has double the number of genes affecting these factors and thus might possess a greater resistance to infection [12]. EONS (29.41%) were lower than LONS (70.59%) Which is in agreement with the reports from other countries [13]. The most common cause

of LONS is nosocomial infection as a complication of neonatal intensive care [14]. The incidence of neonatal septicemia was higher in LBW neonates (58.82%) compared to NBW (41.18%) and also higher in preterm of NNS (64.70%) compared to term of NNS (35.30%). Similar reports in incidence of have been made by other worker [15-16]. The low birth weight and preterm of neonates is a greater risk for infection than the normal birth weight and term because generally require longer hospital stays and more medical procedures and both of which increase their risk for late-onset neonatal sepsis, preterm newborn have less developed immune systems which specially Immunoglobulin type IgG incomplete placental transfer and concentrations decreased and Complement Decreased concentration [17].

BACTERIAL ISOLATES

Gram-positive aerobic bacterial isolates appeared to be predominant type according to the results (52.94%) when compared to Gram-negative aerobic bacteria (47.06%) cases as showed in figure 1. These results were agree with Graham *et al* (2006). Types and frequencies of bacteria isolated from NNS cases which in relation to early and late onset of NNS and the number of death shown in Table 1. Gram-positive were *Staphylococcus aureus* (17.64 %), *Staphylococcus epidermidis* (14.71%), *Staphylococcus capitis* (11.76%), *Staphylococcus hominis* (5.88%), *Staphylococcus xylosus* (2.94%). and Gram-negative were *Escherichia coli* (11.76%), *Enterobacter cloacae* (8.82%), *Klebsiella pneumoniae* (8.82%), *Pseudomonas aeruginosa* (5.88%), *Pasteurella spp* (5.88%), *Burkholderia cepacia* (2.95%), *Serratia marcescens* (2.95%).

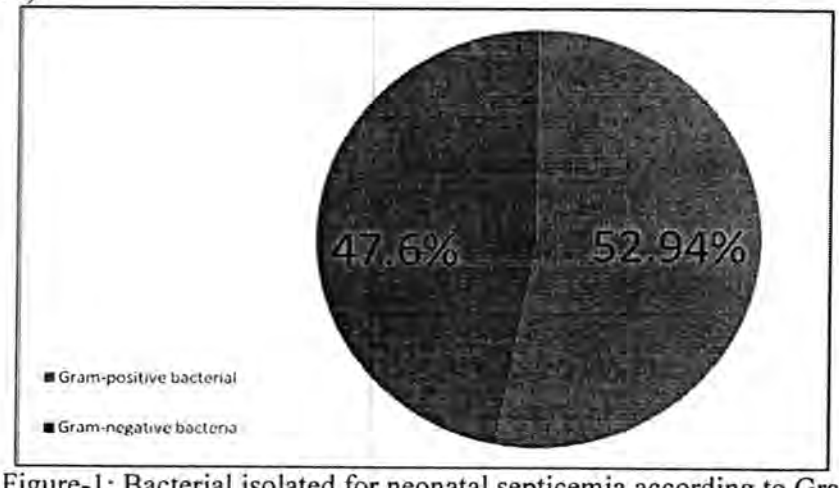

Figure-1: Bacterial isolated for neonatal septicemia according to Gram staining.

Table-1: Type and frequencies of bacteria responsible for (EONS) and (LONS) of NNS and number of death.

Type of bacteria			EONS		LONS		Total		
			NO.	(%)	NO	(%)	NO.	(%)	NO. of Death
Gram positive bacteria	Coagulase Negative *Staphylococcal* (CONS) *group*		3	8.82	9	26.50	12	35.32	0
	I	*Staphylococcus epidermidis*	1	2.95	4	11.76	5	14.70	0
	II	*Staphylococcus capitis*	1	2.95	3	8.82	4	11.76	0
	III	*Staphylococcus hominis*	1	2.95	1	2.95	2	5.88	0
	IV	*Staphylococcus xylosus*	0	0.00	1	2.95	1	2.95	0
	Coagulase positive *Staphylococcal* (COPS) *group* 1- *Staphylococcus aureus*		1	2.95	5	14.70	6	17.64	0
Gram negative bacteria	*Escherichia coli*		3	8.82	1	2.95	4	11.76	0
	Enterobacter cloacae		1	2.95	2	5.88	3	8.82	0
	Klebsiella pneumoniae		1	2.95	2	5.88	3	8.82	0
	Pseudomonas aeruginosa		1	2.95	1	2.95	2	5.88	1
	Pasteurella spp		0	0.00	2	5.88	2	5.88	0
	Burkholderia cepacia		0	0.00	1	2.95	1	2.95	0
	Serratia marcescens		0	0.00	1	2.95	1	2.95	0
Total			10	29.41	24	70.59	34	100	1

ANTIBIOTIC SUSCEPTIBILITIES

Table (2) shows the effect of some antibiotic on the isolates bacteria. According to recommendation of Central Public Health Laboratory to laboratories of Iraq's hospitals and CLSI 2011 [10] the aerobic bacteria isolates divided in groups and genus then select antibiotic for each one of group or genus, the isolates of NSS includes: **Enterobacteriaceae** (*Escherichia coli*, *Enterobacter cloacae*, *Klebsiella pneumonia* and *Serratia marcescens*) these isolates were resist to Ampicillin (AMP), Piperacillin/Tazobactamfrom (PIT), Cefazolin (CZ) and Cefotaxime (CTX) while no resistancy to Imipenem(IMP) and Amikacin(AK) was showed, *E coli* resists to ceftazidime(CAZ), all tested strain of Enterobacteriaceae were sensitive to GEN except *Enterobacter cloacae* resist and CIP was effective against all isolated strain except *Klebsiella pneumoniae* which showed resistance percentage 66%. *Serratia marcescens* was sensitive to most antibiotics except ampicillin and cefazolin. Our findings are similar to other studies display low resist percentage or none to IMP and Ak was low resistance than GEN [19-20] . ***Staphylococcus spp*** Resist to Penicillin and Oxacillin higher than other class of antibiotics including: Chloramphinicol, Ciprofloxacin and Gentamicin. While no resist to Vancomycin. These finding were agreed with Al-Hama wandi J. A., (2005); Al-Talib H. I. (2006). ***Pseudomonas aeruginosa*** was sensitive to Ceftazidime, Imipenem and Amikacin while half of isolate were resist to Piperacillin, Piperacillin/Tazobactam, Gentamicin and Ciprofloxacin. These results are

agreed with Darmstadt *et al.*, (2009). ***Burkholderia cepacia*** were sensitive to Ceftazidime, Imipenem while resist to Trimethoprim-sulfamethoxazole, Gentamicin and Chloramphinicol These results are agreed with Darmstadt *et al.*, (2009). ***Pasteurella spp.*** *Pasteurella spp* were sensitive to most antibiotics except Piperacillin 50% and Piperacillin/Tazobactam 50%.

Table-2: Antibiotic susceptibilities of gram-positive and gram-negative aerobic bacteria.

Antibiotics	Resistant percentages of isolates							
	Escherichia coli	*Enterobacter cloacae*	*Klebsiella pneumonia*	*Serratia marcescens*	*Staphylococcus aureus*	*Pseudomonas aeruginosa*	*Burkholderia cepacia*	*Pasteurella spp*
Amikacin (AK) 30µg	0	0	0	0		0		0
Amoxycillin/Clavulanicacid (AMC) 20/10 µg (30µg)					83			
Ampicillin (AMP) 10µg	100	100	100	100				
Cefazolin (CZ) 30 µg	75	66	66	100				
Cefotaxime (CTX) 30 µg	50	66	66	0	83			
Ceftazidime (CAZ) 30 µg	50	0	0	0		0	0	0
Chloramphinical (C) 30 µg					50		100	
Ciprofloxacin (CIP) 5µg	0	0	66	0	33	50		0
Gentamycin (GEN) 10 µg	0	66	0	0	0	50	100	0
Imipenem (IMP)10 µg	0	0	0	0	66	0	0	0
Oxacillin (OX) 1 µg					83			
Pencillin G (P) 10 units					100			
Piperacillin (PI) 100 µg						50		50
Peperacillin/Tazobactam (PIT) 100/10 µg	75	100	100	0		50		50
Trimethoprim-sulfamethoxazole (COT) 1.25/23.75 µg							100	
Vancomycin (VA) 30 µg					0			

REFERENCES

1. Nimboor K. Bacteriological (aerobic) study of neonatal septicemia in NICU. Department microbiology Mahadev Appa Rampure medical College, Gulbarga, Karnataka (2006).
2. Klinger G.; Levy I.; Sirota L.; Boyko V.; Reichman B. and Lerner L.
3. Epidemiology and risk factors for early onset sepsis among very-low-birthweight infants. Am J Obstet Gynecol. 201(1): 38-46. (2009).
4. Al-Gabban N. I.; Said N. I. and Al-Ani W. A. Neonatal septicemia Iraqi J.comm. Med. 14 (1): 7-9. (2001).
5. AL-Talib H. I. A bacteriological study in early and late onset neonatal sepsis. college of medicine university of Mosul. (2006).

6. Lin F. Y.; Weisman L. E. and Azimi P. Assessment of Intrapartum Antibiotic Prophylaxis for the Prevention of Early-onset Group B Streptococcal Disease. Pediatr Infect Dis J. 30(9): 759-763. (2011).
7. Graham P. L.; Begg M. D. and Larson E. Risk factors for late onset gram-negative sepsis in low birth weight infants hospitalized in the neonatal intensive care unit. Pediatr Infect Dis J. 25(2): 113-117. (2006).
8. Forbes B. A.; Sahm D. F. and Weissfeld A. S. Bailey &Scott's Diagnostic Microbiology, 12thedition. Mosby, U.S.A. (2007).
9. MacFaddin J. F. Biochemical tests for identification of Medical bacteria. Lippincott Williams and wilkins. New York. 214-289. (2000).
10. Bauer A.W.; Kirby W. M. M.; Sherris J. C. and Truck M. Antibiotic susceptibility testing by a standarized single disk method. Am. J.Clin. Path, 43: 493-496. (1966).
11. Franklin R.; Matthew A.; Karen B.; Michael N. George M.; Dwight J. et al., Performance Standards for Antimicrobial Susceptibility Testing; Twenty-First Information Supplement. Clinical and laboratory standards institute (CLSI) (sl. Vol. 31 (1). (2011). Mosayebi Z.; Movahedian A. H. and Moniri R. Profile of Bactrial Sepsis in Neonates from Kashan in Iran. J. Infect. Dis. Antimicrob. Agents. 20:97-102. (2003).
12. Estripeaut D. and Saez-Liorens X. Perinatal bacterial diseases In: Feigin R. D., Chery J. D., Demmler G. J. and Kaplan S. L. Textbook of Pediatric Infectious Diseases, 5th ed. Philadelphia: Saunders, chapter p. 930. (2004).
13. Misallati A.; El-Bargathy S. and Shembesh N. Blood-culture- proven neonatal septicaemia: a review of 36 cases. East Mediterranean Health J. 6(2/3): 483-486. (2000).
14. Fellman V.; Hellstrom-Westas L.; Norman M.; Westgren M. and Kallen K. One- year survival of extremely preterm infants after active perinatal care in Sweden. JAMA. 301: 2225-2233. (2009).
15. Cohen-Wolkowiez M.; Moran C.; Benjamin D. K.; Cotton C. M.; Clark R. H. and Smith P. B. Early and late onset sepsis in late preterm infants. The pediatric infectious disease journal. 28(12): 1052-1056. (2009).
16. Khinchi Y. R.; Kumar A. and Satish Y. Profile of neonatal sepsis. Journal of college of medical sciences-nepal. 6 (2): 1-6. (2010).
17. McKenney W. M. Understanding the neonatal immune system: high risk for infection. Critical Care Nurse. 21(6): 35-47. (2001).
18. Al-hama wandi J. A. (2005). Bacteriological and Immunological Study on infants pneumonia at Babylon Governorate. College of Science Al-Mustansiriya university.
19. Lee N.; Chen S.; Tang R. and Hwang B. (2004). Neonatal bacteremia in a neonatal intensive care unit: analysis of causative organisms and antimicrobial. J. chin. Med. Assoc. 67: 15-20.
20. Seyyed Mohammad H. A.; Azar D. K.; Masood D.; Farshid K.; Seyyed M. M. and Mohammad R. A. Identification of bacterial agents and

antimicrobial susceptibility of neonatal sepsis: A 54-month study in a tertiary hospital. African Journal of Microbiology Research. 5(5): 528-531(2011).

21. Darmstadt G. L.; Saha S. K. and Choi Y. Population-Based Incidence and Etiology of Community-Acquired Neonatal Bacteremia in Mirzapur, Bangladesh: An Observational Study. J Infect Dis. 200(6) : 906–915(2009).

Pictorial Key to Apterous Aphids Species (Homoptera: Aphididae, Aphidinae) Infested Grasses (Gramineae) from Several Provinces of Iraq

Hayder B. Ali[1] and Nassreen N. Mzhr[2]
[1]Baghdad University/College of science/Department of Biology
[2]Al-Mustansiriyah university / college of science/Department of Biology
E mail: hayder.ali1130@yahoo.com

Received 25/10/2011 – Accepted 28/4/2012

الخلاصة

اعتمدت هذه الدراسة على جمع وتعيين انواع من النجيليات من عدة محافظات عراقية، سجلت سبعة انواع من المن تعود الى العويلة (Aphidinea) الانواع هي: ***Hyalopterus pruni*** (Geoffroy, 1762), ***Melanaphis donacis*** (Passerini, 1862), ***M. sacchari*** (Zehntner, 1897), ***Rh. Padi*** (Linnaeus, 1758), ***Schizaphis graminum*** (Rondani, 1852) و ***Rhopalosiphum maidis*** (Fitch, 1856) ***Sitobion avenae*** (Fabricius). هذه الأنواع تصيب أوراق الحنطة، الشعير، الذرة ونباتات نجيلية أخرى في العراق. سجلت الدراسة مختصر للصفات التصنيفية والمضائف المحتملة لكل نوع من الأنواع المسجلة. كما صمم في هذا الدراسة مفتاح ثنائي ومصور.

ABSTRACT

This study was based on the collection and determination of aphid species that infested Graminae in several provinces of Iraq. Seven aphid species belongs to Subfamily Aphidinae were recorded: ***Hyalopterus pruni*** (Geoffroy, 1762), ***Melanaphis donacis*** (Passerini, 1862), ***M. sacchari*** (Zehntner, 1897), ***Rhopalosiphum maidis*** (Fitch, 1856), ***Rh. padi*** (Linnaeus, 1758), ***Schizaphis graminum*** (Rondani, 1852) and ***Sitobion avenae*** (Fabricius). Aphid species are known to colonize leaves of wheat, barley, corn, and other grains related to grasses in Iraq. A summary of taxonomic characters and usual hosts is given here for each species. Couplet key and pictorial plates have been designed here.

Key words: Aphid key, Aphid on Graminae.

INTRODUCTION

Aphids (Hemiptera: Homoptera: Sternorrhyncha: Aphididae) are one of the most economically important groups of insects as agricultural pests and vectors of plant diseases. Slide mounted specimens need to be studied for making taxonomic identifications. Still, it is possible to identify the common species as well as the unusual ones based on external characters and photographs of various stages [1] [2].Small grains, including wheat, barley, corn, and other small grains are attacked throughout the growing season by numerous aphid species. Since economic threshold levels have been established for some, but not all aphid species found feeding on these crops [3]. In Iraq [4] recorded four aphid species infested grasses these species were ***Hyalopterus pruni, Rhopalosiphum maidis***, ***Rh. rufiabdominale*** (Sasaki, 1899), ***Schizaphis graminum***, belongs to Subfamily Aphidinae, while [5] added the aphid species *Aphis craccivora* Koch that infested host plant *Zea mays* L. also he reported the aphid species ***Melanaphis sacchar***i.

Whereas [6],[7] and [8] added ***Melanaphis donacis*** and ***Sitobion avenae*** (Fabricius) to the list of aphids infested graminae.

MATERIALS AND METHODS

Aphid samples infested various Graminae hosts were collected from various locations of Iraqi provinces Baghdad, Babylon, Kerbala, Najaf, Erbil, Sulaimaniya, Dohok, Diyala and Mosul (Sinjar Mountain), over a period from February 2010 to May 2011.

Aphids were collected from their host plants with a fine brush and put in to a tube which contained 70% alcohol. The collecting and preserving technique was based mainly on Eastop and Van Emden [9] method. The aphids were systematically classified from the catalog of [10] All measurements of the aphid are with millimeter (mm) table 1.The parameters measured are as in [2], except that body length (BL) is always measured to the base of the Cauda and does not include any projecting cauda.[1].

Aphid specimens were deposited in the collection of Iraq Natural History Research Center and Museum / University of Baghdad / Baghdad / Iraq.

Morphological Characters of Aphids Identification and Terminology:-

Aphids are determined mainly on the basis of their morphological characters (**Morphometric characters**) To identify an aphid to Family, Tribe or even to genus, qualitative characters are mainly used, but at the species level the characters used are often quantitative [1],[2]. The qualitative features and quantitative of aphid morphological characters were mentioned below for each recorded aphid, used for determinations the species level. The following characters are useful for species determination: degree of sclerotization, nature of the cuticular surface, the number, size and shape of hairs or setae, the color of live aphids, body shape, length, particular characters of head, thorax abdomen, and their respective appendages.

Table-1: Morphometric characters used in this text

Abbreviations	Characters
ANT I - VI	antennal segments I – VI
ANT. VI b	base of antennal segment VI
ANT PT	processus terminalis of antennal segment VI
BD III	basal diameter of antennal segment III
BL	body length
FTC	first tarsi chaetotaxy
HT II	second segment of hind tarsus
URS	ultimate rostral segment

RESULTS AND DUSCUSSION

Seven aphid species were determined related to Subfamily Aphidinae, tribe: Aphidini Subtribe: Aphidina. The descriptions provided are for **apterous viviparous females** because they are found more frequently than any other morph, these species were:

TRIBE **Aphidini** Latreille, 1802

Hyalopterus pruni (Geoffroy, 1762):

(Mealy plum aphid)

Live specimens: Colonies are found on the undersurface of the leaves of *Phragmites* sp.; infested leaves do not curl.

Preserved specimens (based on 10 specimens): Table 2, Figure 1.

Head smooth to slightly wrinkled, pale; antennal tubercles and somewhat median frontal tubercle weakly developed; antenna pale except darker at ANT VI, 0.74-0.7 times as long as body length; longest hair on ANT III with acute apex, 0.71-0.75 times as long as BD of ANT III, which it is without secondary rhinaria; ANT PT 3.32-3.37 times as long as ANT VI b; which 1.61-1.72 times as long as URS. Rostrum short almost reaches mid coxae; URS dark, short, broad, about 1.00-1.05 times as long as basal width, 0.50-0.58 times as long as HT II and bearing two fine and long accessory hairs. Legs pale except dusky in tarsi, FTC 3, 3, 2. Abdominal dorsum pale with dusky anal plates. Siphunculi dusky to dark (at least distally), thin, short, cylindrical, narrow-based, 0.037-0.048 times as long as Body length and 0.4-0.48 times as long as cauda. Cauda dark, tongue-shaped, 0.096-0.105 times as long as Body length and bearing 5-6 long hairs.

Schizaphis graminum (Rondani, 1852): (Greenbug or Wheat Aphid)

Live specimens: small, rather elongate oval, Body length in apteros 1.32-1.75 mm, in alate 1.25-1.80 mm; with head and prothorax yellowish or greenish straw-coloured, rest of thorax and abdomen yellowish green with a darker spinal stripe. Siphunculi are pale but usually have darker apices.They colonize on upper surface of leaves of grasses such as *Hordeum* sp. and *Zea mays* L.

Preserved specimens: (based on 18 specimens): Table 2, Figure 2.

Head smooth to slightly wrinkled, pale; antennal tubercles and median frontal tubercle weakly developed; antenna pale, 0.73-0.77 times as long as body length; longest hair on ANT III minute, with acute apex, 0.5-0.6 times as long as BD of ANT III; ANT III without secondary rhinaria; ANT PT 3.40-3.55 times as long as ANT VI b and 1.33-1.45 times as long as ANT III; ANT VI b 1.14-1.44 times as long as URS. Rostrum short reaches up to mid coxae; URS dark, short, 0.76-0.82

times as long as HT II and bearing two fine and long accessory hairs. Legs pale except dusky in tarsi; FTC 3, 3, 2. Abdominal dorsum pale with dusky anal plates. Siphunculi pale sometime with dark apex, thin, cylindrical, 0.15-0.17 times as long as Body length and 1.53-1.75 times as long as cauda. Cauda pale, finger-shaped, with constriction at middle 0.088-0.100 times as long as Body length and bearing 4-5 long hairs.

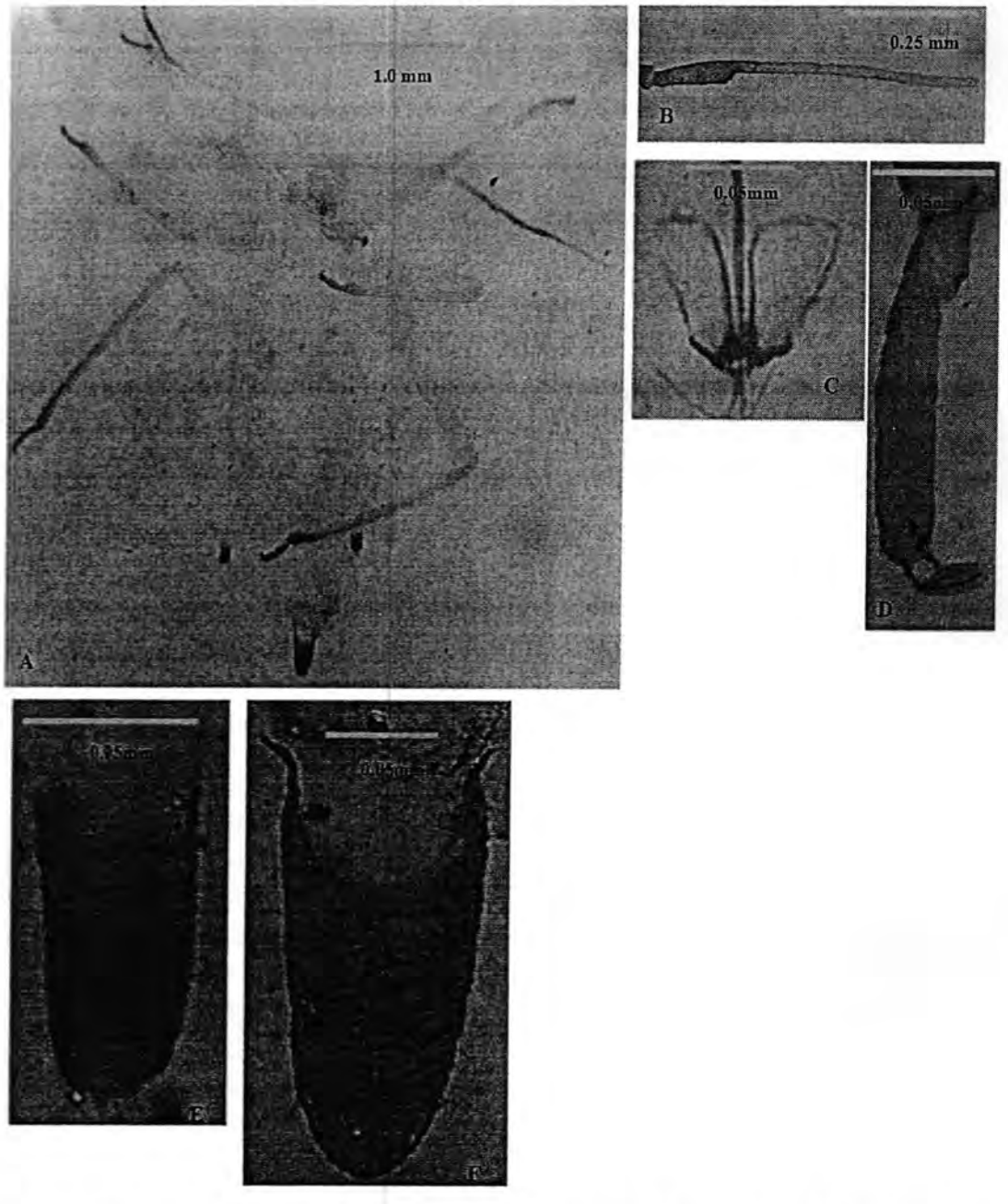

. Figure -1: **H. pruni** . A) Whole body. B) processus terminalis C) Ultimate rostral segment. D) HT II. E) Siphunculi. F) Cauda

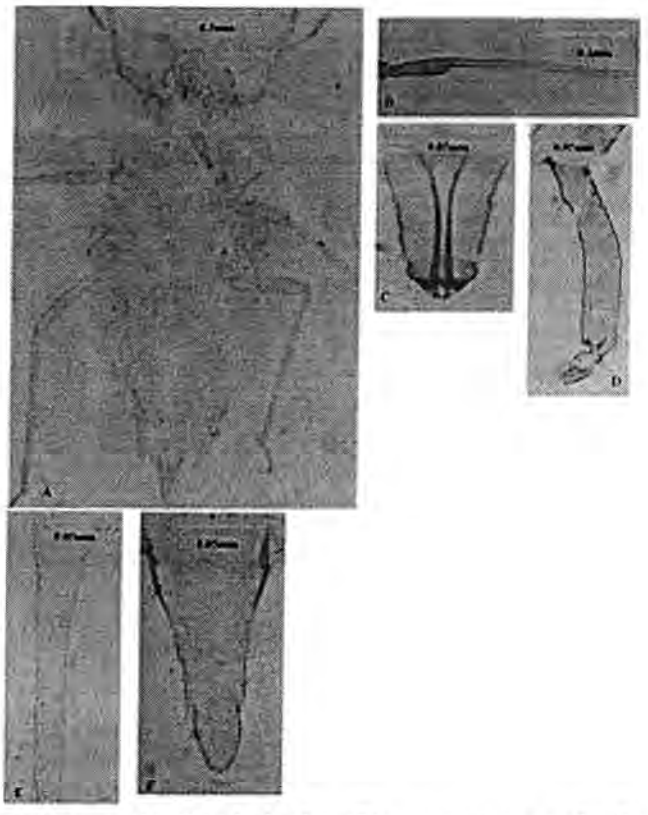

Figure -2: **S. graminum** A) Whole body. B) processus terminalis C) Ultimate rostral segment. D) HT II. E) Siphunculi. F) Cauda

Melanaphis donacis (Passerini, 1862):
Live specimens: small aphid, Body length in apterous 1.2-2.0 mm, alate 1.3-2.0 mm dark grey to blackish brown with white transverse bands marked out by wax, found in large colonies in the central of *Phragmites* sp. leaves.

Preserved specimens: (based on 10 specimens): Table 2, Figure 3.
Head smooth, dark, antennal and median frontal tubercles are moderately developed; antenna short, pale except dark ANT I and VI; 0.56-0.65 times as long as body length; longest hair on ANT III 0.75-1.25 times as long as BD of ANT III and without secondary rhinaria; ANT PT 1.00-1.30 times as long as ANT VI b; which it is 1.60-2.15 times as long as URS. Rostrum short, reaches mid coxae; URS Short broad, sharply tapered, 0.60-0.65 times as long as HT II and bearing two long accessory hairs. Legs pale, except dark cxae and tarsi; FTC 3, 3, 2. Abdominal dorsum pale except dark sub genital and anal plate. Siphunculi dark, short, stump-shaped, broadest at base, with slightly swollen flange, 0.060-0.085 times as long as Body length and 0.66-0.73 times as long as cauda. Cauda dark, finger-shaped with parallel-sides, 0.09-0.12 times as long as Body length and bearing 15-18 long hairs

M. sacchari (Zehntner, 1897): (Sugarcane aphid or Sorghum aphid)

Live specimens: a small aphid Body length in apterous 1.10-1.90 mm; yellow-brown, dark-brown to purple. found on the upper surface of *Phragmites* leaves. Attended by ants.

Preserved specimens: (based on 10 specimens): Table 2, Figure 4.

Head smooth, pale except dusky median frontal tubercles which its moderately developed; antennal tubercles weakly developed; antenna pale except for dark distal half of ANT V and VI, 0.62-0.70 times as long as body length; longest hair on antennal segment III minute, 0.50-0.63 times as long as BD of ANT III; ANT III without secondary rhinaria; processus terminalis 2.70-3.00 times as long as ANT VI b and 1.30-1.75 times as long as antennal segment III; and 1.10-1.24 times as long as URS. Rostrum reaches beyond mid coxae; URS dark, short, broad, sharply tapered, 0.85-0.98 times as long as HT II and bearing two fine and long accessory hairs. Legs pale except dark tarsi; FTC 3, 3, 2. Abdominal dorsum with dark anal plate and dusky sub genital plate. Siphunculi dark, short, tapering, with swollen flange, 0.062-0.075 times as long as Body length and 0.80-0.90 times as long as cauda. Cauda dark finger-shaped, somewhat elongated, 0.070-0.092 times as long as Body length and bearing 10-12 long hairs.

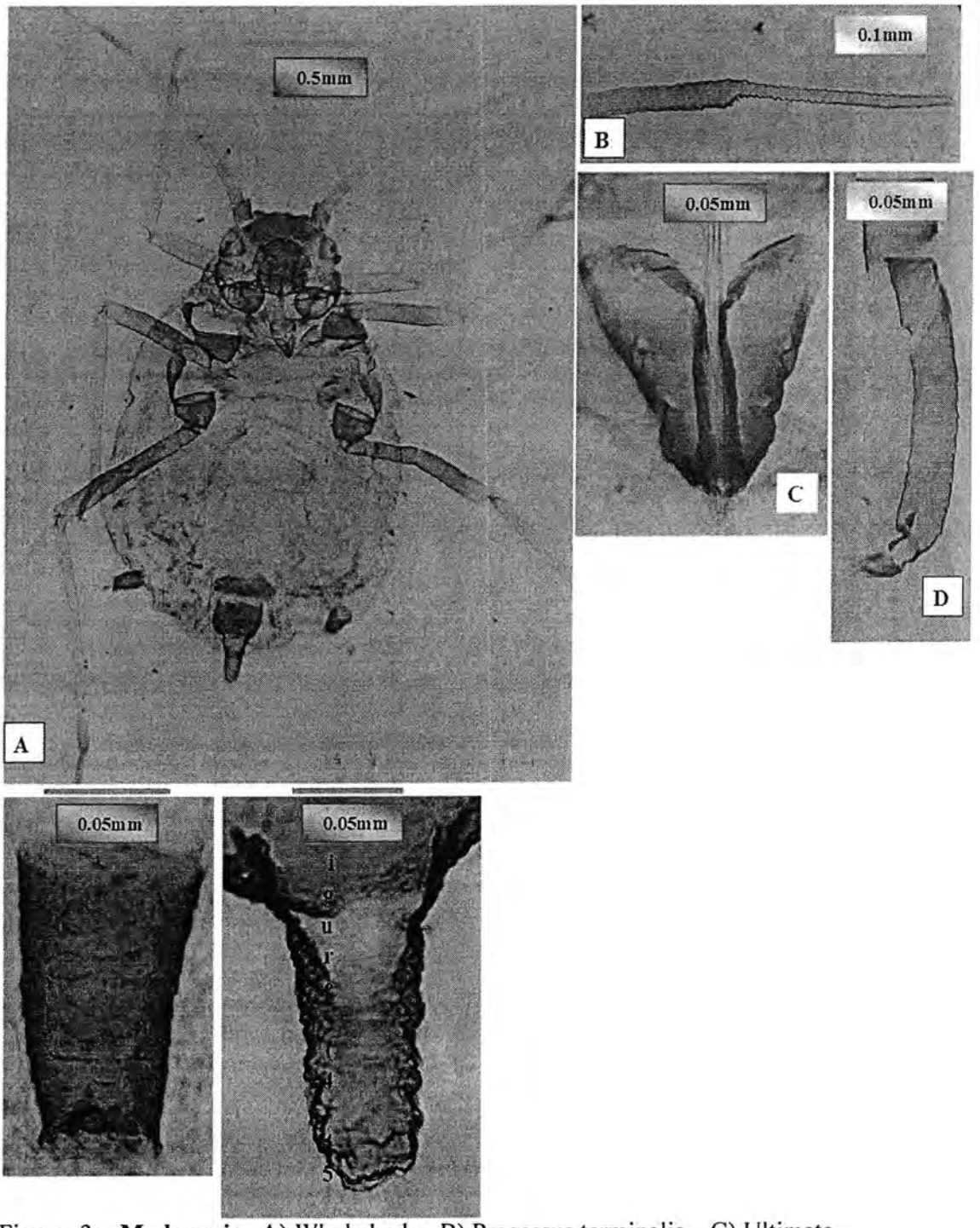

Figure -3: **M. donacis** A) Whole body. B) Processus terminalis C) Ultimate rostral segment. D) HT II. E) Siphunculi. F) Cauda

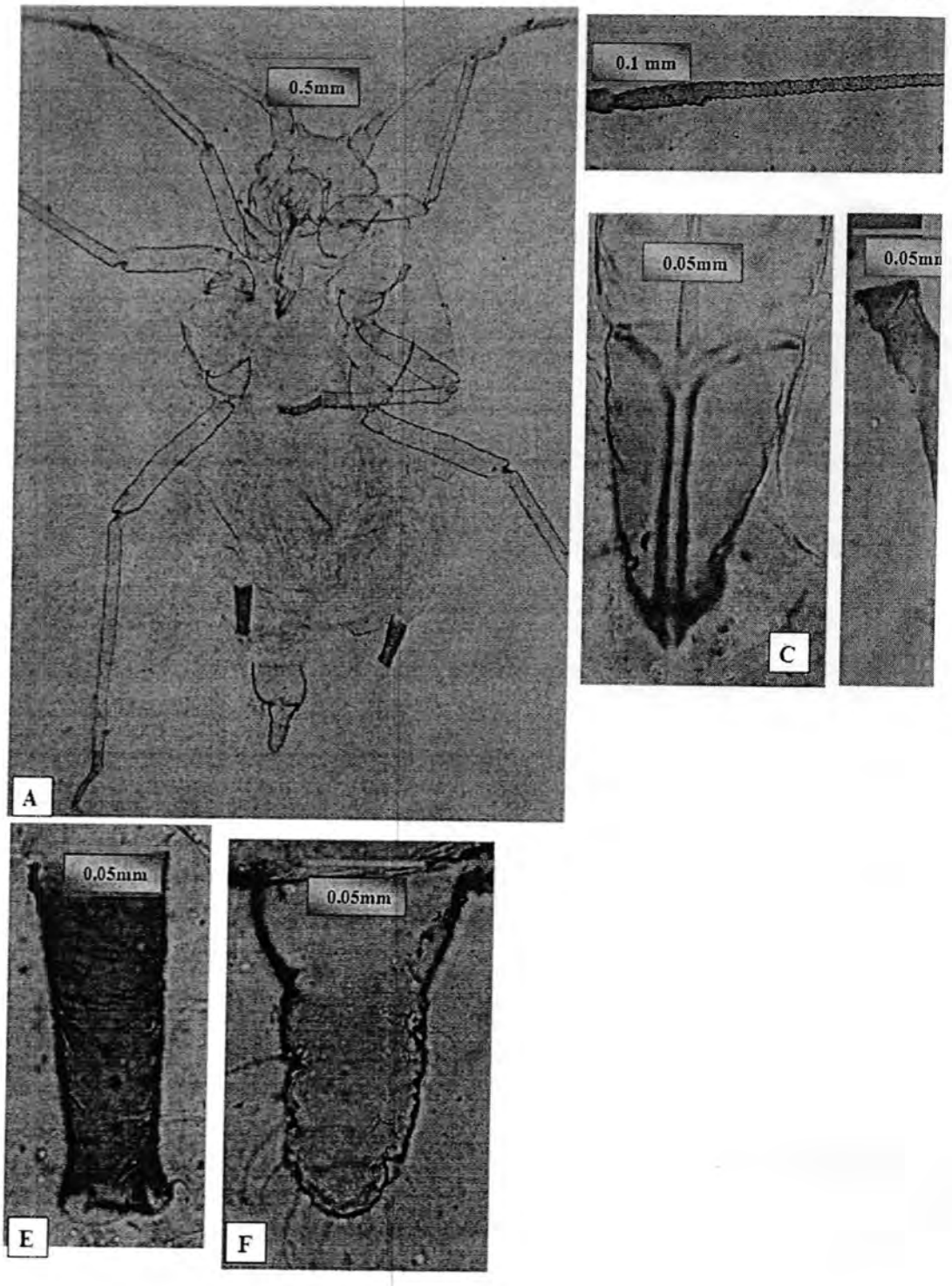

Figure -4: **M. sacchari** . A) Whole body. B) processus terminalis. C) Ultimate rostral segment. D) HT II. E) Siphunculi. F) Cauda

Rhopalosiphum maidis (Fitch, 1856): Green Corn Aphid
Live specimens: Small to medium-sized, rather elongate, Body length in apteros 1.60-2.30 mm, yellow-green to dark olive green, with short dark Siphunculi. Found on young leaves of several grasses such as *Triticum* sp. *Hordeum* sp., *Zea mays* L. and others.
Preserved specimens: (based on 14 specimens): Table 2, Figure 5.
Head smooth dark; antennal tubercles weakly developed, antenna 5- or 6-segments, dark in entire length, 0.38-0.42 times as long as body length, longest hair on ANT III with blunt apex, 0.83-1.00 times as long as BD of ANT III, ANT III without secondary rhinaria. ANT PT 2.00-2.22 times as long as base ANT VI and 0.66-0.77 times as long as ANT III in 5-segments forms, and 0.82-0.92 times as long as ANT III in 6-segments forms; Base ANT VI 1.00-1.12 times as long as URS. Rostrum hardly reaches up to mid coxae; URS dark, short, 0.77-0.88 times as long as HT II, bearing two long accessory hairs. Legs dark in entire length; FTC 3, 3, 2. Abdominal dorsum pale with a net-like pattern and with a pattern of spicules arranged in polygons, sub-genital and anal plates dark. Siphunculi dark, tapering from base with only a slight sub-apical constriction and small flange, 0.078-0.088 times as long as Body length and 1.16-1.29 times as long as cauda. Cauda tongue-shaped, with similar pigmentation to Siphunculi, 0.060-0.075 times as long as Body length and bearing 4-5 long hairs.
Rhopalosiphum padi (Linnaeus, 1758): (Bird Cherry-Oat Aphid)
Live specimens: Small to medium-sized, broadly oval, Body length in apteros 1.65-2.25 mm , in alate 1.5-2.20 mm; green mottled with yellowish green or olive-green, or dark-olive to greenish black; often with rust-coloured patches around the bases of Siphunculi, these patches sometimes meet on the abdominal dorsum. Found On numerous species of Gramineae and Cyperaceae. Such as *Cyperus* sp., *Cynodon dactylon* L., *Canna* sp. and *Hordeum* sp.

Preserved specimens: (based on 14 specimens): Table 2, Figure 6.
Head smooth, dark; antennal tubercles and median frontal tubercle weakly to moderate developed, antenna dark in entire length, 0.72-0.79 times as long as body length, longest hair on ANT III with blunt apex, 0.62-0.75 times as long as BD of ANT III, ANT III without secondary rhinaria. processus terminalis 3.85-4.15 times as long as base antennal VI and 1.02-1.22 times as long as ANT III; ANT VI b 0.92-1.00 times as long as URS. Rostrum reaches mid coxae; URS dark, short with broad base, 1.00-1.14 times as long as HT II, bearing two long accessory hairs. Legs dark in entire length; FTC 3, 3, 2. Abdominal dorsum pale with affiant net-like pattern and with a pattern of spicules arranged in polygons, sub-genital and anal plates dark. Siphunculi dark,

cylindrical for most of length, with slight distal swelling, and with a marked subapical constriction and large flange, 0.14-0.18 times as long as Body length and (1.70-1.94) times as long as cauda. Cauda tongue-shaped, with similar pigmentation to Siphunculi, 0.086-0.095 times as long as Body length and bearing 5-6 long hairs.

TRIBE **Macrosiphini** Wilson, 1910.

Sitobion avenae (Fabricius, 1775). (English Grain Aphid).

Live specimens: Medium to large-sized, Body length in apterous 2.20-3.20 mm, in alate 2.20-2.90 mm; shiny dirty reddish brown, with black antenna and Siphunculi. Found on the upper leaves and flower stems of numerous species of Gramineae.

Preserved specimens: (based on 8 specimens): Table 2, Figure 7.

Head smooth, slightly dusky, antennal tubercles rather weakly to moderately developed; antenna dark except for paler ANT (I and II), 0.90-0.98 times as long as body length; longest hair on ANT III 0.50-0.55 times as long as BD of ANT III, ANT III with 1-2 secondary rhinaria near base, ANT PT 4.30-4.55 times as long as ANT VI b and 0.90-1.08 times as long as ANT III; ANT VI b 1.15-1.35 times as long as URS. Rostrum reaches mid coxae; URS dark, with bulbous sides and blunt apex, 0.62-0.75 times as long as HT II, bearing 6-7 long accessory hairs. Legs dusky to slightly dusky with dark tips, FTC 3, 3, 3. Abdominal dorsum pale. Siphunculi dark, long tapering , cylindrically at distal half , reticulation comprises 20-32 % of total length in about 5-7 transverse rows of closed cells, 0.21-0.25 times as long as Body length and 1.35-1.45 times as long as cauda. Cauda pale, most often constricted near middle, with pointed apex, 0.14-0.19 times as long as body length bearing 6-7 long hairs.

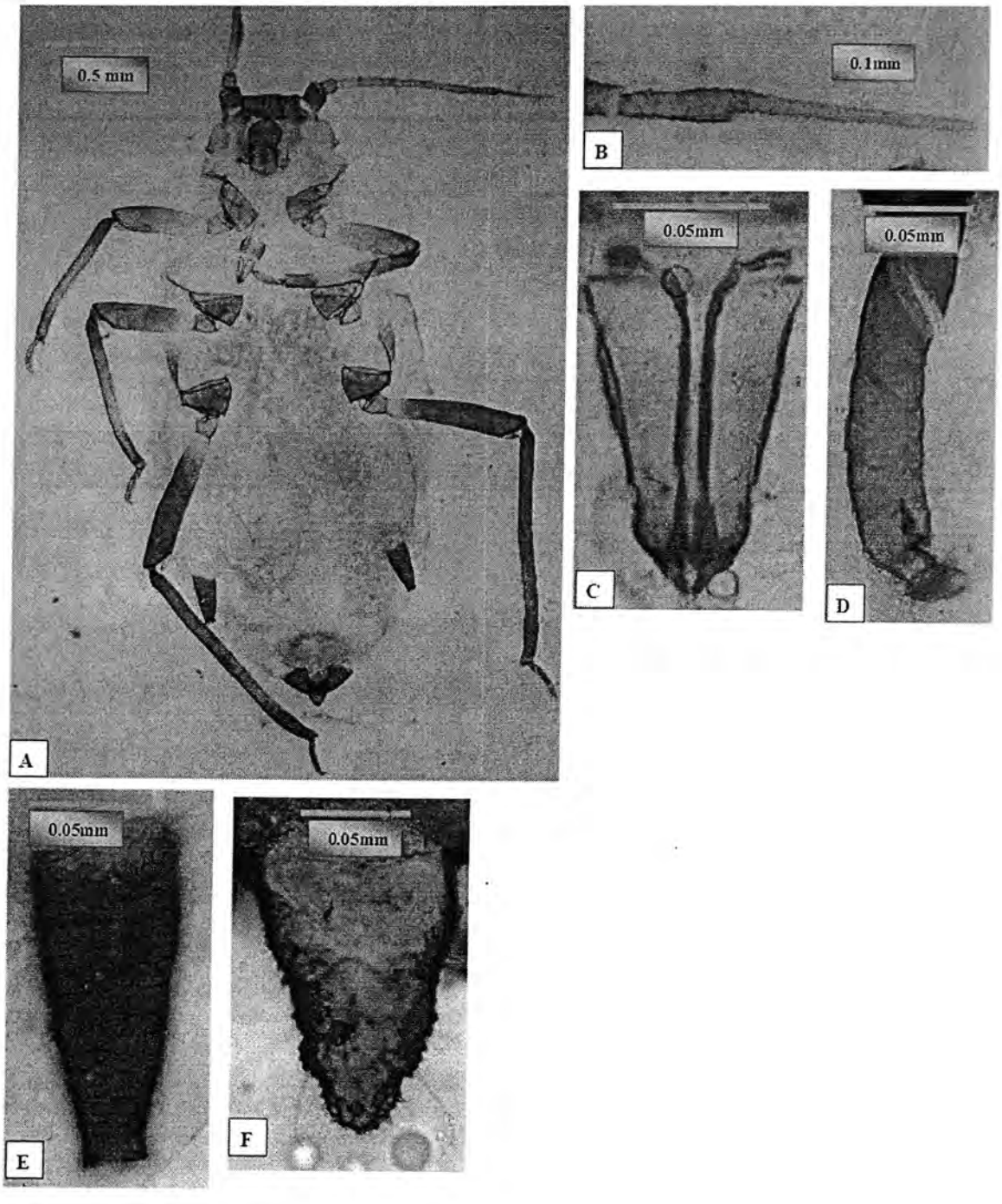

Figure -5: Rh. maidis). A) Whole body. B) Processus terminalis C) Ultimate rostral segment. D) HT II. E) Siphunculi. F) Cauda

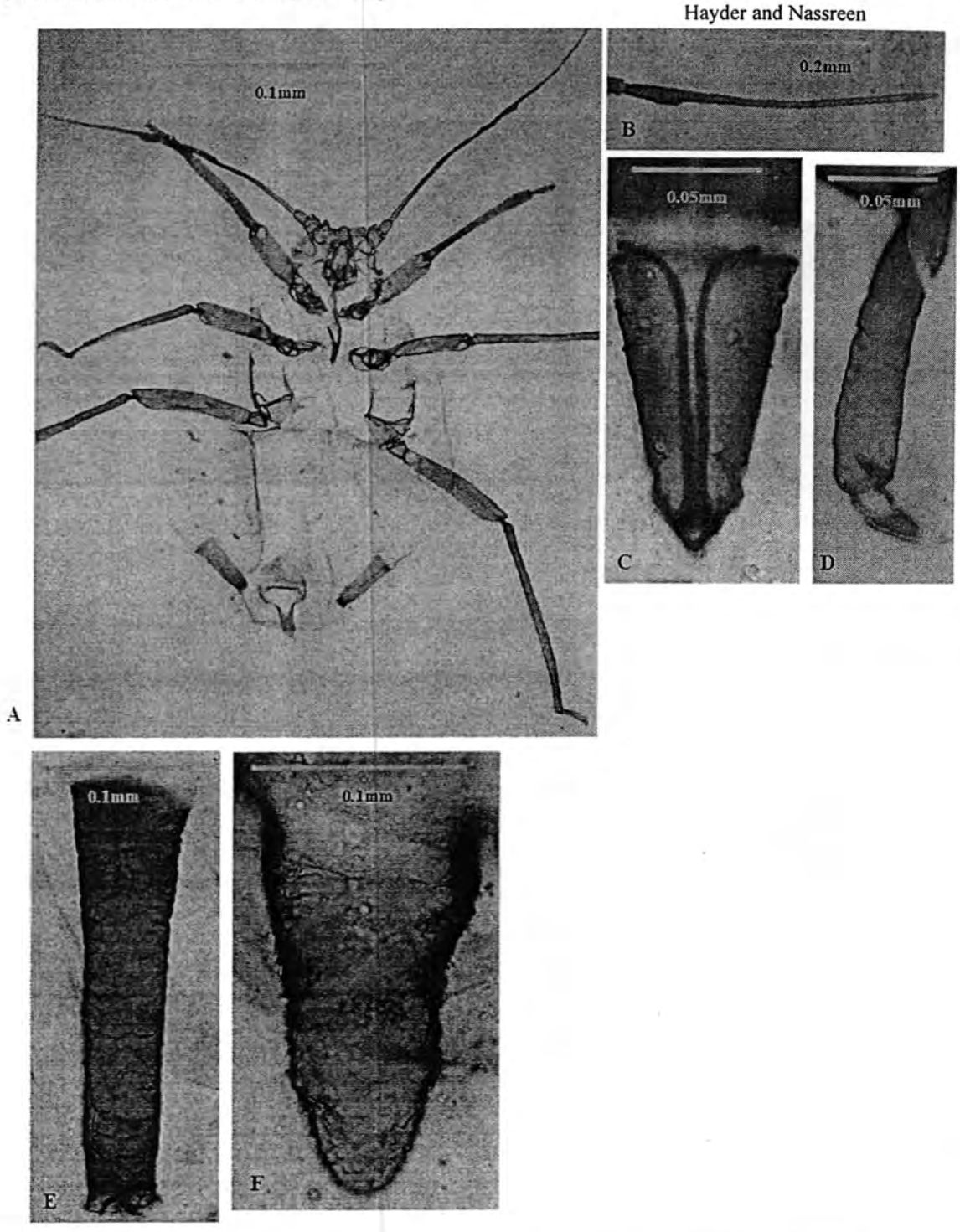

Figure -6: **Rh. padi** A) Whole body. B) Processus terminalis. C) Ultimate rostral segment. D) HT II E) Siphunculi F) Cauda

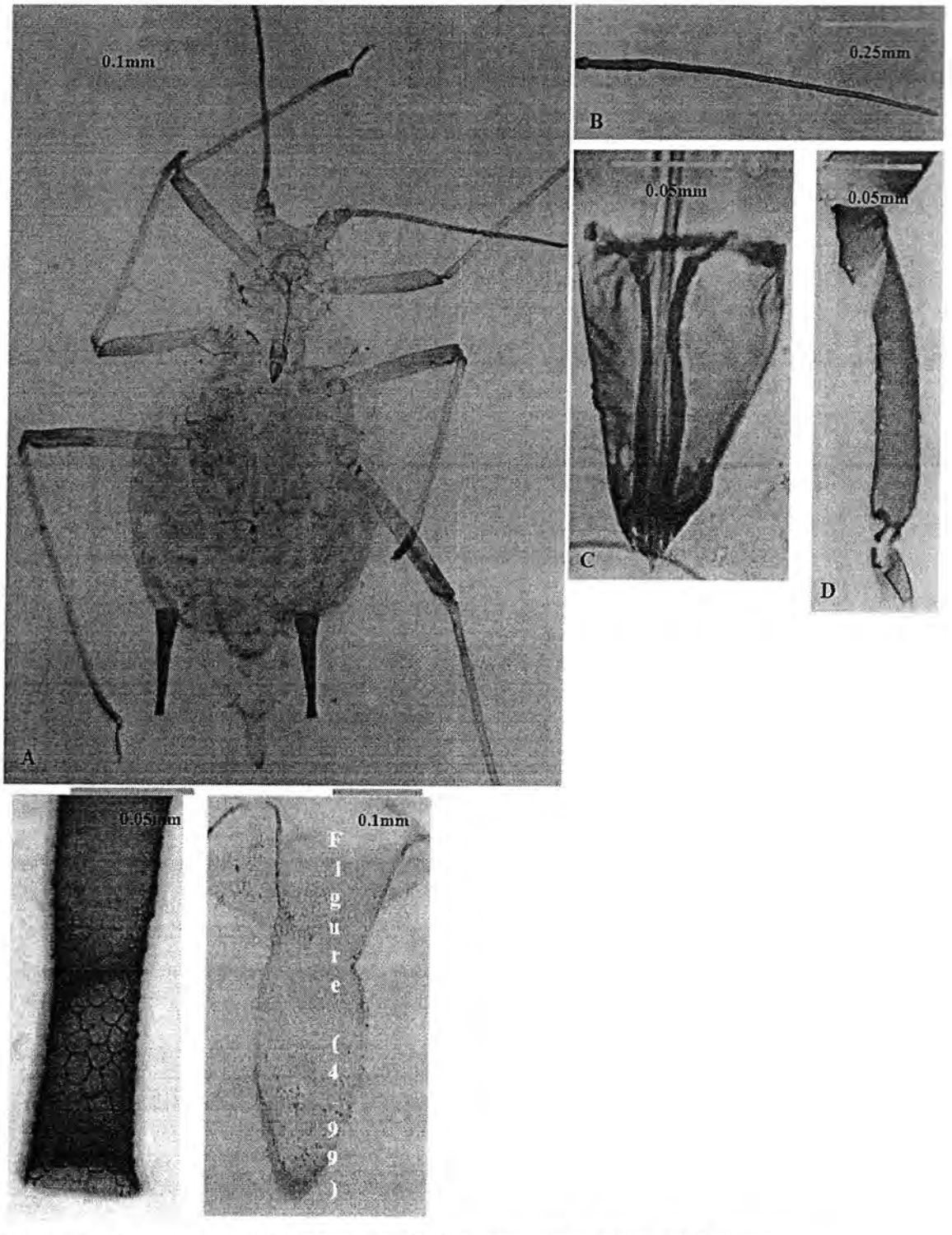

Figure -7: **S. avenae** A) Whole body. B) Processus terminalis C) Ultimate rostral segment. D) HT II. E) Reticulation of Siphunculi. F) Cauda

Table-2: Morphometric characters (mm) and comparisons of the studied adult morphs

Morphometric characters	*H. pruni*	*M. donacis*	*M. sacchari*	*Rh. maidis*	*Rh. padi*	*S. graminum*	*S. avenae*
BL	(1.70-2.25)	(1.20-2.00)	(1.10-1.90)	(1.60-2.30)	(1.65-2.25)	(1.32-1.75)	(2.20-3.20)
Antenna							
ANT(I–VI) (length)	(1.30-1.70)	(0.75-1.15)	(0.75-1.20)	(0.75-1.00)	(1.30-1.70)	(0.95-1.40)	(2.15-2.90)
ANT III (length)	(0.35-0.50)	(0.22-0.30)	(0.14-0.24)	(0.20-0.24)	(0.36-0.47)	(0.19-0.30)	(0.60-0.82)
ANT III (width at base(BD))	(0.0200-0.0275)	(0.02-0.025)	(0.018-0.025)	(0.018-0.030)	(0.022-0.035)	(0.0125-0.0200)	(0.033-0.038)
Processus terminalis (length)	(0.37-0.44)	(0.125-0.190)	(0.24-0.32)	(0.165-0.220)	(0.43-0.50)	(0.28-0.41)	(0.60-0.74)
Base antennal VI	(0.110-0.132)	(0.12-0.15)	(0.085-0.11)	(0.075-0.110)	(0.105-0.125)	(0.080-0.115)	(0.135-0.165)
ANT III secondary rhinaria	(0)	(0)	(0)	(0)	(0)	(0)	(1-2)
Longest hair on ANT III (length)	(0.015-0.020)	(0.015-0.030)	(0.010-0.015)	(0.015-0.030)	(0.016-0.022)	(0.0075-0.0100)	(0.018-0.022)
Ultimate rostral segment (length)	(0.068-0.077)	(0.055-0.090)	(0.070-0.095)	(0.075-0.105)	(0.105-0.130)	(0.066-0.080)	(0.10-0.14)
Ultimate rostral segment (accessory hairs)	(2)	(2)	(2)	(2)	(2)	(2)	(6-7)
Thorax							
Hind tibia (length)	(0.85-1.00)	(0.55-0.90)	(0.50-0.70)	(0.70-1.00)	(0.90-1.15)	(0.46-0.77)	(1.60-1.95)
Hind femora (length)	(0.5-0.6)	(0.38-0.52)	(0.30-0.43)	(0.40-0.60)	(0.60-0.77)	(0.32-0.48)	(0.90-1.18)
HT II (length)	(0.125-0.140)	(0.10-0.14)	(0.08-0.10)	(0.095-0.12)	(0.10-0.12)	(0.085-0.105)	(0.15-0.18)
FTC	3,3,2	3,3,2	3,3,2	3,3,2	3,3,2	3, 3, 2	3,3,3
Diameter of trochantro-femoral suture	(0.0425-0.0525)	(0.040-0.055)	(0.047-0.056)	(0.050-0.055)	(0.062-0.075)	(0.035-0.0425)	(0.063-.0.078)
Ventral hair on hind trochanter	(0.0475-0.0550)	(0.045-0.057)	(0.038-0.043)	(0.045-0.060)	(0.025-0.036)	(0.035-0.045)	(0.037-0.042)
Abdomen							
SIPH (length)	(0.070-0.095)	(0.100-0.125	(0.080-0.125)	(0.14-0.18)	(0.29-0.33)	(0.20-0.28)	(0.55-0.70)
Cauda (length)	(0.175-0.220)	(0.14-0.18)	(0.10-0.14)	(0.12-0.14)	(0.155-0.190)	(0.13-0.16)	(0.40-0.48)
Caudal hairs	(5-6)	(15-18)	(10-12)	(4-5)	(5-6)	(4-5)	(6-7)
Comparisons							
ANT(I–VI) / Body length	(0.74-0.77)	(0.56-0.65)	(0.62-0.70)	(0.38-0.42)	(0.72-0.79)	(0.73-0.77)	(0.90-0.98)
longest hair on ANT III / ANT III(BD)	(0.71-0.75)	(0.75-1.25)	(0.50-0.63)	(0.83-1.00)	(0.62-0.75)	(0.5-0.6)	(0.50-0.55)
Processus terminalis / Base antennal VI	(3.32-3.37)	(1.00-1.30)	(2.70-3.00)	(2.00-2.22)	(3.85-4.15)	(3.40-3.55)	(4.30-4.55)
Ultimate rostral segment / HT II (length)	(0.50-0.58)	(0.60-0.65)	(0.85-0.98)	(0.77-0.88)	(1.00-1.14)	(0.76-0.82)	(0.62-0.75)
SIPH / Body length	(0.037-0.048)	(0.060-0.085)	(0.062-0.075)	(0.078-0.088)	(0.14-0.18)	(0.13-0.17)	(0.21-0.25)
SIPH / cauda (length)	(0.4-0.48)	(0.66-0.73)	(0.80-0.90)	(1.16-1.29)	(1.70-1.94)	(1.53-1.75)	(1.35-1.45)
Cauda / Body length	(0.096-0.105)	(0.09-0.12)	(0.070-0.092)	(0.060-0.075)	(0.086-0.095)	(0.088-0.100)	(0.14-0.19)

Many of the discriminates used in the key are morphometric characters, Key couplets may offer a choice between two ranges of measurements or ratios, these ratios are showed in table 3. For reliable identifications we examined a series of 10 or more apterous adult aphids.

Table-3:Comparisons between morphometric characters or ratios used in the key.

Comparisons
ANT(I–VI) / Body length
longest hair on **ANT III / ANT III**(BD)
Processus terminalis / Base antennal VI
Ultimate rostral segment / HT II (length)
SIPH / Body length
SIPH / Cauda (length)
Cauda / Body length

1

Siphunculi more than 0.05 X BL and more than 0.6 X cauda (Fig. 6)

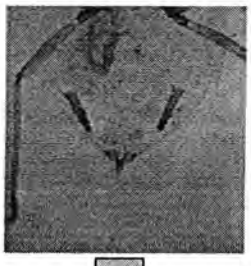

2

Antennal tubercles rather low but always higher than median frontal tubercle; Siphunculi about as long as the distance between their bases or little shorter, with a subapical zone of polygonal reticulation (Fig. 7 E)

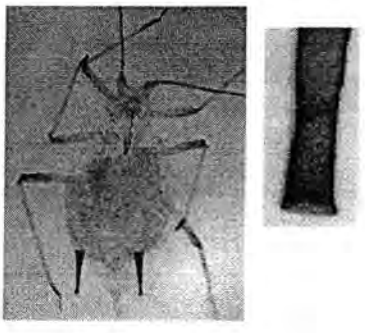

Sitobion avenae

Siphunculi short and thin, 0.037-0.048 X BL and 0.4-0.48 X cauda (Fig. 1)

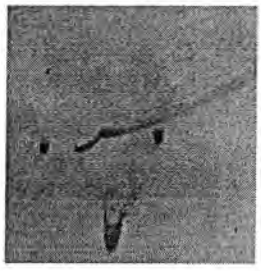

Hyalopterus pruni

Antennal tubercles low or undeveloped not higher than median frontal tubercle; Siphunculi about as long as the distance between their bases or little shorter, with a subapical zone of polygonal reticulation (Fig. 2,3,4.5,6)

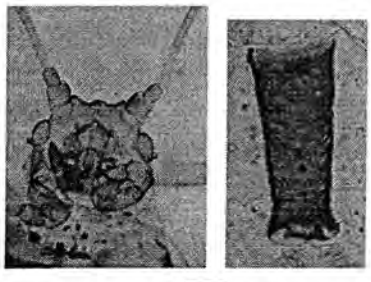

3

3

Cauda longer than Siphunculi, bearing 10-18 hairs

(Fig. 3,4)

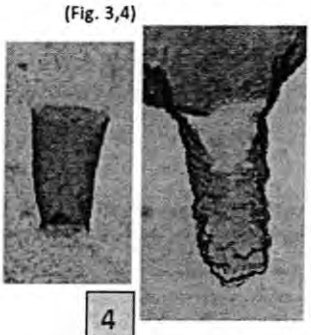

4

ANT PT 1.0-1.3X ANT VI b; URS 0.60-0.65 X HT II;

Longest hair on ANTIII 0.75-1.25 X ANT III BD;

Siphunculi 0.66-0.73 X cauda, which bearing 15-18

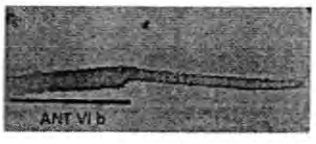

Melanaphis donacis

Cauda shorter than Siphunculi, bearing 4-6 hairs

(Fig. 2,4,6)

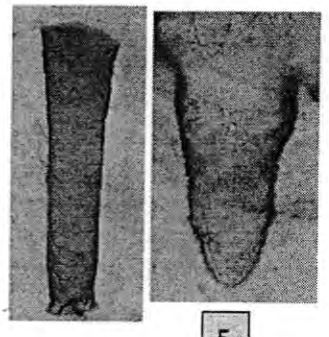

5

ANT PT 2.70-3.00X ANT VI b; URS 0.85-0.98 X HT II;

Longest hair on ANTIII 0.50- 063 X ANT III BD;

Siphunculi 0.80-0.90 X cauda, which bearing 10-12

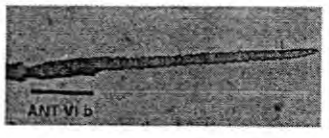

Melanaphis sacchari

15

5

Head, Antenna, Siphunculi and cauda mainly pale

Schizaphis graminum

Head, Antenna, Siphunculi and cauda mainly dark

6

Longest hair on ANTIII 0.83-1.00 X ANT III BD; ANT PT 2.00-2.22 X ANT VI b; URS 0.77-0.88 X HT II; SIPH 0.078-0.088 X BL, 1.16-1.29 X cauda

(Fig. 5)

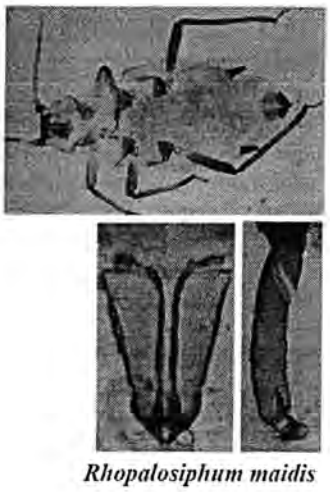

Rhopalosiphum maidis

Longest hair on ANTIII 0.62-0.75 X ANT III BD; ANT PT 3.83-4.15 X ANT VI b; URS 1.00-1.14 X HT II; SIPH 0.14-0.18 X BL, 1.70-1.94 X cauda

(Fig. 6)

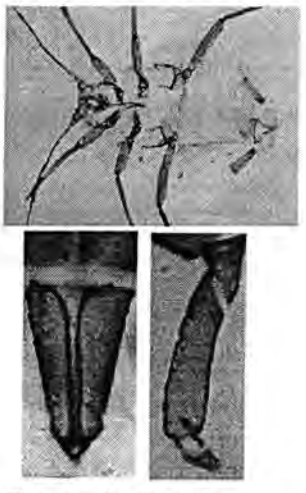

Rhopalosiphum padi

REFERENCES

1. Blackman R. L. and Eastop, V. F. (2006). Aphids on the World's Herbaceous Plants and Shrubs. Chichester: John Wiley and Sons, Ltd 1024 pp.
2. Ilharco F.A. & van Harten, A. (1987) Systematics. pp.51-77 in Minks, A.K. & Harrewijn, P. (eds.) Aphids, their Biology, Natural Enemies and Control. Vol. A. Elsevier, Amsterdam.
3. Summers C.G. and Newton,A.S. (2001). Key to Aphids of Small Grains, Corn, and Sorghum. Plant Protection Quarterly of California university. 11(4): 7-11
4. Bodenheimer F. & Swirski, E. (1957) Aphidoidea of the Middle East. Weizmann Science Press, Jerusalem, 378 pp.

5. Kaddou I.K. (1966). Aphidae from Iraq. Bull. Biol. Res. Cent. 2:21-35.
6. Daoud A. K. & El-Haidari, H.S. (1968) Recorded aphids of Iraq. Iraq Nat. His. Mus. Publs. No. 24, 37 pp.
7. Abdul- Rassoul M. S. (1976) Checklist of Iraq Natural History Museum Insect Collection. Nat. His. Res. Cen. 30: 1-35
8. Al-Ali A.S. (1977). Phytophagous and entomophagous insects and mites of Iraq. Nat. Hist. Res. Cen. Publ. 33:142 pp.
9. Eastop V.F. and VanEmden, H.F. (1972). The insect material. pp.1-45 in Van Emden, H.F. (ed.) Aphid technology. Academic press, London and New York.573 pp.
10. Remaudiere G. and Remaudiere, M. 1997. Catologue des Aphididae du Monde (Catalogue of the WorldÕs Aphididae) Homoptera, Aphidoidea, Preface Par V.F. Eastop, INRA editions, p. 473.

Synthesis of New Heterocyclic Derivatives of Phenothiazine

Souad J. Lafta
Department of Chemistry . College of Science . Al-Mustansiriyah University

Received 8/5/2012 – Accepted 20/6/2012

الخلاصة

يتضمن هذا البحث تحضير عدد من المشتقات الجديدة لمركب الفينوثايازين ذات الفعالية البايولوجية المتوقعة . وقد تم في هذا البحث استعمال مركب 2-امينوبنزوثايازول (1) والمركب فنيل هيدرازين (2) كمادتين اوليتين وتحويلهما الى مشتقات للفينوثايازين ، حيث تم معاملة المركبين مع بارا-هيدروكسي بنزالديهايد في الكحول المطلق لتحضير قواعد شيف (3) و(4) التي عند تفاعلهما على التوالي مع α-مركبتو حامض الخليك تعطي مشتقات تحتوي على حلقة الثايازوليدين (6,5).

عند معاملة المشتقات (5,6) مع امينات اروماتية اولية بوجود كلوريد الزنك اللاماني اعطت امينات اروماتية ثنائية الاريل (7,8) a-c والتي تم تحويلها الى مشتقات الفينوثايازين (9،10) a-c عند صهرها مع عنصر الكبريت بوجود كمية قليلة من اليود كعامل مساعد لاجراء الغلق الحلقي للامينات ثنائية الاريل المحضرة . شخصت المركبات المحضرة بدراسة خصائصها الطيفية والفيزياوية .

ABSTRACT

In this study was synthesized new phenothiazine derivatives for their potent biological activities, from compounds phenylhydrazine (1) & compound (2), as starting materials. The route of preparation involved the refluxing of compounds (1) & (2) with p-hydroxy benzaldehyde in absolute ethanol to form Schiff bases (3) & (4) , which on cyclization by mercaptoacetic acid yielded thiazolidine derivatives (5) and (6) respectively, reaction of the heterocyclic derivatives (5&6) with p-substituted anilines in presence of anhydrous zinc chloride gave substituted diarylamines (7&8)a-c . The fusion of diarylamines with sulphur in presence of catalytic amount of iodine resulted in the substituted phenothiazines (9&10)a-c . The structure of all the synthesized compounds have been supported by their physical properties and spectral data .

INTRODUCTION

Phenothiazine derivatives constitutes an important class of thiazines [1] heterocyclic ring system and posses diverse activities as neuroleptics [2], tranquilizers [3], antimalarian [4], antiparkinson [5] , anticonvulsant, antihistaminic [6], antiviral, antihelminic , anticancer [7-8], antibacterial and CNS-depresent.[9] Furthermore, a wide spectrum of biological activates including antibacterial, antitumor, antituberculotic and insectesides [9] have been reported in different benzothiazole [10] derivatives . Heterocyclic compounds particularly five or six membered ring compounds have the first place among various classes of organic compounds for their diverse biological activities. A broad spectrum of biological activity is associated with both thiazole [11-13] and thiazolidine ring and a large number of natural and synthetic compounds containing such moieties find pharmaceuticals applications.

MATERIALS AND METHODS

All the melting points were determined in open capillaries and are uncorrected. The FT-IR spectra were run in KBr disc on a Pva-Unicam SP3-100 spectrophotometer. UV spectra were recorded with a Hitachi-2000 spectrophotometer . H^1-NMR spectra were recorded on Burker DMX-500 NMR (300-600 MHZ) Spectrophotometer in ALalbet university – Jordon using DMSO as a solvent .

General Procedure for the Synthesis of the Compounds (3,4) [14] :

(0.01 mole 1.22g) of p-hydroxybenzaldehyde was added to (0.01 mole 1.08g) of the compound 1 or (0.01 mol. 1.50g) of the compound 2 in absolute ethanol (30 ml) and the mixture was refluxed to 3 hrs. The resulted mixture was cooled for 24 hrs. until the product was precipitated . The ppt. was filtered and crystallized from ethanol . The physical properties of the synthesized compounds are listed in table (1).

General Procedure for the Synthesis of the Compounds (5,6) [15] :

(0.002 mole, 0.184g) of α-mercaptoacetic acid was added gradually to a mixture consisted from (0.002 mole, 0.424g) of compound 3 or (0.002 mol. 0.508g) of compound 4 in (30 ml) of ethanol and the resulted mixture was refluxed for (6-7) hrs. After cooling, the solution was neutralized by cold dist. water and recrystallized from suitable solvent. The physical properties of the synthesized compounds are listed in table (1).

General Procedure for the Synthesis of the Compounds (7,8) [16] :

A mixture of (0.005 mole, 1.370g) from compound 5 or (0.005 mol. 1.530g) of compound 6 and (0.05 mole) from primary aromatic amine in (50 ml) of absolute ethanol was heated under reflux in the presence of anhydrous ZnCl2 (0.5 g) for 6 hrs. On cooling , a solid mass separated out which was washed with acidified water to remove inorganic materials, then it was filtered off to obtain the product and crystallized from suitable solvent. The physical properties are listed in table (1).

General Procedure for the Synthesis of the Compounds (9,10) [17] :

A mixture of (0.01 mole) from compounds (7)a-c with (0.1 mole) of sulfur and (0.5 g) of iodine was heated at 120° C in oil bath for 2 hr. The hot melt was rapidly poured into a mortar and crushed to a fine powder. It was washed with water, dried and crystallized from suitable solvent. The physical properties are listed in table (1).

RESULTS AND DISCUSSION

Synthetic routes leading to target compounds are summarized in schemes 3 and 4. The structures of all the synthesized compounds have been supported by their physical properties and their spectral studies. The treatment of the starting materials 1 & 2 with p-hydroxybenzaldehyde leads to the generation of two Schiff's bases 3 & 4, which exhibited IR [18] absorption bands at 3200 cm-1 (NH stretching) and 3400 cm-1 (OH stretching) . The spectra shows also bands at 1599-1580 cm^{-1} which belong to (C=N stretching) out of plane vibration . The disappearance of NH_2 stretching vibration bands confirmed the structure of these bases.

The UV-Vis spectra of the base 3 shows peak at (338 nm) which belong to the electronic transitions (n-π^*) of the (C=N) group out of the ring , and peak at (283 nm) of the transition (n-π^*) which belong to (C-OH) , and at (207 nm) of the transitions (π-π^*) for the benzene ring . The UV-Vis spectra of compound 4 shows peak at (269 nm) belongs to the transitions (n-π^*) of the (C=N) group and peak at (222 nm) for the (π-π^*) transitions of the benzene ring.

The treatment of compounds 3 & 4 with mercaptoacetic acid gives the [16] heterocyclic compounds 5 & 6 , which shows the bands of (C=O) group at 1700 cm^{-1} in its IR spectra and disappearance of the band at 1599-1580 cm^{-1} which belongs to (C=N) group and appearance of a band at (1662 cm^{-1}) which belongs to the cyclic carbonyl group which shows enolic character which cause the broad band of (NH) group at (3260-3200 cm^{-1}). The UV-Vis spectra of the compound (5) shows maxima at (278 nm) for the (n-π^*) transitions of (C=O) group and peak at (218 nm) for the [17] electronic transitions (π-π^*) of the benzene ring , while the compound (6) shows peak at (355 nm) for (n-π^*) for the (C=O) group, and at (268 nm) for the transitions of (C=N) group and at (222 nm) for the (π-π^*) of the benzene ring.

The reaction of the compounds (5 & 6) with primary aromatic amines in presence of anhydrous zinc chloride affords the formation of diaryl aromatic amines (7 & 8)a-c , through bimolecular nucleophilic aromatic mechanism , the reaction of compounds (5&6) with primary aromatic in presence of anhydrous zinc chloride furnished the substituted diphenylamines through bimolecular nucleophilic aromatic substitution mechanism [21]. Zinc chloride in this reaction acts as Lewis acid, effects formation of complex ion with hydroxide group, which activate the nucleophilic aromatic substitution by increasing the positivity of the carbon atom linked to OH group, through inductive withdrawing electrons towards oxygen atom, followed by the nucleophilic reaction of the aromatic amine to give the diphenylamine after releasing of the HO-

$ZnCl_2$ complex ion which abstract proton from nitrogen atom and dissociate to H_2O & $ZnCl_2$, as showen in the scheme 1:

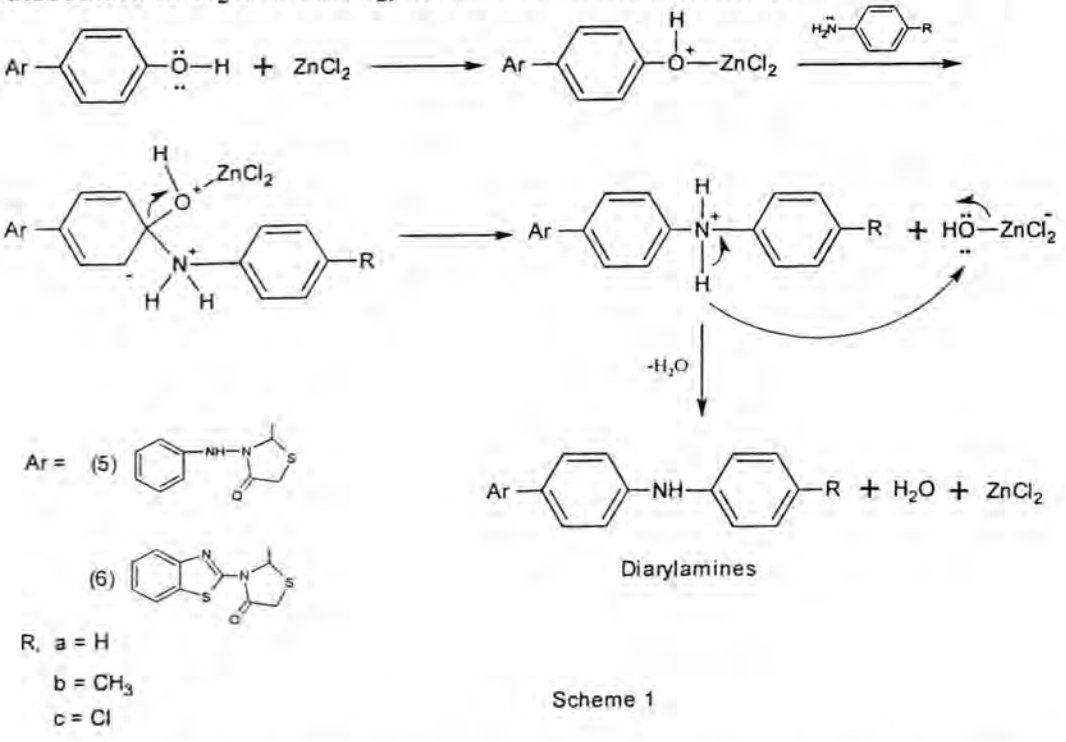

Scheme 1

The structures of these compounds were confirmed through the IR spectrums which shows disappearance of stretching vibrations of (OH) group and appearance of stretching band for (NH) group of the diaryl amines . The UV-Vis spectra for compounds (7 & 8)a-c shows peak at (344 nm) for the transitions (n-π^*) of (C=O) group and absorption peak at (210 nm) for the transitions (π-π^*) of the benzene ring .

The fusion of the diarylamines (7 & 8)a-c with sulphur in presence of elemental iodine affords the phenothiazine derivatives (9 & 10)a-c, through thionation cyclization reaction. The mechanism of this reaction is still not fully clear. The reaction (22) proceeds by fusion with sulphur in presence of organic or inorganic base, the first step is the formation of the S-nucloephile, followed by the addition of sulphur to the double bond in the aromatic ring to creat reactive ylidene sulphur adduct, finally the intramolecular ring closure, to give the three rings heterocyclic compound (phenothiazine). The suggested mechanism could be as shown in the scheme 2 :

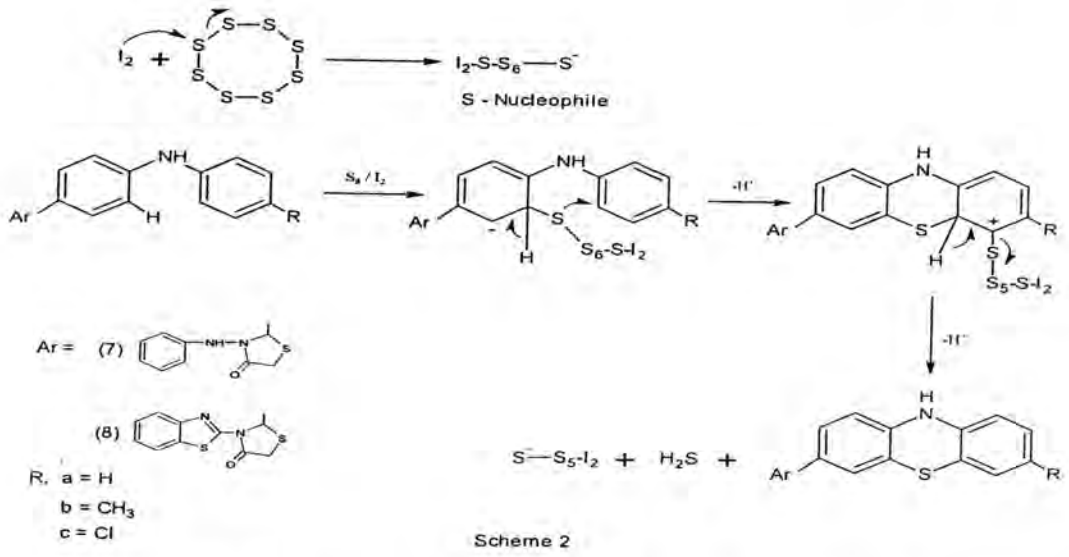

Scheme 2

The structures of these compounds were checked through their spectral data. IR spectra of phenthiazine derivatives shows stretching bands at range (3450-3200 cm^{-1}) belong to (NH) group in phenothiazine ring and bands at (1270-1200 cm^{-1}) of the bond (C-S).

The UV-Vis spectra shows the peaks of the electronic transitions (n-π^*) of the cyclic carbonyl group at (346 nm) and for the transitions (π-π^*) at (216 nm) of the benzene ring.

^{1}H-NMR spectrum for the phenothiazine derivatives shows the following results :

Comp. No.	R	^{1}H-NMR ($CDCl_3$, 300 MH_Z) δ in ppm
9a	H	7.06(2H, arom. Benzene) , 4.0 (1H, proton of amino group in phenylhydrazine) , 5.92 (1H, proton of N-CH-S group) , 6.7-7.08 (6H , aromatic , phenothiazine) , 4.12 (2H, CH_2 group in thiazolidinone) , 6.71-6.79 (3H , arom. Phenothiazine) , 7.37 (2H , arom. Benzene)
9b	CH_3	6.71-6.79 (4H, arom. phenothiazine) , 7.08 (2H, arom. phenothiazine) , 2.34 (3H, methyl group) , 4.12 (1H, proton of NH phenothiazine) , 4.0 (1H, proton of NH phenylhydrazine) , 5.92 (1H, proton of N-CH-S group) , 3.95,3.85 (2H, protons of methylene group in thiazolidinene) , 7.06 (2H, arom. In benzene) , 7.37 (2H, arom. In benzene) .
9c	Cl	7.06 (2H, arom. In benzene) , 7.57 (2H, arom. benzene) , 6.9 (1H, arom. benzene) , 4.0 (1H, proton of NH of phenylhydrazine) , 7.08 (1H, arom. In phenothiazine) , 6.71-6.92 (3H, arom. In phenothiazine) , 7.0,7.14 (2H, arom. phenothiazine) , 4.12 (1H, proton of NH in phenothiazine) , 5.92 (1H, in N-CH-S group) , 3.95,3.85 (2H, of methylene group) .
10a	H	6.44 (1H, proton of methane group N-CH-S) , 3.95,3.85 (2H, protons of methylene group in thiazolidine) , 6.71-6.79 (3H, arom. phenothiazine) , 7.08-7.21 (3H, arom. In phenothiazine) , 4.12 (1H, proton of NH in phenothiazine) , 8.01,8.18 (2H, arom in benzene) , 7.53 (2H, arom. In benzene)
10b	CH_3	6.71-6.79 (4H, arom. In phenothiazine) , 7.08 (2H, arom. In phenothiazine) , 2.34 (3H, protons of methyl group) , 6.44 (1H, proton in N-CH-S group) , 3.95,3.85 (2H, protons of methylene group) , 8.01,8.18 (2H, arom. In benzene) , 7.53 (2H, arom. In benzene) , 4.12 (1H, proton of NH in phenothiazine)
10c	Cl	6.71-6.92 (3H, arom. In phenothiazine) , 7.0-7.14 (3H, arom. In phenothiazine) , 4.12 (1H, proton of NH in phenothiazine) , 6.44 (1H, proton in N-CH-S group) , 8.01,8.18(2H, arom. In benzothiazol) , 7.53 (2H, arom. of benzene ring in benzothiazol)

All the values of the spectral data for all of the derivatives are listed in table (2) and their physical properties are listed in table (1).

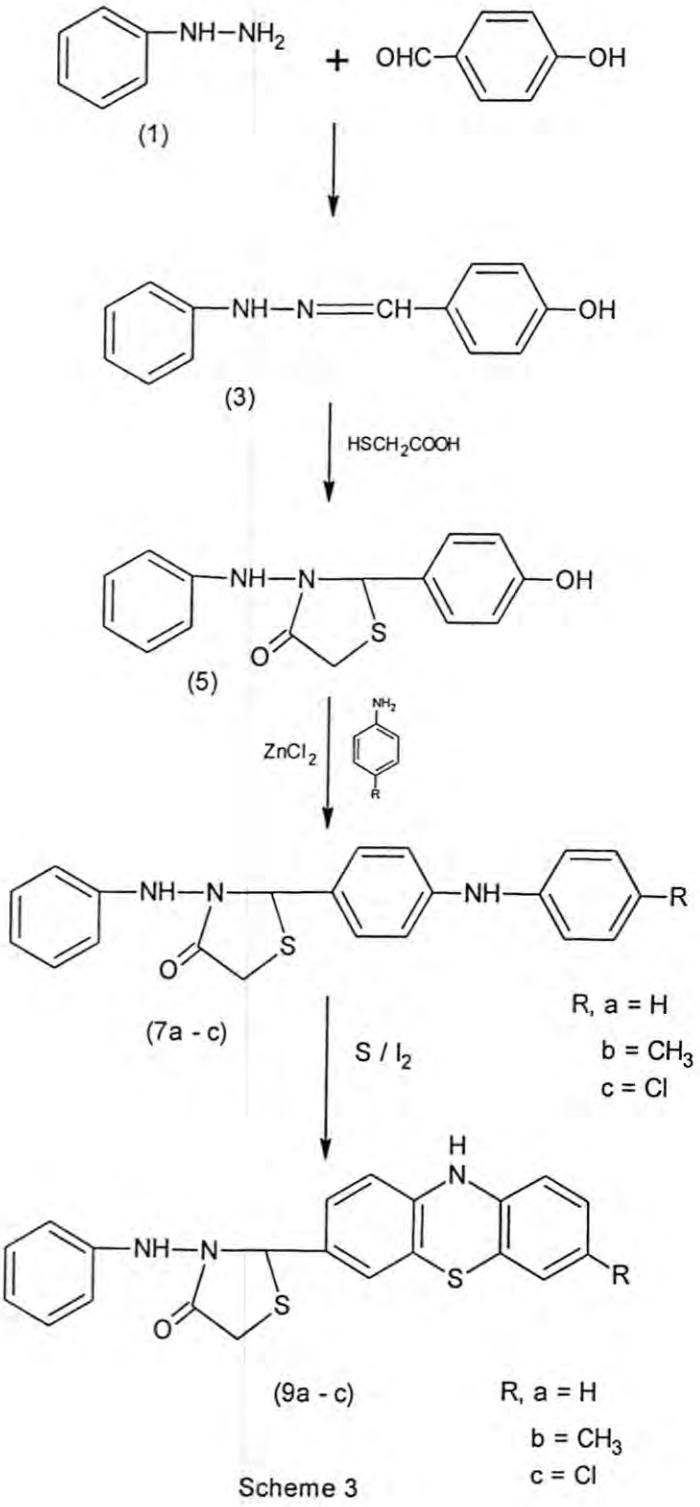

Scheme 3

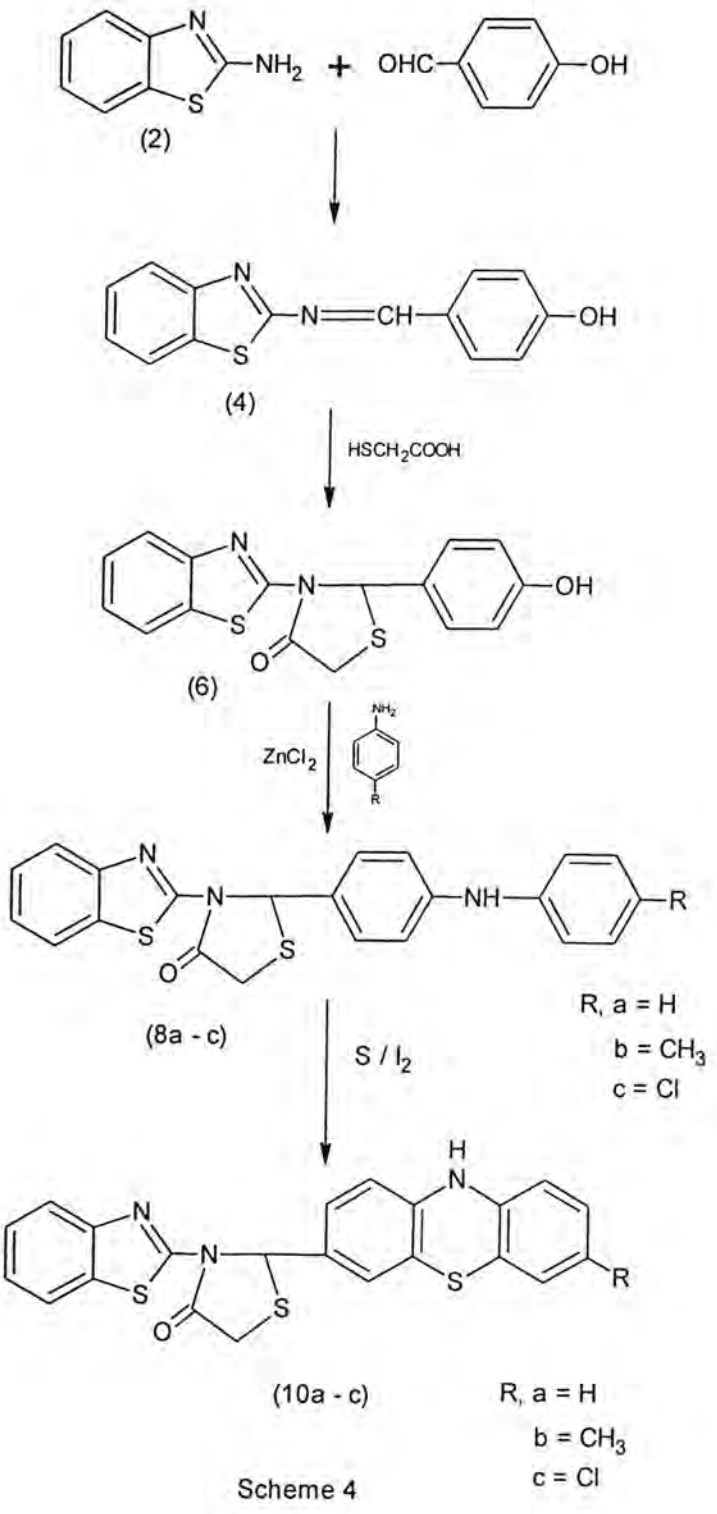
NH2
OHC
OH
(2)
N=CH
OH
(4)
HSCH2COOH
OH
(6)
ZnCl2
NH2
R
NH
R
(8a - c)
S / I2
R, a = H
b = CH3
c = Cl
H
N
S
R
(10a - c)
R, a = H
b = CH3
c = Cl

Scheme 4

Table-1: Physico-Chemical data of synthesized compounds

Comp. No.	R	Recryst. Solvent	Melting Point C°	Molecular Formula	Yield %	Color of ppt.
3		Ethanol	123-125	$C_{13}H_{10}N_2O$	84	Yellow
4		Ethanol	110-112	$C_{14}H_{10}N_2O$	80	Orange
5		Ethanol	135-138	$C_{15}H_{14}N_2O_2S$	72	Pale yellow
6		Ethanol	137-140	$C_{16}H_{16}N_2O_2S_2$	70	Pale yellow
7a-c	a = H	Ethanol	148-150	$C_{21}H_{19}N_3OS$	71	Pale brown
	b = CH_3	Ethanol	138-140	$C_{22}H_{21}N_3OS$	60	Yellow
	c = Cl	Ethanol	145-147	$C_{21}H_{18}N_3OSCl$	63	Orange
8a-c	a = H	Ethanol	178-180	$C_{22}H_{17}N_3OS_2$	70	Pale yellow
	b = CH_3	Ethanol	182-184	$C_{23}H_{19}N_3OS_2$	65	Deep yellow
	c = Cl	Ethanol	170-173	$C_{22}H_{16}N_3OS_2$	63	Pale yellow
9a-c	a = H	Ethanol	169-171	$C_{21}H_{17}N_3OS_2$	61	Red
	b = CH_3	Ether	172-174	$C_{22}H_{19}N_3OS_2$	59	Pale red
	c = Cl	Ether	180-182	$C_{21}H_{16}N_3OS_2$	66	Black
10a-c	a = H	Ether	223-225	$C_{22}H_{15}N_3OS_2$	59	Green
	b = CH_3	Ethanol	219-221	$C_{23}H_{17}N_3OS_2$	67	Green
	c = Cl	Ether	201-204	$C_{22}H_{14}N_3OS_2$	54	Green

Table-2: the spectral data of the synthesized compounds

Compd. No.	UV-Vis λ_{max} nm	FT-IR cm-1				
		υ C-H	υ O-H	υ N-H	υ C=O	Others
3	338 207 283	3053 ar 2980 al	3404	3200		υ C=N 1599 υ C=C 1500,1600 υ C-N 1253
4	269 222	3059 ar 2950 al	3404	3240		υ C=N 1580 υ C-S 1311 υ C-N 1240 υ C=C 1500,1600
5	278 218	3050 ar 2950 al	3545	3460	1700	υ C-N 1350 υ C-S 1261 υ C=C 1500,1612
6	355 268 222	3000 ar 2848 al	3400	3261	1662	υ C-N 1392 υ C-S 1271 υ C=C 1500,1612 υ C=N 1590
7a-c	344 296 254 210	3051 ar 2916 al		3329	1700	υ C-N 1309 υ C-S 1288 υ C-Cl 825 υ C=C 1500,1600
8a-c	268 222 206	3070 ar 2920 al		3400	1699	υ C=N 1500,1600 υ C=N 1612 υ C-N 1265 υ C=C 1512,1589
9a-c	346 242 216	3032 ar 2900 al		3446-3190	1680	υ C=N 1654 υ C-S 1237 υ C-Cl 819 υ C-N 1300 υ C=C 1608,1519
10a-c	277 231 201	3000 ar 2918 al		3441-3209	1699	υ C=N 1645 υ C-S 1271 υ C-N 1349 υ C=C 1610,1520

REFERENCES

1. Ritu S , Pushkal S , Srivastava S. D. and Srivastava S. K., Synthesis and biological activity of 2-oxo-azetidine derivatives of phenothiazine , Org. Commun , 4:2 (2011) 42-51 .
2. Reld W. R, Wright J. R, Koflote H. G, Hunter J. H., Synthesis and antimicrobial activity of 10 N{[(Aryl-)amino]-methyl}3-methoxy-10,10a dihydro-4s-H-phenothiazine-9-Carboxylic acid . J. Am. Chem. 1948, 70 .
3. El-Said, M. K. Pharmazie 1981, 36, 678.
4. Dominguez J. N., Lopez S., Carns J., Iarruso L., Lobo G., Semenow A., Olson J. E., Rosenthal P. J., Synthesis and antimalarial effects of phenothiazine inhibitors of a plasmodium falciparum cysteine protease. J. Med. Chem. 1997: 40 : 2726-2732.
5. Khanna R., Palit G., Srivastava V. K., Shanker K., Newer heterocycles of phenothiazine and their antiparkinsan activity, Indian J. Chem., 1990, 298, 556-560.
6. Leancer D, Mitscher I. A., Organic Chemistry of drug synthesis , Vol. 1, 372-392.
7. Motohasho N., Kawase M., Saito S., Sakagami H., Antitumor potential and possible targets of phenothiazine-related compounds. Curr. Drug. Targets 2000: 1: 237-245.
8. Motohashi N., Kauase M., Saito S., Kurihara T., Satoh K., Nakashima H., Premoulathan M., Arakaki R., Sakagami H., Molnar J., Synthesis and biological activity of N-acylphenothiazines. Int. J. Antimicrob. Ag. 2000, 14(3), 203-7.
9. Swarnkar P. K., Kriplani P., Gupta G. N., Ojha K. G., Synthesis and Antibacterial Activity of Some new phenothiazine Derivatives , E. J. Chem., 2007, 4, 14-20.
10. Gupta S., Ajmera N., Gautam N., Sharma P. and Gauatma D., Novel Synthesis and biological activity study of pyrimido[2,1-b]benzothiazines, Ind. J. Chem., 2009, 488, 853-858.
11. A. D. Baramde , Synthesis and invitro antifungal activity of some novel thiazoles , pharmaceutical chemistry , March 2010 .
12. N. Siddiqui , et al ; Diverse biological activities of Thiazoles, Int. J. Drug Der. & Res., oct-dec . 2011, 3(4) 55-67 .
13. Zhang , Qiu , Zhou , Zhai , Shumei , Yan , Bing ; Natural product-Inspired Synthesis of Thiazolidine and Thiazolidinone Compounds and their Anticancer Activities ; Current pharmaceutical Design , V16, No. 16, p 1836-1842 , June 2010 .
14. V, Kumar , K. Yashovardhan , S, Kumar ; Synthesis of new 10-substituted phenothiazines and anti-inflammatory and analgesic agent , Int. J. of phom. Bio. Sci., 2010; Vol. 1, issue-3 , 1-10 .

15. Ashraf A. Khalil, Sami G. Abdel Hamide , Abdul rahman M. Al-Obaid and Hussein I. Al-Subbagh,; Substituted quinazolines , part 2 , Synthesis and invitro anticancer evaluation of new 2-substituted mercapto-3-H-quinazoline analogs , Arch. Pharm. Med. Chem.; 2003 , 2, 95-103 .
16. Himani N. Chopde, J. S. Mesharm and R. Pagadala ; Synthesis – Characterization and antibacterial activity of some new 3-(aryl)-1-(4-quinoline-8-yl) amino)phenyl] prop-2-en-1-one , Schol. Res. Lib. 2010, 2(3) , 294-300 .
17. A. O. Fitton and R. K. Smalley , Practical heterocyclic Chemistry , Academic press , London and New york , 1968 , p 128.
18. Williamson and Fleming , Spectroscopic methods in Organic Chemistry 2nd Ed , McGraw Hill , London , 1973 .
19. M. T. Shreenivas , B. P. Chetan and A. R. Bhat , Synthesis and Pharmacological Evaluation of Certain Schiff bases and Thiazolidine Derivatives as ATI Angiotension-II (AII) Receptor Antagonists , J. Pharm. Sci. and Tech. Vol. 1(2) 2009 , 88-94.
20. R. M. Silverstein , F, X. Webster , D. J. Kiemle , Spectrometric Introduction of Organic Compounds , 7th Ed .; John Wiley & Sons , USA , 2005 .

Synthesis and Spectroscopic study of 2-methyl-1,3- oxazole-5(4H)-one Derivatives

Zeina Kudair Hassan AL-Dulaimy
Department of chemistry, College of Science, AL-Mustansiriyah University

Received 30/1/2011 – Accepted 20/6/2012

الخلاصة

في هذا البحث تم تحضير المركب (2-methyl-1,3-oxazol-5(4H)-one) (A) من تفاعل الكلايسين مع أنهدريد الخليك وبمفاعلة المركب (A) مع عدد من الألديهايدات المختلفة أعطت قواعد شيف (a3-a1) وعند تفاعل هذه المركبات مع الهيدرازين المائي ($NH_2NH_2.H_2O$) تم الحصول على مشتقات الايميدازول (a4-a6). وحضرت قواعد شيف اخرى (a15-a7)، إضافة إلى تحضير مشتقات البيتا لاكتام (a24-a16). وقد شخصت هذه المركبات بواسطة درجة الأنصهار و FT-IR و UV.Vis.

ABSTRACT

2-methyl -1,3-oxazole -5(4H)- one (A) was synthesized from the reaction of glycine with acetic anhydride . The end product (A) was reacted with different aldehydes to from Schiff basses (a1-a3). Furthermore, the reaction of these Schiff basses with hydrated hydrazine afforded Imidazole derivatives (a4-a6). Another Schiff basses (a7-a15) and β-Lactam derivatives (a16-a24) were then prepared. The structures of the synthesized compounds were confirmed by their melting point , Infrared and UV-Visible spectra.

INTRODUCTION

Many heterocyclic compounds are biosynthesized by plants and animals and are biologically active. Imidazole is incorporated into many important biological molecules, the most pervasive is the amino acid histidine, which has an imidazole side-chain. Histidine presents in many proteins and enzymes and plays a vital part in the structure and binding functions of hemoglobin.

Imidazole has become an important part of many pharmaceuticals. Synthetic imidazoles are present in many fungicides and antifungal, antiprotozoal, and antihypertensive medications. Imidazole is part of the theophylline molecule, found in tea leaves and coffee beans, that stimulates the central nervous system. It is present in the anticancer medication mercaptopurine, which combats leukemia by interfering with DNA activities [1-4].

Moreover, 1,3-oxazole derivatives are interesting series of heterocyclic compounds which have been shown to be diverse fungicidal and bacterial properties [5-9]. Also, Schiff bases have widely reported to be biologically versatile compounds having antifungal herbicidal and plant growth regulating properties [10-11].

The final product in this research, β-Lactam, represent a broad class of antibiotics, consisting of all antibiotic agents that contains a β-Lactam nucleus in their molecular structures. This includes penicillin derivatives (penams), cephalosporins (cephems), monobactams and carbapenems [5].

In view of these observations, new derivatives have been synthesized by groups linked of these moieties which might result in potential biologically active agents.

4-Benzylidene -2-phenyl -1,3-oxazol-5(4*H*)-ones (azloctones) are compounds with a significant synthetic potential and several biological and technological applications [9-13]. The compounds can be for example, used as inhibitors of the enzyme activity or as fluorescent sensors[12-13].

MATERIALS AND METHODS

Melting points were measured in open capillary tubes on a Gallenkamp melting point apparatus and were uncorrected.

The IR. Spectra (KBr) disc were recorded with shimadzu-2N, FTIR-8400S. UV spectra were recorded on varian, UV-Vis spectro photometer using absolute ethanol as solvent.

1- Synthesis of 2-methyl-1,3-oxazole-5(4*H*)-one[14] (A):

A mixture of amino acid (glycine) (o.o67mole) and (o.o67mole) acetic anhydride was refluxed for 3hr. Excess of acetic anhydride was evaporated and the residue was purified by column chromatography silica gel and mixture of (ethanol:water)(7:3) as eluant and recrystaltized from methanol to give compounds (A).

2- Synthesis of 4-(4-substitution benzylidine)-2-methyl-1,3-oxazole -5(4H)-one (a1-a3) [15]:

A mixture of compound (A)(0.005mole), Aryl aldehyde (0.005mole) and anhydrous sodium acetate in glacial acetic acid/acetic ahydride (30+10)ml was reflued for 3hr. the reaction mixture was allawed to cool and was poured in to water (100ml) . the solid substance was filtered off and recrystallized from dioxane to give the product.

3- Synthesis of 3-Amino-5-(4-substitution benzylidene)-2-methyl-3,5-dihydro-4H-imidazol-4-one (a4-a6) [14] :

A solution of compound (a1-a3) (0.01mole) in dry Benzene (10ml), hydrazine hydrate 80% (0.015mole) was added. The mixture was refluxed for (7hr.) the solvent was removed and the solid product was collected and crystallized from methanol.

4- Synthesis of 5-(4-substitution benzylidene)-3-{[(4-substitution phenyl) methylene] amino}-2-methyl-3,5-dihydro -4H-imidazol -4-one (a7-a15) [16] :

General procedure:

To stirring solute of compound (a4-a6) (0.01)mole in absolute ethanol (15ml) and appropriate aldehydes (0.01mole) was added, the mixture was refluxed for (6hrs) then cooled to room temperature. the precipitate was filtered and recrystallized from ethanol.

5- Synthesis of 5-(4-substitution benzylidene)-3-[2-(4-substitution phenyl) -3-phenyl -4-oxoazetidin-1-yl] -2-metyl-3,5-dihydro-4H-imidazol-4-one (a16 - a24) [17-18] :

To a suspension of phenyl Acetic acid (0.005)mole , Schiff Bases (a7-a15) (0.005mole) and triethylamine (0.01mole) in 40ml of dry dichloro methane , was added dropwise , under nitrogen atm at OC° asolution of Thionyl chloride (0.1 mole) in 20ml of dry dichloro methane the constant stirring , The reactants were stirred over night at room temperature , Thereafter , The contents were washed successively with (1N)HCl (30ml) , water (3X30ml) ,5% NaHCO3 (30ml) and brine (30ml). The organic Layer was separated and dried over an hydrous sodium sulphate (Na2SO4). The solvent was removed under reduced pressure and the crude product was column chromotographed over silica gel using ethyl acetate – hexane (3:7) as eluent , solvent evaporation furnished pure β –Lactam .

RESULTS AND DISCUSSION

The starting material for the synthesis of the targeted compound (A) which was prepared by reaction of glycine with acetic anhydride according to the reported method [14].

Reaction between (A) and different aldehyde afforded the compounds (a1-a3) in a good yield.

The IR spectra showed the (C=O) stretching at (1656 cm^{-1}) and (C=N) in (1260 cm^{-1}) . The reaction between compounds (a1-a3) and hydrazine hydrate afforded the N-amino derivatives (a4-a6) (scheme (1)) (table-1-).

The spectrum showed the (N-H) stretching absorption near (3358-3282 cm^{-1}) and the (C=O) stretching one (1670cm^{-1}). UV. Spectrum of compound (a4-a6) mostly showed intense maxima at 220nm and 309nm belonged to $\pi \rightarrow \pi^*$ and $n \rightarrow \pi^*$ electronic transition respectively. Condensation of compounds (a4-a6) with aryl aldehyde in absolute ethanol gave Schiff bases (a7-a15) (scheme(1)) (table-2-) . the formation of these azomethines was indicated by the presence in their IR spectra of the azomethine (CH=N) stretching band at (1610-1615)cm^{-1} combined with the disappearance also of the NH2 streching band . UV. Spectra showed mainly intense maxima at (205-221)nm and (309-382)nm which belonged to $\pi \rightarrow \pi^*$ and $n \rightarrow \pi^*$ transition respectively. Treatment of some above Schiff bases with SOCl2 and dichloro methan led to the ring closure (a16- a24) table (3) . the IR spectra of these derivatives showed the disappearance of bands (CH-N) in the region (1610-1615)cm^{-1} combined with the appearance of absorption bands at (1675-1705) cm^{-1} and (C-Cl) stretching bands . UV. Spectra of these derivatives showed intense maxima at (232-236nm) and (303-322nm) due to $\pi \rightarrow \pi^*$ and $n \rightarrow \pi^*$ transitions.

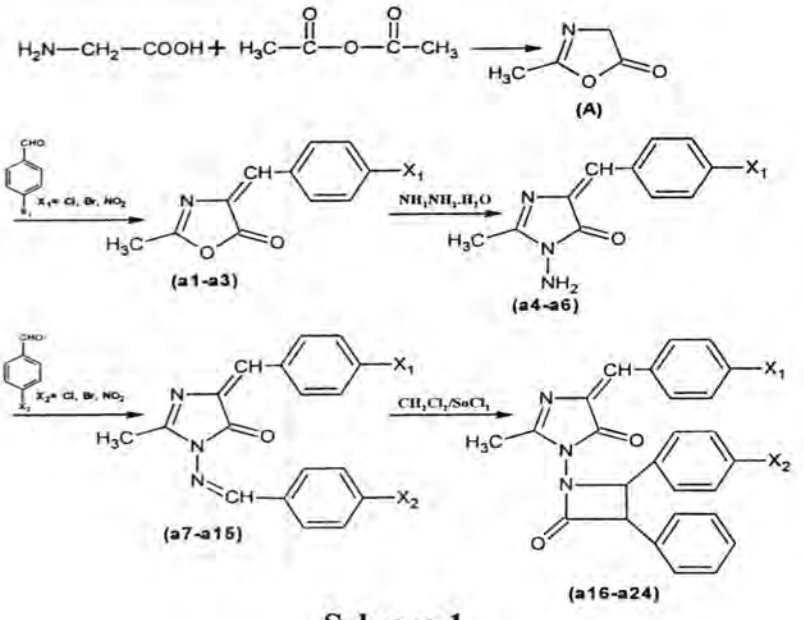

Scheme 1

Table-1: Properties of compounds (a1-a5)

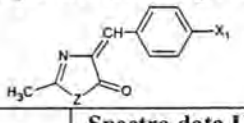

Comp. No.	Z	X1	Mp. C°	Spectra data UV Λ max (EtOH)	I.R cm^{-1}
a1	-O-	Cl	132-134	220-309	1656(C=O),3082(C=H) 585(C=C), 1201(C-O)808(C-Cl),1620 (C=N)
a2	-O-	Br	165-168	215,330	1695(C=O), 3070(C-N) 560(C=C), 1210(C-O) 758(C-Br),1600(C=N)
a3	-O-	NO_2	118-120	308,259,208	1615(C=O), 3050(C-H)580(C=C), 1230(C-O) (C-NO_2)
a4	N-NH_2	Cl	195-197	309,220	3358, 3282 (N-H), 3034(C-H) 1670(C=O), 1591(C=C) 810(C-Cl), 1219(C-O) 1600(C-N)
a5	N-NH_2	Br	169-172	307,259,208	3350, 3280(N-H), 3030(C-H) 1687(C=O), 1590(C=C) 723(C-Br), 1219(C-O)

Table-2: Properties of compounds (a7-a9)

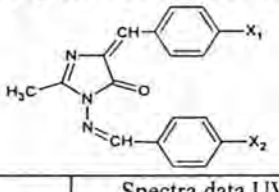

Comp. No.	X1	X2	Mp. C°	Spectra data UV Λ max (EtOH)	I.R cm^{-1}
a7	Br	Br	157-159	205, 221	1610-1615(C=N), 1680(C=O), 704(C-Br), 1583(C=C ar.)
a8	Br	No2	198-201	309-220	3080(C-H ar.),1699(C=O) 1624(C=N), 1583(C=C ar.) 1398,1629(NO_2),700(C-Br)
a9	Br	Cl	199-203	309, 221	3040(C-H ar.),1688(C=O) 1615(C=N), 1587(C=C ar.) 702(C-Br), 808(C-Cl)

Table-3: Properties of compounds (a19-a24)

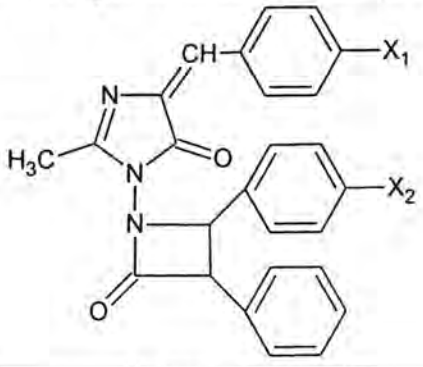

Comp No.	X1	X2	Mp. C°	Spectra data UV Λ max (Et oH)	I.R cm^{-1}
a19	NO	Br	154-156	232-236	3091(C-H ar.), 2943(C-H al.), 1698-1675(C=0), 1545(C=C), 1348(NO_2), 725(C-Br)
a20	NO	NO_2	145-147	204-233	3010(C-H), 2920(C-H), 1694(C=O), 1587(C=C), 1348(C-NO_2)
a21	NO	Cl	141-143	309,235	3030(C-H), 2929(C-H), 1690-1697(C=O), 1545(C=C), 801(C-Cl)
a22	Cl	Br	184-186	206,230,280	3091(C-H) , 2956(C-H), 1688(C=O), 1584(C=C), 721(C-Br)
a23	Cl	NO_2	157-159		3050(C-H), 1695-1677(C=O), 1583(C=Cl), 1453(NO_2)
a24	Cl	Cl	89-93		1680(C=O), 1624(C=N), 3070(C-H ar.), 1587(C=C), 808(C-Cl)

REFERENCES

1. Shargel L., Comprehensive Pharmacy Review, 6th edition, p930.
2. ARKIVOC, (V) 48-61, (2002).
3. Mar. Drugs,7,705-753, (2009).
4. Synthesis of imidazole Schiff base ligands, their silver(I) complexes and their activities against candida Albicans a thesis .
5. Holten K.B., Onusko E.M., "Appropriate Prescribing of Oral Beta-Lactam Antibiotics", Am Fam Physician, 62(3) :611-620, (2000).
6. Bath H. S., "Inorganic synthesis", Mc Gram-Hill Book, New York and Landon, 485, (1939).
7. Al-Rawi J. M., AL-Shahiry K. F., "Synthesis of oxo -2-thio-3,4-dihydro -2H-1,3-shbsitiuted benzoxaxine-Their Transformation with water diazomethane and Amines", Asian J. of chem., 2 :343-350, (1990).
8. Ibrahim M. N., Saeed M. and Fadhil S., "Carbon 13 spectral of some Unsaturated Amino acids and dihydro-peptides derived from oxaze L-5- one", Iraqi, J. chem. soc., 12, 179, (1987).
9. Ballamy L. J., "The infrared spectra of complex Molecule" second Edition , Methuen , London, (1958).

10. AL-Bayati R. I., Al-Rwai, J. M. and AL-Naimi K. H., "Reaction of 2,4-dioxo-3,4- dihydro -2H-1,3-benzoxazine with some secondary Amines". Iraqi J. of chem., 23, 2, (1997).
11. Al-Bayati R. I., Al-Rawi J. and Al-Naimi K. H., "Studies on the reaction of substituted -4- oxo-2- thio and 2,4-dioxo -3,4-dihydro - 2H- 1,3-benzoxazine", Muth J., 9 :243-262, (1994).
12. Al-Bayati R. I., Thani M. Z. and Abdullah A. M., "Synthesis of new 4-amino-1,5- dimethyl-2-phenyl-pyrazol-3-derivatives", Journal of college of Education, 3, :79-86, (2008).
13. Roui I. H, "Synthesis and biological activity of some new Twin compounds containing hetero cyclic unit", Al-Mustansiriya J.Sci, 19(4) :41-52, (2008).
14. Mukerjee A. K., Hetrocyclic, 26 :1077-1097, (1987).
15. Fisk J. S., Mosey R. A., Tepe J., J. chem. soc. Rev., 36 :1432-1440, (2007).
16. Kham K. M., Mughal U. R., Khan M. T. H., Z. Ullah, Perrn. S., Choudhary M. I., Bioorg. Med. chem.,14 :6027-6033, (2006).
17. Khan K. M., Mughal U. R., Lodhi M. A., Chaudhary M. I., Lett. Drug Design Discovery, 5 :52-56, (2008).
18. Kitazawa M., Higuchi R., Takahashi M., Wada T., Sasabe H., J.phys. chem., 99 :147-92, (1995).
19. Sharba A. K., AL-Bayati R. H., Aouod M. and Rezki N., Molecules, 10 :1161-1168, (2005).
20. Shuka S. B., Horan A. A., amino Acta., 40 :80-85, (1997).
21. Rowi I. H., "Synthesis and biological activity of some new Twin compounds containing heterocyclic unit", Al-Mustansiriya J. sci. 19(4) :41-52, (2008).
22. Alcaide Bi., Almendros P., Salgado N. R., A. J. org. Chem., 65 :44-53, (2000).
23. Madan S., Arora R., Venugopalan P., Bari S. S., Tetrahedron Lett, 41 :55-77, (2000).

Accelerated Stability Evaluation of Captopril Tablets

Hayder Hamed Abed
College of dentistry, Al - Mustansiria University

Received 7/4/2011 – Accepted 17/1/2012

الخلاصة

يعد الكابتوبريل من علاجات الواسعة الاستخدام في ضبط ضغط الدم المرتفع. يعمل الكابتوبريل على خفض التضخم عند مرضى عجز القلب واعادته الى المستوى الطبيعي من خلال خفض ضغط القلب وتقليل الجهد على القلب. كما يظهر تأثير فسلجي على مستلمات الانسولين (تيروسين كاينيز). يعد اختبار الاستقرارية من اهم الاختبارات التي تجرى على الادوية و المستحضرات الدوائية لبيان كفاءة وصلاحية الادوية والمستحضرات عند الخزن ومدة الخزن الواجب اتباعها مع الظروف الملائمة لبقاء المستحضر ضمن المواصفات والمحددات الدستورية.

نم اجراء اختبار الاستقرارية المسرعة على ثلاث نماذج مختلفة من حبوب الكابتوبريل 25 ملغ بدون تكسيه والمطابقة للمواصفات الدستورية الامريكية. تم الخزن حسب مواصفات دراسات الاستقرارية المعتمدة في هذا المجال من درجة حرارة و رطوبة. اظهرت النتائج عدم وجود تغير ملحوظ في تركيز الكابتوبريل عند الخزن مع استقرار الصفات الكيميائية والفزيائية (مثل اللون، الوزن، القساوة، زمن التكسر و الانحلالية) . كما تم حساب عمر صلاحية حبوب الكابتوبريل المنتجة من خلال تطبيق معادلة ارنيوس.

بينت النتائج استقراريه المنتج لثلاث سنوات عند الخزن بدرجة حرارة الغرفة. كما بينت النتائج كفاءة طريقة التحضير وجودة التركيبة المستخدمة. قادت نتائج طريقة حساب الاستقرارية الى معلومات مميزة وأظهرت الملائمة مع حبوب الكابتوبريل وكفاءة الطريقة المستخدمة عند التحضير للكميات الكبيرة.

ABSTRACT

Captopril is one of the most important drugs used to control high blood pressure and help in the relief of chronic heart failure. It may have an effect on reduction of left atrial size in mild to moderate hypertension and on insulin receptor (tyrosine kinase) activity in essential hypertension.

Three different batches of Iraqi manufactured captopril tablets were investigated in this research for stability condition. The collected data of assays represent non significant ($p>0.05$) changes during the storage period with no changes in physico-chemical properties (color, weight variation, hardness, disintegration, and dissolution). The shelf life of tablets were calculated using Arrhernues equation. The estimation of product shelf life predicted three years validity at room temperature storage.

The study concluded that the used formula in manufactured tablets were very stable for three year of date of manufacturing and very suitable for mass production. The applied stability method was very useful in providing information about the stability of manufactured tablets and provides an efficient investigation for mass production.

Key word : captopril, accelerated stability study, Arrhenues equation.

INTRODUCTION

Captopril [(2S)-1-[3-mercapto-2-methylpropionyl]- L proline] has been widely used in medicine as an angiotensin-converting enzyme inhibitor since 1981, for the treatment of hypertensive and congestive heart failure patients Captopril has also been postulated as a free radical scavenger because of its terminal sulfhydryl group. [1] In vitro a combination of captopril with aspirin significantly inhibitors the platelet

aggregation Captopril shows 75% bioavailability but presence of food reduces the oral absorption by 30-50% [2].

Several methods have been reported for the quantitative determination of captopril in formulations and biological fluids. [3] A method based on the oxidation of captopril with excess potassium permanganate and measuring the remaining drug using different dyes was reported, however the United States pharmacopeias were reported very efficient procedure for determination of captopril in pharmaceutical preparations by using high performance liquid chromatography. [4,5]

International conference of harmonization and world health organization guidelines were provided successful method for determination of stability of pharmaceutical products. The major advantage of this method to develop pharmaceutical formulations is that the potential factors could be studied simultaneously, systematically and quickly. By using design of experiments, the effect of each formulation factor on each response can be evaluated and critical factors can be identified based on statistical analysis.[6] In addition, the United States Pharmacopoeia (USP) requirements and the International Conference on Harmonization (ICH) guidelines all provide various techniques that are widely used to monitor the possible decomposition pathways and degradation products. Understanding of the nature of active compounds in a combination formulation is the essential component of a successful product development. More importantly the stability, physical and chemical compatibility is the primary concern when facing complicated combinations of drugs in the design formulas [7,8].

The aim of this study is to investigate an Iraqi manufactured Captopril tablets (uncoated 25 mg.) in term of shelf life in a different accelerated stability condition, stability of formula in drastic condition and its liability for mass production. No such stability study were observed to the time of writing of this research.

MATERIALS AND METHODS

A high purity chemicals and reagents were used in this study for analytical purposes (complying the U.S. pharmacopeia's). Tablets investigated in this study were manufactured by AL - Safa pharmaceutical company, tablets, packed in aluminum plaster. each sheet contain 10 tablets. The manufacturing properties were comply the U.S. pharmaceutical criteria.[9] Three different batches of studied tablets were selected and stored for accelerated stability conditions. All reported result predicted the average of these three batches.

initial physical properties of tablets are listed bellow:-

Test	Initial Result	Normal range
Color	White color tablet	White color tablet
Weight variation	3.35	NMT 5 %
Tablets weight (mg.)	0.13	NMT 5%
Hardness (kg/cm2)	4.33	NMT 5 %
Disintegration (minutes)	3.57	NMT 5 minutes
Dissolution (as %)	88.62	NLT 80 %
Assay (%)	93.25	90-110 %

Where NMT: not more than

Investigated stability conditions :

The storage stability conditions were performed by using thermo lab oven with temperature range of 25-180 °C ± 1 °C. The applied storage condition were listed below:

Temperature in centigrade	% Relative humidity
Room temperature (25 °C ± 2°C)	35 % ± 5%
40 °C ± 2°C	40 % ± 5%
50 °C ± 2°C	65 % ±5%
60 °C ± 2°C	75 % ±5%

Captopril assay method:

The sassy of tablets were achieved according the USP method:

Mobile phase: A filtered degassed mixture of 550 ml methanol and 450 ml of water contained 0.50 ml of phosphoric acid .

Standard preparation: suitable quantity of U.S. pharmacopeia's reference standard in mobile phase to obtain a solution having know concentration of about 1 mg. / ml and 0.05 ml, respectively.

Assay preparation: Transfer not fewer than 20 tablets to a suitable volumetric flask, add mobile phase to fill the flask to about half of its capacity, and sonicated for 15 minutes. Dilute with mobile phase to volume, shake by mechanical means for 15 minutes, and filter [9].

Chromatographic system:

The liquid chromatograph is equipped with 220 nm detector and a 4.6mm X 25 cm column that contains packing C18 with about 1 % load. the flow rate is about 1 ml per minute. Chromatograph the standard preparation, recorded the peak response as directed in procedure, the relative retention times are about 0.5 [10].

Procedure:

Separately inject equal volumes (20 µL) of the standard preparation and the assay preparation into the chromatograph, recorded the chromatograms, and measured the response for the major peak. The quantity of Captopril in tablets by using the formula:

$$(L/D)C(ru/rs)$$

In which L is the labeled amount in mg. of captopril in each tablet. D is the concentration in mg./ml of captopril in the assay preparation based on labeled quantity per tablet and the extent of dilution, C is the concentration in mg, per ml of captopril united state pharmacopeia's reference standard , and ru and rs are captopril peaks responses obtained from the assay preparation and the standard preparation, respectively [11].

RESULTS AND DISCUSSION

All analysis were performed by using SPSS -15 and Microsoft axel .

The physco-chemical properties of captopril tablets are listed in table

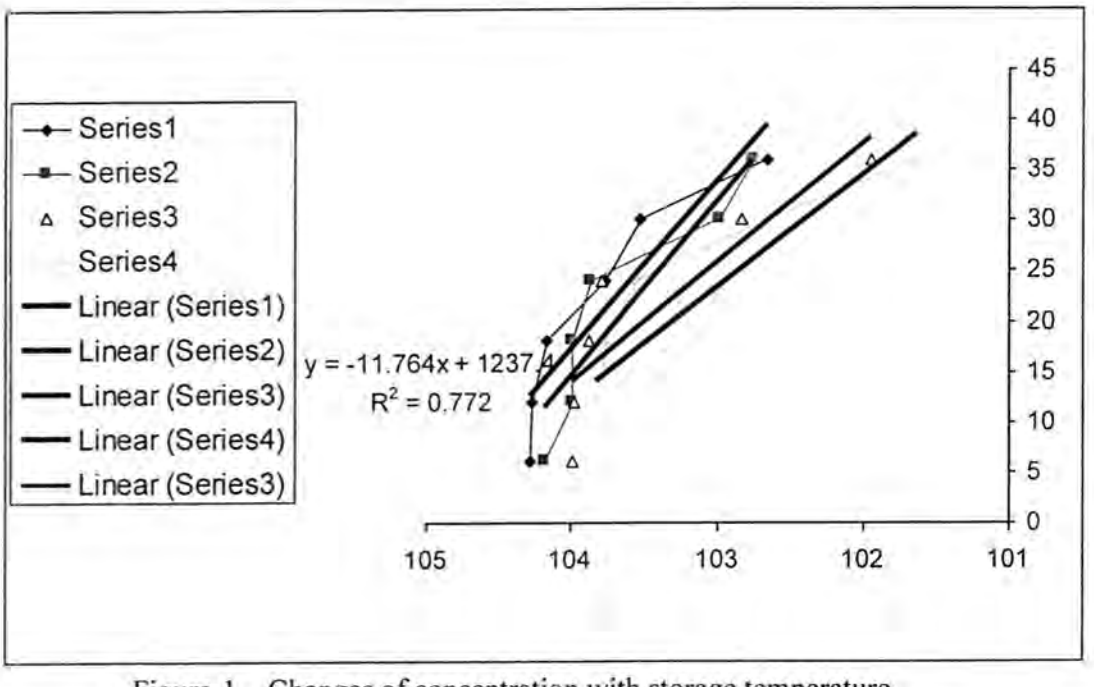

Figure-1. Changes of concentration with storage temperature

Where Series 1 represent the room temperate
Series 2 represent 40 °C
Series 3 represent 50 °C
Series 4 represent 60 ° C

Table-1: The physco-chemical properties of captopril tablets.

Conditions		Assay	Color	Weight variation	Disintegration	Hardness $Kg./cm^2$	dissolution
R.T	30 days	104.255	White	3.34	4.22	4.33	88.62
	60 days	104.160	White	3.34	4.22	4.33	88.62
	90 days	103.985	White	3.34	4.22	4.34	88.62
	120 days	103.927	White	3.34	4.22	4.34	88.62
	150 days	103.935	White	3.34	4.22	4.34	88.60
	180 days	103.896	White	3.34	4.22	4.34	88.60
40 °C	30 days	104.117	White	3.34	4.22	4.34	88.60
	60 days	103.976	White	3.34	4.22	4.34	88.60
	90 days	103.897	White	3.34	4.22	4.34	88.60
	120 days	103.872	White	3.34	4.22	4.35	88.56
	150 days	103.869	White	3.34	4.22	4.35	88.56
	180 days	103.834	white3	3.34	4.22	4.35	88.56
50°C	30 days	104.016	White	3.34	4.22	4.35	88.56
	60 days	103.876	White	3.34	4.22	4.35	88.53
	90 days	103.869	White	3.34	4.22	4.35	88.53
	120 days	103.739	White	3.34	4.22	4.35	88.53
	150 days	103.681	White	3.34	4.22	4.35	88.53
	180 days	103.668	White	3.34	4.22	4.36	88.53
60 °C	30 days	103.925	White	3.34	4.22	4.36	88.50
	60 days	103.765	White	3.34	4.22	4.36	88.48
	90 days	103.628	White	3.34	4.22	4.36	88.48
	120 days	103.486	White	3.34	4.22	4.36	88.42
	150 days	103.071	White	3.34	4.22	4.37	88.42
	180 days	102.865	White	3.34	4.22	4.37	88.37

The changes in concentration with temperatures (room temperature, 40 °C, 50 °C, and 60 °C) are plotted in figure 1.
The evaluated Arrhenues Activation energy were listed in table 2.
The evaluated slope values are for Arrhenues activation constant are listed in table 3.
The slop values for activation constant with concentration are listed table 4.

Table-2: The evaluated activation constant (Ka).

Temperature	Slope from direct plot of K a With 1/T
Room temperature	0.25
40 ° C	0.03
50 °C	0.37
60 ° C	0.43

The evaluation of expiration date with time are listed in table -5

Table-3: The evaluated Captopril tablets life in years.

Temperature	T *90* / years
Room temperature	3.48
40 ° C	2.90
50 °C	2.37
60 °C	2.02

Where T 90 represent the degradation time for 90 % of original concentration of the evaluated tablets.

Statistical evaluation:

All analysis were performed by using SPSS -10 and Microsoft axel.

The statistical evaluation of tablets assays:

Test	Result
Mean	103.8047
Std. Error of Mean	6.326E-02
Median	103.8740
Mode	103.87
Std. Deviation	0.3099
Variance	9.605E-02
Skewness	-1.708
Std. Error of Skewness	0.472
Range	1.39
Minimum	102.87
Maximum	104.26
Sum	2491.31
Percentiles 25	103.6955
50	103.8740
75	103.9658
Sig.	Non significant

Captopril usually manufactured into two pharmaceutical formula 25 and 50 mg. Captopril compounds considered very sensitive to light and heating changes [13]. No changes were recorded out of the U.S. pharmacopeias criteria. All collected physical parameter were predicted stability without any changes in tablets. However, This result consider very important for active gradients [14].

Accelerated stability and long term stability considered one of the most effected methods for evaluation Captopril stability in designed formula. The applying of Arrhenues equation provided, accurate, simplest and sophisticated method for evaluation the tablets life during the study. [15] The collected assays predicted long life for the used formula and long stability in drastic storage conditions, however all collected data predicted non significant changes for the active substances. The non significant changes predicted the stability of tablets during changes of temperature and humidity. However, all Collected

assays predicted changes in Captopril assays values with elevated temperature but it remain within the accepted limit of united state pharmacopeias. The raising of temperature during storage reduce the storage time, this could be attributed to the sensitivity of Captopril to temperature changes. The stability data recorded non significant changes of physical properties for the tested tablets.

High analysis performance liquid chromatography provided fast sensitive method of evaluation of captopril in tablet matrix. [15] The analysis procedure were observed free from any technical problems or any other analytical difficulties, thus help us to collect wide range of result in short time period. The degradation of captopril with storage time in the investigated temperatures were have a randomly behavior. This randomly result required ANOVA plotting of the result to evaluate the degradation slope and evaluated the Arrhenues constant for evaluation expiration date.Many research were recorded such result and report the requirements of statistical evaluation to solve the problem. [16-18]

We concluded that the investigated stable were very stable for more than three years from the time of manufacturing without any changes in physico-chemical properties.

REFERENCES:

1. Bhuyan, KC., Bhuyan, DK., Santos, O. and Podos, SM.. Antioxidant and anti cataractogenic effects of topical captopril in diquat-induced cataract in rabbits. *Free Radical Biology and Medicine* **12**: 251 (1992).
2. Abubkar O Nur, Zhang JS. Recent progress in sustained/controlled oral delivery of captopril: An overview. Int J Pharm; 194: 139-146, (2000).
3. Zhou XH, Li Wan PA. Stability and in-vitro absorption of captopril, enalapril and lisinopril across the rat intestine. Biochem Pharmacol; 47: 1121- 1126 (1994)
4. Parfitt K, Martindale W. *Martindale: the Complete Drug Reference*. 32nd ed. London, UK: Pharmaceutical Press; 836, 7 (1999).
5. Deray G. Captopril pharmacokinetics. *Br J Clin Pharmacol.* **20:** 90 – 2 (1985).
6. Food and Drug Administration Guideline for submitting Documentation for the stability of Human Drugs and Biologics, U.S Department of Health and Human services, Washington DC (1987).
7. Guidance for Industry: Q1E Evaluation of Stability Data. U.S Department of Health and Human Services, FDA, CDER, CBER, Rockville, MD, ICH, June (2004).

8. Rajesh H. Parikh., Stability of pharmaceuticals, *Pharma Times,* 18, 16-17 (1986).
9. The united state pharmacopeias, USP-30, NF -25 (2007).
10. Amini M, Zarghi A, Vatanpour H. Sensitive high performance liquid chromatographic method for determination of captopril in plasma. *Pharm Acta Helv.* **73:** 303 – 6 (1999).
11. S.A. Shama, A. E. Amin, H. Omara . J Quantitative Spectroscopy & Radiative Transfer. vol. 102, pp. 261–268 (2006).
12. A. V. Chobanian, G. L. Bakris, H. R. Black, W. C. Cushman, L. A. Green, J. L. Izzo Jr., D. W. Jones, B. J. Materson, S. Oparil, J. T. Wight Jr. and E. J. Rocella, Seventh report of the joint national committee on prevention, detection, evaluation, and treatment of high blood pressure, *Hypertension* **42,** 1206–1252 (2003).
13. L. Xu, F-M. Shen, H. Shu, C-Y. Miao, Y-Y. Jiang and D-F. Su, Synergism of atenolol and amlodipine on lowering and stabilizing blood pressure in spontaneously hypertensive rats, *Fund. Clin. Pharmacol.* **18,** 33–38(2004).
14. Pal Sprauten1,2, Paul Beringer2, Mark Gill2, Stan Lloue, and Tim Synold , Temperature Stability And Antibacterial Activity Of Cefepime (CFP) During Continuous Infusion (CI) Administration-3 University of Oslo1, Norway; Laboratory for Pharmacodynamic Research, University of Southern California2 School of Pharmacy; City of Hope3, Duarte, CA. (2010).
15. Bald, E., Sypniewski, S., Drzewoski, J. and Stepien, M. Application of 2-halopyrinidium salts as ultraviolet derivatization reagents and solid-phase extraction for determination of captopril in human plasma by high performance liquid chromatography. *Journal of Chromatography B: Biomedical Applications* **681**: 283 (1996).
16. B. R. Mathews, Regulatory aspects of stability testing in Europe, *Drug Dev. Ind. Pharm.* **25,** 831–856. (1999).
17. 6. K. R. Naidu, U. N. Kale and M. S. Shingare, Stability indicating RP-HPLC method for simultaneous determination of amlodipine and benezepril hydrochloride from their combination drug product, *J. Pharm. Biomed. Anal.* **39,** 147–155; DOI: 10.1016 /J.JPBA. 04.001, (2005).
18. Tripathi KD. Essentials of Medical Pharmacology. New Delhi, India, Jaypee Brothers, pp 449-454(2003).

Synthesis of Heterocyclic Compounds of Cyclohexenone Derived From Chalcone of Acetophenone

Nabil B. Ayrim
Department of chemistry , college of science , Al-Mustansyriah University

Received 13/11/2011 – Accepted 20/6/2012

الخلاصة

تم تحضير مشتقات للسايكلوهيكسينون من اضافة مركب اثيل اسيتواسيتات الى مركب الجالكون المحضر من تفاعل الاسيتوفينون او مشتقاته مع البنزالديهايد في الكحول بوجود قاعدة NaOH 40 % ، ثم عومل السايكلوهيكسينون المحضر مع الهيدرازين المائي لتحضير مشتق الكاربوهيدرازايد الذي تمت معاملته مع حامض الفورميك ، حامض الخليك ، كلوروثايوسيانات ، اثيل اسيتواسيتات والاسيتايل اسيتون لتحضير مشتقات جديدة مهمة يتوقع لها فعالية بايولوجية والاهمية الصناعية ، تم تشخيص المركبات المحضرة من خلال صفاتها الفيزياوية وكذلك اطياف الاشعة تحت الحمراء وفوق البنفسجية واطياف الرنين النووي المغناطيسي .

ABSTRACT

Derivatives of cyclo hexenone were prepared from addition of ethylacetoacetate to chalcone compound which was prepared from the reaction of acetophenone or it's derivatives with benzaldehyde in ethanol in presence of 40 % NaOH . The synthesized cyclo hexenone was treated with hydrazine hydrate to prepare carbohydrazide derivative , which was treated with formic acid , acetic acid , chloro isothiocyante , ethyl acetoacetate and acetyl acetone to prepare new important derivatives with expected biological activity . The structures of the synthesized compounds were confirmed through their physical properties and spectral data .

INTRODUCTION

Chalcones and the corresponding heterocyclic analoge are valuabl intermediates in organic synthesis [1] , and exhibit multitude of biological activates [2] . from a chemical point of view , an important feature of chalcones and their heteroanalogs is the ability to act as activated unsaturated systems in conjugated addition reaction of carbanions in the presence of basic catalysis [3,4]. This type of reaction may be exploited with the view of obtaining highly functionalized cyclohexene derivatives [5] , but is more commonly used for the preparation of 3,5-diaryl-6-carbethoxy cyclohexenones via Michael addition of ethyl acetoacetate . The mentioned cyclohexenones are efficient synthons in building spiranic compounds [6] or intermediates in the synthesis of fused heterocycles such as benzoselenadiazoles and benzothiazoles [7] , benzopyrazoles and benzisoxazoles [8,9] or carbazole derivatives [10] .

Hydrazinolysis of ester is the conventional methods for preparing acyl hydrazide [11,12] . However , when this method was applied to an α,β-unsaturated ester , the predominant product was the corresponding pyrazolidinone , the result of hydrazinolysis and an undesired subsequent itramolecular michael-type addition [13] . a number of natural and synthetic hydrazide derivatives have been reported to exert

notably antimicrobial [14,15] as will as antifungal [16,17] and tuberculostatic [18] activity .

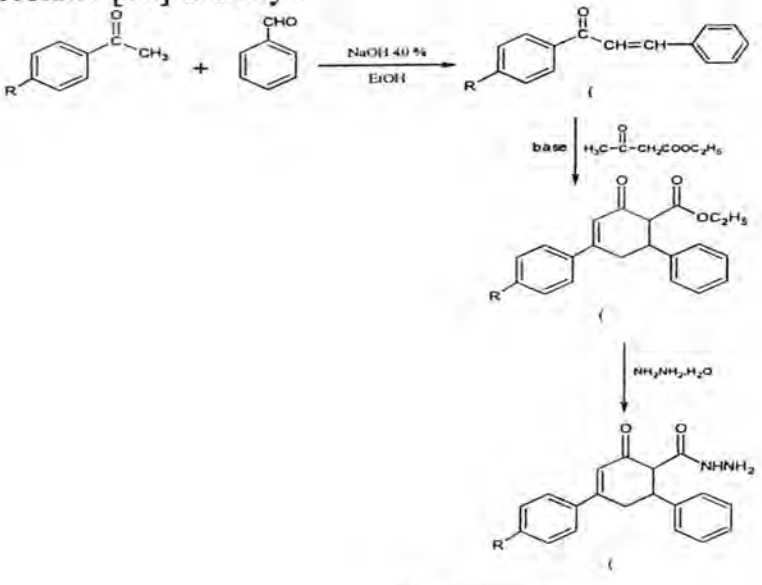

Scheme 1

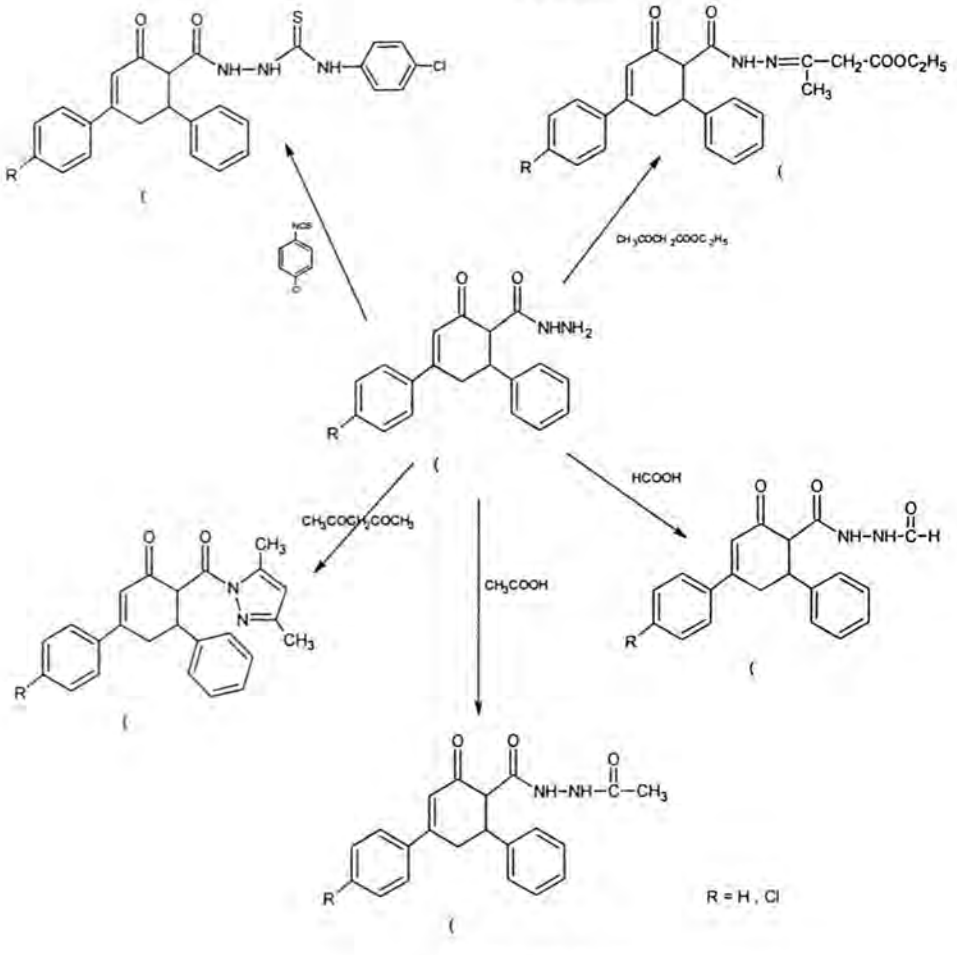

Scheme 2

MATERIALS AND METHODS

Melting points were determined in open capillary tube on Gallen Kamp melting point apparatus and uncorrected. The IR spectra KBr disc were recorded with Shimadzu-2N , FT-IR-8400S. UV. Spectra were recorded on Varian UV-Vis spectrophotometer using absolute ethanol as solvent. 1HNMR spectra were recorded on Bruker spectrophotometer model ultra shield at 300 MHz in DMSO-d6 solution with the TMS as internal standard .

Synthesis of compounds (1a ,1b) : [19]

A mixture of acetophenone or derivatives (0.1 mol) and benzaldehyde (0.1 mol) in ethanol (40 ml) and 40 % NaOH solution was stirred for (24 hrs.) at RT. The reaction mixture was acidified by 10 % HCl solution , The product formed was filtered and recrystallized from ethanol to give compounds (1a , 1b) .

Synthesis of compounds (2a , ab): [20]

A mixture of compounds (1a ,1b) (0.01 mol) and ethyl acetoacetate (0.1 mol) in ethanol (25 ml) was refluxed for (6 hrs.) in the presence of (3ml) 10 % NaOH solution . The reaction mixture was then poured with good stirring into (200 ml) ice-cold water until the reaction product separated as a solid , which was filtered and recrystallized from ethanol to give compounds (2a , 2b) .

Synthesis of compounds (3a , 3b) : [21]

Compound (2a or 2b) was dissolved in a solution containing ethanol (30 ml) and hydrazine hydrate (12 ml) and the mixture was refluxed for (5 hrs.) after cooling the precipitate was filtered and recrystallized from ethanol to give compounds (3a , 3b).

Synthesis of compounds (4a , 4b) : [22]

A solution of compound (3a or 3b) (1 mmol) in formic acid (20 ml) was refluxed for (1 hrs.) . The solvent was evaporated and the residue was crystallized from ethanol to give compounds (4a, ab).

Synthesis of compounds (5a , 5b) : [22]

A solution of compound (3a or 3b) (1 mmol) was refluxed in acetic acid (20 ml) for (5 hrs.). The reaction mixture was cooled and the crystalline product was collected by filtration to give compounds (5a, 5b).

Synthesis of compounds (6a , ab) : [22]

To a solution of compound (3a or 3b) (1 mmol) in ethanol (10 ml) , phenyl isothiocyante (1 mmol) and sodium hydroxide (40 mg) were added . The mixture was stirred for (24 hrs.) and the filtrate was acidified with hydrochloric acid . The precipitate was filtered and recrystallized from (ethanol : water) to give compounds (6a , 6b).

Synthesis of compounds (7a , 7b) : [22]

A mixture of compounds (3a or 3b) (1 mmol) and ethyl acetoacetate (1 mmol) was condensed without solvent at (145-155 C°) for 10 min. The reaction mixture was cooled and refluxed in ethanol (15 ml) for (2 hrs.). The precipitate formed after cooling was collected by filtration and recrystallized from ethanol to give compounds (7a , 7b).

Synthesis of compounds (8a , 8b) : [22]

A mixture of compound (3a or 3b) (1mmol) with acetyl acetone (1 mmol) and acetic acid (1 ml) was refluxed in ethanol (10 ml) for (5 hrs.). The precipitate which formed after cooling was collected by filtration and recrystallized from ethanol to give compounds (8a , 8b).

RESULTS AND DISCUSSION

The new derivatives of compounds (1a,1b) were prepared following the reaction sequences depicated in scheme (1). The starting material for the synthesis of the targeted compound is chalcone or derivatives (1a,1b) which was prepared by the reaction of acetophenone or derivatives with benzaldehyde in ethanol in the presence of 40 % NaOH solution table (1). The formation of compound (1a) was indicated by appearance of the carbonyl group band (C=O) at 1654 cm^{-1} in their IR spectra combined with disappearance of the (OH) stretching band. In addition , ^{1}HNMR of compound (1a) showed CH=CH (2H, S) δ= 3.5 ppm and aromatic proton (10 H, m) δ= 6.7-8. UV spectra of compound (1a) mostly showed intense maxima at 208 nm , 249 nm, 357 nm, which belonged to (π-π*) and (n-π*) transition respectively. The values of IR and UV spectra of compound (1a) are reported in table (1).

The IR spectra of compound (2a) showed the ester functional group absorption band at 1730 cm^{-1} . The structure of cyclo hexenone a sharp strong absorption band was noticed at approximately 1664 cm^{-1} and was assigned to the carbonyl group conjugated with a carbon-carbon double bond . In addition , ^{1}HNMR of compound (2a) showed OCH_2CH_3 (3H, t) δ= 1.3 ppm , OCH_2CH_3 (2 H, q) δ= 4.1 ppm, cyclohexenone (3H, m) δ =3.1-3.3 ppm, cyclohexenone (CH_2, 2H, d) δ = 1.8 ppm and aromatic (10H, m) δ = 6.8-8 ppm. UV spectra of compound (2a) mostly showed intense maxima at 204 nm and 258 nm which belonged to (π-π*) and (n-π*) transition respectively. The values of IR and UV spectra of compound (2b) are reported in table (1). The IR spectra of compound (3a) carbohydrazide showed absorption band in the 3317 cm^{-1} (-NH_2) and 1668 cm^{-1} (-CO-NHNH_2) group . In addition , ^{1}HNMR of compound (3a) showed in cyclohexenone (3H, m) δ= 2.7-2.9 ppm, cyclohexenone (-CH_2, 2H, d) δ= 2 ppm, -NH- (1H, S) δ= 6 ppm , -NH_2 (2H, d) δ= 5.1-5.3 ppm and aromatic (10 H, m) δ =6.5-8 ppm. UV spectra mostly showed intense maxima at 204 nm and 251 nm which

belonged to (π-π^*) and (n-π^*) transition respectively. The values of IR and UV spectra of compound (3b) are reported in table (1).

The IR spectra of compound (4a) showed absorption band in the 3441 cm^{-1} (-NH) and the absorption band in the 1670 cm^{-1} for (-NH-CO-) . In addition , ^{1}HNMR of compound (4a) showed in cyclohexenone (3H, m) δ= 3-3.2 ppm, cyclohexenone (-CH_2, 2H, d) δ= 2.2 ppm, -NH- (1H, S) δ= 8.3 ppm , -NH-CO (1H, S) δ= 9 ppm, -COH (1H, S) δ= 10.1 ppm and aromatic (10 H, m) δ =6.8-7.3 ppm . UV spectra mostly showed intense maxima at 205 nm and 244 nm which belonged to (π-π^*) and (n-π^*) transition respectively. The values of IR and UV spectra of compound (4b) are reported in table (2).

The IR spectra of compound (5a) showed absorption bands in the 3431 cm^{-1} (-NH) and 1708 cm^{-1} (-NH-CO-) group . In addition , ^{1}HNMR of compound (5a) showed in cyclohexenone (3H, m) δ= 3-3.1 ppm, cyclohexenone (-CH_2, 2H, d) δ= 1.8 ppm, -CH_3 (3H, S) δ= 2.3 ppm , -CONH (1H, S) δ= 10.3 ppm, -$NHCOCH_3$ (1H, S) δ= 9.8 ppm and aromatic (10 H, m) δ =6.9-7.8 ppm. UV spectra mostly showed intense maxima at 204 nm and 247 nm which belonged to (π-π^*) and (n-π^*) transition respectively. The values of IR and UV spectra of compound (5b) are reported in table (2).

The IR spectra of compound (6a) contain 3444-3240 cm^{-1} (-NH-CS-NH-) and band at 1662 cm^{-1} (-C=O) group and 1039 cm^{-1} (C=S) and (C-Cl) at 756 cm^{-1}. In addition , ^{1}HNMR of compound (6a) showed in cyclohexenone (3H, m) δ= 2.8.1 ppm, cyclohexenone (2H, d) δ= 1.8 ppm, -CONH (1H, S) δ= 9.8 ppm, -NHCS- (1H, S) δ= 8 ppm, -CSNH- (1H, S) δ= 11.2 ppm and aromatic (14 H, m) δ =6.7-7.9 ppm . UV spectra mostly showed intense maxima at 202 nm , 276 nm and 352 nm which belonged to (π-π^*) and (n-π^*) transition respectively. The values of IR and UV spectra of compound (6b) are reported in table (1).

The IR spectra of compound (7a) contains 3462 cm^{-1} (-NH-) and absorption band in the (C=O) group function appeared at 1653 cm^{-1} and (-C=O) ester function appeared at 1743 cm^{-1} and appearance of (C=N) at 1612 cm^{-1}. In addition , ^{1}HNMR of compound (7a) showed in cyclohexenone (3H, m) δ= 2.9-3.1 ppm, cyclohexenone (-CH_2, 2H, d) δ= 1.8 ppm, -CO-CH_2CH_3 (3H, t) δ= 1.5 ppm , --CO-CH_2CH_3 (2H, q) δ= 4.2 ppm, -N=C-CH_3 (3H, S) δ= 2.2 ppm, -N=C-CH_2 (2H, S) δ= 3.8 ppm, -NH- (1H, S) δ= 10.8 ppm and aromatic (10 H, m) δ =6.9-7.8 ppm. UV spectra mostly showed intense maxima at 205 nm , 249 nm and 365 nm due to (π-π^*) and (n-π^*) transition respectively. The values of IR and UV spectra of compound (7b) are reported in table (2).

The IR spectra of compound (8a) contains 1656 cm^{-1} (C=O) carbonyl group and absorption at 1597 cm^{-1} (-C=N) , 1220 cm^{-1} (C-N) and (C-$H_{al.}$) at 2918 cm^{-1}. In addition , ^{1}HNMR of compound (8a) showed in

cyclohexenone (3H, m) δ= 3 ppm, cyclohexenone (-CH_2, 2H, d) δ= 2 ppm, -CH_3 (3H, s) δ= 1.2 ppm , -CH_3 (3H, S) δ= 4 ppm, -CH=C- (1H, S) δ= 5.5 ppm, and aromatic (10 H, m) δ =6.8-7.6 ppm UV spectra showed intense maxima at 208 nm , 249 nm and 357 nm due to (π-π^*) and (n-π^*) transition respectively. The values of IR and UV spectra of compound (8b) are reported in table (2).

Table -1 : physical properties and spectral data for compounds (1-3 a,b)

Comp.	R	M.P C°	Yeild%	Spectral data	
				UV λ_{max}	IR (cm^{-1})
1a	H	170-172	82.7	357,249 208	1654(C=O), 3030(CH)ar, 1610(C=C)
1b	4-Cl	165-167	85	258, 208	1670(C=O), 3050(CH)ar, 1600(C=C), 746(C-Cl)
2a	H	138-140	72.2	248, 204	1660(C=O), 1730(C=O ester), 3064(CH)ar, 1590(C=C)
2b	4-Cl	88-90	68.5	327,251 204	1670(C=O), 1745(C=Oester), 3050(CH)ar, 1600(C=C), 780(C-Cl).
3a	H	95-97	60.3	251, 204	1656(C=O), 1668(-CONHNH2), 3059(CH)ar, 1595(C=C), 3317(3317)
3b	4-Cl	100-102	63.5	259, 204	1660(C=O), 1681(-CONHNH2), 3063(CH)ar, 1589(C=C), 3396(NH2), 829(C-Cl)

Table-2 : physical properties and spectral data for compounds (4-8 a,b)

Comp	R	M.P C°	Yeild%	Spectral data	
				UV λ_{max}	IR (cm^{-1})
4a	H	110-112	53	244,205	1660(C=O), 1676(-NH-CO-), 3061(CH)ar, 1591(C=C), 3440(-NH-),
4b	4-Cl	115-117	55.4	255,203	1630(C=O), 1670(-NH-CO-), 3030(C=C)ar, 3390(-NH-), 756(C-Cl)
5a	H	116-118	68.2	352,247 204	1670(C=O), 1708(-NH-CO-), 3059(CH)ar, 1593(C=C), 2922(CH)al, 3431(NH)
5b	4-Cl	128-130	58	266, 205	1672(C=O), 1713(-NH-CO-), 3070(CH)ar, 2930(CH)al, 1588(C=C), 3231(NH), 780(C-Cl)
6a	H	152-154	51	352, 276 202	1662(C=O), 3055(CH)ar, 3444-3240(-NH-CS-NH-), 1039(C=S), 1211(C-N), 852(C-Cl)
6b	4-Cl	85-87	57	248, 265	1658(C=O), 3059(CH)ar, 3462-3300(-NH-CS-NH-), 1039(C=S), 1217(C-N), 726(C-Cl)
7a	H	135-137	67	365,249 205	1653(C=O), 1743(C=O), 3061(CH)ar, 2931(CH)al, 3462(NH), 1612(C=N), 1589(C=C)
7b	4-Cl	144-146	69	258, 204	1657(C=O), 1710(C=O), 3076(CH)ar, 2910(CH)al,3381(NH),1629(C=N), 1601(C=C), 759(C-Cl)
8a	H	152-154	73	357, 249 208	1656(C=O), 1597(C=C), 1492(C=N), 3059(CH)ar, 2854(CH)al, 1210(C-N)
8b	4-Cl	133-135	74	320, 251 212	1662(C=O), 1590(C=C), 1560(C=N), 756(C-Cl),1219(C-N)

REFERENCES

1. D.N.Dhar, The chemistry of chalcones and related compounds, Wiley-Intarcience, New York (1981).
2. M. A. Rahman, Chalcone : Avaluable Insight into the Recent Advances and Potential Pharmacological Activities. Chemical Sciences Journal, Review (2011).
3. H.O.House, Modern Synthtic Reactions, 2nd edition, W.A.Benjamin, Menlo park, California, p595 (1972).
4. M.E.Jurg, Comprehensive Organic Synthesis, Vol. 4, Eds. B.M.Trost, I. Fleming, pergamon press, oxford, p1 (1991).
5. H.D.Tabba, N.M.Yousef and M.M.Al-Arab, Coll.Czech. Chem. Commun. 60, 594-604 (1995).
6. A. N. Mayekar, H. Li, H. S. Yathirajan, B. Narayana and N. S. Kumari, Synthesis Characterization and Antimicrobial Study of Some New Cyclohexenone Derivatives, International Journal of Chemistry, V.2 , No. 2 (2010) .
7. M. Bella, M. Schultz, and V. Milata, Synthesis of [1,2,5] seleradiazolo [5,4-f] quinolone derivatives by the could Jacobs reaction of 5-amino-2,3-benzoselenodiazole. ARKIVOC, 242-251, (2012) (iv).
8. R. G. Xing, Ya, N. Li. And Q. L. Qing, Facile and Efficient Synthesis of Benzoxazoles and Benzimidazoles; Eur. J. Org. Chem. Issue 34, 6627-6632, Dec. (2010).
9. A. V. Dubrovskiy and R. C. Lavock, Synthesis of Benzisoxazoles by the [3+2] cycloaddition of in situ Generated Nitrile Oxides and Arynes, 1180-1183, pubmed (2011).
10. A. E. Martin, K. R. Prasad, Synthesis and characterization of Carbazole derivatives and their antimicrobial studies , Acta pharm. 79-86 , 56(2006) .
11. M. K. Dahlgren, C. T. Oberg, E. A. Wallin, P. G. Janson and M. Elofsson . Synthesis of 2-(2-Amino pyrimidine)-2,2-difluoroethands as potential Bioisosters of salicylidene Acyl hydrazides, Molecules, 15, 4423-4438 (2010) .
12. M. Cacic and M. Trkovnik, Synthesis and Antimicrobial Activity of Some Derivatives of (7-hydroxy-2-oxo-2H-Chroman-4-yl) acetic acid hydrazide . Molecules , 11, 134-147 (2006) .
13. T. Oishi and K. Yoshimura, An Efficient copper mediated 1,3-Dipolar cycloaddition of Pyrazolidinone-based Dipoles to Terminal Alkynes to produce N,N-Bicyclic Pyrazolidinone derivatives . Chemistry letters, V. 39, issue 10, 1086-1087 (2010) .
14. S. Pulac, X. Sem, A. Negrea and M. Rhem, Small-molecular virulence inhibitors show divergent and immunomodulatery effects

in infection models of Salmonella enterica servor Typhimurium, Int. J. Antimicrobial Agent, V. 38, issues 409-416, Nov. (2011).

15. R. M. Modhareb, D. H. Fleita and O. b. K. Sakka, Novel Synthesis of hydrazide-hydrazone derivatives and their utilization in the synthesis of coumarin, pyridine, thiazole and thiophene derivatives with antitumor activity, Molecules, No. 16, p. 16-27 (2011).
16. P. M. Sivakumar, S. Ganesan, P. Veluchamy and M. Dobe, Novel Chalcones and 1,3,5-triphenyl-2-pyrazoline derivatives as antibacterial agents, Chemical Biology & Drug Design , V. 76,issue 5, p. 407-411, Nov. (2010) .
17. I. Lacka, M. Konieczny, A. Bulakowska, T. Rzymowski and S. Milewski, Antifungal action of the oxathiolone-fused Chalcone derivatives mycoses, V. 54, issue 5, p. 407-414 (2011) .
18. O.A.Abdallah, Synthesis and biological studies of some benzopyrano[2,3-C]pyrazole derivatives. IL Farmaco, 55, 641- 649 (2000).
19. A.I. Vogel, Partical Organic Chemistry, 3rd Ed., Longmans, London (1956).
20. G.Roman, Cyclo Hexenones Through Addition of Ethyl acetoacetate to Chalcones Derived from 2-Acetyl Thiophene, Act Chem. Solv, 51,537-544 (2004).
21. E.H.EI.Tamany, E.M.Salem, R.N.Metwally, and A.H.EI-Soghier, Egypt. J.Chem., Vo.40, No. 5, p23 (1997).
22. [22] - M.Cacic, M.Trkovnik, F. Cacic and E.Has-Schon, Synthesis and Anti Microbial Activity of Some Derivatives of (7-Hydroxy-2-oxo-2H-Chromen-4-yl)-acetic acid Hydrazide, Molecules, 11, 134-147 (2006).

Potential Energy Surfaces for Heavy Nuclei $^{228}_{88}Ra$, $^{230}_{90}Th$ and $^{232}_{92}U$

Rana Oday Al-Habib
Department of physics, College of Science, Al-Mustanseria University

Received 25/12/2011 – Accepted 18/4/2012

الخلاصة

يهدف البحث الى دراسة التركيب النووي لبعض النوى الثقيلة ^{232}U و ^{230}Th و ^{228}Ra والواقعة جميعها ضمن التصرف الديناميكي SU(3) باستخدام نموذج البوزونات المتفاعلة الاول (IBM-1). حيث تم حساب مستويات الطاقة بعد اجراء سلسلة من العمليات الحسابية لتحديد نوع التناظر الديناميكي التي تنتمي اليها هذه النوى وتقسيم حزم طاقاتها من حساب مستويات الطاقة لها باستخدام برنامج اساسي لهذا النموذج هو (IBSS1.For) وحساب جهد طاقة السطح و ذلك لمعرفة مقدار التشوه النووي الذي تعانيه هذه النوى وذلك بالاعتماد على النتا ئج التي حصلنا عليها من حساب مستويات الطاقة. تم مقارنة اغلب النتائج التي حصلنا عليها مع القيم العملية الموجودة لدينا فكانت متوافقة جدا.

ABSTRACT

The main purpose of this paper is to study the nuclear structure of the heavy nuclei ^{228}Ra, ^{230}Th and ^{232}U with N=140 for the dynamical symmetry SU (3) by using interacting boson model version -1. Where the calculation of energy levels after a series of calculation to determine the type of dynamic symmetry, which belong to these cores and split their packs of calculating energy levels by using a basic program for this model hootm (IBSS1.For) and calculate the potential energy surface to know the range of deformations nuclear for these nuclei based on the results obtained from the calculation of energy levels. We have compared the results obtained with our existing process with the practical values and they were very compatible.

INTRODUCTION

The interacting boson models (IBM) had been introduced by Iachello [1] and then developed by Arima and Iachello [2-5] in the field of nuclear – energy phenomena. The model has already gained significant success in both single – particle and collective behavior of nuclei. There are essentially two models: the first, IBM-1when no distinction between the proton and neutron pairs is made then the IBM is referred to as IBM-1. If protons and neutrons are explicitly introduced then the model is known as IBM-2 [6].

The IBM [7] provides a unified description of collective nuclear states in terms of a system of interacting bosons. The shell for the nuclei ^{228}Ra, ^{230}Th and ^{232}U are taken at the neutron number N=126 and the proton number at Z=82, resulting in boson number, formed by proton (particle) pairs and neutron (hole) pairs.

The potential energy surface function V(N,β,γ) depends on the shape variables parameters β and γ, where β is the magnitude of the nuclear deformation and γ gives the turn away from axial symmetry (asymmetry angle), and they are different for different states of nucleus. The values of β are between (0 --- 2.4), and for γ are between (0° ---- 60°) [8].

THEORETICAL PART

Hamiltonian operator

The IBM-1 model was applied to the positive and negative parity low – lying states even-even ^{228}Ra, ^{230}Th and ^{232}U nuclei. The proton, π, and neutron, υ, bosons are treated as one boson and the system is considered as in interaction between s-bosons and d-bosons. Creation and annihilation operators for the IBM bosons are denoted by $\{s^{\dagger}, d_{\upsilon}^{\dagger}\}$ and $\{s, \hat{d}_{\upsilon}\}$with; $\upsilon = 0, \pm 1, \pm 2$ [9] .The general IBM Hamiltonian [10] employed for the present calculation is given as:-

$\hat{H} = \varepsilon\hat{n}_d + a_0(\hat{P}^{\dagger}\cdot\hat{P}) + a_1(\hat{L}\cdot\hat{L}) + a_2(\hat{Q}\cdot\hat{Q}) + a_3(\hat{T}_3\cdot\hat{T}_3) + a_4(\hat{T}_4\cdot\hat{T}_4) --(1)$

Where the interaction parameters in the [PHINT] program are given below: ε=EPS, $a_0 = 2PAIR$, $a_1 = \frac{ELL}{2}$, $a_2 = \frac{QQ}{2}$, $a_3 = 5OCT$ *and* $a_4 = 5HEX$; OCT and HEX is the octupole and hexadecupole interactions.

$\varepsilon(\varepsilon_d - \varepsilon_s) -------(2)$

$\varepsilon - Boson\ energy$

ε_d- Energy of d- boson

ε_s- Energy of s- boson

$\hat{n}_d = [\hat{d}^{\dagger}\cdot\hat{\tilde{d}}] ----------(3)$

$\hat{P} = \frac{1}{2}(\hat{\tilde{d}}\cdot\hat{\tilde{d}}) - \frac{1}{2}(\hat{s}\cdot\hat{s}) -----(4)$

$\hat{L} = \sqrt{10}(\hat{d}^{\dagger}\times\hat{\tilde{d}}) ----------(5)$

$\hat{Q} = [\hat{d}^{\dagger}\times\hat{\tilde{d}}]^2 + [\hat{s}^{\dagger}\times\hat{\tilde{d}}]^2 + CHI\ [\hat{d}^{\dagger}\times\hat{\tilde{d}}]^2 ---(6)$

$\hat{T}_3 = [\hat{d}^{\dagger}\times\hat{\tilde{d}}]^3 ----------(7)$

$\hat{T}_4 = [\hat{d}^{\dagger}\times\hat{\tilde{d}}]^4 ----------(8)$

In the previous formula, n_d is the number of boson; P.P, Q.Q, $T_3.T_3$ and $T_4.T_4$ represent pairing, angular momentum, quadruple, octupole and Hexadecapole interactions between the bosons.

The rotational SU (3) limit

The rotational symmetry for SU (3) group is used to describe the rotational spectrum of nuclei that have an axial symmetrical rotor.

The rotational group and the classification representation labels for this group are [11-12]:

$$\begin{array}{l} \text{U (6)} \supset SU(3) \supset O(3) \supset O(2) \\ \text{[N]} \quad (\lambda,\mu)\widehat{K}, \quad \text{I}, \quad \mu_I \end{array} \quad \text{-------(9)}$$

Where the quantum numbers are [7, 8, and 9]

[N] , I and μ_I are as before

$\widehat{K}$: is an extra quantum number, which is needed to classify the state uniquely, since the SU (3) $\supset O(3)$in, not fully decomposable.

The value of (λ,μ) contained in asymmetric representation[N].

The potential energy surface for SU(3)rotational symmetry

The potential energy surface (EPS) can be leads to the knowledge of nuclear

Deformation shape. This deformation shape depends on two parameters (β,γ) for a given N, as the following:

β deformation parameters:-

When the value of parameters is approach to zero, the shape of nuclei will be spherical and when these values are greater than zero the deformation of nuclei dominant.

γ distortion parameters:-

When the value of γ parameters equal to (0°) this leads to triplet symmetric from prolate type, and when the value of γ equal to (60°) the distortion will be triplet symmetric from oblate type.

The most commonly general equation for the potential energy surface as a function of geometrical variables β and γ is given by [8, 13, and 14]

$$V(N,\beta,\gamma) = \frac{N(\epsilon_s + \epsilon_d\beta^2)}{1+\beta^2} + \frac{N(N-1)}{(1+\beta^2)^2}(\alpha_1\beta^4 + \alpha_2\beta^3\cos 3\gamma + \alpha_3\beta^3 + \alpha_4) \text{ --(10)}$$

Where:

N: the total number of boson

β: the axial quadrupole deformation from 0 ⟶ 2.4

γ: the distortion parameter (asymmetry angle) 0°⟶60°

RESULTS AND DISCUSSION

Table 1, gives the best fit parameters of the Hamiltonian IBM-1 for each nucleus $^{228}_{88}Ra$, $^{230}_{90}Th$ and $^{232}_{92}U$ used in the present work according to their atomic mass number, and dynamical symmetry. (IBS1.for) program is a sub-program follows up with the general program (IBM-1) which was written in [Fortran 90].

The calculated energy levels $for\ ^{228}_{88}Ra$, $^{230}_{90}Th$ and $^{232}_{92}U respectively$ are shown in figures (1-3) and compared with the experimental levels.

Table-1: The Hamiltonian parameters set used in the research work for the IBM-1 calculations of $^{228}_{88}$Ra, $^{230}_{90}$Th and $^{232}_{92}$U nuclei by using (IBSS1.For) program

$^{A}_{Z}X$	N	EPS (MeV)	$\hat{P}^{\dagger}.\hat{P}$ (MeV)	$\hat{I}.\hat{I}$ (MeV)	$\hat{Q}.\hat{Q}$ (MeV)	$\widehat{T_3}.\widehat{T_3}$ (MeV)	$\widehat{T_4}.\widehat{T_4}$ (MeV)	CHI (MeV)
$^{228}_{88}Ra$	10	0.0000	0.0000	0.0055	-0.0125	0.0000	0.0000	-1.3200
$^{230}_{90}Th$	11	0.0000	0.0000	0.0047	-0.0104	0.0000	0.0000	-1.3200
$^{232}_{92}U$	12	0.0000	0.0000	0.0039	-0.0104	0.0000	0.0000	-1.3200

The results of the present calculation for energy spectrum are presented in table (2). In general, g-, β and γ,β_2,β_3, and γ_2 bands are well established in Sakai [15].the calculated energy levels for the same bands are a good agreement at shown in sakai[15] in addition, new energy levels are be found for these nuclei at shown in fig(1-3) as follows:

1. For $^{228}_{88}Ra$ nuclei, in g- band the new energy levels are 8^{+}(0.7334) , 10^{+}(1.1205)and 12^{+}(1.5891),inβ_1- band the new energy levels are 6^{+}(1.1390) , 8^{+}(1.4446)and10^{+}(1.8317),in γ_1-band the new energy levels are 4^{+}(0.9156) , 5^{+}(1.0168), 6^{+}(1.1397)and7^{+}(1.2816), in β_2-band the new energy levels are 4^{+}(1.4763), 6^{+}(1.7005)and 8^{+}(2.0061) and in γ_2-band the new energy levels are 4^{+}(1.4769), 5^{+}(1.5782), 6^{+}(1.7010)and7^{+}(1.8431) states.
2. For $^{230}_{90}Th$ nuclei, in β_1- band the new energy levels are 6^{+}(1.0151) , 8^{+}(1.2731)and10^{+}(1.5999),in γ_1-band the new energy levels are 5^{+}(0.9119)and 6^{+}(1.0158), in β_2-band the new energy levels are 4^{+}(1.3559)and 6^{+}(1.5451) and in γ_2-band the new energy levels are 4^{+}(1.3553), 5^{+}(1.4413)and 6^{+}(1.7010) states.
3. For $^{232}_{92}U$ nuclei, in γ_1-band the new energy levels are 5^{+}(0.9517) , 6^{+}(1.0466),7^{+}(1.1558), 8^{+}(1.2821)and 9^{+}(1.4227) states.

In general, the comparisons between calculated and experimental values [15] of energy levels for each nucleus [see figs. (1-3) and table 2], the agreement is good, especially for the ground – state and levels for the dynamical symmetry SU (3).

Table -2: The theoretical both of energy level, energy transition and the ground state , quasi beta and gamma band energies compare with experimental value of $^{228}_{88}Ra$, $^{230}_{90}Th$ and $^{232}_{92}U$ nuclei.

Nuclei	Bands	I_i^+	Energy level(MeV)		Spin Sequence	Energy transition(MeV)	
			Exp.(15)	IBM-1		Exp.(15)	IBM-1
$^{228}_{88}Ra$ (SU(3))	g-band	0_1^+	0.0000	0.0000	---------	--------	-------
		2_1^+	0.0638	0.0611	2_1^+------ 0_1^+	0.0638	0.0611
		4_1^+	0.2047	0.2037	4_1^+------ 2_1^+	0.1409	0.1426
		6_1^+	0.4117	0.4278	6_1^+------ 4_1^+	0.2070	0.2241
		8_1^+	--------	0.7334	8_1^+------ 6_1^+	--------	0.3056
		10_1^+	--------	1.1205	10_1^+------ 8_1^+	--------	0.3871
		12_1^+	--------	1.5891	12_1^+------ 10_1^+	--------	0.4686
	β_1- band	0_2^+	0.7212	0.7118	0_2^+------ 2_1^+	0.6574	0.6507
		2_2^+	0.7707	0.7723	2_2^+------ 0_2^+	0.0495	0.0605
		4_2^+	0.8803	0.9149	4_2^+------ 4_1^+	0.6756	0.7112
		6_2^+	--------	1.1390	6_2^+------ 4_2^+	--------	0.2241
		8_2^+	--------	1.4446	8_2^+------ 6_1^+	--------	1.0168
		10_2^+	--------	1.8317	10_2^+------ 8_2^+	--------	0.3871
	β_2- band	0_3^+	1.0419	1.2734	0_3^+------ 2_2^+	0.2712	0.5011
		2_5^+	1.0873	0.7730	2_5^+------ 4_1^+	0.8826	0.5693
		4_4^+	--------	1.4763	4_4^+------ 6_1^+	--------	1.0485
		6_4^+	--------	1.7005	6_4^+------ 4_4^+	--------	0.2242
		8_4^+	--------	2.0061	8_4^+------ 8_2^+	--------	0.5615
	γ_1- band	2_3^+	0.8462	0.7730	2_3^+------ 2_2^+	0.0755	0.7119
		3_1^+	0.8989	0.8334	3_1^+------ 4_1^+	0.6942	0.6297
		4_3^+	--------	0.9156	4_3^+------ 3_1^+	--------	0.0822
		5_1^+	--------	1.0168	5_1^+------ 4_1^+	--------	0.8131
		6_3^+	--------	1.1397	6_3^+------ 5_1^+	--------	0.1229
		7_1^+	--------	1.2816	7_1^+------ 5_1^+	--------	0.2648
	γ_2- band	2_4^+	1.0133	1.3343	2_4^+------ 2_2^+	0.2426	0.5620
		3_2^+	1.0703	1.3954	3_2^+------ 4_1^+	0.8656	1.1917
		4_5^+	--------	1.4769	4_5^+------ 2_3^+	--------	0.7039
		5_2^+	--------	1.5782	5_2^+------ 5_1^+	--------	0.5614
		6_5^+	--------	1.7010	6_5^+------ 6_4^+	--------	0.5613
		7_2^+	--------	1.8431	7_2^+------ 5_1^+	--------	0.8263
$^{230}_{90}Th$ (SU(3))	g-band	0_1^+	0.0000	0.0000	---------	--------	--------
		2_1^+	0.5320	0.5159	2_1^+------ 0_1^+	0.0532	0.0516
		4_1^+	0.1741	0.1720	4_1^+------ 2_1^+	0.1209	0.1204
		6_1^+	0.3566	0.3612	6_1^+------ 4_1^+	0.1825	0.1892
		8_1^+	0.5941	0.6191	8_1^+------ 6_1^+	0.2375	0.2579
		10_1^+	0.8797	0.9459	10_1^+------ 8_1^+	0.2856	0.3268
		12_1^+	1.2078	1.3414	12_1^+------ 10_1^+	0.3281	0.3955
	β_1- band	0_2^+	0.6346	0.6546	0_2^+------ 2_1^+	0.5814	0.6030
		2_2^+	0.6777	0.7055	2_2^+------ 2_1^+	0.6245	0.6539
		4_2^+	0.7695	0.8259	4_2^+------ 4_1^+	0.5954	0.6539
		6_2^+	--------	1.0151	6_2^+------ 4_1^+	--------	0.8431
		8_2^+	--------	1.2731	8_2^+------ 6_1^+	--------	0.9119
		10_2^+	--------	1.5999	10_2^+------ 8_2^+	--------	0.3268
	β_2- band	0_3^+	1.5900	1.1841	0_3^+------ 0_2^+	0.9554	0.5277
		2_5^+	1.6360	1.2357	2_5^+------ 2_2^+	0.9583	0.5302
		4_5^+	--------	1.3559	4_5^+------ 0_3^+	--------	0.1718
		6_5^+	--------	1.5451	6_5^+------ 4_2^+	--------	0.7192
	γ_1- band	2_3^+	0.7813	0.7062	2_3^+------ 2_1^+	0.7281	0.6546
		3_1^+	0.8258	0.7571	3_1^+------ 4_1^+	0.6517	0.5851
		4_3^+	0.8810	0.8266	4_3^+------ 2_1^+	0.8278	0.7750
		5_1^+	--------	0.9119	5_1^+------ 6_1^+	--------	0.5507
		6_3^+	--------	1.0158	6_3^+------ 5_1^+	--------	0.1039
		7_1^+	1.1300	1.1355	7_1^+------ 5_1^+	1.1300	0.2236
	γ_2- band	2_4^+	1.0096	1.2355	2_4^+------ 2_2^+	0.3319	0.5300
		3_2^+	1.0520	1.2871	3_2^+------ 4_1^+	0.8779	1.1151
		4_4^+	--------	1.3553	4_4^+------ 2_1^+	--------	1.3037
		5_2^+	--------	1.4413	5_2^+------ 6_1^+	--------	1.0801
		6_4^+	--------	1.7010	6_4^+------ 4_1^+	--------	1.5290
		7_2^+	1.6630	1.6650	7_2^+------ 5_2^+	1.6630	0.2237
$^{232}_{92}U$ (SU(3))	g-band	0_1^+	0.0000	0.0000	---------	--------	--------
		2_1^+	0.0476	0.0471	2_1^+------ 0_1^+	0.0476	0.0471
		4_1^+	0.1566	0.1570	4_1^+------ 2_1^+	0.1090	0.1099
		6_1^+	0.3216	0.3297	6_1^+------ 4_1^+	0.1650	0.1727
		8_1^+	0.5410	0.5651	8_1^+------ 6_1^+	0.2194	0.2354

		10_1^+	0.8050	0.8634	10_1^+------ 8_1^+	0.2640	0.2983
		12_1^+	1.1112	1.2244	12_1^+------ 10_1^+	0.3062	0.3610
	β_1- band	0_2^+	0.6913	0.7169	0_2^+------ 2_1^+	0.6437	0.6698
		2_2^+	0.7346	0.7633	2_2^+------ 2_1^+	0.6870	0.7162
		4_2^+	0.8331	0.8732	4_2^+------ 4_1^+	0.6765	0.7162
		6_2^+	0.9852	1.0459	6_2^+------ 4_1^+	0.8286	0.8889
		8_2^+	1.1873	1.2814	8_2^+------ 6_1^+	0.8657	0.9517
		10_2^+	1.4349	1.5797	10_2^+------ 8_2^+	0.2476	0.2983
	γ_1- band	2_3^+	0.8667	0.7640	2_3^+------ 2_2^+	0.1321	0.0007
		3_1^+	0.9114	0.8104	3_1^+------ 4_1^+	0.7548	0.6534
		4_3^+	0.9708	0.8739	4_3^+------ 2_1^+	0.9232	0.8268
		5_1^+	--------	0.9517	5_1^+------ 4_1^+	--------	0.7947
		6_3^+	--------	1.0466	6_2^+------ 6_2^+	--------	0.0007
		7_1^+	--------	1.1558	7_1^+------ 5_1^+	--------	0.2041
		8_3^+	--------	1.2821	8_3^+------ 6_2^+	--------	0.2362
		9_1^+	--------	1.4227	9_1^+------ 7_1^+	--------	0.2669

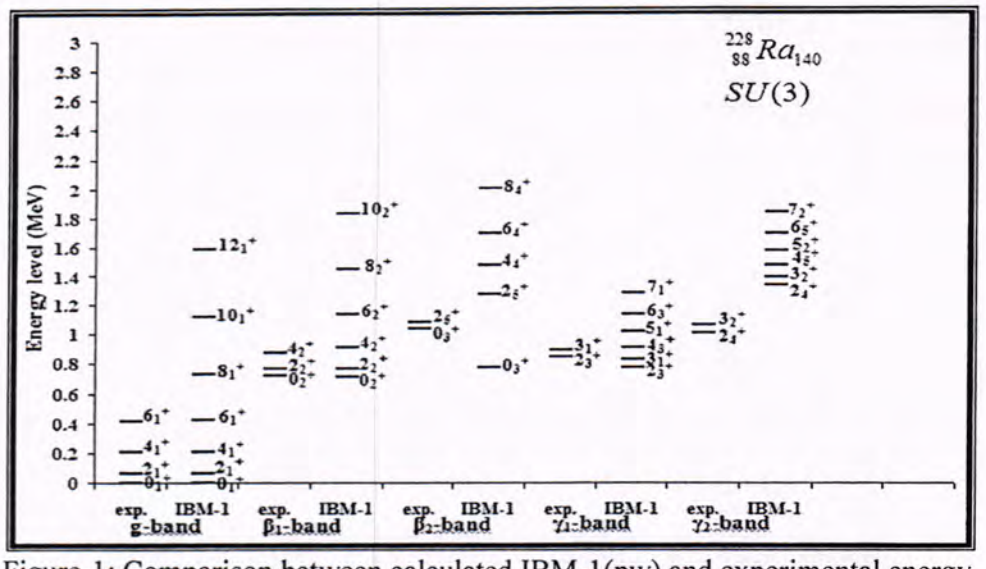

Figure-1: Comparison between calculated IBM-1(pw) and experimental energy bands states (g,β,γ)bands in ^{228}Ra for the dynamical symmetry SU(3)

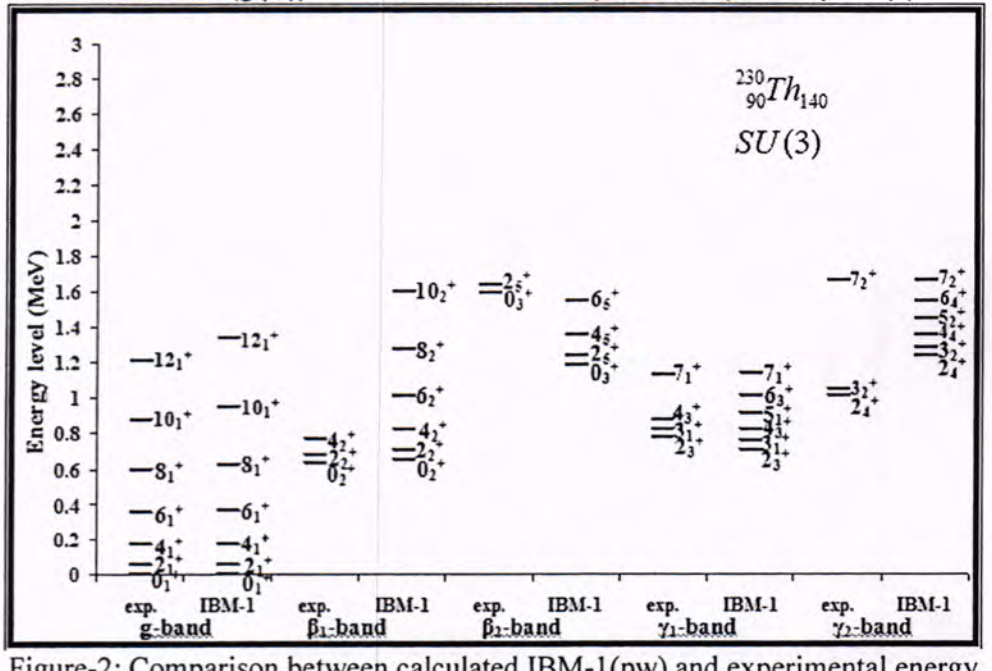

Figure-2: Comparison between calculated IBM-1(pw) and experimental energy bands states (g,β,γ)bands in ^{230}Th for the dynamical symmetry SU(3)

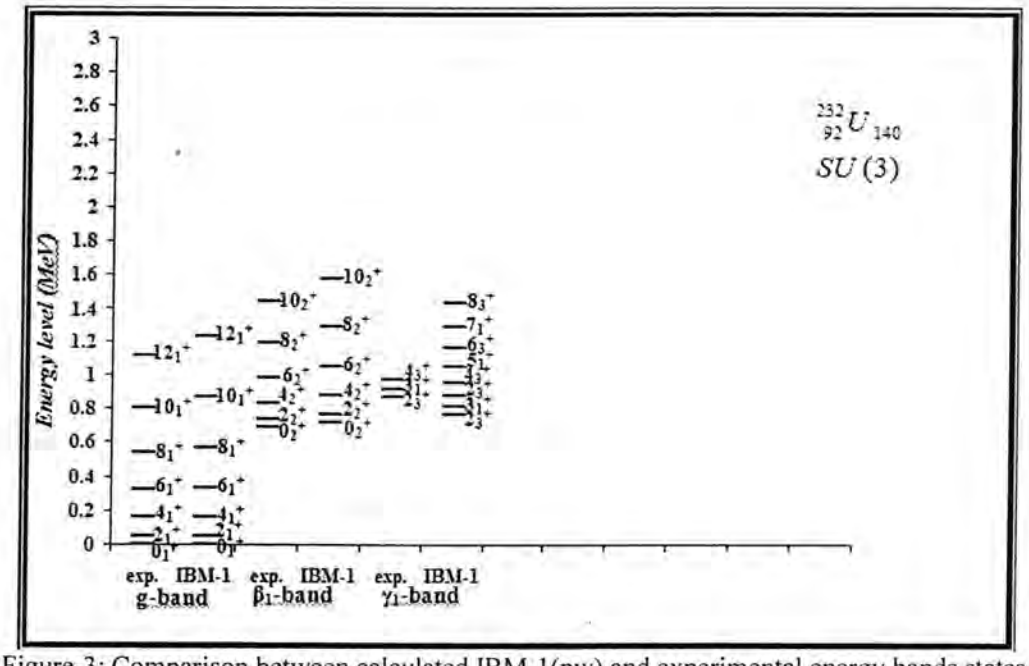

Figure-3: Comparison between calculated IBM-1(pw) and experimental energy bands states (g,β,γ)bands in ^{232}U for the dynamical symmetry SU(3)

The potential energy surface for is one of many methods to predict the deformation of nuclear structure, In this research, we were used the IBM-1 analysis solutions for the set of the counter plots of potential energy surface function V (N, β, γ) which is calculated by using the parameters (α's) infer from (IBSS1.For) program, as shown in table (3).

Table-3: parameters used for potential energy surface calculations in (IBSS1.) program.

Nuclei	N	ϵ_s	ϵ_d	α_1	α_2	α_3	α_4
$^{228}_{88}Ra$	10	-0.063	-0.001	-0.006	-0.035	-0.050	0.000
$^{230}_{90}Th$	11	-0.052	0.000	-0.005	-0.029	-0.042	0.000
$^{232}_{92}U$	12	-0.052	0.005	-0.005	-0.029	-0.042	0.000

Figures (4, 5, 6 – a) indicates the contour plots deduced from the potential energy surface as a function of deformed (β, γ), the contour lines are in a good agreement with typical plots [12].the axially symmetric ($\gamma=0^o$,$\gamma=30^o$,$\gamma=60^o$)plots of the potential energy calculated in this research are shown in figures(4,5,6-b). This figure shows the behaviors of the potential energy surface for $^{228}_{88}Ra$ with deep minimum of (0) MeV on the oblate side at $\beta=1.2$, $\gamma=0^o$ and a minimum for prolate shape at $\beta=-0.6$,$\gamma=60^o$ which is (1.443)MeV and for $^{230}_{90}Th$ with deep minimum of (0) MeV on the oblate side at $\beta=1.2$, $\gamma=0^o$ and a minimum for

prolate shape at β= -0.6,γ=60° which is (1.483)MeV and for $^{232}_{92}U$ with deep minimum of (0.005) MeV on the oblate side at β=1.2, γ=0° and a minimum for prolate shape at β= -0.6,γ=60° which is (1.821).

The effect of these minimum are deduced by normalization of potential energy to zero at the lowest minimum. The energy of zero point motion (EZPM) is (0)MeV for $^{228}_{88}Ra$, (0)MeV for $^{230}_{90}Th$ and (0.005) MeV for $^{232}_{92}U$.

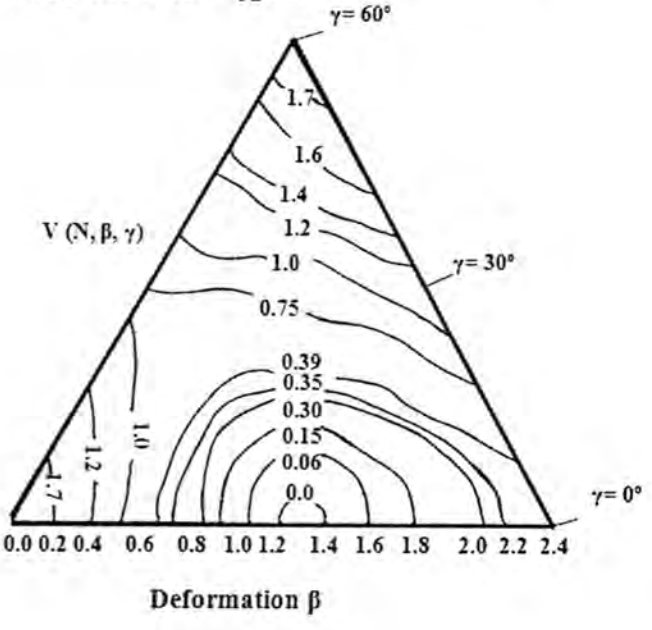

(a)

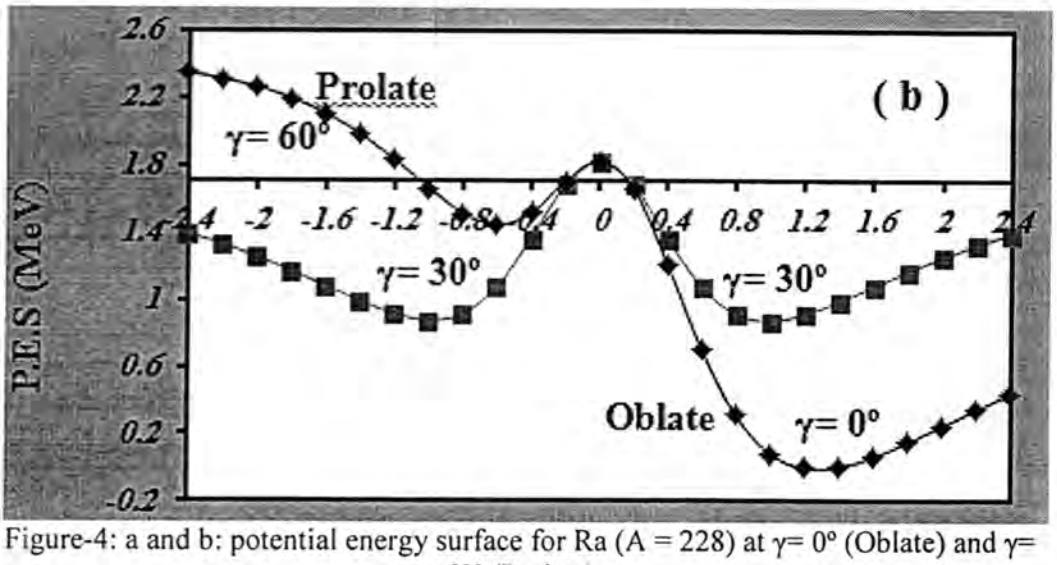

Figure-4: a and b: potential energy surface for Ra (A = 228) at γ= 0° (Oblate) and γ= 60° (Prolate)

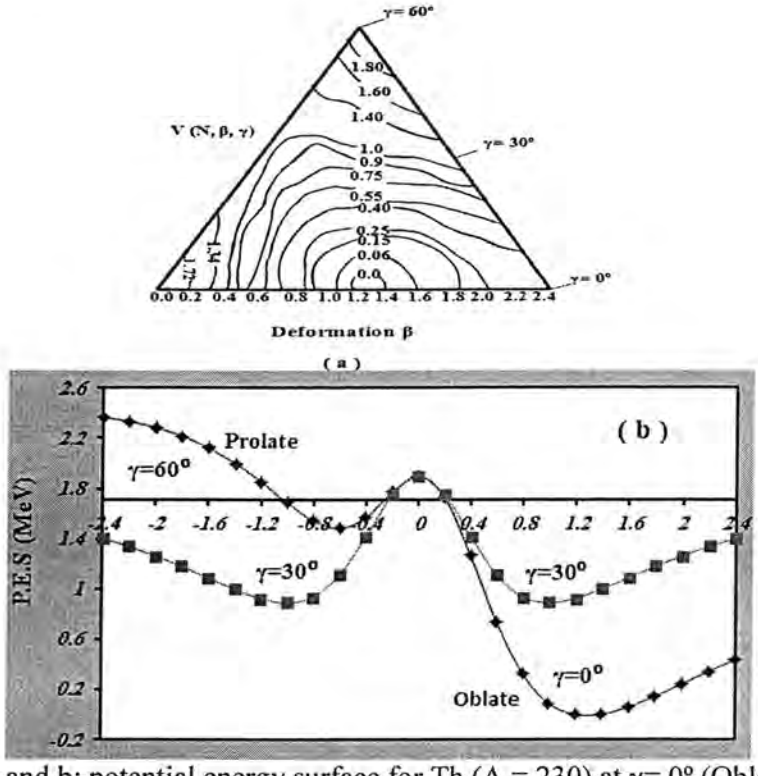

Figure-5: a and b: potential energy surface for Th (A = 230) at γ= 0° (Oblate) and γ= 60° (Prolate)

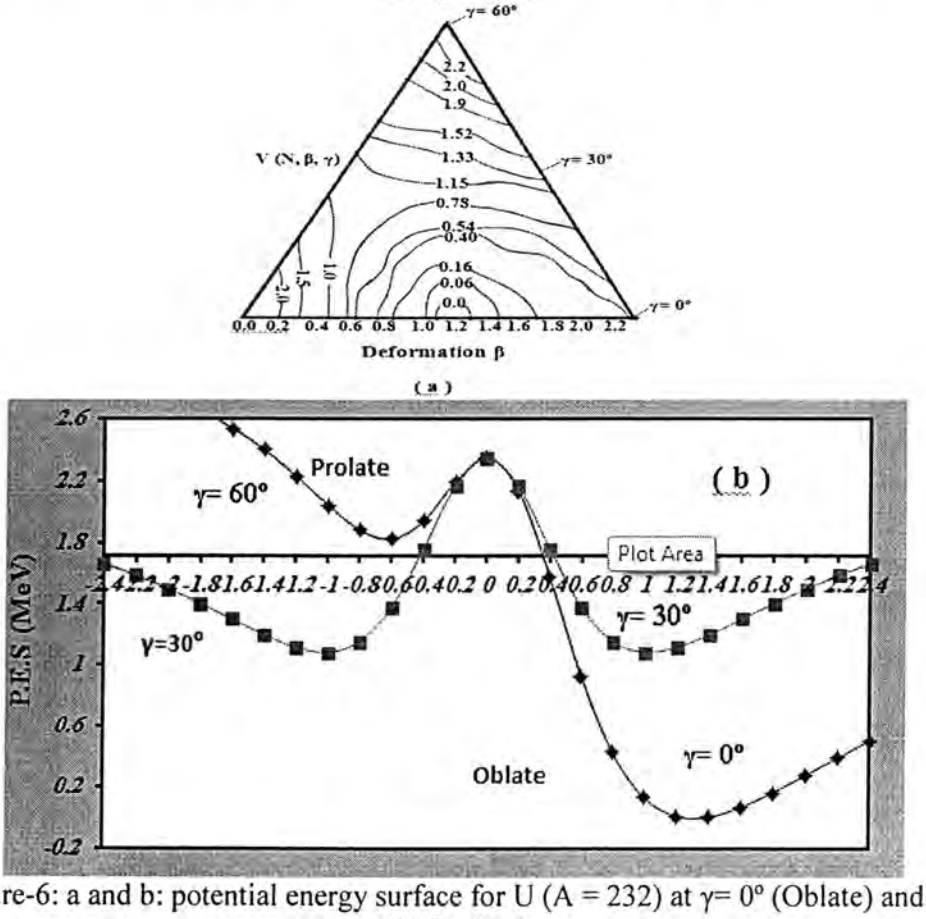

Figure-6: a and b: potential energy surface for U (A = 232) at γ= 0° (Oblate) and γ= 60° (Prolate)

REFERENCES

1. F. Iachello, collective aspects of the shell model, Proc. Int. Conf. on Nucl. Structure and Spectroscopy, Amsterdam (1974).
2. A. Arima, F. Iachello, Ann. Phys. 99, 293 (1976).
3. A. Arima, F. Iachello, Ann. Phys. 111, 201 (1978).
4. O. Scholten, F. Iachello, A. Arima, Ann. Phys. 115,325 (1979).
5. A. Arima, F. Iachello, Ann. Phys. 123, 468 (1979).
6. F.S. Radhi, N.M. Stewart, Z. Phys. A 356, 145-153 (1996).
7. A. Arima, A., Iachello, F., Ann. Phys. (N.Y) 99, 253 (1976).
8. R.F. Casten, and D.D. Warner: Rev. Mod. Phys. Vol. 60, 391 (1988).
9. M. Sohair Diab and A. Salah Eid. Potential Energy Surfaces of the Even- Even $^{230\text{-}238}$U Isotopes, Vol. 3, July, (2008).
10. H. Freshband and F. Iachello, Ann. Phys., Vol. 84, 211(1974).
11. D.D Warner and R.F. Casten: Phys. Rev. Vol. 25, 1 (1982).
12. A. Arima, F. Iachello, "Interacting boson Model" Ed. Iachello; Pub. Cambridge, England. PP. 3-236 (1987).
13. W. Pfeifer: "Introduction to interacting boson model of atomic nucleus" PI, PP. 5, (1998).
14. J. Lang, K. Kumer, and J. Hamilton, Rev. Mod. Phys. Vol. 54, 119 (1982).
15. M. Sakai " Atomic Data and Nuclear Data Tables"Vol.31, 410 (1984).

A Single Machine Scheduling Problem to Minimize the Sum of Total Completion Times and Total Late Works

Manal G. Ahmed Al-Ayoubi
Mathematic Dept College of science Al- Mustansiriyah University

Received 27/2/2012 – Accepted 20/6/2012

الخلاصه

كما وقدمنا تم في هذا البحث تناول مسألة جدولة ثنائية المعاير على ماكنة واحده. المقياسان المراد تصغيرهما $\sum C_i$, $\sum V_i$. خوارزمية التفرع والتقييد لإيجاد الحل الأمثل لمسألة تصغير الدالة الخطية ($\sum C_i + \sum V_i$,.i.e).واعطينا تجارب حسابية لطريقة التفرع والتقييد على مجموعة كبيرة لمسائل اختبارية. واستخدمنا طرائق البحث المحلية Local search heuristics methods لايجاد حلول مثلى قريبة من الحل الامثل وبزمن حسابي اقل . وأيضا قدمنا تقرير عن نتائج العمليات الحسابيه Genetic Algorithm (GA) , Particle Swarm Optimization (PSO)
الاستنتاج الرئيسي الذي يمكن استخلاصه من نتائجنا الحسابية هو ان (GA) هي اكثر طريقة فعالة لمسألتنا تليها (PSO).

ABSTRACT

In this paper bi-criteria scheduling problem on a single machine are considered. The two criteria to be minimized are $\sum V_i$ and $\sum C_i$.

We present a Branch and Bound algorithm to find optimal solution for the problem of minimizing a linear function (i.e., $\sum C_i + \sum V_i$). A computational experiment for the BAB algorithm on a large set of test problems is given. We use local search heuristics methods to find near optimal solutions that are close to the optimum with less computational time. Also, we report on the results of extensive computations test of the Genetic Algorithm (GA) and Particle Swarm Optimization (PSO) Method.

The main conclusion to be drawn for our computation results is that (GA) is more effective method for our problem followed by (PSO).

Keywords: single machine scheduling, bi-criteria, Genetic algorithm, Particleswarm optimization method

INTRODUCTION

Machine Scheduling Problems (MSPs) are one of the classical combinatorial optimization problems which exists in many diverse areas such as flexible manufacturing systems, production planning, airline industry, etc.[1]

In real life situations, decisions to be made are often constrained by specific requirements. More importantly, these constraints are typically conflicting in nature. The decision making process gets increasingly more complicated with increment in the number of constraints. Modeling and development of solution methodologies for these scenarios have been the challenge for operations researchers from the outset. A variety of algorithms and formulations have been developed for various classes of problems. Scheduling is one of such classes of problems [2].

Scheduling theory has been developed to solve problems occurring in for instance production facilities. The basic scheduling problem can be described as finding for each of the tasks, which are also called jobs, an execution interval on one of the machines that are able to execute it, such that all side-constraints are met; obviously, this should be done in such a way that the resulting solution, which is called a schedule, is best possible, that is, it minimizes the given objective function [3].

Because the one-machine problem provides a useful laboratory for the development of ideas for heuristics and interactive procedure that may prove to be useful in more general models, we consider the one-machine case in this study.

Scheduling has received much attention in the literature since the pioneering work of Jonson in 1954. In the first 30 years, it was usual to consider only one objective function as performance criterion. However, in many practical situations a decision-maker has to take into account simultaneously several objectives. Therefore, the investigation of multi-criteria scheduling problems has begun about 20 years ago with a growing interest nowadays [4].

Recently, much research has been directed to scheduling problems with multiple criteria. A comprehensive overview for the development of this topic can be found in Nagar et al. (1995) [5] as well as Hoogeveen (2005)[3].

This paper consists of these sections; section 1 is a problem formulation. Section 2 is using branch and bound method to find an optimal solution. Section 3 local search heuristics methods. Section 4 computational experience. Section 5 conclusion. Section 6 future work.

Problem Formulation

We are given n jobs to be scheduled on a single machine which can handle only one job at a time. All jobs are available for processing at time zero. The objective is to find a processing order of the jobs that minimize the sum of total completion times and total late works (the objective function is denoted by $\sum C_i + \sum V_i$)

Let $N=\{1,2,3,\ldots,n\}$ be a set of independent jobs which are processed on a single machine . Each job has positive integer P_i (processing time) and positive integer d_i (due date). Using the three field classification suggested by Graham et. al.[6] , this problem denoted as $1//\sum C_i + \sum V_i$ where for each job i $C_i = \sum_{j=1}^{i} P_j$ for a given schedule $(1,2,\ldots\ldots,n)$ and

$$V_i = \begin{cases} 0 & \text{if} \quad C_i \le d_i \\ C_i - d_i & \text{if} \quad d_i < C_i < d_i + p_i \\ P_i & \text{if} \quad C_i \ge d_i + p_i \end{cases}$$

Since $1//\sum V_i$ is NP –hard [7] then the problem under investigation is known to be NP –hard .

The objective to find the schedule $\sigma = (\sigma(1),\ldots, \sigma(n))$ of the jobs that minimize the total cost $W(\sigma)$ for the following problem:

$$\underset{\sigma\in S}{Min} W(\sigma) = \min_{\sigma\in S}\{\sum_{i=1}^{n} C\sigma(i) + \sum_{i=1}^{n} V\sigma(i)\}$$

s.t.

$C_{\sigma(i)} \geq P_{\sigma(i)} \quad \forall i = 1,2,\ldots,n$

$C_{\sigma(i)} = C_{\sigma(i-1)} + P_{\sigma(i)} \quad , i = 2,\ldots,n$

$V_{\sigma(i)} = 0 \quad \text{if} \quad C_{\sigma(i)} \leq d_{\sigma(i)}$

$V_{\sigma(i)} = C_{\sigma(i)} - d_{\sigma(i)} \quad \text{if} \quad d_{\sigma(i)} < C_{\sigma(i)} < d_{\sigma(i)} + P_{\sigma(i)}$

$V_{\sigma(i)} = P_{\sigma(i)} \quad \text{if} \quad C_{\sigma(i)} \geq d_{\sigma(i)} + p_{\sigma(i)}$

$V_{\sigma(i)} = \min\{P_{\sigma(i)}, T_{\sigma(i)}\}$ (P)

Where

S is the set of all feasible schedules and σ is a schedule in S .

Using Branch and Bound Method to Find an Optimal Solution

1- Derivation of Lower Bound for the problem

Our problem can be decomposed into two subproblems SP1 and SP2 then the lower bound (LB) of the problem is the sum of the minimum value of the subproblem SP1 and SP2 .

$$W1 = \underset{\sigma\in S}{Min} \sum_{i=1}^{n} C\sigma(i)$$

s.t.

$C_{\sigma(i)} \geq P_{\sigma(i)} \quad \forall i = 1,2,\ldots,n$

$C_{\sigma(i)} = C_{\sigma(i-1)} + P_{\sigma(i)} \quad , i = 2,\ldots,n$ (SP1)

$$W2 = \underset{\sigma\in S}{Min} \sum_{i=1}^{n} V\sigma(i)$$

s.t.

$V_{\sigma(i)} = 0 \quad \text{if} \quad C_{\sigma(i)} \leq d_{\sigma(i)}$

$V_{\sigma(i)} = C_{\sigma(i)} - d_{\sigma(i)} \quad \text{if} \quad d_{\sigma(i)} < C_{\sigma(i)} < d_{\sigma(i)} + P_{\sigma(i)}$

$V_{\sigma(i)} = P_{\sigma(i)} \quad \text{if} \quad C_{\sigma(i)} \geq d_{\sigma(i)} + p_{\sigma(i)}$

$V_{\sigma(i)} = \min\{P_{\sigma(i)}, T_{\sigma(i)}\}$ (SP2)

It is clear from the decomposition that SP1 and SP2 have simpler structures than P , and thus appear easily to solve optimality for SP1 (SP1 is solved by shortest processing time (SPT)rule (i.e. $p1 \leq p2 \leq \ldots\ldots \leq pn$)) then SPT gives a lower bound LB1 = W1 for SP1,and a lower bound LB2 for SP2 is obtained as follows: ordered the jobs by

EDD rule (i.e. d1≤ d2≤ .....≤ dn) and calculate T_{max} = max $\{T_i\}$=max$\{\max(C_i - d_i,0)\}$, and LB2 = T_{max}[7].

Then LB = LB1+LB2.The lower bound of each node in solution search tree is written against each node of the tree .

2- Derivation of Upper Bound

We can find upper bound (UB) for our problem (P) by using (SPT) rule, since SPT rule gives the optimal solution to $\sum C_i$ problem. This upper bound is applied at the root node of (BAB) search tree.

if $\sigma = (\sigma(1),\ldots, \sigma(n))$ is obtained by SPT rule ,

$$\text{then} \quad UB = \sum_{i=1}^{n} C\sigma(i) + \sum_{i=1}^{n} V\sigma(i)$$

The BAB method is determined by the following procedures [8] :

1- **The Branching Procedure :** This describes the method to partition a subset of possible solution .The subsets can be treated as a set of solutions of corresponding subproblems of the original problem.

2- **The Bounding Procedure :** This indicates how to calculate a lower bound (LB) on the optimal solution value for each subproblem generated in the branching process.

3- **The Search Strategy :** This strategy describes the method of choosing a node of the search tree to branch from it, we usually branch from a node with the smallest lower bound (LB) among the recently created nodes.

Using Dynamic Programming Dominance (DP Dominance)

For any two nodes of search tree corresponding to two final partial sequences containing the same jobs. The one which has the largest cost of objective function of its sequence jobs can be discarded .This means compare cost of σ ij with cost σ ji.

We use (DP) dominance so that some branches can be eliminated from further examination and then the number of nodes with the time spend on solving our problem are reduced .

Local Search Heuristic Method

The word heuristic comes from Greek word (heuriskein) which means to find or to discover[8]. Reeves [9] define a heuristic as a technique which seeks good (near optimal) solutions at a reasonable computational time without being able to guarantee either optimality, or even in many cases to state how close to optimality a particular feasible solution. It is clear to solve scheduling problems one tends to use (BAB) or (DP) method to find optimal solutions, but these approaches has two main disadvantages :

1- It is mathematically complex and thus a lot of time be invested [10] .

2- When it concerns NP-hard problem, the computational time requirements are enormous for large sized problem, to avoid these drawbacks we can appeal to heuristics methods.

In this paper we used two methods of local search methods which are Genetic Algorithm and Particle Swarm Optimization Method .

Genetic Algorithm

Genetic Algorithms (GAs) were first proposed by John Holland [11] in the 1960s. The GA is a heuristic search technique that simulates the rocesses of natural selection and evolution. A GA maintains a population of individuals over many generations. An initial population of individuals, each representing a feasible solution to the given problem is constructed at random. For each generation, the fitness value of each individual in the population is measured, where a high fitness value would exhibit a better solution compared to a low fitness value. Fitter members are more likely to be selected from the population using a selection mechanism to produce offspring for the subsequent generation via crossover and mutation. After many generations the result is hopefully a population that is substantially fitter than the original. [1]

The following steps describe each of GA mechanisms in our problem:

- Initial population

In this problem the initial population with size 20 chromosomes (solutions) which are generated randomly.

- Parent selection

The selection strategy is a procedure to choose the individuals in the current population for creating offspring of subsequent generation. Two parent solutions (chromosomes) are selected from a current population according to their values, the better fitness, the bigger chance to be selection.

- The crossover operator

The crossover operation is the most important operator in GA, we use Uniform Order–Based Crossover [12].

- The mutation operator

Swap mutation is applied on each pair of parent solutions to generate two new solutions.

- Replacement Strategy

The elitist strategy is applied in this problem. In each generation we select the best chromosome as one of the chromosomes in the next population, in addition to the chromosomes (parents and offsprings) which are ranked after crossover and mutation according to their fitness values.

- Stopping Condition

The GA procedure stops when a fixed number of generations (or iterations) are executed here 1000 iterations. This means that GA procedure continuous until the population is converged to a good, if not optimal solution to our problem (P).

2- Particle Swarm Optimization [13]

Particle Swarm Optimization (PSO) is one of the latest evolutionary optimization methods. It is a population-based technique, which was originally developed by Kennedy & Eberhart in 1995 [14]. PSO is based on the metaphor of social interaction and communication, such as bird flecking and fish schooling.

Since it is population-based and evolutionary in nature, the members in a PSO algorithm tend to follow the leader of the group, i.e., the one with the best performance.

PSO shares many common points with GA. Both algorithms starts with a group of randomly generated population, both have fitness values to evaluate the population. Both update the population and search for the optimum with random techniques. Both systems do not guarantee success.

But, PSO is distinctly different from other evolutionary-type methods in a way that it does not use the filtering operation (such as crossover and/or mutation) and the members of the entire population are maintained through the search procedure so that information is socially shared among individuals to direct the search towards the best position in the search space.

PSO can be easily implemented and it is computationally inexpensive, since its memory and CPU speed requirements are low [15]. Moreover, it does not require gradient information of the objective function under consideration, but only its values, and it uses only primitive mathematical operators. PSO has been proved to be an efficient method for many global optimization problems and some cases it does not suffer the difficulties encountered by other evolutionary computation techniques [16].

In evolutionary computation techniques, three main operators are involved: the recombination, the mutation and the selection operators.

PSO does not have a direct recombination operator. However, the stochastic acceleration of a particle towards its previous best position, as well as towards the best particle of the swarm (or towards the best in its neighborhood in the local version), resembles the recombination procedure in evolutionary computation [17],[18],[19].

In a PSO algorithm, each member is called "particle", and each particle flies around in the multi-dimensional search space with a velocity, which is constantly updated by the particle's own experience

and the experience of the particle's neighbors or the experience of the whole swarm, instead of being carried from fitness dependent selected "parents" to descendants as in GAs.

PSO is actually the only evolutionary algorithm that does not use the "survival of the fittest" concept. It does not utilize a direct selection function. Thus, particles with lower fitness can survive during the optimization and potentially visit any point of the search space [17].

The original PSO algorithm is described as below:

$$V_{ij}^{k} = V_{ij}^{k-1} + c_1 r_1 (pb_{ij}^{k-1} - x_{ij}^{k-1}) + c_2 r_2 (gb_j^{k-1} - x_{ij}^{k-1}) \quad (1a)$$

$$x_{ij}^{k} = x_{ij}^{k-1} + v_{ij}^{k} \quad (1b)$$

Where c_1 and c_2 are positive constants, and r_1 and r_2 are two random functions in the range [0,1].

The above equations describe the flying trajectory of a population of particles. Equation (1a) describes how the velocity is dynamically updated and Equation (1b) the position update of the "flying" particles.

Equation (1a) consists of three parts. The first part is the "momentum" part. The velocity can't be changed abruptly. It is changed from the current velocity. The second part is the "cognitive" part which represents private thinking of itself-learning from its own flying experience. The third part is the "social" part which represents the collaboration among particles-learning from group flying experience[20].

Two variants of the PSO algorithm are developed, namely PSO with a local neighborhood, and PSO with a global neighborhood. According to the global neighborhood, each particle moves towards its best previous position and towards the best particle in the whole swarm, called gbest model. On the other hand, according to the local variant so called lbest, each particle moves towards its best previous position and towards the best particle in its restricted neighborhood [21].

The velocities of particles are constrained to a maximum velocity, V_{max}. If a velocity on a dimension of a particle exceeds V_{max}, then it is limited to V_{max}. V_{max} controls the exploration and exploitation ability of a particle. It helps to search the regions between the current position and the target position.

Fine-tuning V_{max} is so important that a large value of V_{max} facilitates global exploration, while a smaller V_{max} encourages local exploitation. If V_{max} is set too high or too small, the particles can't explore the search space sufficiently and they could stuck at local optima.

Eberhart & Shi introduced a new concept to PSO in 1998; the inertia weight (w) which highly increased the performance of PSO in a number of applications. Before PSO was not searching neighbors

sufficiently. Dynamically adjusting the velocity by means of w provided the local search.

The inertia weight controls the effect of previous velocity of the particle to its current velocity as seen in the formulas below:

$$V_{ij}^{k} = w^{k-1} V_{ij}^{k-1} + c_1 r_1 (pb_{ij}^{k-1} - x_{ij}^{k-1}) + c_2 r_2 (gb_j^{k-1} - x_{ij}^{k-1}) \quad (1c)$$

$$x_{ij}^{k} = x_{ij}^{k-1} + v_{ij}^{k} \quad (1d)$$

Where r_1 , $r_2 \sim$ Uniform (0,1), w:inertia weight
and $w^k = w^{k-1} * \alpha$, where α is the decrement factor.

Setting high values to w at the beginning and small values at the end of the search is found to be better. When suitably set, the inertia weight helps to balance the local and global exploration, thus the optimal value can be obtained in a few iterations. High values encourage global exploration, while low values facilitate local exploitation.

Some of the wide application area of PSO are, power and voltage control, neural network training, supplier selection and ordering problem, ingredient mix optimization, system design, pattern recognition, biological system modeling, signal processing, robotic applications, decision-making, simulation,...etc. More literature can be found in [21].

The PSO used in our problem is PSO with a global neighborhood starts with 20 particles population and the equation (1c), (1d) used in this paper with $V_{max} = 2$, $V_{min} = -V_{max}$, $w \in [0.4, 0.9]$, $c_2 = c_1 = 2$, r_1 and $r_2 \in [0, 1]$ and the algorithm is stopped when iterations are executed 1000 iterations .

Computational experience

An intensive work of numerical experimentations has been performed. We first present how instances (tests problem) can be randomly generated.

There exists in the literature a classical way to randomly generate tests problem of scheduling problems.

- The processing time P_i is uniformly distributed in the interval [1,10].
- The due dates d_i are uniformly distributed in the interval $[P(1-TF-RDD/2), P(1+TF+RDD/2)]$; where $P=\sum P_i$, depending on the relative range of due date (RDD) and on the average tardiness factor (TF). For both parameters, the values 0.2 , 0.4 , 0.6 , 0.8 ,1.0 are considered. For each selected value of n two problems were generated for each of the values of parameters producing 10 problems for each values of n.

The BAB algorithm was tested in Fortran Power Station and GA , PSO algorithms were tested in Delphi Language and running on

Pentium (R) at 2.20 GHz with Ram 2 GB computer processor-type PDCT 4400.

In table (1) n = 11 jobs , 13 jobs and 15 jobs we list 10 problems for each value of n. Test problems are tested to show the efficiency of our lower bound (LB) used in BAB algorithm to obtain the optimal solution. Results of comparing the lower bound , upper bound and the optimal solutions are given in table (1). The first column is the number of problems. The second column gives the value of an optimal solution found by using BAB algorithm. The third column gives the value of the initial lower bound (ILB). The fourth column gives the value of our upper bound (UB). The fifth column gives the number of nodes (Nodes). The six column gives the time in seconds (Time).

Table -1: The performance of initial lower bound, upper bound, number of nodes and computational time in seconds of BAB algorithm.

n	Number	Opt.	ILB	UB	Nodes	Time
11	1	293*	285	293	5501	0.0005
	2	298	283	309	9156	0.00066
	3	304	295	309	12554	0.0001
	4	297	283	305	5943	0.0005
	5	293	291	299	5783	0.0006
	6	296	288	302	5232	0.0003
	7	311	299	313	8087	0.00083
	8	317	307	323	7810	0.00083
	9	300	293	305	6264	0.0005
	10	313	304	314	11821	0.001
13	1	489*	484	489	131402	0.01333
	2	488	479	499	103032	0.01083
	3	493	479	505	144772	0.00833
	4	494	479	507	174555	0.010
	5	515	500	528	229575	0.0130
	6	509	484	531	228226	0.0130
	7	508	493	514	213240	0.01433
	8	516	498	529	289101	0.0255
	9	521	498	527	317218	0.0203
	10	525	508	539	390906	0.0266
15	1	**	474	491		
	2	481	469	486	1984494	0.20983
	3	471	469	482	784567	0.10700
	4	483	469	486	1314184	0.14983
	5	**	483	513		
	6	496	476	511	1900446	0.24166
	7	**	473	513		
	8	490	489	504	1181915	0.1135
	9	490	482	496	1392911	0.1660
	10	**	498	519		

Opt. = The optimal value obtained by BAB algorithm.
ILB = Initial lower bound.
UB = Upper bound.
Nodes = The number of generated nodes.
Time = Computational time in seconds.
* = The optimal value equal to upper bound.
** = The number of nodes are greater than 2000000.

Table -2: comparison optimal solutions in BAB with genetic and Particle Swarm Optimization methods .

n	Number	Optimal	GA	PSO
12	1	308	308	323
	2	307	307	326
	3	297	297	314
	4	298	298	313
	5	318	318	330
	6	311	311	323
	7	312	312	323
	8	336	336	352
	9	324	324	328
	10	338	338	345
No. of optimal			10	-
14	1	427	427	442
	2	424	424	438
	3	427	428	444
	4	424	424	444
	5	437	437	448
	6	433	433	449
	7	429	429	447
	8	443	443	459
	9	445	445	465
	10	441	442	465
No. of optimal			8	-

Optimal = Optimal solution in BAB.
GA = Genetic Algorithm.
PSO = Particle Swarm Optimization Method.

Comparative Results for Local Search Methods

Table (3) shows the comparative of local search methods which are GA and PSO .

The results in table (3) show that (GA) has good performance results, followed by (PSO).

Table -3: comparison between Local Search Methods

			N=500
N	**G A**	**PSO**	**Best**
1	547235	650906	547235
2	548127	649765	548127
3	554753	650273	554753
4	555096	650944	555096
5	559416	642095	559416
6	543895	652518	543895
7	553925	646926	553925
8	544254	649322	544254
9	556325	648380	556325
10	555285	649968	555285
No. of best	10	-	-
Av. time	13	6.8	-
			N=1000
1	2446375	2735921	2446375
2	2415292	2733290	2415292
3	2480605	2726175	2480605
4	2489448	2726600	2489448
5	2472945	2732574	2472945
6	2475155	2732835	2475155
7	2407027	2733811	2407027
8	2434110	2741051	2434110
9	2427874	2717555	2427874
10	2444450	2731973	2444450
No. of best	10	-	-
Av. time	36.7	19.5	-
			N=1500
1	5436325	5951516	5436325
2	5435249	5945804	5435249
3	5388584	5979512	5388584
4	5521891	5936747	5521891
5	5419784	5966182	5419784
6	5445155	5942386	5445155
7	5455254	5952615	5455254
8	5432081	5962459	5432081
9	5382387	5937703	5382387
10	5524879	5945766	5524879
No. of best	10	-	-
Av. time	69.2	30.8	-

GA = Genetic Algorithm.
PSO = Particle Swarm Optimization.
Best = The best solution by using GA and PSO.
No. of best = Number of best solutions.
Av. time = Average time of ten examples.

CONCLUSIONS

In this study, the problem of scheduling jobs on one machine to minimize bi-criteria are considered. The two criteria to be minimized are $\sum V_i$ and $\sum C_i$.

We present a Branch and Bound algorithm to find optimal solution for the problem of minimizing a linear function (i.e., $\sum V_i + \sum C_i$). A computational experiment for BAB algorithm on a large set of test problems are given and BAB algorithm solve our test problem up to (15) jobs . The NP−hardness of this problem and the optimal solutions of the BAB algorithm are not always quickly. Hence , this problem is solved by using local search methods Genetic Algorithm and Particle Swarm Optimization method. Also , we report on the results of extensive computations test of local search methods.

The main conclusion to be drawn for our computation results is that GA is more effective method for our problem followed by PSO . Whereas the computational time of (PSO) is very small but the computational time of (GA) is larger than (PSO).

An interesting future research topic would involve experimentation with the following problems:

F2/ / $\sum V_i + \sum C_i$.

1 / / $\sum V_i + \sum C_i + V_{max}$.

REFRENCES

1. Nazif H. and Lee L.S., "A Genetic Algorithm on Single Machine Scheduling Problem to Minimize Total Weighted Completion Time ", European Journal of Scientific Research ISSN 1450-216X Vol.35 No.3 pp.444-452 (2009).
2. Divya Prakash , " Bi-criteria Scheduling Problem on Parallel Machines " , M.Sc. thesis , Virginia Polytenchnic Institute and State University (2007).
3. Hoogeveen J.A, " Invited Review Multi-criteria Scheduling " , European Journal of Operational Research 167 , 592−623 (2005).
4. Kindt T,Billaut J., " Multi-criteria Scheduling. Theory, Models and Algorithms " , Spring Verlag, ISBN 3-540-43617-0, 303 pp., EUR 74.95(2002).
5. Nagar A., Jorge H., and Sunderesh H., " Multiple and bi-criteria scheduling : A literature survey " , European Journal of Operational Research North-Holland, 81,88-104 (1995).

6. Graham R. L., Lawler E. L., Lenstra J. K., Rinnooy Kan A. H. G. " Optimization and approximation in deterministic sequencing and scheduling ". A survey. Ann Discrete Math, 5 (287-326) 1979.
7. Potts C. N. and Van Wassenhove L. N., " Single Machine To Minimize Total Late Work " Operations Research Vol.40 , No.3 (1992).
8. Hummadi L.Z. "Using Genetic algorithm to solve (NP-complete) problems " . M.Sc. Thesis. College of Science, University of Al-Mustansiriyah, (2005).
9. Reeves CR. " Modern Heuristic Techniques for Combinatorial Problems ". John Wiley and Sons, Inc, New York, (1993).
10. Crauwels, H. " A comparative study of local search methods for one machine sequence problem " . Ph.D. thesis Katholieke University, Heverlee. Belgium (1998).
11. Holland, J.H., "Adaptations in natural and artificial systems " , Ann Arbor: The university of Michigan Press(1975).
12. Hameed W. M., "The Role of Crossover in Genetic Algorithms ",M.Sc. Al-Mustansiriya Univ.,(2005).
13. Ozgur Uysal and Serol Bulkan " Comparison of Genetic Algorithm and Particle Swarm Optimization for Bicriteria Permutation Flowshop Scheduling Problem" International Journal of Computational Intelligence Research. ISSN 0973-1873 Vol.4, No. 2, pp.159-175, (2008).
14. Kennedy J., Eberhart R. C. : "Particle swarm optimization" , In Proceedings of IEEE International Conference on Neural Networks, Piscataway, NJ, USA, PP. 1942-1948, 1995.
15. Eberhart R. C. , Simpson P.K. , Dobbins R. W. Computational Intelligent PC Tools, Boston, MA., Academic Press Professional, 1996.
16. Eberhart R.C. , Kennedy J. " A new optimizer using particle swarm theory " , In Proceedings of the sixth International Symposium on Micro Machine and Human Science, Nagoya, Japan, pp. 39-43, 1995.
17. Eberhart R.C. , Shi Y. " Comparison between genetic algorithms and particle swarm optimization " . In Evolutionary Programming VII, Porto, V.W., Saravanan, N., Waggen, D. and Eiben, A.E. (eds.), Springer, pp.611-616, 1998.

18. Rechenberg I. , " Evolution Strategy" , In Computational Intelligence: Imitating life, Zurada, J.M., Marks, R.J.II and Robinson, C. (eds.), IEEE Press, Piscataway, NJ, 1994.
19. Schwefel H-P., Evolution and Optimum Seeking, Wiley, New York, 1995.
20. Shi Y., Eberhart R.C., " A modified particles swarm optimizer " , In Proceedings of the 1998 IEEE International Conference on Evolutionary Computation, pp. 69-73, 1998b.
21. Kennedy J. , Eberhart R.C. , Shi Y. , Swarm intelligence, Morgan Kaufmann, San Mateo, CA., 2001.

Estimation of Daily Diffuse Solar Radiation for Different Iraqi Cities

Ali Raheem Tuaimah
Atmospheric science Department, College of science, AL-Mustansiryah University

Received 8/5/2012 – Accepted 20/6/2012

الخلاصة

إن الطاقة الشمسية هي موضع اهتمام لكونها مصدر طاقة نظيفة ومتجددة . تم تحليل واستخدام بيانات متوسط قراءات الإشعاع الشمسي الكلي والمنتشر الساقط على سطح أفقي لمدة 22 سنة لمناطق مختلفة من العراق ولتحقيق هذا الهدف استخدم نموذج رياضية خاص تقوم بتقدير قيم الإشعاع الشمسي المنتشر من القيم اليومية للجو الصحو لمناطق مختلفة في العراق .أظهرت النتائج انه يمكن لهذا النموذج الرياضي إن يقدر قيم الإشعاع الشمسي المنتشر الساقط على سطح أفقي وبدقة عالية . وأظهرت النتائج كذلك بان علاقة الارتباط جيد بين نتائج النموذج الرياضي والقيم المسجلة .

ABSTRACT

Solar radiation energy is a very attraction issue for study because it is renewable and clean energy. Analysis of 22 year of daily solar radiation (global and diffuse) on horizontal surfaces at different cities in Iraq . To achieve this goal , a special statistical model was used to estimate diffuse fraction from clearness index at a daily scale at different Iraqi regions. The results showed that this model can estimate diffuse solar radiation on a horizontal surface with high resolution. It also showed a good correlation between the model and observation.

Keywords; diffuse fraction, solar energy, solar radiation, diffuse radiation.

INTRODUCTION

All sources of solar energy may be grouped into two general categories, incoming energy, which is the energy reaching the earth from outer space, and capital energy, which is the energy that already, exists on or within the earth[1].

One of the promising usages of renewable energy technology is the installation of the solar collector system .The applications of the solar collector system have become more widespread in both developed and developing countries [2 ,3].

Solar radiation varies with season and time of the day due to the various Sun positions under the unpredictable weather conditions [4].The global solar radiation reaching the earth's surface is made up of two components, direct and diffuse. Direct radiation is the part which travels unobstructed through space and the atmosphere to the surface, it's depends on the time of day, the time of year, the local latitude , the amount of cloud cover, and the amount of atmospheric pollution [5] .

Diffuse solar radiation is the solar radiation received from the sun after its direction has been changed by reflection and scattering by the atmosphere [6].

On a planetary scale, 17% of solar radiation is absorbed by the atmosphere, 30% is reflected by the constituents of the atmosphere, and

53% (31% as direct radiation and 22% as diffuse radiation) reaches the surface of the earth [7] .

However, most solar radiation recording stations measure only the total horizontal solar intensity Thus researchers resort to theoretical studies to estimate the diffuse radiation at that places , to determine direct radiation which is of vital importance for the development of solar energy devices and for estimates of their performances [8].

The first attempt at estimating global solar radiation was the well-known empirical relation between global solar radiation under clear sky conditions and bright sunshine duration, given by Angstrom [9]. Theoretical and empirical models have been postulated to compute the components of the insolation. Some of these models are theoretical, dealing with the solution of the radiative transfer equation, while others are simply regression models [10 ,11,12,13,14,15].

MATERIALS AND METHODS

Solar radiation data used in this study were obtained from NASA Surface Meteorology and Solar Energy (16) for different regions of Iraq : Basra (south Iraq), Baghdad (middle Iraq) ,Rutbah (east Iraq) and Mosul (north Iraq) , Table (1) gives the geographical locations of these stations:

Table -1: Geographical locations of recording stations [17]

stations	Latitude N	Longitude E	Elevation m
Basrah	30.34	47.47	2
Baghdad	33.23	46.14	34
Rutbah	33.03	40.28	800
Mosul	36.14	43.09	223

A 22-year period (1983-2005) of daily diffuse and global radiation were used in this study. All data were manually checked for errors. The data which violate of physical laws, such as diffuse radiation being greater than global radiation, or global radiation being greater than extraterrestrial radiation were subsequently discarded.

The data set was organized into two groups. The first group (1983-2004) was used for estimating the models, whereas the second group (2005) was employed for models validation. To formulate the model for each station, daily diffuse fraction (k_d) (the ratio of daily diffuse radiation to daily global radiation) and daily clearness index (k_t) (the ratio of daily global radiation to daily extraterrestrial radiation) were plotted .

After choosing the best correlation formula that gives a good fitting through most reading, by used Nonlinear Regression Polynomial Inverse Third Order .The equations are employed to calculate the diffuse radiation for the four stations. The values of

diffuse radiation are then compared with the measured data for Basra, Baghdad ,Rutbah and Mosul . The accuracy of the estimated diffuse radiation data is tested by calculating the correlations coefficients(R) the correlations coefficients is one of the most important statistic tool to compare two variables and indications about the correlation formula. If its value close to one, this means that the regression formula is fitting through most of measurement data) , the mean bias (MBE) (w/m^2 day), root mean square (RMSE) (w/m^2 day) and the mean percentage (MPE) errors(%) are defined as follows:

$$R=\frac{\sum(Hical-\overline{Hc})(Himeas-\overline{Hm})}{\sqrt{\sum(Hical-\overline{Hc})^2(Himeas-\overline{Hm})^2}} \quad .....(1)$$

$$MBE=\frac{(\sum(Hical-Himeas)}{n-1} \quad .....(2)$$

$$RMSE\sqrt{\frac{(\sum(Hical-Himeas))^2}{n-1}} .....(3)$$

$$MPE=\frac{\left[\sum(\frac{(Himeas-Hical)}{Himeas}\times 100)\right]}{n-1} \quad .....(4)$$

Where H is the calculated and measured values and n is the total number of observations and $\overline{Hc}, \overline{Hm}$ was the arithmetic mean value of the calculate and measured values of the diffuse solar radiation.

In general, a low RMSE is desirable. The positive MBE shows overestimation while a negative MBE indicates underestimation.

RESULTS AND DISCUSSIONS

One of the most important energy sources in our economy is still oil, which is not renewable. In this paper, studies on the prediction of daily diffuse solar radiation on horizontal surfaces have been carried out and predicted formulas were used to calculate the Solar Radiation in Iraq. Diffuse fraction (k_d) are plotted against clearness index (k_t) ,the results are shown in Fig 1.

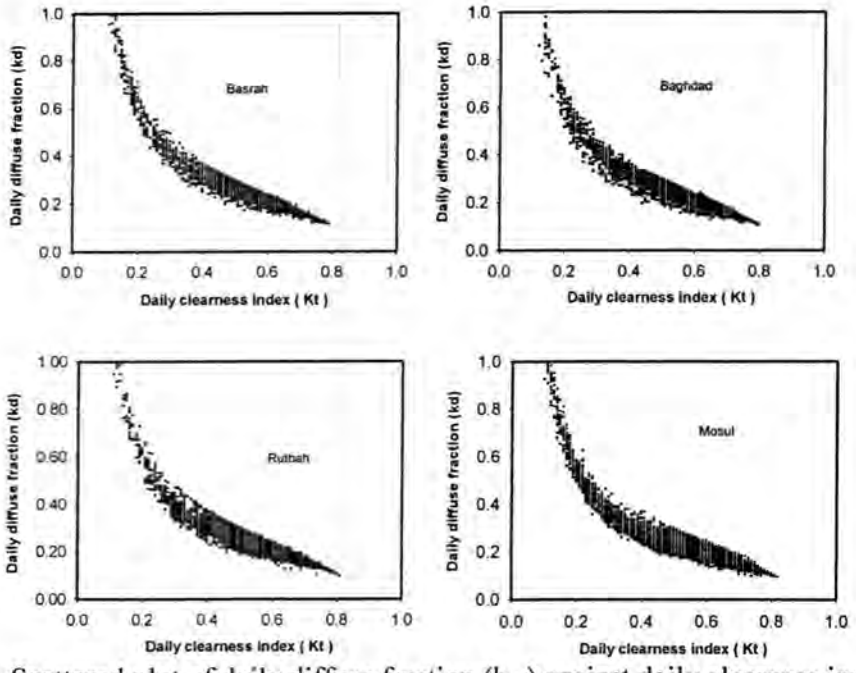

Fig-1:. Scattered plot of daily diffuse fraction (k_d) against daily clearness index (k_t,) for all stations (1983- 2004)

Figure 1 shows considerable scatter in all stations. This is due to the fact that the main factor affecting diffuse solar radiation and global solar radiation are clouds and cloud structure has a random nature. Although the data points are scattered, the graphs of all stations exhibit a similar trend. This trend shows that the relation between diffuse fraction (k_d) and clearness index (k_t) is inverse. This corresponds to the fact that the clearer of the atmosphere, the less the quantity of diffuse global radiation. In general, diffuse radiation in the tropics is mainly generated by the scattering of direct radiation by air molecules, atmospheric aerosols and clouds. The Polynomial Nonlinear Regression Inverse First, Second and Third Order are used to choose the best correlation formula that gives agood fitting between the diffuse fraction (k_d) and the clearness index (K_t),as show in table 2.

Table -2: Comparisions in Degree of order, correlation coefficient (R) and Standard Error of Estimate to choose the best fitting :

Stations	Degree of order	R	R^2	Standard Error of Estimate
Basrah	Inverse First Order	0.9693	0.9396	0.0226
	Inverse Second Order	0.9725	0.9457	0.0214
	Inverse Third Order	0.9750	0.9506	0.0205
Baghdad	Inverse First Order	0.9612	0.9240	0.0242
	Inverse Second Order	0.9637	0.9287	0.0234
	Inverse Third Order	0.9672	0.9356	0.0223
Rutbah	Inverse First Order	0.9530	0.9082	0.0262
	Inverse Second Order	0.9583	0.9183	0.0248
	Inverse Third Order	0.9626	0.9267	0.0235
Mosul	Inverse First Order	0.9690	0.9389	0.0277
	Inverse Second Order	0.9690	0.9390	0.0277
	Inverse Third Order	0.9693	0.9396	0.0276

After choosing the best correlation formula that gives a good fitting through most reading, by using Polynomial Nonlinear Regression Inverse Third Order because it gave the chance to chose the best exponential faction that gave best correlation and less Standard Error of Estimate between calculated and estimate data ,as show in figure 2 while the empirical models in Table 3.

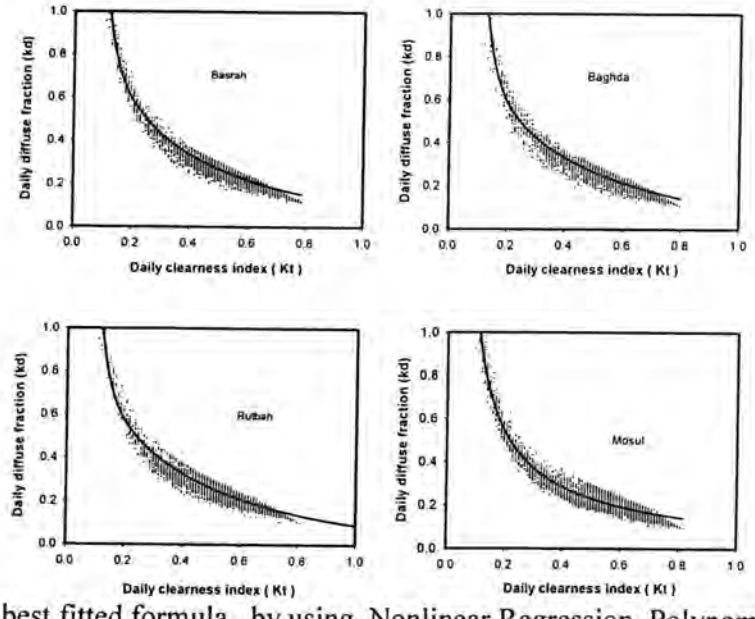

Figure -2: best fitted formula , by using Nonlinear Regression Polynomial Inverse Third Order for the all stations (1983- 2004).

From the results of Table 3 it is clear that for all selected stations, the values of the correlations coefficients (R) from Equations (1) of the proposed correlations are
Higher than 0.91 which indicate good fitting between the clearness index (k_t) and diffuse fraction (k_d).

Table -3: Equations relating the diffuse fraction (k_d) and clearness index (k_t). R is correlation coefficient.

Stations	Equations	R	R^2
Basrah	$k_d = -0.1140 + (0.2461/Kt) + (-0.0321/Kt^2) + (0.0023/kt^3)$	0.975	0.950
Baghdad	$k_d = -0.1426 + (0.2776/Kt) + (-0.0439/Kt^2) + (0.0035/kt^3)$	0.967	0.935
Rutbah	$k_d = -0.1851 + (0.2639/Kt) + (-0.0240/Kt^2) + (0.0007/kt^3)$	0.958	0.918
Mosul	$k_d = -0.0156 + (0.1374/Kt) + (-0.0080/Kt^2) + (0.0006/kt^3)$	0.969	0.939

Then these Equations are employed to calculate the diffuse radiation for the four stations. The calculated values of diffuse radiation are then compared with the 2005 measured data for all stations . The accuracy of the calculate diffuse radiation data is tested by:

The correlations coefficients (R) , the mean bias (MBE) (w/m^2 day), root mean square (RMSE) (w/m^2 day) and the mean percentage (MPE) errors(%) from Equations (1) ,(2) ,(3) and (4), respectively, which summarized in table4:

Table-4: Statistical test results of models:

Stations	R	MBE	RMSE	MPE %
Basra	0.916	19.60	106.23	1.97
Baghdad	0.956	-9.16	82.35	-0.43
Rutbah	0.946	16.17	86.37	-1.21
Mosul	0.939	1.95	122.01	-2.84

As can be seen in Table 4 , that show the compare between the calculated values of diffuse radiation by using Equations in table 3 with the 2005 measured data for all stations, it is obvious that for all selected locations, the values of the correlations coefficients (R) of the proposed correlations are higher than 0.91 in all stations which indicate good fitting between the calculate and measured diffuse radiation data. Positive MBE% shows over estimation and a negative MBE% shows under estimation. From Table 4, the MBE% values obtained from the models are positive in some cases and negative in others, which shows that these models vary between under and over estimate of diffuse solar radiation.

However, values of MBE% for Basra, Rutbah and Mosul indicates an over estimation, While for Baghdad model gives us under estimation.

The negative values of the MPE indicate that the present correlations slightly overestimate as we saw in Baghdad, Rutbah and Mosul . The highest value of the MPE equals 1,97 % that obtained for Basra .

After that the results obtained from the suggestion formal in Table3 (the calculated value of diffuse radiation) for Basra, Baghdad ,Rutbah and Mosul were plotted against the 2005 measure values of diffuse radiation as show in figure 3 ,which employed for models validation , as mentioned in the third paragraph of methodology .

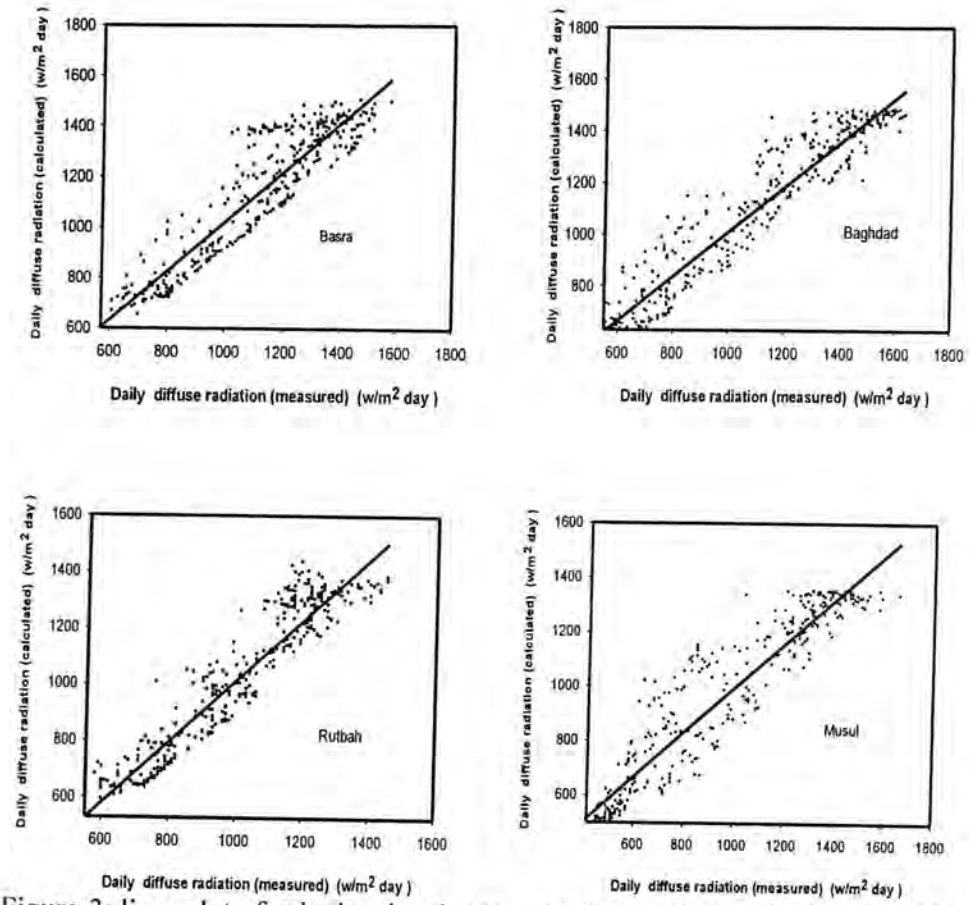

Figure-3: liner plot of calculated and measured daily diffuse radiation for 2005 .

Figures 3 Show the above four suggested correlation formulas plotted together with the measurements of diffuse daily solar radiation for these stations. A linear trend between predicted and measured radiation data is evident for each model- Most of the predicted data are in a very good agreement with the corresponding measured results ,the linear equations between calculated and measured data of diffuse radiation summarized in table 5 .

Table-5:the linear equations between calculated and measured data of diffuse radiation.

Stations	Liner equations	R
Basrah	$H_{cal} = 47.69 + 0.97 * H_{meas}$	0.916
Baghdad	$H_{cal} = 144.71 + 0.86 * H_{meas}$	0.956
Rutbah	$H_{cal} = -69.21 + 1.08 * H_{meas}$	0.946
Mosul	$H_{cal} = 180.85 + 0.81 * H_{meas}$	0.939

Then the Equation (Nonlinear Regression Polynomial Inverse Third Order are employed, which get from NASA data, to calculate the diffuse radiation for February 1994 for Baghdad stations and compared with the measured data get from Solar Radiation And Collacteral Weather Data at AL-Jadria in Baghdad[18] as show in figure 4. The accuracy of the calculate diffuse radiation data is tested by Statistical test

(R = 0.701) , (MBE% = -327.83) , (RMSE = 469.72) and (MPE = 20.29)

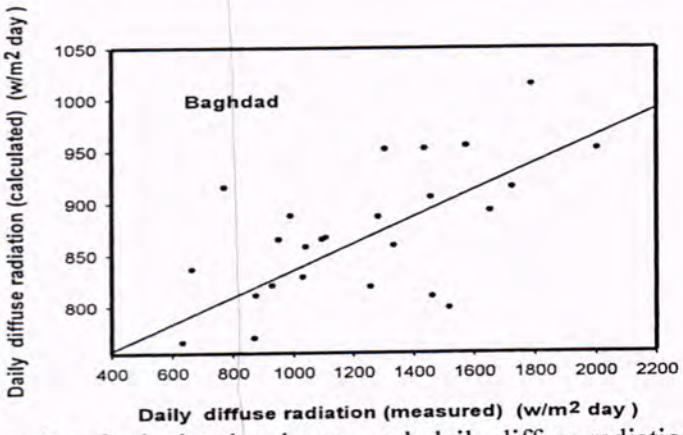

Figure-4: liner plot of calculated and measured daily diffuse radiation for Baghdad Feb.1994 .

The liner equation obtained from figure 4 is :

$H_{cal} = 706.0076 + 0.12 * H_{meas}$

CONCLUSIONS

1. An evaluation of the predicted solar-radiation for (Basrah, Baghdad, Rutbah and Mosul) horizontal surface using measured data has been conducted in the present paper.
2. The proposed suggested models provided an excellent predictive method for the daily averaged value of solar diffuse radiation . The comparison of the predictions with the tabulated values proved that the suggested developed model could be used to successfully model the solar radiation in Amman area.
3. 3) It has been found that the Polynomial Nonlinear Regression Inverse Third Order formulas give excellent fitting , very good correlation, and less Standard Error of Estimate in all stations .
4. Good agreement has been found between measured values and data estimated by the suggested models, which makes it useful in estimating diffuse solar radiation (where there is no data).
5. The models are expected to be applicable to other locations with similar environments.

REFERENCE

1- Culp, A. W. Principles of Energy Conversion,2nd Ed., McGraw Hill. New York,1991.

2- Kurokawa, k. and Ikki, O., 2001. The Japanese experiences with national PV-system programmes. *Solar Energy*, **70(6)**, 457-466.

3- Al-lsmaily, H. A. and Probert , D., 1998.Photovoltaic electricity prospects in Oman. AppI Energy, 59(2), 97-124.

4- Li, D. H. W. and Lam, J. C., 1999. An analysis of climatic variables and design implications. Architect Rev, 42(1), 15-25.

5- Muneer, T., 1997. Perez slope radiation and illuminance models: evaluation against Japanese date. Lighting Res Technol. 29(2)

6- Abdel Salam MS. Higazy NA. ,1978. Solar data application to Egypt, In: T. Nejat Veziroglu, editor. Proceedings of the International Symposium Workshop on Solar Energy, 1, 20-40.

7- Mosalam Shaltout M.A. , Hassan A.H., and A.M. Fathy , 2001.Total suspended particles and solar radiation over Cairo and Aswan , Renewable energy ,23, 605-619 .

8- Iqbal, M., An Introduction to Solar Radiation, Academic Press, New York. 1983.

9- Angstrom, A.1924.Solar and Terrestrial Radiation, *Roy.Met. Sor.*,**50**,121-127.

10- Hourmitz, B. 1945. Insolation in Relation **to** Cloudiness and Cloud Density, J.Met., 2, 154-156.

11- Dancshyar, M., 1978. Solar Radiation Statistics for Iran, Solar Energy. 21, 345-340.

12- AL-Hassabi ,A . Modeling of Solar Spectral Irradiance On Horizontal Surfaces.M.S.C.Thesis, AL-Mustansiriyah Univercity,Iraq,1998 .

13- AL-Hassani ,D . Attenuation of Solar Radiation for Baghdad. .M.S.C.Thesis, AL-Mustansiriyah Univercity,Iraq,2004 .

14- Hamd, R. H.2003. Formulation of the Global Solar Radiation Using Sunshine Duration over Egypt. Journal Astronomical Society of Egypt.11, 39-52.

15- Beheary. M. M.,2004. Using the Global Solar Radiation to Estimate the Spectroscopic Structure of the Normal Incident Solar

Radiation at Selected Sites in Egypt, Al-Azhar Bull. Sci. 15 , 93-106.

16- NASA Surface meteorology and Solar Energy http://www.eosweb.larc.nasa.gov

17- وزارة النقل والمواصلات – الهيئة العامة للانواء الجوية والرصد الزلزالي – اطلس مناخ العراق – 2000

18- وزارة الصناعة والمعادن – مركز بحوث الطاقة والبيئة- بيانات مركز الطاقة الشمسية –بغداد –الجادرية -1994

Predicting the Astronomical Events in Iraq By Using Backpropagation and Radial Basis Function Networks: A Comparative Analysis

Ahmad Hashim Hussein Aal-Yhia
Post-Graduate Institute for Accounting and Financial Studies, University of Baghdad
E-mail: fingerprint192003@yahoo.com

Received 9/4/2012 – Accepted 20/6/2012

الخلاصة

هذا البحث يصف شبكتين عصبيتين، شبكة Backpropagation وشبكة Radial Basis Function. الشبكات العصبية طُبِقت للتنبؤ بالأحداث الفلكية: كسوف الشمس وخسوف القمر وشروق وغروب الشمس لعدّة مدن عراقية. تم استعمال أدوات الشبكة العصبية في لغة Matlab لتدريب ومحاكاة كلّ شبكة حدث، والبيانات المستعملة في البحث هي بيانات حقيقية. كلّ شبكة حدث طُبِّقت خمس مرات، وبعد ذلك يُحسَب المعدل. يتم مقارنة انجاز شبكة Backpropagation وشبكة Radial basis function لكلّ معدل من ناحية عدد الدورات، الوقت المأخوذ للتدريب، الوقت المأخوذ للاسترجاع او التقارب ونسبة الأخطاء في النتائج. النتائج تبين بأنّ شبكة Radial basis function شبكة عصبية كفوءة وأكثر عملية من شبكة Backpropagation.

ABSTRACT

This paper describes two neural networks Backpropagation network (BPN) and Radial basis function network (RBFN). Neural networks were applied for predicting of astronomical events: solar eclipse, lunar eclipse, sunrise and sunset for several Iraqi cities. Neural network toolbox in MATLAB was used for training and simulation each event network and the used data in the paper is real data. Each event network was implemented five times, and then the average was computed. The performances of BPN and RBFN are compared for each average in terms of the number of epochs, the taken time for training, the taken time for convergence and ratio of errors in results. The results show that RBFN is a more efficient and practical neural network than BPN.

Keywords: radial basis function network, backpropagation network, astronomical events, prediction.

INTRODUCTION

In recent years, astronomers and artificial intelligence researchers have started collaborating towards the goal of automating the task of analyzing astronomical data [1]. An event is defined to be any source that has changed in position and/or brightness relative to the baseline "template sky" [2]. The Naval Observatory frequently receives requests for the formulas or algorithms used to compute times of sunrise, sunset, twilight, moonrise, and moonset. Unfortunately there is no single formula that can be used to accurately predict times of these phenomena over an acceptably wide range of dates and places [3]. Many researchers compared statistical methods with that of artificial neural network based modeling and concluded that in their studies artificial neural networks performed better when compared to traditional multiple Regression and other classes of statistical modeling techniques [4]. The use of artificial neural networks is increasing in various fields, like astronomy [5].

Artificial neural networks at most, can be used to mimic a few simple capabilities of the mind such as: modeling memory, pattern recognition, short term dynamical predictions, etc. [6]. Artificial neural networks are more flexible, and are found to be more suitable for prediction purposes as they produce more accurate results that could be replicated [4].

Feedforward backpropagation neural networks (BPN), the most commonly used method in automated astronomical prediction and classification [7]. But, the BPN has the limitation of slow convergence [8] and lengthy training cycles [9] and problems with local minima [10]. While, radial basis function network (RBFN) have rapid training time and do not have problems with local minima [10], and it is particularly well suited for function interpolation, and have consistently outperformed other approaches in a variety of tasks [11].

In previous studies, Tagliaferri and .et al. summarized the methodological background and focused our attention on some of the most interesting fields of application, namely: object extraction and classification, time series analysis, noise identification, and data mining [6].

Ciaramella and et al. showed that neural networks have also been applied to the study and prediction of solar activity and phenomena. The use of neural networks for the analysis of the data collected by the new generation of instruments for astroparticle physics such as, the solar energetic proton events [12].

Carballo and et al. used the supervised artificial neural networks for quasar selection from combined radio and optical surveys with photometric and morphological data, using the list of candidates and their classification. Predictions of the probabilities for the 98 candidates are presented and compared with the results from their work. The values obtained for the two ANN models and the decision trees are found to be in good agreement. This is the first analysis of the performance of ANNs for the selection of quasars. The work showed that ANNs provide a promising technique for the selection of specific object types in astronomical databases [13].

Aal-Yhia used one of artificial neural networks. Backpropagation algorithm is implemented to construct the two nets for predicting astronomical events: solar eclipse, lunar eclipse, sunrise and sunset in cites of Iraq. The errors in results are 21.9% for the application of sunrise, 25% for the application of sunset, 15.6% for the application of solar eclipse and 23.3% for the application of lunar eclipse [14].

In this study, Radial basis function neural network is implemented on same data in [14] and the results are compared with the results of implementation Backpropagation network, the study analysis the

performance of BPN and RBFN to determine the best neural network for predicting the astronomical events.
This paper is structured as follows. Section 2 presents artificial neural networks, the first backpropagation network, the second Radial basis function network. Section 3 presents the application of BPN and RBFN for predicting astronomical events. Section 4 presents results and discussion. Finally; Conclusions are presented in section 5.

2.Artificial Neural Networks

Basic processing elements of the network, the neurons, are interconnected, and the strengths of the interconnections are denoted by parameters called weights. A neuron comprises weighted inputs that are processed by a certain nonlinear function and called the activation function. The output of the neuron, ~ Y, is then computed by the equation (1) [15]:

$$Y = f\left(\sum_{i=0}^{N-1} w_i x_i - \theta\right) \quad \ldots\ldots\ldots (1)$$

The parameter θ serves as a threshold or bias. The network, therefore, is defined by the number and the way in which the neurons are interconnected, the activation function used, and the learning algorithm [15].

2.1. Backpropagation Neural Network (BPN)

A successful BPN requires internal parameters determination such as network architecture and initial weights to meet the required performance. An ineffective design of the network will result in unreliable consequences. Finding a suitable architecture and the corresponding weights of the network is a complex task due to the lack of theoretical parameters or optimal values and need the trial and error approach using different initializations and architecture [16].
The backpropagation training algorithm is an iterative gradient algorithm designed to minimize the mean square error (MSE) between the actual output of a multilayer feedforward perceptron and the desired output. It requires continuous differentiable non-linearities.[17].
The feedforward BPN is a very popular model in neural networks. It does not have feedback connections, but errors are backpropagated during training. Least mean squared error (LMST) is used. Multilayer feed forward networks trained using the backpropagation learning algorithm. The network edges connect the processing units called neurons. With each neuron input there is associated a weight, representing its relative importance in the set of the neuron's inputs. The inputs' values to each neuron are accumulated through the net function to yield the net value: the net value is a weighted linear combination of

the neuron's inputs' values. Architecture and calculation of output for BP training network in Figure 1 [18].

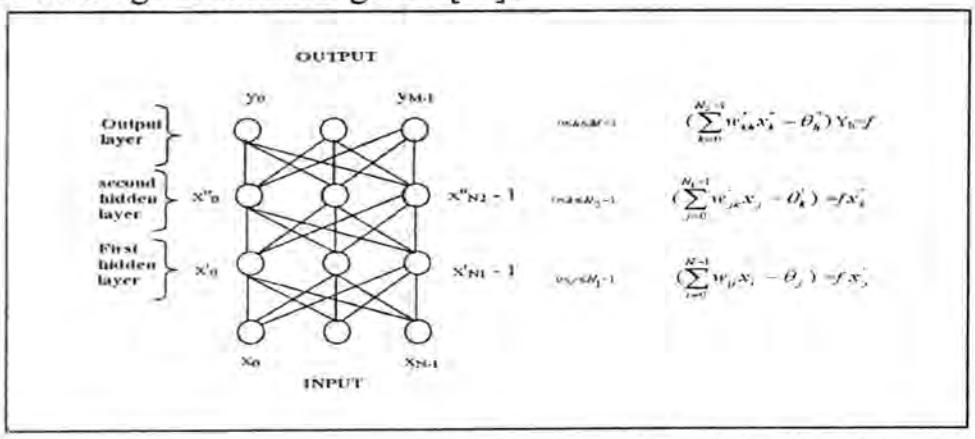

Figure -1: Calculation of output for backpropagation training algorithm [18].

2.2. Radial basis function Neural Network (RBFN)

Radial basis function network is a special case of neural networks, which is originally used for regression problems, i.e. function approximation. In recent decades, RBF is well suited for classification problems and provided valuable results. First time in 1964 RBFN are used for classification problems and since then RBF opened its way toward classification problems, and today it is known as a reliable classifier [19].

RBFN consists of three layers: input layer, radial basis functions and output layer. Input layer takes features extracted from training samples and directly delivers them to the RBF layer. Hidden neurons are radial basis functions. These functions should have four specifications [19]:

1. Attaining the maximum value in the center (zero distance).
2. Having a considerable value in the close neighborhood of the center.
3. Having a negligible value in far distances (where are close to other centers).
4. Differentiability.

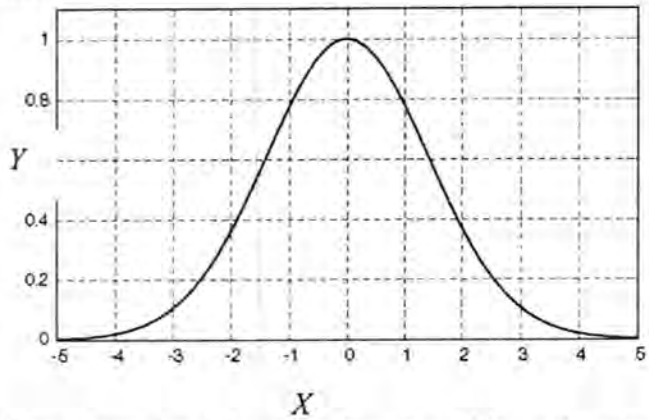

Figure-2: One dimensional Gaussian function with $\mu = 0$ and $\sigma = 2$ [19].

Figure 2 shows a typical function commonly used in RBF layer is Gaussian function (2) [19]:

$$y_m = f_m(X) = \exp\left(-\frac{\|X-\mu_m\|^2}{2\sigma_m^2}\right) \quad \ldots\ldots\ldots (2)$$

Here m is index of the hidden neuron, X is the input vector, μm is mean vector or prototype vector of mth neuron and σm is the spread parameter. In regression problems, number of hidden neurons can be equal to the number of training samples so that mean vector, μm, for each neuron would be the same as one of the training samples. In fact, in this way each Gaussian function will cover part of input space and if training samples have suitable distribution, the network will perform well [19]. The figure 3 shows topology of RBFN [20].

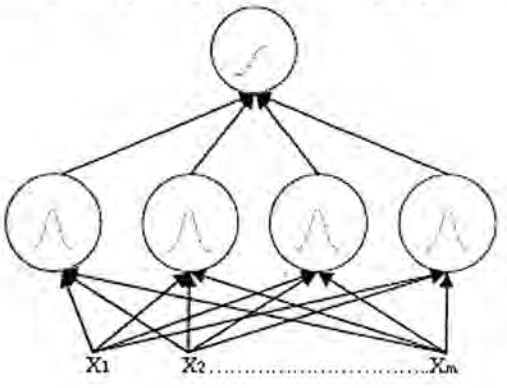

Figure-3: A Topology of Radial basis function network (RBFN) [20].

2.3. Training, learning and testing RBF network

The RBF network employed the orthogonal least squares (OLS) learning method. The OLS method is one of the most efficient learning methods reported for RBF neural modeling. During learning the OLS receives a net input vector distance ||x-w|| between its weight vector w and the input vector x, multiplied by the bias b. The bias is a direct function of the spread parameter 0 which determines the proportion of the input space where the jth RBF neuron has sufficient non-zero response. Thus the valve of the spread should be such that it results in neurons responding strongly to overlapping regions of the input space. Neurons are created one at a time during the training cycle. At each iteration, the input vector which will result in lowering the network error the most is used to create a RBF neuron. The error of the network is checked and if lower than the set of error, training is terminated otherwise the next neuron is added. This procedure is repeated until the error level set is met or the set maximum number of neurons is

exhausted. A mathematical summary of OLS is presented below [21].

3. The proposed method for Prediction in Astronomical Events

In this paper, the BPN and RBFN were implemented to create the two nets for predicting astronomical events: solar eclipse or lunar eclipse and sunrise or sunset. The representation of data for input layer and output layer is in the original digits. The two nets for predicting astronomical events were implemented by using programs written in MATLAB application.

The experiments data is captured from MrEclipse site [22], [23] and site of rafed net [24].

The Table 1 contains the requested data for input layer and output layer of the first net (application of sunrise or sunset). The data are for 16 cities in Iraq and they represent times of sunrise and sunset at 1/3/2011 [14].

Table-1: The data of 16 cities in Iraq for times of sunrise and sunset [14].

City	Day	Month	Sunrise	Sunset
Baghdad	1	3	6:31	17:59
Al-Basra	1	3	6:16	17:47
Al-Mousel	1	3	6:39	18:02
Al-Najaf	1	3	6:31	18:00
Al-Sulamania	1	3	6:29	17:53
Irbil	1	3	6:35	17:59
Babel	1	3	6:31	18:00
Al-Diwaniyah	1	3	6:28	17:58
Al-Ramadi	1	3	6:35	18:04
Al-Samawah	1	3	6:26	17:57
Al-Amarah	1	3	6:19	17:49
Al-Kut	1	3	6:25	17:54
Al-Nasiriyah	1	3	6:22	17:53
Ba'qubah	1	3	6:31	17:58
Karbala	1	3	6:32	18:01
Kirkuk	1	3	6:33	17:58

The Table 2 contains the requested data for input layer and output layer of the second net (application of solar eclipse). The data are for 16 cities in Iraq and they represent the start of solar eclipse, end of solar eclipse and status of solar eclipse at 4/1/2011 [14].

Table-2: The data of 16 cities in Iraq for solar eclipse [14].

Solar eclipse						
Day	Month	Year	City	Start of events	End of event	Status of event
4	1	2011	Baghdad	10:43	13:30	Partial
4	1	2011	Basra	10:56	13:34	Partial
4	1	2011	Mousel	10:39	13:30	Partial
4	1	2011	Najaf	10:39	13:29	Partial
4	1	2011	Sulamania	10:46	13:34	Partial
4	1	2011	Irbil	10:42	13:32	Partial
4	1	2011	Babel	10:43	13:29	Partial
4	1	2011	Al-Diwaniyah	10:45	13:30	Partial
4	1	2011	Al-Ramadi	10:39	13:27	Partial
4	1	2011	Al-Samawah	10:46	13:30	Partial
4	1	2011	Al-Amarah	10:53	13:35	Partial
4	1	2011	Al-Kut	10:48	13:32	Partial
4	1	2011	Al-Nasiriyah	10:50	13:32	Partial
4	1	2011	Ba'qubah	10:44	13:31	Partial
4	1	2011	Karbala	10:42	13:29	Partial
4	1	2011	Kirkuk	10:43	13:32	Partial

The Table 3 contains the requested data for input layer and output layer of the second net (application of lunar eclipse). The data are for 5 different countries and they represent the start of lunar eclipse, end of lunar eclipse and status of lunar eclipse at 28/11/2012. Times of start and end of lunar eclipse for Iraqi cites are similar, therefore the data was selected for different countries in times are not similar. The Table 4 shows types of solar eclipse, lunar eclipse and their codes [14].

Table-3: The data of 5 different countries for lunar eclipse [14].

Lunar eclipse						
Day	Month	Year	Country	Start of events	End of event	Status of event
28	11	2012	Iraq	15:14	19:55	Penumbral
28	11	2012	Jordan	14:14	18:55	Penumbral
28	11	2012	Iran	15:44	20:25	Penumbral
28	11	2012	Libya	13:14	17:55	Penumbral
28	11	2012	Oman	12:14	16:55	Penumbral

Table-4: The types of solar eclipse, lunar eclipse and their codes [14].

lunar eclipse	Total	Partial	penumbral	
solar eclipse	Total	Partial	hybrid	annular
The code	0	1	2	3

3.1. The net of prediction sunrise or sunset by BPN

In this prediction net, the data in the input layer denotes the city, day and month, while the data in the output layer denotes the hours and minutes (time of sunrise or sunset). Architecture of the net by BPN consists of 3 neurons in input layer, 22 neurons in hidden layer and 2 neurons in output layer. The figure 4 shows architecture of the net of sunrise or sunset by BPN [14].

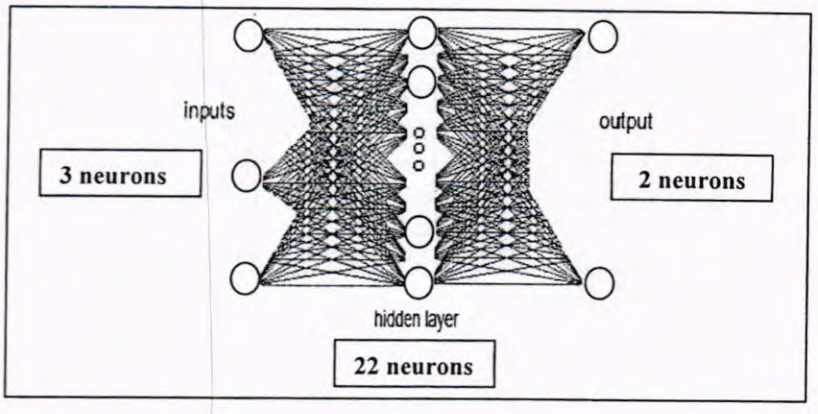

Figure-4: Architecture of the prediction net of sunrise or sunset by BPN [14].

3.2. The net of prediction solar eclipse or lunar eclipse by BPN

In this net (application of solar eclipse or lunar eclipse), the data in the input layer denotes the city, month and year, while the data in the output layer denotes the day, hours, minutes (start of event), hours, minutes (end of event) and status of event [14].

Architecture of the second prediction net (application of solar eclipse) by BPN consists of 3 neurons in input layer, 22 neurons in hidden layer and 6 neurons in output layer. The figure 5 shows architecture of the prediction net of solar eclipse by BPN [14].

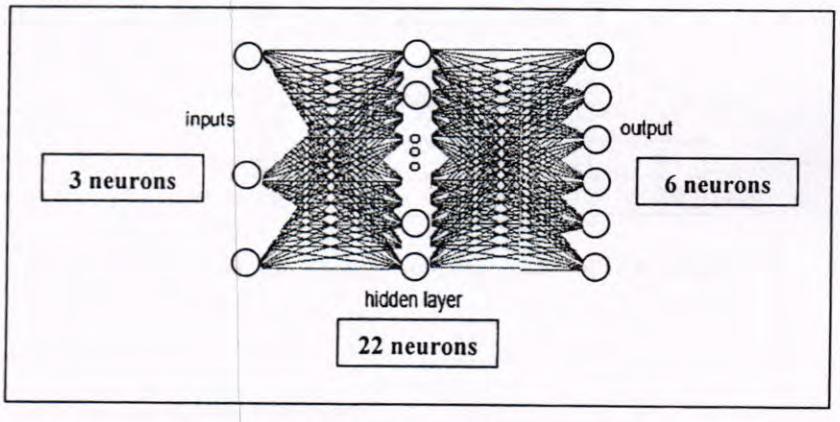

Figure-5: Architecture of the prediction net of solar eclipse by BPN [14].

Architecture of the second prediction net (application of lunar eclipse) by BPN consists of 3 neurons in input layer, 4 neurons in hidden layer and 6 neurons in output layer. The figure 6 shows architecture of the prediction net of lunar eclipse by BPN [14].

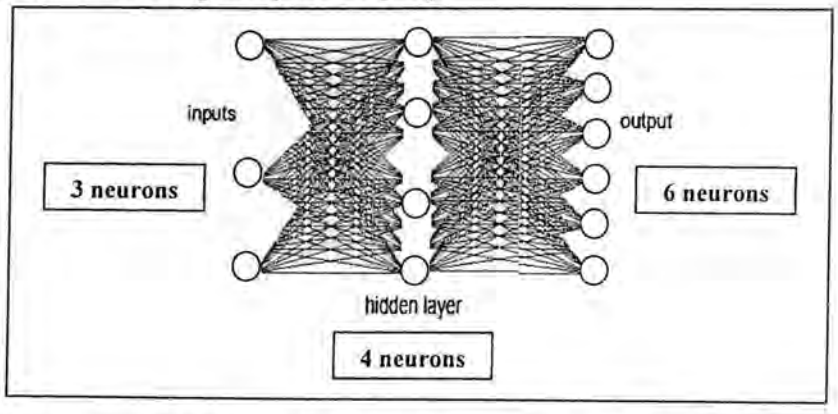

Figure-6: Architecture of the prediction net of lunar eclipse by BPN [14].

3.3. The net of prediction sunrise or sunset by RBFN

In this prediction net, the data in the input layer denotes the city, day and month, while the data in the output layer denotes the hours and minutes (time of sunrise or sunset). Architecture of the net by RBFN consists of 3 neurons in input layer, 0 neurons in hidden layer and 2 neurons in output layer. The figure 7 shows architecture of the net of sunrise or sunset by RBFN.

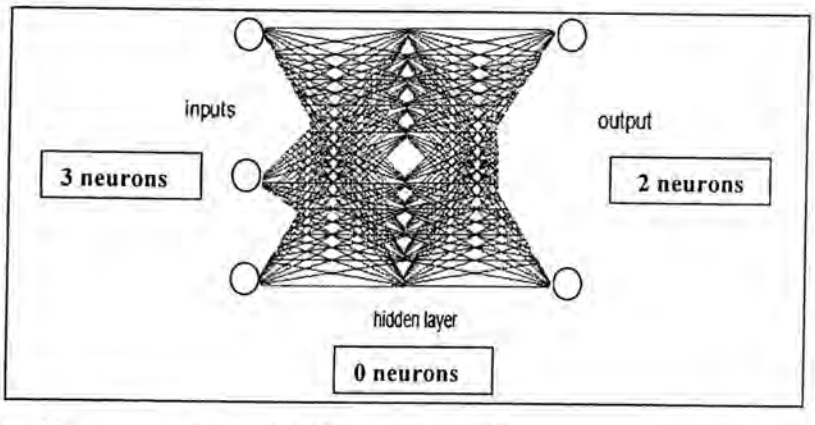

Figure-7: Architecture of the prediction net of sunrise or sunset by RBFN.

3.4. The net of prediction solar eclipse or lunar eclipse by RBFN

In this net (application of solar eclipse or lunar eclipse), the data in the input layer denotes the city, month and year, while the data in the output layer denotes the day, hours, minutes (start of event), hours, minutes (end of event) and status of event.

Architecture of the second prediction net (application of solar eclipse or lunar eclipse) by RBFN consists of 3 neurons in input layer, 0 neurons

in hidden layer and 6 neurons in output layer. The figure 8 shows architecture of the net of prediction solar eclipse or lunar eclipse by RBFN.

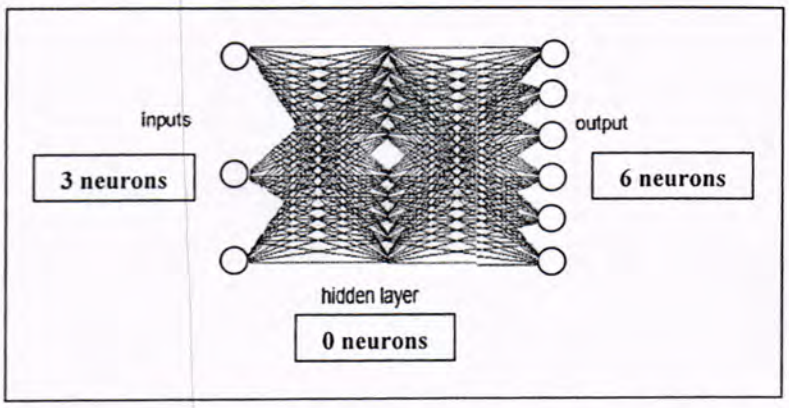

Figure-8: Architecture of the net of prediction solar eclipse or lunar eclipse by RBFN.

Radial basis networks may be contained neurons or not in hidden layer because the neurons are added to the hidden layer of a radial basis network until it meets the specified mean squared error goal while the backpropagation feedforward networks often have one or more hidden layers.

4. RESULTS AND DISCUSSION

In this study, simulations have been performed in Matlab 7.6.0.324 (R2008a) by computer had the following properties: Intel™ Core™2 Duo CPU T5800@ 2.00 GHz 2.00 GHz, 3.00 GB of RAM. Five independent runs were carried out for four applications in RBFN and BPN.

Experimental results of the performance in terms of number of epochs required, time taken for training, time taken for convergence and ratio of errors in results for four applications (sunrise, sunset, solar eclipse and lunar eclipse) in RBFN and BPN. Those results are shown in Table 5 through Table 12.

Table-5: The results for the application of sunrise in RBFN.

N.	The epochs	Training time (Second)	Convergence time (Second)	Errors in results
1	8	0.0932	0.0174	43.75%
2	8	0.0796	0.01	43.75%
3	8	0.0827	0.0102	43.75%
4	8	0.081	0.01	43.75%
5	8	0.079	0.0109	43.75%

Table-6: The results for the application of sunrise in BPN.

N.	The epochs	Training time (Second)	Convergence time (Second)	Errors in results
1	4	0.4733	0.0141	43.75%
2	3	0.481	0.0183	50%
3	4	0.47	0.0152	50%
4	4	0.464	0.02	50%
5	4	0.4761	0.0188	43.75%

Table-7: The results for the application of sunset in RBFN.

N.	**The epochs**	**Training time (Second)**	**Convergence time (Second)**	**Errors in results**
1	8	0.0843	0.0121	87.50%
2	8	0.0778	0.0094	87.50%
3	8	0.0775	0.0102	87.50%
4	8	0.0809	0.01	87.50%
5	8	0.0848	0.0101	87.50%

Table-8: The results for the application of sunset in BPN.

N.	The epochs	Training time (Second)	Convergence time (Second)	Errors in results
1	4	0.4698	0.0207	87.5%
2	4	0.4656	0.0172	81.25%
3	4	0.4721	0.0171	100%
4	4	0.4779	0.0175	81.25%
5	4	0.4705	0.0184	81.25%

Table-9: The results for the application of solar eclipse in RBFN.

N.	The epochs	Training time (Second)	Convergence time (Second)	Errors in results
1	8	0.0782	0.01	41.67%
2	8	0.0832	0.01	41.67%
3	8	0.1209	0.01	41.67%
4	8	0.1408	0.0113	41.67%
5	8	0.0819	0.0099	41.67%

Table-10: The results for the application of solar eclipse in BPN.

N.	The epochs	Training time (Second)	Convergence time (Second)	Errors in results
1	4	0.0267	0.0267	31.25%
2	4	0.459	0.0152	29.17%
3	4	0.4808	0.0215	31.25%
4	4	0.4708	0.015	31.25%
5	4	0.5257	0.0226	33.33%

Table-11: The results for the application of lunar eclipse in RBFN.

N.	The epochs	Training time (Second)	Convergence time (Second)	Errors in results
1	3	0.0829	0.0176	58.33%
2	3	0.0735	0.0101	58.33%
3	3	0.0854	0.0113	58.33%
4	3	0.0787	0.0104	58.33%
5	3	0.0798	0.0105	58.33%

Table-12: The results for the application of lunar eclipse in BPN.

N.	The epochs	Training time (Second)	Convergence time (Second)	Errors in results
1	4	0.4223	0.0098	41.67%
2	4	0.4763	0.0133	58.33%
3	4	0.4429	0.0155	50%
4	4	0.4517	0.0182	58.33%
5	4	0.4186	0.0148	66.67%

The results average of five runs for four applications (sunrise, sunset, solar eclipse and lunar eclipse) in RBFN and BPN are shown in Table 13 through Table 16 and their charts are shown in figure 9 through figure 12. The results of comparisons showed that the errors ratios in results of the four applications for RBFN are less than that of BPN, the RBFN is the best. Commonly, the training time of the four applications for RBFN is less than that of BPN, the RBFN is the best. The convergence time of the four applications for RBFN is less than that of BPN, Commonly, the RBFN is the best. The number of epochs for BPN is less than that of RBFN.

Table-13: The average of errors ratio in results for BPN and RBFN.

Name of application	The error ratio in results		The best
	BPN	RBFN	
Sunrise	47.5%	43.75%	RBFN
Sunset	86.25%	87.50%	BPN
Solar eclipse	31.25%	41.67%	BPN
lunar eclipse	55%	58.33%	BPN

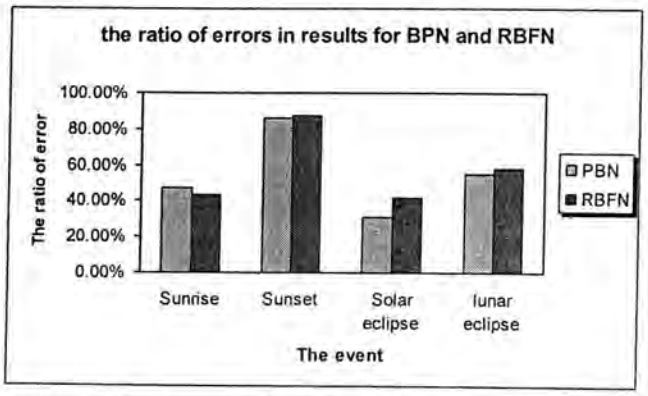

Figure-9: Chart for ratio of errors in results for BPN and RBFN.

Table-14: The average of training times for BPN and RBFN.

Name of application	The training time (Second)		The best
	BPN	RBFN	
Sunrise	0.4729	0.0831	RBFN
Sunset	0.4712	0.0811	RBFN
Solar eclipse	0.3926	0.101	RBFN
lunar eclipse	0.4424	0.0801	RBFN

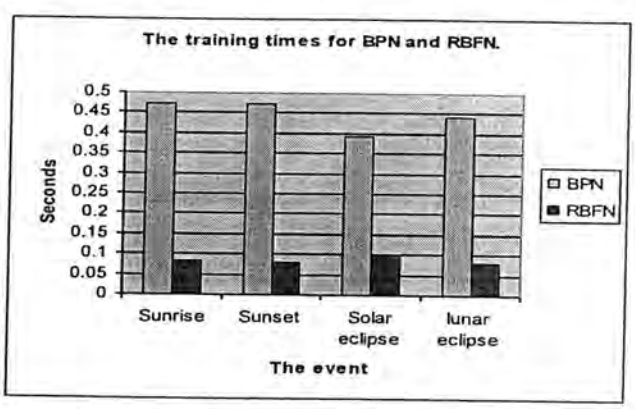

Figure-10: Chart for times of training for BPN and RBFN.

Table-15: The average of convergence times for BPN and RBFN.

Name of application	The convergence time (Second)		The best
	BPN	RBFN	
Sunrise	0.0173	0.0117	RBFN
Sunset	0.0182	0.0104	RBFN
Solar eclipse	0.0202	0.0102	RBFN
lunar eclipse	0.0143	0.012	RBFN

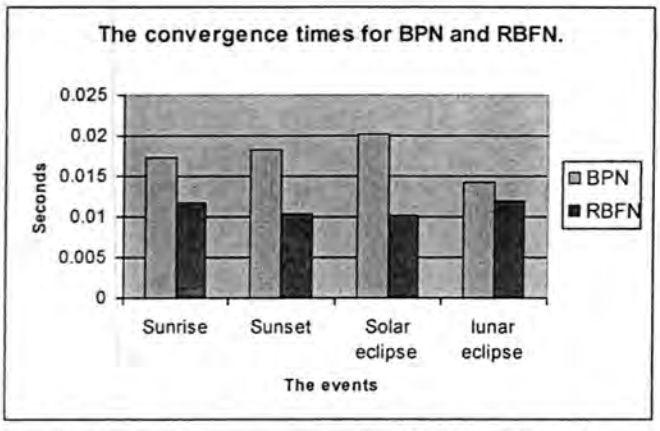

Figure-11: Chart for times of convergence for BPN and RBFN.

Table-16: The average of epoch's numbers for BPN and RBFN.

Name of application	The number of epochs		The best
	BPN	RBFN	
Sunrise	4	8	BPN
Sunset	4	8	BPN
Solar eclipse	4	8	BPN
lunar eclipse	4	3	RBFN

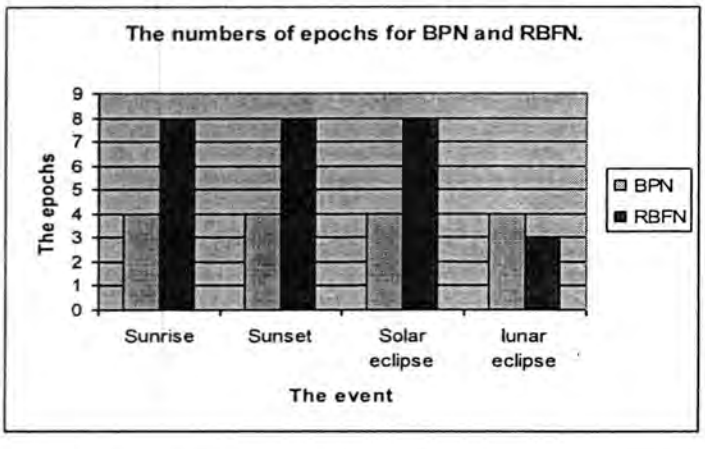

Figure-12: Chart for numbers of epochs for BPN and RBFN.

5. Conclusions

The both of backpropagation (BPN) and radial basis function networks (RBFN) have been successfully applied to problems in classification and prediction applications. Subsequently, to know the best neural network, this paper presents a comparison between RBFN and BPN. To determine the best performance of RBFN and BPN, we make comparisons by implementation both of RBFN and BPN on real and original data in this study. The results are as follows:

1. The accuracy of BPN is far superior to that of the RBFN.
2. The training speed of RBFN is faster than that of BPN, although the number of epochs of RBFN is grater than that of BPN.
3. The convergence speed of RBFN is faster than that of BPN.

Therefore, BPN is a more efficient neural network than that of RBFN in the term of accuracy and RBFN is a more efficient neural network than that of BPN in the terms of speed of training and convergence.

REFERENCES

1. Fuentes O., "Automatic determination of stellar atmospheric parameters using neural networks and instance-based machine learning," *Experimental Astronomy*, 12, pp. 21–31(2001)
2. Borne K., Laher R., Ivezic Z., and Hamam N., "Petascale Object Classification of the LSST Event Stream," *American Astronomical Society*, Vol. 41, pp.372, January (2009).
3. Naval Oceanography Portal, the United States Naval Meteorology and Oceanography Command (NMOC), (n. d.) Retrieved August 26 (2010). Available: http://www.usno.navy.mil/ USNO/astronomical-applications/astronomical-information- center/algor-astro
4. Talib A., Abu Hasan Y., and Abdul Rahman N., "Predicting Biochemical Oxygen Demand As Indicator Of River Pollution Using Artificial Neural Networks," *in Proceedings of the 18th World IMACS / MODSIM Congress*, Cairns, Australia, pp. 824-830 (2009).
5. Gulati R., and Altamirano L., "Artificial neural networks in stellar astronomy," *in Proceedings of the RevMexAA (Serie de Conferencias)*, Vol. 11, Mexico, pp. 85-86 (2001).
6. Tagliaferri R., Longo G., Milano L., Acernese F., Barone F., Ciaramella A., De Rosa R., Donalek C., Eleuteri A., Raiconi G., Sessa S., Staiano A., and Volpicelli A., "Neural networks in astronomy," *Neural Networks*, 16, pp. 297–319 (2003).
7. Coppola Jr E., McLane C., Poulton M., Szidarovszky F., and Magelky R., "Predicting Conductance Due to Upconing Using Neural Networks," *ground water*, Vol. 43, no.6, pp. 827-836(2005).
8. Wu J., *Neural networks and simulation methods.* New York: Marcel Dekker, (1994).
9. Kosko B., *Neural networks and fuzzy systems: A dynamical systems approach to machine intelligence.* USA: Prentice-Hall international, (1992).

10. Rao V., and Rao H., *C++ Neural Networks and Fuzzy Logic.* (2nd ed.), USA: M&T publishing (1996).
11. Cochenour G., Das S., Pahwa A., and Simon J., "A Multi-Objective Evolutionary Strategy Based Radial Basis Function Network Approach for Predicting Failure Rates in Distribution Systems," *ISAST Transactions on Intelligent Systems,* No. 1, Vol. 1, pp. 7-14 (2008).
12. Ciaramella A., Donalek C., Staiano A., Ambrosio M., Aramo C., Benvenuti P., Longo G., Milano L., Raiconil G., Tagliaferril R., and Volpicelli A., "Applications of neural networks in astronomy and astroparticle physics," *Research Signpost,* 2, pp. 1-32 (2005).
13. Carballo R., CofinoA., and Gonzalez-Serrano J., "Selection of quasar candidates from combined radio and optical surveys using neural networks," *MNRAS,* pp. 1-11, (2008).
14. Aal-Yhia A., "Artificial Neural Networks For Predicting the Astronomical Events," Acceptable for publisher, *Iraqi Journal for Information Technology*, College of Sciences, Al-Mustansirya University, Baghdad, Iraq, (2011).
15. Bhushan B., Singh M., and Hage Y., "Identification and control using MLP, Elman, NARXSP and radial basis function networks: a comparative analysis," *Artif Intell Rev*, No. 37, pp. 133–156 (2012).
16. Sargolzaei J., Asl M., and Moghaddam A., "Membrane permeate flux and rejection factor prediction using intelligent systems," *Desalination*, No. 284, pp. 92–99 (2012).
17. Aal-Yhia A., and Sharieh, A., "An energy backpropagation algorithm," *in Proceedings of the World Congress on Engineering*, London, vol. 1, pp. 122-127(2007).
18. Aal-Yhia A., "Enhanced energy backpropagation algorithm," *Iraqi Journal of Science*, Vol. 50, No.4, pp. 553-560, College of Sciences, Baghdad University, Baghdad, Iraq(2009).
19. Khosravi H., "A Novel Structure for Radial Basis Function Networks—WRBF," *Neural Process Lett*, No. 35, pp. 177-186 (2012)
20. Yeh I., Chen C., Zhang X., Wu C., and Huang K., "Adaptive radial basis function networks with kernel shape parameters," *Neural Comput & Applic*, No. 21, pp. 469-480 (2012).
21. Tortoe C., Orchard J., Beezer A., and Tetteh J., "Application of Radial Basis Function Network with a Gaussian Function of Artificial Neural Networks in Osmo-dehydration of Plant Materials," *Journal of Artificial Intelligence*, Vol. 4 No. 4, pp. 233-244 (2011).
22. Mreclipse.com, (n.d.) Retrieved August 26, 2010. Available: http://www.mreclipse.com/ Special/SEprimer.html
23. Mreclipse.com, (n.d.) Retrieved August 26, 2010. Available: http://www.mreclipse.com/Special/LEprimer.html
24. Rafed net, (n.d.) Retrieved August 26, 2010. Available: http://rafed.net/calendar

Discrete Cosine Transform using in Hiding Image Technique

Jameelah H.S.
Al-Mustenesiriyh University, College of Science, Dept.Computer Scie. Iraq
Jamela1232002@yahoo.com

Received 21/9/2011 – Accepted 18/4/2012

الخلاصة

اخفاء المعلومات هو فن اخفاء حقيقة الاتصالات التي تجري عن طريق اخفاء المعلومات في غيرها من المعلومات. هناك الكثير من صيغ ملفات ناقل المعلومات المختلفة ، لكن الصور الرقمية هي اكثر الملفات شعبية بسبب كثرة استخداماتها في شبكة الانترنت. في هذا البحث تم تصميم تقنية اخفاء معتمدة على مبدا استبدال كتلة مماثلة من الصورة المضمنة في صورة الغلاف. تقنية ادراج البت الاقل اهمية (LSB) استخدمت في تضمين المعلومات في صورة الغلاف.

تقنية التحويل لعبت ايضا دورا هاما في عملية تضمين المعاملات بالمجال الترددي بدلا من المعاملات الموجودة بالمجال الحيزي و قد استخمت تقنية تحويل جيب التمام (DCT) من خلال تكميم الاجزاء الاقل اهمية في الصورة بالاعتماد على المقارنة مع القدرات البصرية للانسان.

ABSTRACT

Steganography is the art of hiding the fact that communication is taking place, by hiding information in other information. Many different carrier file formats can be used, but digital images are the most popular because of their frequency on the internet. In this paper a steganography technique designed based on substituting a similar block of embedded image within a cover image. Least significant bit (LSB) insertion technique is an approach for embedding information in a cover image. Transform technique has also played some important role in embedding the message by modulating coefficients in a domain transform. Discrete cosines transform (DCT) works by using quantization on the least important parts of the image in respect to human visual capabilities.

INTRODUCTION

The main goal of steganography is to communicate message security in a complete undetectable manner [1]. The general idea of hiding some information in digital content has a wider class of applications that go beyond steganography (see Figure1 [2].

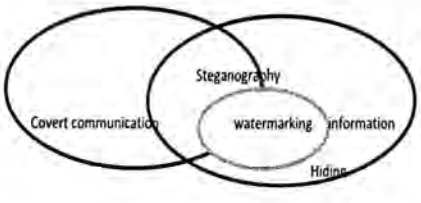

Figure-1: relationship of steganography to related fields.

Image steganography has gotten more popular press in recent years than other kinds of steganography, possibly because of the flood of electronic image information available with the advent of digital cameras and high speed Internet distribution. Image steganography often involves hiding information in naturally occurring "noise" within

the image, generally refers to the imperfections inherent in the process of rendering an analog picture as digital image [3]. Digital technology gives us a new way to relate steganography techniques including hiding information in digital image, it not only goes well beyond simply by embedding a text in an image, but also pertains to other media, including voice, text, binary files and communication channels .Therefore, information security will be important to you . Due to growth and progress of science in the world, computers and the Internet to send data are used [4]. Steganography refers to the technique of hiding information in digital media in order to conceal the existence of the information. The media with and without hidden information are called stego media and cover media, respectively [5].

IMAGE AND TRANSFORM DOMAIN

Image steganography techniques can be divided into two groups: those in the image domain and those in the transform domain [6]. Image (also known as spatial) domain techniques embed message in the intensity of pixel directly, while for transform (also known as frequency) domain, images are first transformed and then the message is embedded in the image [7], see Figure2.

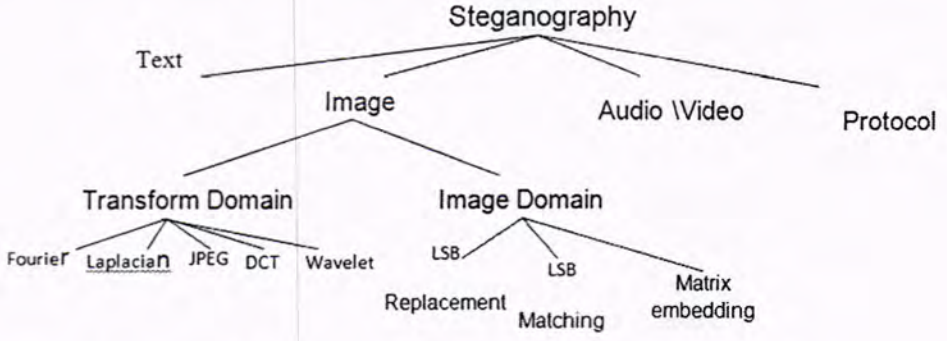

Figure-2: Categories of image steganography

IMAGE DOMAIN

Image domain techniques encompass Least Significant Bit (LSB) insertion is a common, simple approach to embedding information in a cover image [4]. LSB (in other words, the 8th bit) of some or all the bytes inside an image is changed to a bit of the secret message. When using a 24 bit image, a bit of each of the red, green, and blue color components can be used, since they are each represented by a byte [8]. When embedding a message in a "raw' image, that has not been changed with compressing such as a BMP, there exists a trade-off between the invisibility of the message and the amount of information that can be embedded, therefore, LSB in BMP is most suitable for applications where the focus is on the amount of information to be transmitted [7].

DISCRETE COSINE TRANSFORM

The Discrete Cosine Transform (DCT) a signal from an image representation into a frequency representation, by grouping the pixels into 8x8 pixel blocks and transforming the pixel blocks into 64 DCT coefficients [8]. During the DCT transformation phase of the compression algorithm, rounding error occur in the coefficient data that are not noticeable by human eye (i.e. a subjective quality is degraded). Assuming N*N image, its two dimensional DCT produces the (N *N) array of numbers, it's given by [4]:

$$T(u,v) = \alpha(u)\alpha(v)\sum_{r=0}^{N-1}\sum_{c=0}^{N-1} I(r,c)\cos\frac{(2r+1)u\pi}{2n}\cos\frac{(2c+1)v\pi}{2n} \quad ...(1)$$

Where $\alpha(u),\alpha(v) = \begin{cases} \frac{1}{\sqrt{n}} & \text{if } u,v = 0 \\ \frac{2}{\sqrt{n}} & \text{if } u,v = 1,2,...,n-1 \end{cases}$

IDCT is the inverse of DCT which can be obtained by:

$$I(u,v) = \sum_{u=0}^{N-1}\sum_{v=0}^{N-1} \alpha(u)\alpha(v)I(r,c)\cos\frac{(2r+1)u\pi}{2n}\cos\frac{(2c+1)v\pi}{2n} \quad ...(2)$$

Where u, v are varies from 0 to n-1.

The result of the DCT is the square (NxN) array T (u, v) of real numbers, The coefficient T(0,0) is called the "DC coefficient" and the remaining are called the AC coefficients.

QUANTIZATION PROCESS

Quantization is the process of selectively discarding visual information without a significant loss in the visual effect. Quantization reduces the number of bits needed to store an integer value by reducing the precision of the integer. Quantization is done to achieve better compression. A reduction in the number of bits reduces storage capacity needed, improves bandwidth, and lowers implementation costs [9].

After each (N xN) matrix of DCT coefficients is calculated, it is quantized, this is the step where the information loss occurs. Each number in the DCT coefficient matrix is divided by the corresponding number from the particular "quantization table" used, and the result is rounded to the nearest integer. In practice few users have the time or expertise to experiment with

so many parameters, so JPEG software normally uses the two approaches below:

1- Default quantization tables were the elements in the table generally grow as moved from the upper left corner to the bottom right one.

2- A simple quantization table Q is computed, based on one parameter R supplied by the user. A simple expression such as

$$Q_{ij} = 1 + (i + j) \times R \quad .....(3)$$

GENERAL STEGANOGRAPHY SYSTEM

A general Steganography system is shown in Figure3.

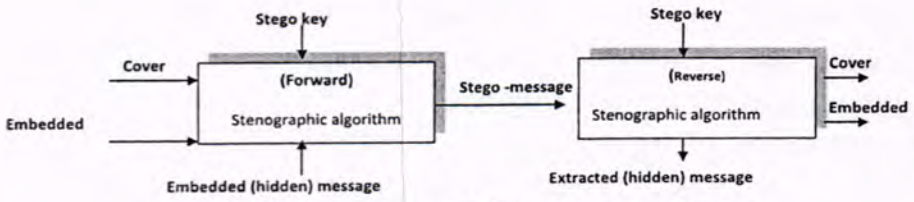

Figure-3: General Steganography System

It is assumed that the sender wishes to send, via stenographic transmission, a message to a receiver. The sender starts with a cover message, which is an input to the stego-system, in which the embedded message will be hidden. The hidden message is called the embedded message. A stenographic algorithm combines the cover message with the embedded message (new), which is something to be hidden in something else.

The algorithm may, or may not, use a Steganography key (Stegokey), which is additional secret data that may be needed in the hidden process. The same key (or related one) is usually needed to extract the embedded message again. The output of the Steganography algorithm is the stego message. The cover message and stego message must be of the same data type, but the embedded message may be of another data type. The receiver reverses the embedding process to extract the embedded message [10, 11].

THE PROPOSED SYSTEM

The proposed systems depends on the substitution of blocks of bytes between embedded and cover image rather than substitution of bit or byte as in more steganography methods. The existing block in the embedded image is replaced by the similar block in the cover image. DCT is used in this work to transform block of (N × N) pixel to (N × N) coefficients of real numbers, and a Quantization process is used to transform real number to integer number.

The proposed system consists of two parts:

1. The Embedding Process

The embedding process of our proposed system consists of the following stages:

i. Testing embedded image and cover image:

In this test, we will check the size of the cover-image and the size of the embedded-image, the size of the embedded-image must be smaller than the size of the cover-image by ratio1:2. The size of both the cover-image and embedded image is calculated by using the equation (4):

$$S_e = \text{embedded hight} \times \text{embedded width}$$

$$S_c = \text{cover hight} \times \text{cover width} \qquad \ldots(4)$$

where S_e and S_c : are the size of the embedded and the cover image respectively.

After the size of the embedded and cover images are checked, now the selected cover image must be decided is it suitable to hold the embedded image or not. It is too difficult to accurately judge whether the testing image carries some hidden data or not, and to predict the hiding ratio r, without the original cover and based only on the distribution density of the histogram.
, as in the following two equations [12]:-

$$S\{H(E), H(C)\} = \frac{\sum_{j=1}^{n} \min\{hj(E), hj(c)\}}{Nc \times Mc} \quad ..(5)$$

$$D\{H(E), H(C)\} = \sum_{j=1}^{n} \left| \frac{hj(E)}{Ne \times Me} - \frac{hj(C)}{Nc \times Mc} \right| \quad ..(6)$$

Equation (5) is used to measure the similarity between the histogram of the embedded image (E) and the cover image (C), where $h_j(E)$ and $h_j(c)$: is the number of elements which have the color (J) in the (E) and (C) images respectively.

$Mc \times Nc$: is the size of the cover image.

Equation (6) is used to measure the dissimilarity between the histogram of the embedded image (E) and the cover image (C), where

$Me \times Ne$: is the size of the embedded image (E).

ii. Transformation stage

After choosing a suitable cover for holding the image to be embedded, the cover-image and the embedding-image are partitions into blocks of (n × n) pixels. In our work, we used (2, 4 or 8) pixels. when, the size of blocks is decreases , the embedding process will be better, so, the distortion in stego image become least, because the blocks which are used in Substitution process have small sizes. Using DCT (equation (3)) to transform these blocks and get the coefficient of real numbers and quantized them to integer number. Each number in the DCT coefficient block is divided by the corresponding number (quantized number), and the result is rounded to the nearest integer. The quantized value based on one parameter R is supplied by the user. wherever, the R value is increases , the error between the original image and reconstructed image will be least. Therefore, the value of R in the proposed system will be choose as small value in order to keep the quality of reconstructed image .

iii. Matching stage:

When performing the first match between the first embedded block and other cover blocks and determining the best block to hold it, using the goodness of fit:

$$S = \sum_{i=1}^{n} \frac{(E_i - C_i)^2}{E_i} \quad ...(7)$$

Where: E: represents the value embedded image pixels, C: represents the value of cover image pixels, and n: represents the block size.

Then we will try to decrease the number of embedded block inside the cover image by comparing between the first embedded block and other embedded blocks to find the block similar to it, then, it gives all the similar block to the first embedded block the same cover block position (which will be used to hold them) in index matrix. This process is performed in order to decrease the number of blocks inside the embedded image; therefore the size of embedded image will decrease. When the size of embedded image decreases, the hidden will be invisible due to less distortion in the stego-image.

iv. Substituting stage:

Substituting stage is the important stage in the embedded process; in this stage we hide each embedding block inside the corresponding cover block.

v. Inverse transformation stage:

After construct an image, which consists of an embedded image and a cover image, then we will perform inverse Quantization (dequantization), by each number in DCT quantization coefficient is multiplied by the corresponding number (the same number which used in quantization steps).Then, we will perform inverse transformation stage (IDCT from equation (2.4)) to reconstructed the original number of pixel from stego-image.

vi. Key Generating-stage:

Key generating is a final stage in this paper. The key is generating and hidden inside the stego-image. The key is encrypted to increase the security of our proposed system. It consists of three stages:-

1) Generating Stage

In this stage, we generate two types of key depending on image type:

1. 24 bit image Key: The key in 24 bit image consists of the hidden location (index matrix) for each block of embedding image inside cover image, the number of embedded block, the header of embedded image, and the size of the key.

2. 8 bit image Key: The key in 8 bit image consists of the hidden location (index matrix) for each block of embedding image, the palette of embedded image, the header of embedded image, the number of embedded block, and the size of the key.

2) Encryption Stage

In this stage, we will cipher the key which results from the generating stage, by using exclusive-or (XOR) operation. The plaintext is Xored with a keyword to generate the cipher text as in the equation (4) [13]:

$$p \oplus k = c \ldots (8)$$

Where, P: is a plaintext, K: is a keyword, and C: is a cipher text.

3) Hidden Stage

In this stage, we will hide the key after being encrypted inside stego-image by using Pseudo random Permutations method for stego-image pixels, where the secret key bit is distributed randomly over the stego-image pixel. The first and the second bytes in the hidden process represent the size of the key, the third byte represents the encipher key, and other bytes is the remaining key. The distributing between pixel and pixel by the distribution distance is calculated by:

$$mm = (wid \times hig) div (size\ of\ the\ key \times 8) \ldots (9)$$

2. The Extraction Process

To start the extraction process, the extractor must have the stego-image, and the stego-key to extract the original image. The extraction processes are described in Figure4:

Each stage in Fig.(4) can be described as following:

1. Stego Key Extraction

It is the first step in the extracting process. We will extract the key from the stego-image in order to extract the embedded image.

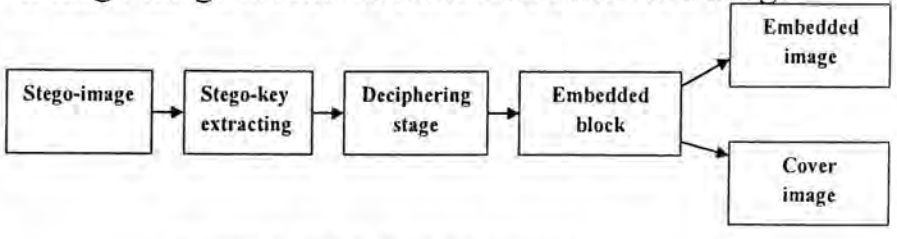

Figure-4: The Extracting Process

From the first and second bytes, the extractor will know the size of the key. From the third byte, the extractor will know the encipher key, which is important in the deciphering stage. The other byte represents the hidden location (move index) for each embedded block inside the cover block, the embedded header, the palette (if the image is 8 bit per pixel) and the number of embedded block. The secret key is extracted by applying Pseudorandom Permutation extraction for stego image pixel, therefore, must have the hidden distance (mm) between pixels.

2. Deciphering Stage

When the extractor knows the secret key, the original key (important information to extract the original image) will be

extracted after deciphering the secret key. The extractor knows the encipher key, which represents the third byte from the extracting key.

The key is Xored with cipher key to generate the plaintext as in the equation (10)[13]:-

$$c \oplus k = p \quad \text{.....(10)}$$

Where, c: is the cipher text, K: is the keyword, and P: is the plaintext.

3. Embedded Block Extraction

After deciphering the key, the extractor knows all the important information to extract the embedded image. We will extract the embedded block by using the hidden location (move index array) for each embedded block in the cover block. The extraction is performed by restoring the embedded block to reach into original arrange for this block.

After extracting the original arrangement for embedded block and knowing the embedded header and image palette (if the image is 8 bit /pixel), the extractor reaches the embedded image.

EXPERIMENTAL RESULTS

To evaluate the proposed works, and analyzing their results we need at first to implement the main interface of our proposed system , Figure5 illustrate the main window of hide image system, which includes have the original image and hide the image , also includes the parameters can be interred the key parameter , block size, and the correlation.

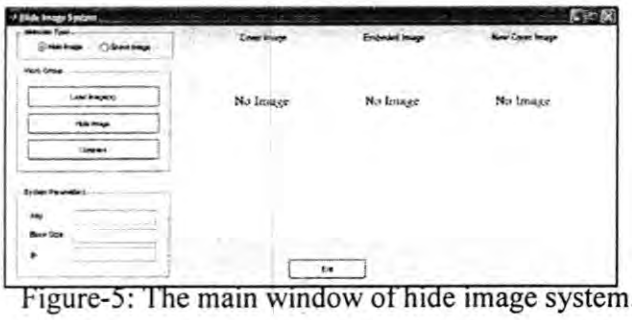

Figure-5: The main window of hide image system.

In Figure6 the cover image is loading as bitmap file and the embedded image. We chose the value of secret key at

128, block size=4x4 pixels, and R= 0.5.

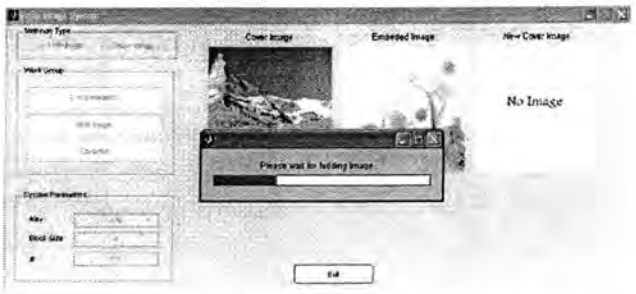

Figure-6: The first stage of hiding image.

After the hide image (small image) will be hided this process has time called time of hide image. This time saved; Figure7 show the second stage.

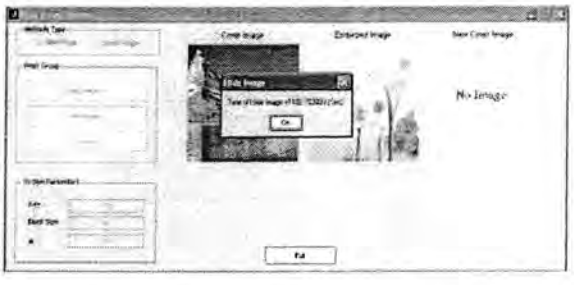

Figure-7 :Show the second stage.

Figure8 included the compare between embedded image and the original image as shown .

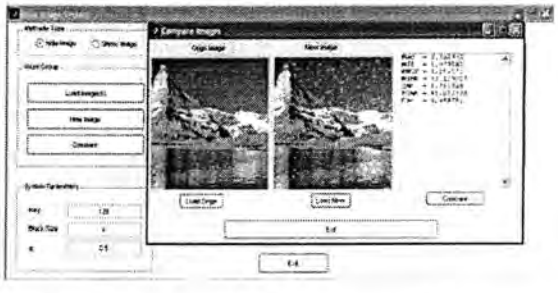

Figure-8 :Showing the original image and the cover image.

If we chose the second key (i.e., show image) and we will inter the password in the key parameter, which can be see in figure9.

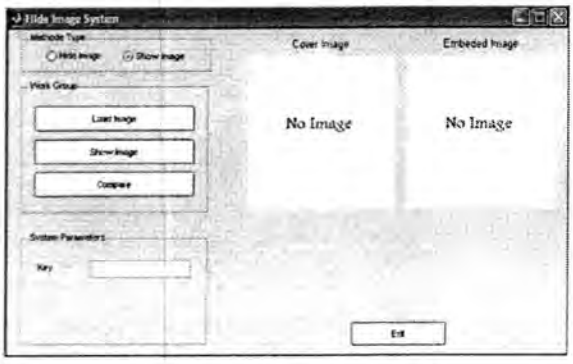

Figure-9: Showing the window of show image.

The performance results of implementing of steganography technique, the block size=4x4 pixels, r (resolution) = 0.2 . Figure10 show the embedded and cover images.

Embedded image

Cover image

Figure10: Show the embedded and cover image, chose the block size=4 and the R=0.2

After we interred the password =128 in the key parameter we can extract the image of size (128x 128) pixel from the covered image of size (256 x 256) pixels, see figure11.

Extract

Stego

Figure-11: The extract image.

The results of fidelity criteria of embedded image and cover image are measured and shown in table (1).

Table -1: the results of comparing between embedded and cover image.

Fidelity Criteria	Embedded image	Cover image
MAD	0.204	0.182
MSE	0.214	0.191
RMSE	0.463	0.437
MSNR	1107.7	1277.75
SNR	33.28	35.75
PSNR	54.81	55.30
Cor.	0.999	0.999

CONCLUSIONS

The proposed system can be defined as sacred key steganography system, therefore we can conclude:

1. The stego key is generated during the embedded process and stored inside the stego image to increase the security of the proposed system. Without knowledge of the stego key, the receiver cannot extract the original message.
2. The block size effects on the quality of the stego image, if the size of blocks is decreases, the embedding process will be better. So, the distortion in stego image become least , because the blocks which are used in substitution process have small sizes. The similarity between the cover image and the stego image can be consider good since the correlation test for both the stego and reconstructed image is nearly equal to 1 .

REFERENCES

1. Niels Provos and Peter Hone Yman,"Hide and Seek: an Introduction to steganography", IEEE 1540-7993, 2003.
2. Mehdi Kharrazi, Husrev T. Senlar, and Nasir Memon," Image Steganography: Concepts and Practice",WSPC, April,22,2004.
3. Wayner, Peter," Diapering Cryptography: Information hiding: steganography &Watermarking", 2nd edition, San Francisco:Morgon Kanfman,2002.
4. Asghar Sh., Akbar Sh. " A Hybrid Method for Color Image Steganography in Spatial and Frequency Domain "IJCSI International Journal of Computer Science Issues, Vol. 8, Issue 3, No. 2, May 2011
5. Huaiqing Wang and Shuozhong Wang, Cyber warfare: Steganography vs. steganalysis, Communications of the ACM, vol. 47, no. 10, pp. 76-82, 2004.
6. P.Nithyanandam, T.Ravichandran, N.M.Santron & E.Priyadarshini, "A Spatial Domain Image Steganography Technique Based on

Matrix Embedding and Huffman Encoding", International Journal of Computer Science and Security (IJCSS), Volume (5), Issue (5), 2011.

7. Lee,Y.K.&Chen,L.H.," High Capacity Image Stenographic Model", Visual Image Signal Processing, 147:03,June2000.
8. Dilip Vishwakarma1, Satyam Maheshwari2,& Sunil Joshi3" Efficient Information Hiding Technique Using Steganography",International Journal of Emerging Technology and Advanced Engineering Website: www.ijetae.com (ISSN 2250-2459, Volume 2, Issue 1, January 2012.
9. Matsumoto, H.; Sasazaki, K.; Suzuki, Y., "Color image compression with vector quantization ", IEEE Conference on Soft Computing in Industrial Applications, 2008.
10. Arafat Ali, " Qualitative Spatial Image Data Hiding for Secure Data Transmission ", GVIP Journal, Volume 7, Issue 2, August, 2007
11. L. Chang, "Issues In Information Hiding Techniques", Research Supported By The Office OF Naval Research, 2002.
12. T. A. AL-Asadia," A Hybrid algorithm for image compression", Ph. D Thesis, University of Technology, 2004.
13. Bruce Schneier, "Applied Cryptography ", second edition, protocols, algorithms and source code in C, J. Wiley and Sons ,2007

E-Commerce Security: Website Authentication Protocol Based On Developed Rubik Notation

Enas H. Salih[1], Reyadh Hazim.Mahdi[2], and Ammar J. Fattah[3]
[1]Al-Rafeadin University Collage Department of software engineering
[2]Department of Computer science College of science University of Al-Mustansiriyah
[3]Al-Tifaf Co. for Communication and Information Technology

Received 8/12/2011 – Accepted 20/6/2012

الخلاصة

صدر عن شركة kaspersky المعروفة في مجال الامنية المعلوماتية تقرير في منتصف سنة 2011 بخصوص البرامجيات الضارة حيث ينص التقرير على ان انظمة الدفع عبر الانترنيت مثل PayPal و eBay ما زالت الهدف الرئيسي لهجمات الصيادين والتي تتسبب بخسارات هائلة بالنسبة لزبائن هذه الانظمة وفي نفس الوقت للشركات التي تدير انظمة الدفع هذه.

قد تم استخدام وتوظيف الكثير من الطرق لمكافحة مثل هذه الهجمات والتي تعتمد بشكل رئيسي على هجوم الرجل في الوسط وهو طريقة يقوم من خلالها المهاجم بخداع الزبون على انه الموقع الالكتروني الرسمي والذي يمثل الهدف وبالتالي سوف يقنع الزبون بكشف معلومات حساسة عن حسابه ، هذا الاسلوب يعتمد على تحليل وتفسير البيانات المتبادلة لغرض سرقتها.

ان هذا البحث يقوم بتصميم وتنفيذ صيغة رمزية تستخدم لتحقيق الهوية للموقع الالكتروني الذي يهدفه الزبون والذي قد يمثل بنك الكتروني او موقع تجاري وذلك لعقد الصفقات الالكترونية ، ان هذه الصيغة الرمزية المقدمة في هذا البحث تم اشتقاقها من الصيغة الرمزية والتي تعرف Singmaster والتي تم استخدامها لنمذجة حركات المكعب المعروف Rubik حيث ان البيانات المتبادلة في النموذج المقترح لا تمثل البيانات ولا تحويلاتها كما يحدث في التشفير او الترميز.

ABSTRACT

Kaspersky the famous security firm has issued a report in May 2011 regarding spam activity stated that online payment system like PayPal and EBay continued to be the main target for phishers attacks; causing a tremendous losses for customers and companies running these payment systems at the same level.

A lot of hacking methodologies have been used to fraud a web site to act as man-middle-attack to deceive the client urging him to expose crucial and sensitive personal information, all methodologies relying on the interpretation on the intercepted traffic.

This paper is presenting a design and implementation of a notation used to authenticate online payment systems and electronic Bank web sites for ecommerce transactions, the notation is derived from 'Singmaster notation' which was used to model Rubik cube movements where which the exchanged traffic between client and bank does not represent the data nor its transformations (i.e., encrypted or coded).

1- Introduction

Phishing is the practice of sending out fake emails, or spam, written to appear as if they have been sent by banks or other reputable organizations, with the intent of luring the recipient into revealing sensitive information such as usernames, passwords, account IDs, ATM PINs or credit card details. Typically, phishing attacks will direct the recipient to a web page designed to mimic a target organization's own

visual identity and to harvest the user's personal information, often leaving the victim unaware of the attack.[1,2]

The term was coined in the 1996 timeframe by hackers who were stealing America Online (AOL) accounts by scamming passwords from unsuspecting AOL users. The popularized first mention on the Internet of phishing was made in alt.2600 hacker newsgroup in January 1996, however the term may have been used even earlier in the popular hacker newsletter "2600".[1,3,4]

By 1996, hacked accounts were called "phish", and by 1997 phish were actively being traded between hackers as a form of electronic currency. There are instances whereby Phishes would routinely trade 10 working AOL phish for a piece of hacking software or warez (stolen copyrighted applications and games). The earliest media citation referring to phishing wasn't made until March 1997.[3]

Phishing is an example of social engineering techniques used to fool users,] and exploits the poor usability of current web security technologies. Phishing attacks generally rely on a number of simple tools and techniques to trick unsuspecting users. The underlying infrastructure to support a phishing scam may be as basic as a simple copied HTML page uploaded to a freshly compromised web server and a server side script to process any user input data, or it may involve more complex web sites and content redirection, but generally the objectives are the same - to set up a fake web presence for a trusted brand with the necessary back end capabilities to process user input data and make it available to the attacker.[1,3]

Over time, the definition of what constitutes a phishing attack has blurred and expanded. The term Phishing covers not only obtaining user account details, but now includes access to all personal and financial data. What originally entailed tricking users into replying to emails for passwords and credit card details, has now expanded into fake websites, installation of Trojan horse key-loggers and screen captures, and man-in-the-middle data proxies – delivered through any electronic communication channel.[3,4]

2- Phishing a Website

The fraudulent web site that supports the phishing email is designed to mirror the legitimate web site it is purporting to be. The fraudsters use multiple methods to do this, including using genuine looking images and text, disguising the URL in the address bar or removing the address bar altogether. The purpose of the web site is to trick consumers into thinking they are at the company's genuine web site, and giving their personal information to the trusted company they think they are dealing with. [1,3,4]

Using modern HTML editing tools it is very easy to produce a web site mimicking a target organization, and poorly secured web servers can easily be located and compromised if an attacker is not adverse to scanning entire portions of Internet IP address space in the search for vulnerable target hosts. Once compromised, even home PCs can make effective hosts for phishing web sites, so not only well known corporate or academic systems are targeted. Attackers are often indiscriminate in their choice of target computers, purely selecting large IP address blocks to scan at random for a particular exploitable security vulnerability.[1,3]

Once a victim visits the phishing website the deception is not over. Some phishing scams use JavaScript commands in order to alter the address bar. This is done either by placing a picture of a legitimate URL over the address bar, or by closing the original address bar and opening a new one with the legitimate URL. [1,3,5]

An attacker can even use flaws in a trusted website's own scripts against the victim. These types of attacks (known as cross-site scripting) are particularly problematic, because they direct the user to sign in at their bank or service's own web page, where everything from the web address to the security certificates appears correct. In reality, the link to the website is crafted to carry out the attack, making it very difficult to spot without specialist knowledge. Just such a flaw was used in 2006 against PayPal. [3,5]

A Universal Man-in-the-middle (MITM) Phishing Kit, discovered in 2007, provides a simple-to-use interface that allows a phisher to convincingly reproduce websites and capture log-in details entered at the fake site as it can seen in figure (1).

For man-in-the-middle attacks to be successful, the attacker must be able to direct the customer to their proxy server instead of the real server. This may be carried out through a number of methods:[5,6]

- Transparent Proxies
- DNS Cache Poisoning
- URL Obfuscation
- Browser Proxy Configuration

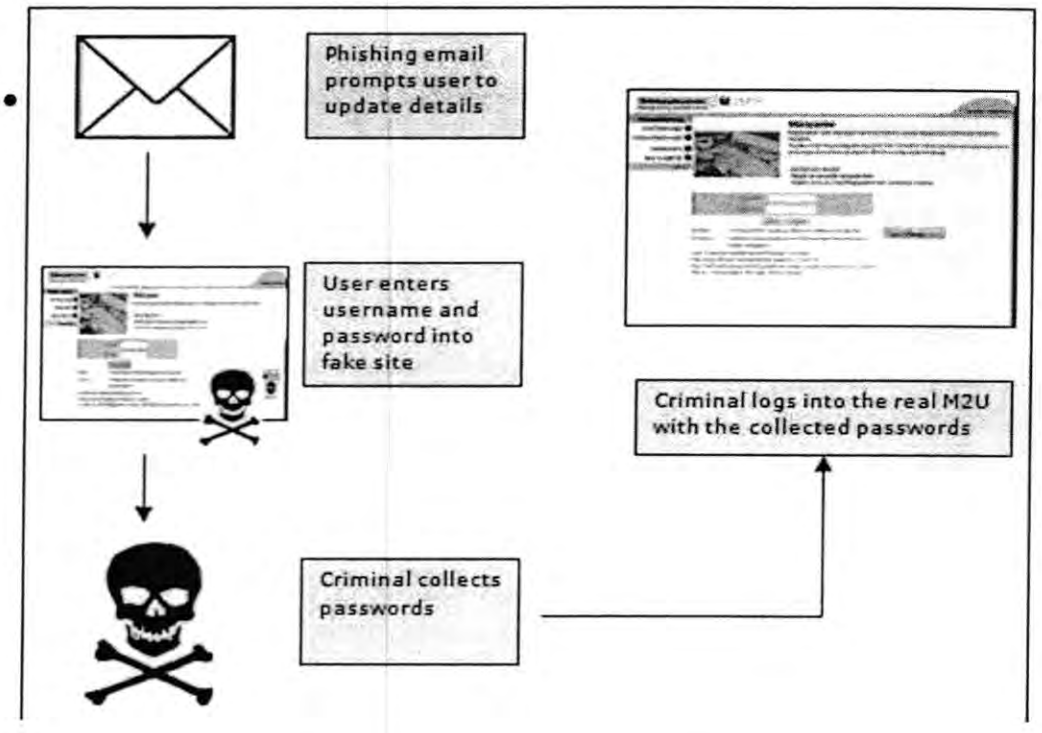

Figure-1: shows website phishing process

4. Phishing eBay website scheme

The following is a real case taken as a demonstration on phishing a website, this hit was really conducted on the targeted famous site 'www.eBay.com', the attack was detected and contained with a minimum collateral damages. [6]

Two critical pieces of information were targeted in this scheme: the authentication credentials (i.e., username and password) and the user's credit card information. Figure (2) shows the critical steps of the scheme from beginning to end.[1]

To build the fraudulent web site, the attacker simply sends requests to eBay for the HTML markup and images needed to render critical pages of the eBay site. Because the Web works by having clients (such as Mozilla or Internet Explorer) download HTML from the server and then display the results to the user, there is no way for eBay to stop users from downloading its source. In fact, easy replicability of content from one Web site to another is a critical feature of the Web.[1,5,6]

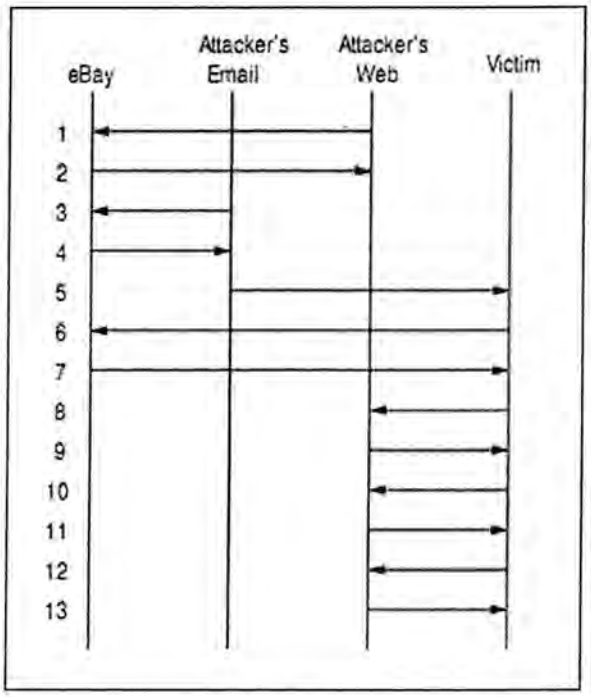

Attacker sends request to eBay for source eBay web server gives source Attacker pulls additional source from eBay web server gives source
''Please resubmit credit card'' Mail client requests real eBay images eBay web site delivers images as requested Victim clicks on a link, thinking it is to eBay Attacker's web site display, looks like eBay User puts in username and password Attacker accepts password, asks for credit card User uploads credit card information Attacker thanks victim for the ''update''

Figure-2: Interaction Diagram Showing Scheme

Instructing the eBay site to send a copy of the source is as simple as having the attacker point his browser to http://www.ebay.com. Each of the thirteen steps identified in figure2 supports one of three goals needed for the thief to achieve his objective. Those goals are creation of the fraudulent eBay site, directing users to the fraudulent site, and then operating the fraudulent site such that users never suspect what has happened.[1,6]

5. Augmented passwords logins

The Bank of America's website is one of several that ask users to select a personal image, and display this user-selected image with any forms that request a password. Users of the bank's online services are instructed to enter a password only when they see the image they selected. However, a recent study suggests few users refrain from entering their password when images are absent. In addition, this feature (like other forms of two-factor authentication) is susceptible to other attacks, such as those suffered by Scandinavian bank Nordea in late 2005, and Citibank in 2006.[8]

A similar system, in which an automatically-generated "Identity Cue" consisting of a colored word within a colored box is displayed to each website user, is in use at other financial institutions.[8]

Security skins are a related technique that involves overlaying a user-selected image onto the login form as a visual cue that the form is

legitimate. Unlike the website-based image schemes, however, the image itself is shared only between the user and the browser, and not between the user and the website. The scheme also relies on a mutual authentication protocol, which makes it less vulnerable to attacks that affect user-only authentication schemes.[7,8]

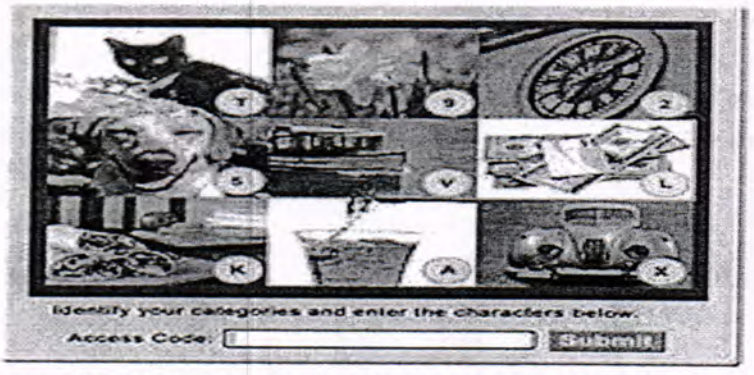

Figure-3 : Dynamic image-based authentication for anti-phishing

Still another technique relies on a dynamic grid of images that is different for each login attempt. The user must identify the pictures that fit their pre-chosen categories (such as dogs, cars and flowers). Only after they have correctly identified the pictures that fit their categories are they allowed to enter their alphanumeric password to complete the login. Unlike the static images used on the Bank of America website, a dynamic image-based authentication method creates a one-time pass code for the login, requires active participation from the user, and is very difficult for a phishing website to correctly replicate because it would need to display a different grid of randomly generated images that includes the user's secret categories.[6]

6. Rubik Move notation

Many 3×3×3 Rubik's Cube enthusiasts use a notation developed by David Singmaster to denote a sequence of moves, referred to as "Singmaster notation". Its relative nature allows algorithms to be written in such a way that they can be applied regardless of which side is designated the top or how the colours are organized on a particular cube.

- *F* (Front): the side currently facing the solver
- *B* (Back): the side opposite the front
- *U* (Up): the side above or on top of the front side
- *D* (Down): the side opposite the top, underneath the Cube
- *L* (Left): the side directly to the left of the front
- *R* (Right): the side directly to the right of the front

• *f* (Front two layers): the side facing the solver and the corresponding middle layer
• *b* (Back two layers): the side opposite the front and the corresponding middle layer
• *u* (Up two layers) : the top side and the corresponding middle layer
• *d* (Down two layers) : the bottom layer and the corresponding middle layer
• *l* (Left two layers) : the side to the left of the front and the corresponding middle layer
• *r* (Right two layers) : the side to the right of the front and the corresponding middle layer
• *x* (rotate): rotate the entire Cube on *R*
• *y* (rotate): rotate the entire Cube on *U*
• *z* (rotate): rotate the entire Cube on *F*

7. Rubik Based Authentication Protocol

Rubik's dimensions are (4 x 4 x 4) which gives 96 place holder, which are to be selected randomly from the 256 ASCII character set. The proposal is using modified Singmaster notation mentioned in previous section to inform the other members about the moves taken at each side.

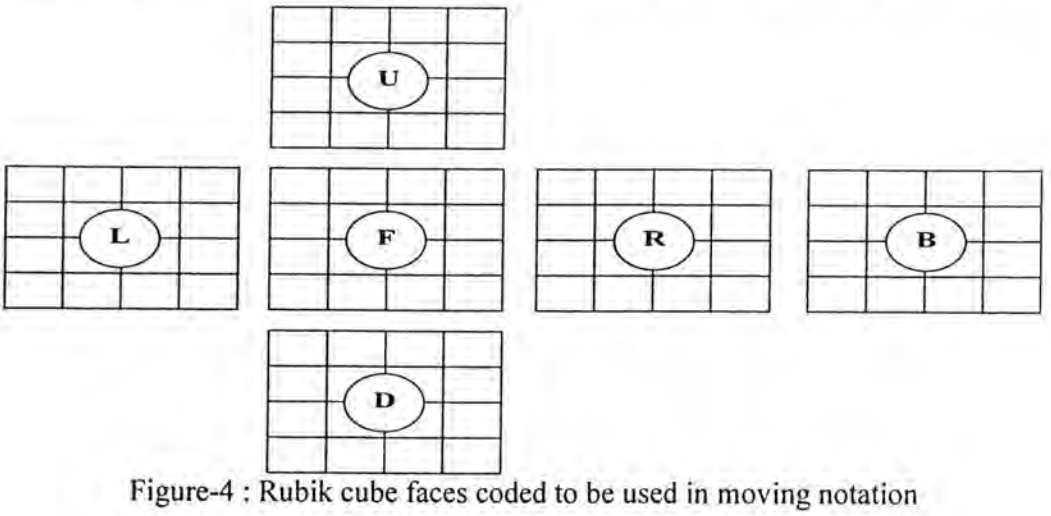

Figure-4 : Rubik cube faces coded to be used in moving notation

The Proposed move notation has the following prototype:

M = {S,RC,I,PN,R,A}
S: Which Side of the cube (i.e., F,B,U,D,R,L)
RC: Row or Column (0 → Row , 1→column and -1 → entire cube)
I: index within RC (0-3 if initialization , -1 if authentication), knobs and place holders should not be declared in authentication session
R: Rotation (i.e., 0→ to left if RC= 0, 0→down if RC=1 and 1→to right if RC=0, 1→to up if RC = 1), this parameter has no effect in initialization
PN: (0→ knob , 1→ place holder)
A: 0→Initialization , 1→Move

Figure-5: Proposed Rubik movement notation

For example
(F,0,1,X,0,0) → means set knob at front face in first Row with index 1
(F,0,X,X,0,1) → means move knob at first row in front face (known by client) to the left
Where X is don't care regarding the value.
By that a stream of moves or initialization can be sent to each directions (i.e., client and Bank) representing required moves or initialization for both sides.
Client and Bank will initialize their Rubik cube which will be used later to authenticate both the web page and client, client and Bank have to agree on each other before starting authenticated session.
The following is the algorithm used in registration phase:
1- [Initial Rubik cube – client side] Client will receive his/her cubic with 96 characters randomly distributed over the place holder of the cube, private email can be used to send initialization for the cube, other secure channels are also an option.
2- [Initial Client knobs and place holders – client side] using proposed notation presented in figure (5), client will get his/her cubic's faces marked for client knobs – at least 1 mark for each face and marked place holders (for client and bank), client and bank might not have the same count of knobs or marked place holders.
3- [Initial Bank Server Rubik cube] Server will receive the same instance of the client cube with the same initialization but not necessarily same locations of knobs or place holders.
4- [Start Authentication session] The session will start by client sending his moves to Bank server side. Rubik movements will be manually generated (i.e., using mouse or write proposed notation script directly).

5- [Bank Sever read the message] Bank Server side will read what has been **assigned** for client place holders.
6- [Bank Server Reply] Bank Server will decide how to move his knobs to get his place holders filled with same sequence as client place holders. Again moves will be generated manually (i.e., using mouse or writing script using proposed notation).
7- [Send Reply to client] Bank Server will send moves as a sequence of the proposed notation to client side
8- [Client Verify Bank Reply] Client side will move server knobs in his/her own instance and check if the same sequence has been obtained from server moved knobs.
9- [Client convinced] client can repeat steps 1-8 for convincing or just authorize this site as the legal web site for the Bank.
After the registration session Band and client will get their Rubik cube initialized with random sequence of ASCII, knobs and place holders. Rubik cube can be used now to send and interpret moves exchanged in the proposed notation. Figure (5) presents Rubik cube after getting initialized and moved by client to generate challenge message 'EENVND OOIVEV'.

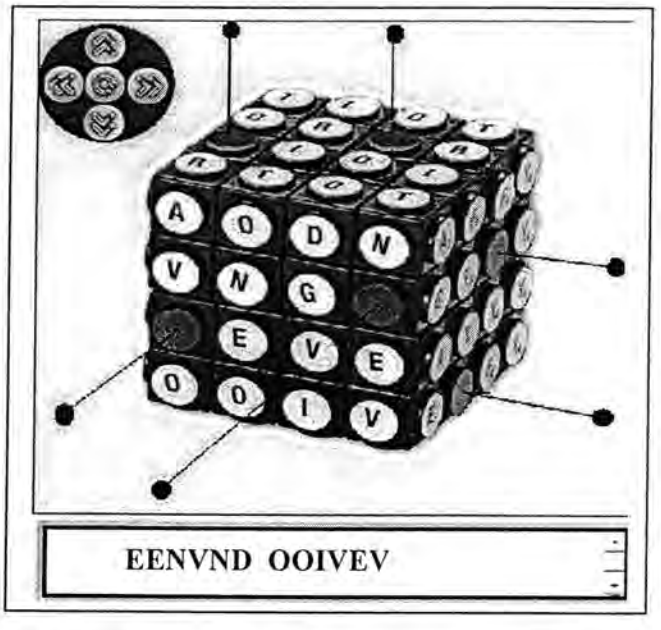

Figure-5 : Rubik cube simulation in Client web page

Figure (6) presents Rubik cube representing Bank side been initialized and moved using Bank knobs to generate same challenge message. Figure (7) presents authentication protocol using proposed Rubik based notation.

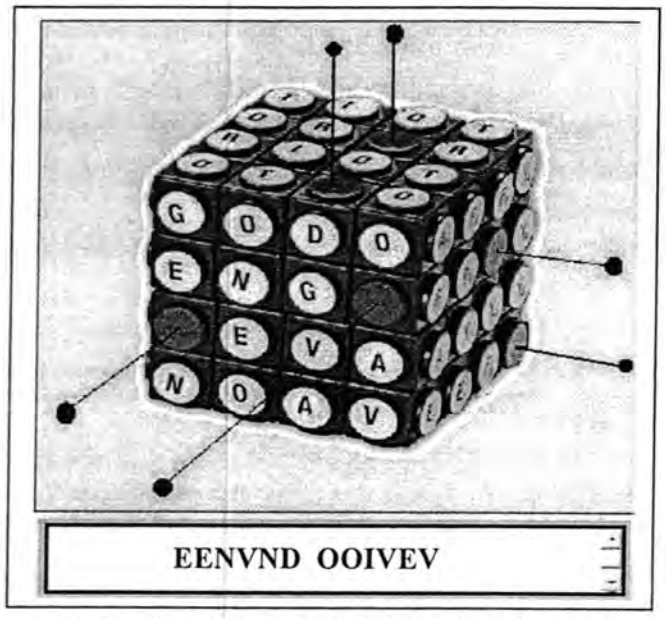

Figure-6 : Bank Rubik cube simulation in Client web page

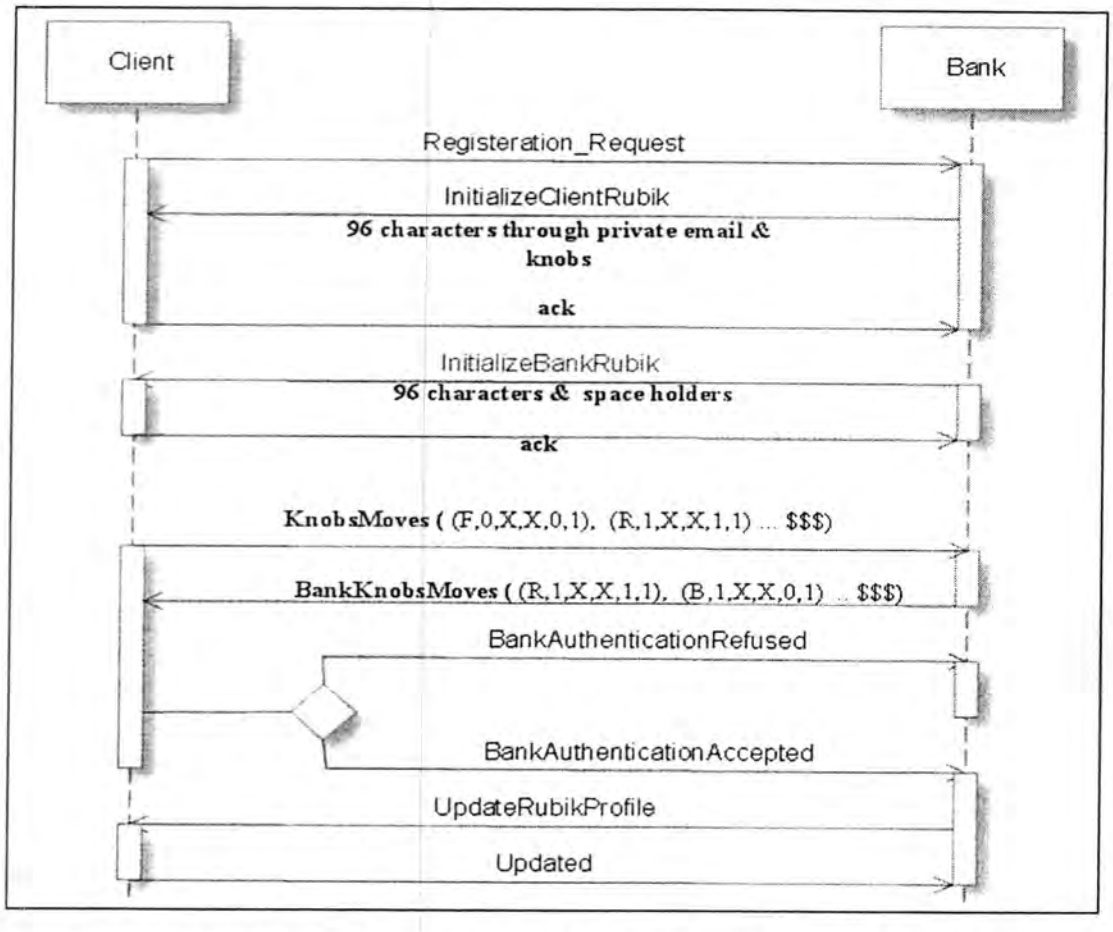

Figure-7: Website (Bank) Authentication Protocol Based on Rubik Notation

Each authentication session will end up with updating knobs positions at client side and Bank side; updated locations will be stored in client profile within Bank database. Update locations can be determined as the following:

$l_{i+1} = l_i + m_i$

Where

l_{i+1} : Next locations of knobs

l_i : Initial locations of knobs

m_i : Moves of knobs

Figure (8) presents components of Bank Authentication system proposed by this paper

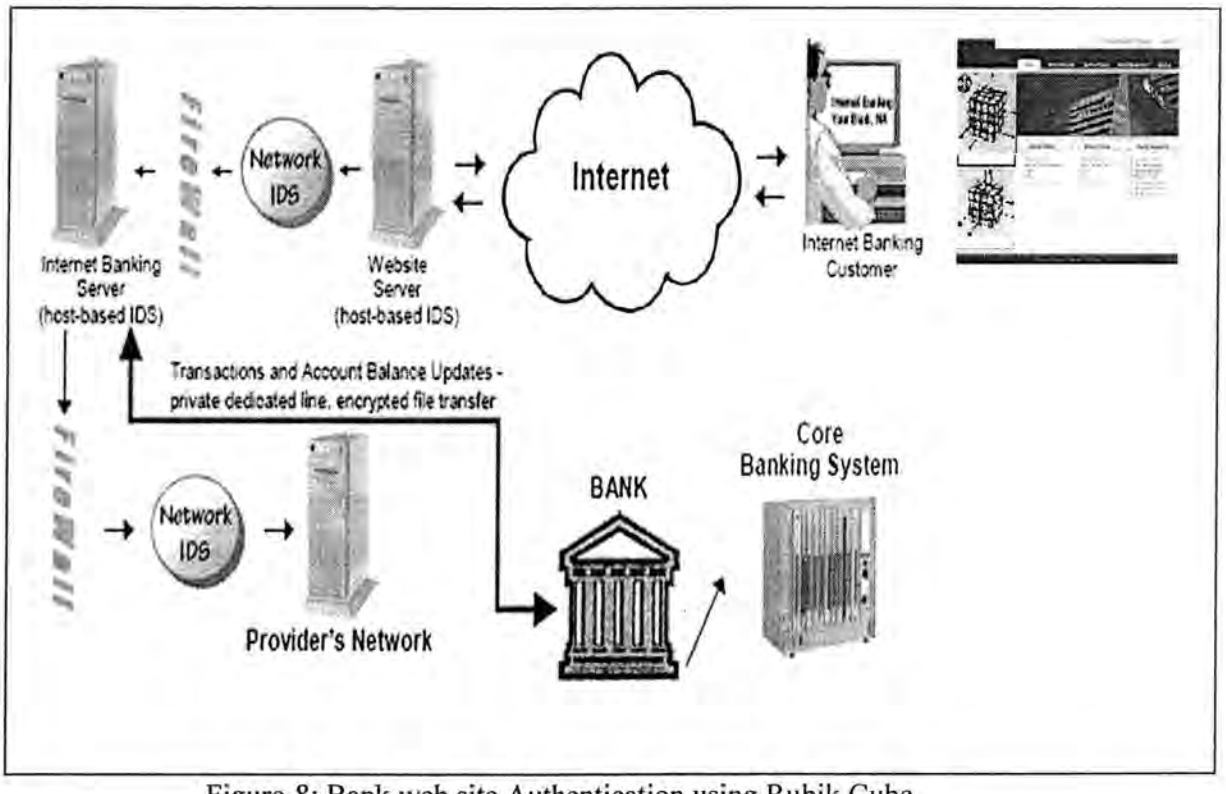

Figure-8: Bank web site Authentication using Rubik Cube

8. Analysis

1- Server and client will exchange moves that do not in any way refer to the data, even it does not point to the size of the data (i.e., rubik's cubic can be moved different number of moves and yet obtain the same data from client place holders).

2- Attacker can't map client sequence to server sequence due to that it is not one-to-one mapping, where client can use different routes to get into the same result.

3- Attacker can't interpret intercepted movement due to non-existing of evaluation function to get the feasibility of certain distribution especially if client and Bank does not use meaningful information (i.e., when matching is the goal rather than the meaning of what is exchanged).

9. Conclusions

1- Electronic transactions still vulnerable to phishing threats due to traditional security technologies it uses to maintain clients' privacy and confidentiality.

2- Web site phishing is easy to be conducted due to open source languages used to build web sites and to the availability of mass downloading tools on the internet; a complete web site with its entire links can easily be downloaded.

3- Web based Mining tools could be used by attackers to automatically collect information regarding security algorithms, where automatic analysis for user interaction with the fake web site can reveal important information regarding privacy and security policies, this information could be used later to compromise that web site.

4- Web site authentication is a serious challenge for e-commerce due to Internet architecture where routing a request to a server could pass through multiple routers to end up with the designation target, each router is a vulnerable point in that chain, thus the large number of routers to the e-commerce server the more serious is the challenge.

10. REFERENCES

1- David Watson, Thorsten Holz and Sven Mueller, "Behind the scene of phishing attack", Honeynet Project & Research Alliance, 2005.
2- Koon Yaw Tan,"phishing and Spamming Via IM ", 2006
3- http://www.fraudwatchinternational.com/phishing-fraud/phishing-web-site-methods.html
4- http://www.technicalinfo.net/papers/Phishing.html
5- Joel Scambray, Vincent Liu and Caleb Sima,"Hacking Exposed: Web Application Security Secrets & Solutions", McGraw-Hill, 2011.
6- Matt Curtin, "Anatomy of Online Fraud", interhack,2003
7- http://www.wordspy.com/words/phishing.asp
8- http://en.wikipedia.org/wiki/phishing
9- David Joyner. "Adventures in group theory: Rubik's Cube, Merlin's machine, and Other Mathematical Toys". Baltimore: Johns Hopkins University Press, 2002.

Socializing Snort Firewall Alerts using Multi Agent Platform

Ethar abdul wahhab hachim
Assistant Lecture Department of Computer Science
College of Science Al-Mustansiriya University , Iraq
ethar_201124@yahoo.com

Received 20/7/2011 – Accepted 18/4/2012

الخلاصة

ان "snort" هي عبارة عن نظام لكشف الاختراقات مع امكانية الاستحواذ على البيانات المنقولة في الشبكة للقيام بتحليل اكثر وكشف الاختراقات المحتملة ومن ثم اصدار تحذير بوقوع حدث الاختراق (نقصد باحداث الاختراق هي تلك التصرفات الشاذة والتي يتم استشعارها عن طريق مراقبة بيانات الشبكة مثل طوفان الشبكة ، تقليد ARP ، طوفان الشبكة من نوع SYNC)

هذا البحث يقوم بتقديم هيكلية تطوير لهذا النظام من خلال ربط منظومة الانذار الخاصة بالنظام snort مع جدار نار تام التوزيع من خلال استخدام مفاهيم واليات الايجنت، حيث ان الايجنت يستطيع العمل بشكل مستقل لادراك فايل التهيئة الخاص بالـ snort ومن ثم القيام باضافة قانون جديد الى جدار النار، ان القانون الجديد يعتمد على مستوى الادراك للاحداث التي تجري في الشبكة. واخيرا يقوم الايجنت بنشر الانذار المستلم الى كل اعضاء النظام الشرعيين بغض النظر عن الهندسة الموقعية للشبكة واجزائها .

ABSTRACT

Snort is Intrusion Detection System (IDS) with capabilities to sniff network traffic for further analysis, detect and alert intrusion events (i.e., any malicious action sensed from monitoring network traffic such as network flooding, ARP spoofing, SYNC flood and others).

This paper is presenting development schema to integrate Snort alerts system with a fully distributed firewall by using Agent terminology, where agent can act autonomously to perceive Snort configuration file and add firewall rule according to this perceiving. Eventually, agent will broadcast detected alert to all platform members regardless network topology and segmentation.

Keywords: Snort firewall, rule file, Java programming, Agent , JADE

1. INTRODUCTION

Network intrusion detection systems (NIDS) are an important part of any network security architecture. They provide a layer of defense which monitors network traffic for predefined suspicious activity or patterns, and alert system administrators when potential hostile traffic is detected. Commercial NIDS have many differences, but information Systems departments must face the commonalities that they share such as significant system footprint, complex deployment and high monetary cost. Snort was designed to address these issues.[1]

All malicious activities have signatures through which security software can identify and neutralize these activities, and even tools and techniques used to conduct malicious activities are listed in a dedicated database as well as the vulnerabilities that intruders want to exploit. These signatures are used to create Snort rules to investigate network

packets against possible suspicious signatures in their header and payload parts. [1]

2. Managing Network Security with Snort

Snort is a modern security application with three main functions: it can serve as a packet sniffer (in which Snort gathers packet headers and data and writes them to the screen), a packet logger (in which data and /or headers are dumped to the hard drive); or a Network-based Intrusion Detection System (IDS)(which does not record packets but instead analyzes their content in comparison to rules that have been chosen). [1,2,3] There are also many add-on programs to Snort to provide different ways of recording and managing Snort log files, fetching and maintaining current Snort rule sets, and alerting to let your administrators know when potentially malicious traffic has been seen. Although not part of the core Snort suite, the add-ons provide a rich variety of features to the security administrator. There are many ways to use Snort as part of company's security design.[2]

The Snort intrusion detection mode has four main components : the packet capture engine (which collects traffic using libpcap or WinPcap), the preprocessor plug-ins (which analyze packet data they obtain from pcap, determining what to do with each packet, and also dropping weird input), the detection engine (which systematically compares data in each packet it collects to rules), and the output plug-ins (which generate alerts and perform other functions such as terminating undesirable sessions).[2,3]

Snort rules have a defined format and are numbered in a systematic manner, so related rules are mostly within the same numerical range. Although Snort offers a large number of rules, not all of them must be used. Snort, in fact, runs more efficiently if a reduced rule set is used. Custom rules can also be created to supplement the existing Snort rules. Snort 2.0 performs selective searches of data within rule sets, resulting in better performance. Snort's alerting function enables alert data to be sent in a variety of ways, including using SNMP, or written to a log file or a database. [1,2,3]

The hardware Snort depends on the size of the Snort deployment. Disk space, memory, and processor speed are important considerations. Software used in connection with Snort is also critical. Choosing an appropriate OS to run on the Snort platform is the first step. You also need software, such as pcap, gcc, automake, autoconf, lex and yacc or flex and bison, and flexrep.[3]

Snort 2.0 offers numerous improvements, among which is the Snort 2.0 Protocol Flow Analyzer. This analyzer conducts a high-level analysis of application protocol traffic, breaking it into client-to-server and also server-to-client data flows. For the sake of efficiency, the analyzer

inspects only certain portions of the data in data flows. Snort 2.0 also has improved protocol decoding in which the preprocessor function transforms a wide range of data to a single format to facilitate processing the data.[2,3]

One of Snort's real strengths are the options available for output of alerts and other detection information. While running tail -f on the alert file in /var/log/snort certainly lets you see that alerts that Snort generates, using that information effectively requires more horsepower. Many Snort administrators use third-party applications to monitor and investigate the information generated by Snort. To do this, Snort must output the data a particular format. The output plug-ins perform this task. Note that using some of these plug-ins require the administrator to take some steps at the time that Snort is compiled. For example, to allow Snort to output to a MySQL database, a MySQL client needs to be installed on the Snort system and the --with-mysql option must be specified with the ../configure command. Some of these options are only available on a particular platform. For instance, only a Windows system can log directly to Microsoft SQL Server with the mssql plug-in (Unix-based systems must use ODBC with the odbc plug-in).[2,3,4]

3. Creating and Managing Snort Rules

Snort is a signature-based intrusion detection system. While the preprocessors do not rely on signatures to generate alerts on potential malicious traffic, the heart of Snort's ability to detect intrusion is the catalog of signatures located in the rules files. Being a signature-based IDS is both a strength and weakness.[4]

Because Snort is signature-based, it can be configured for specific threats—the latest worm, the latest IIS exploit, and so on. The rules watch for the specific contents of a packet or for strange settings in the headers. This allows the security administrator to quickly determine the nature of the potential attack since he can easily examine the rule that triggered the alert (as well as the packet itself with some of the other tools available, like ACID or SnortCenter). Rules are records stored in snort rule file and it has the structure presented in Figure(1). A comparison is commonly made between signature-based IDS and antivirus software. Both have a catalog of signatures that they use to match against a stream of data flowing by a sensor component. In antivirus software, this process is accomplished by a software component that watches memory and filesystem access. An IDS, on the other hand, watches packets traveling the network. [1,3,4]

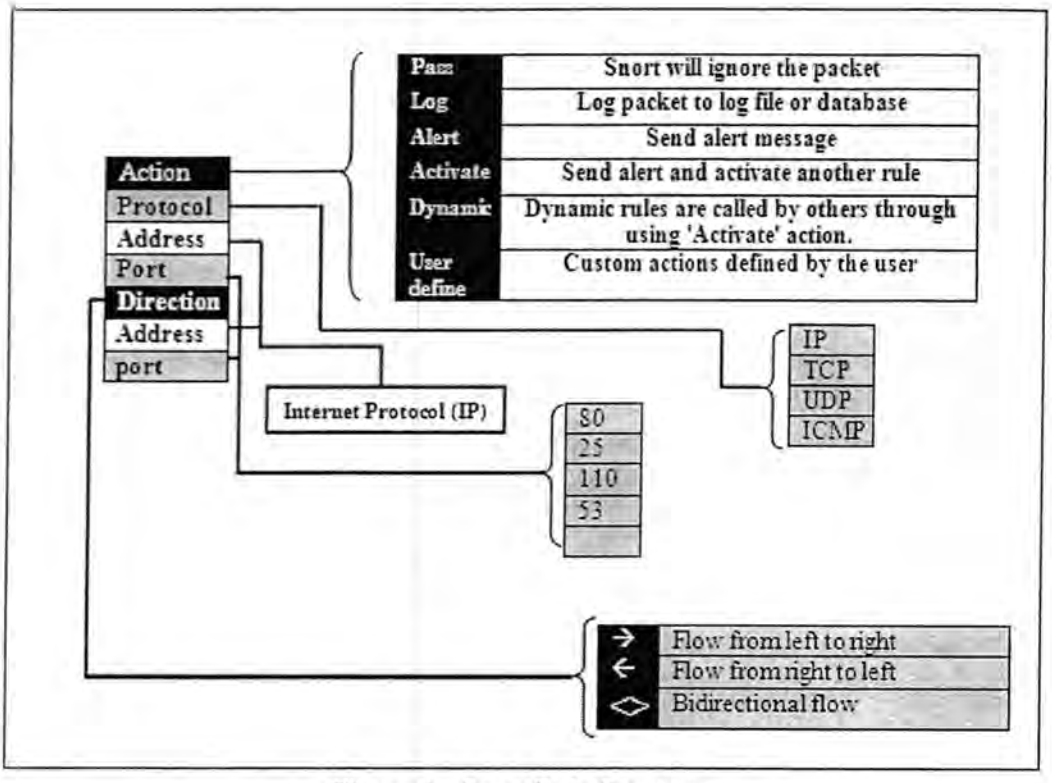

Figure-1: Snort Rule Structure

To detect the latest attack methods , the latest is needed. As a result, it is important to keep the rules as up to date as is reasonable. A schedule of updating the entire rule set once every two weeks will be enough

4. Agent based software design

Software development process is an imposing structures and technologies engaged in software production. These technologies have been directing software development process, which in other term is the software development lifecycle, toward different engineering concepts due to the wide spectrum of applications demanded by the revolutionary growing of society needs.[5,6]

In recent years, Agent Oriented Software Engineering (AOSE) has been increasingly adopting new concepts in software production to add more interactivities and autonomous behavior to software modules. This approach was due to the developed environment which the software has been designed to work within, where there is a real-time changing in states and unforeseen run-time conditions and fluctuations. Agent-based software design, and development and deployment was emerged into software technologies to add new perspective to building software components.[5,7]

Agent is a software module that can generally defined as an entity that perceives an environment and acts on this environment[7], and it is a relatively new software paradigm that adopts concepts from theories of artificial intelligence and deploy these concepts into mainstream realm of distributed systems. Agent-based software development process is an abstraction of applications as a collection of software modules called Agents that are characterized by the following attributes: [5,7,8]

- Temporal continuity: Agent process keep going without a stop.
- Autonomy: Agent is completely autonomous within its environment where Agent can perceive, conceptualize and react to environment events.
- Sociability: Agent keep communicating other Agents and software module to increase his knowledge and experience.
- Rationality: Agent has the ability to conceptualize and react in reasoning environment events.
- Reactivity: Agent mutually interact with the environment through effectors wither it is software effectors or hardware effectors.
- Proactivity: Agent can predicate changes within the environment before changing states.

5. Java Agent Development Framework (JADE)

JADE is the most widespread Agent-oriented middleware and it is a completely distributed middleware system with a flexible infrastructure allowing easy extension with add-on modules. The framework facilitates the development of complete Agent-based applications by means of a run-time environment implementing the life-cycle support features required by Agents, the core logic of Agents themselves, and of language features.[8] figure (2) presents Agent Management reference model used by JADE environment

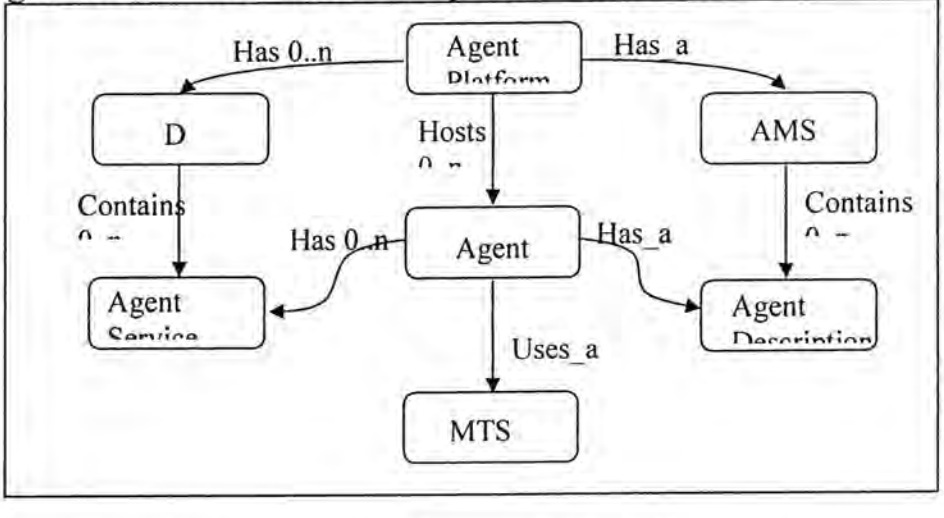

Figure-2 : Java Agent Development Platform Components

From figure(2) main components of the model can be briefly described as the following:

- Agent Platform (AP): Agent physical infrastructure in which Agents are deployed, this component includes machines, operating systems, FIPA agent management components, Agents.
- Agent: computational process that inhavits an AP and typically offers one or more computational services that can be published as a service description.
- Directory Facilitator (DF): the DF is an optional component of an AP providing yellow pages services to other agents. It maintains an accurate, complete and timely list of agents and must provide the most current information about agents in its directory on a non-discriminatory basis to all authorized agents. An AP may support any number of DFs which may register with one another to for federations. [7,8]

6. The proposal

The aim of this paper is to present SNORT integration environment ontology where Java Intelligent agents can communicate and update personal firewall rule list autonomously and intellectually as figure (3) depicts.

Java agents will work autonomously in the network environment and will monitor network status for certain suspicious events (spoofing, flooding,..., etc) and eventually add rule to SNORT rule file.

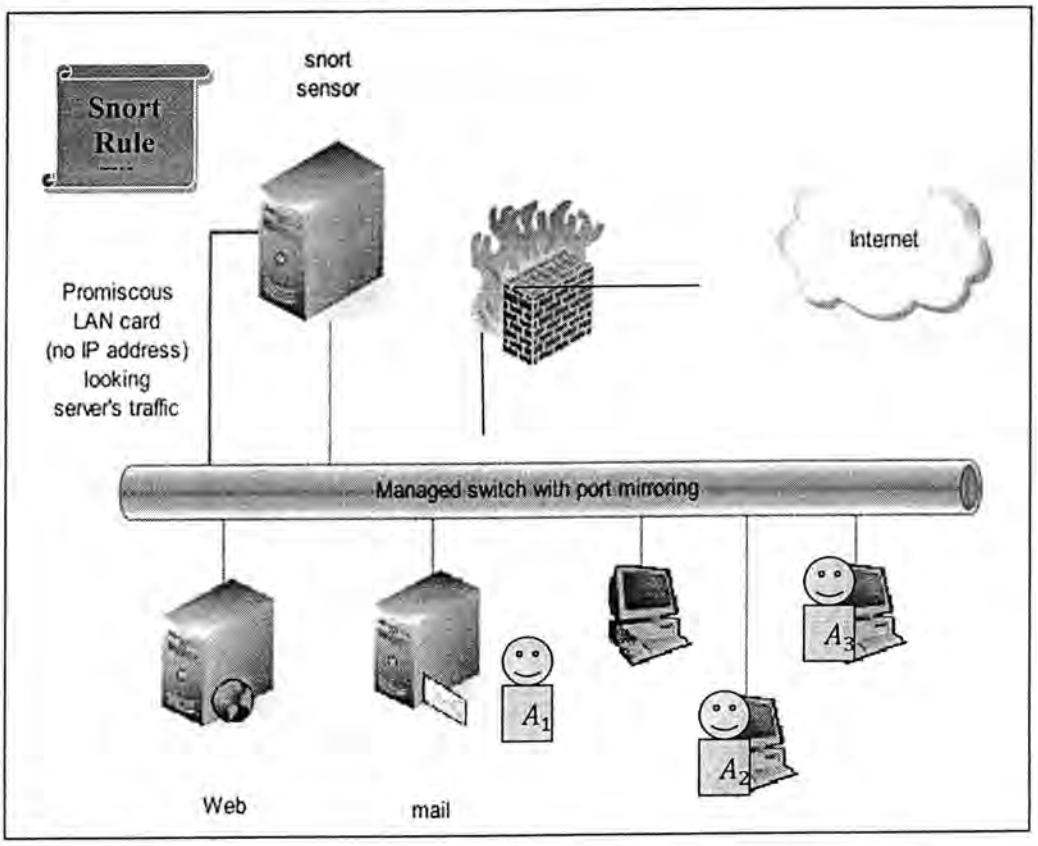

Figure-3: autonomous Agents deployed to automatically update snort rule file

Environment Concepts

For an Agent to be active within an environment, the domain of the environment must be abstracted into its basic concepts much like abstracting problem domain into a collection of objects in object oriented programming. A data structure can be promoted to be an object if there is a possibility to define its attributes and methods, but this is not enough to be a concept, thus there is a need to have inference rules to tell what propositions can be revealed from the existence of such an object (i.e., reasoning the existence).

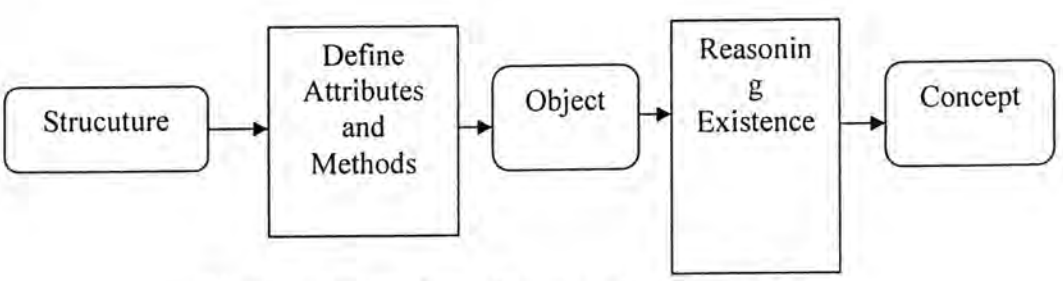

Figure-4 : Promoting a Structure to a Concept life

This proposal will define the concepts of ARP-Spoofing to grant Agents the ability to perceive this network event and act according to some ontology define by this paper. The data structure will the TCP/IP packet which posses ARP packet. This paper will not introduce these structures due to its standardization and publicity.

In this domain the concepts that agent will have the ability to perceive are:

1- ARP(IN IP,IN Type, OUT MAC). Type→{request, reply}
2- RARP(IN MAC, IN Type, OUT IP). Type→{request, reply}
3- SNORT_PASS(IN action=PASS, IN protocol, IN IPsrc, IN PortSrc ...)
4- BINDED_TO_MAC(IN IP)
5- BINDED_TO_IP(IN MAC)

Environment Ontology

1- ARP(IP_i, request, X)
2- ARP(IP_i, reply, MAC_i)
3- RARP(X, request, IP_i)
4- RARP(MAC_i,reply, IP_i)
5- ARP(IP_i, request, X) and ARP(IP_i, reply, MAC_i) and NOT BINDED_TO_MAC(IP_i)→ ARP_SESSION
6- ARP(IP_i, request, X) and ARP(IP_i, reply, MAC_i) and BINDED_TO_MAC(IP_i)→ SUSPECIOUS_ARP_SESSION

JADE is a Java library that can be embedded in any Java program, but unfortunately Java dose have ability to talk to real machine but it talks to Java Virtual Machine (JVM), thus to allow Agent to perceive within network environment; Java Agent has to access network traffic. This paper has designed and implemented C++ socket based network module to interface Java Agent to the real machine, and Java Agent in its turn will activate its kernel processing components (i.e., Behaviours) to inference the incoming packets. As it is presented in figure (5).

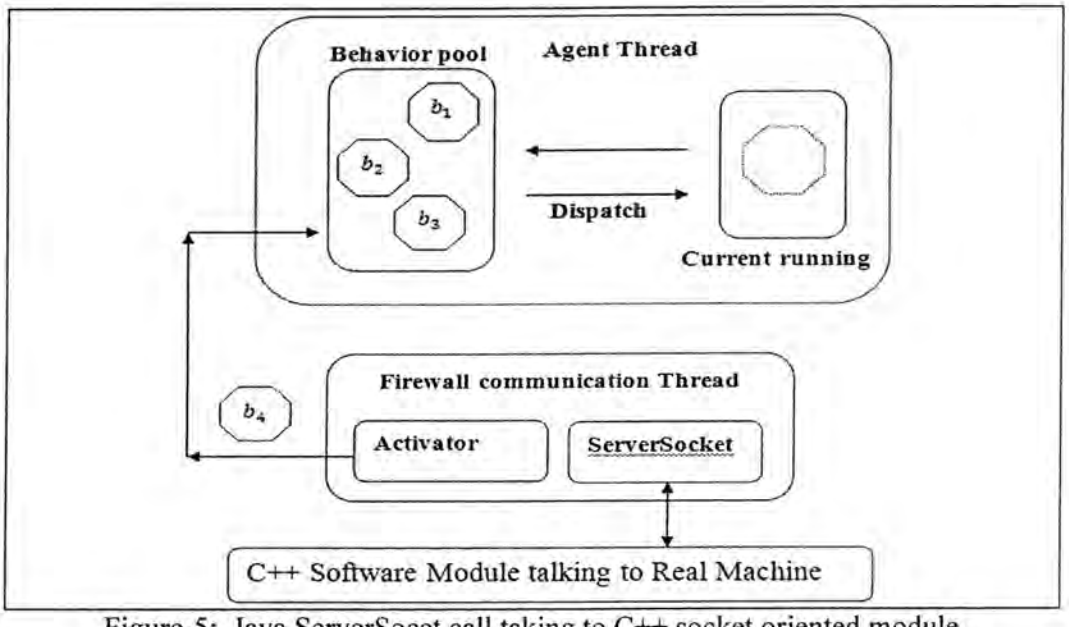

Figure-5: Java ServerSocet call taking to C++ socket oriented module

When one Agent intercept network threat such ARP spoofing it will Alert other Agents for this threat, Agent will use XML syntax to represent the threat due to its readability and being tagged document. Figure (6) presents communication session conducted between agents within the same platform.

Snort firewall will handle the detection of the alert and register it in its rule file and firewall agent will interpret this rule and propogate it to the entire platform.

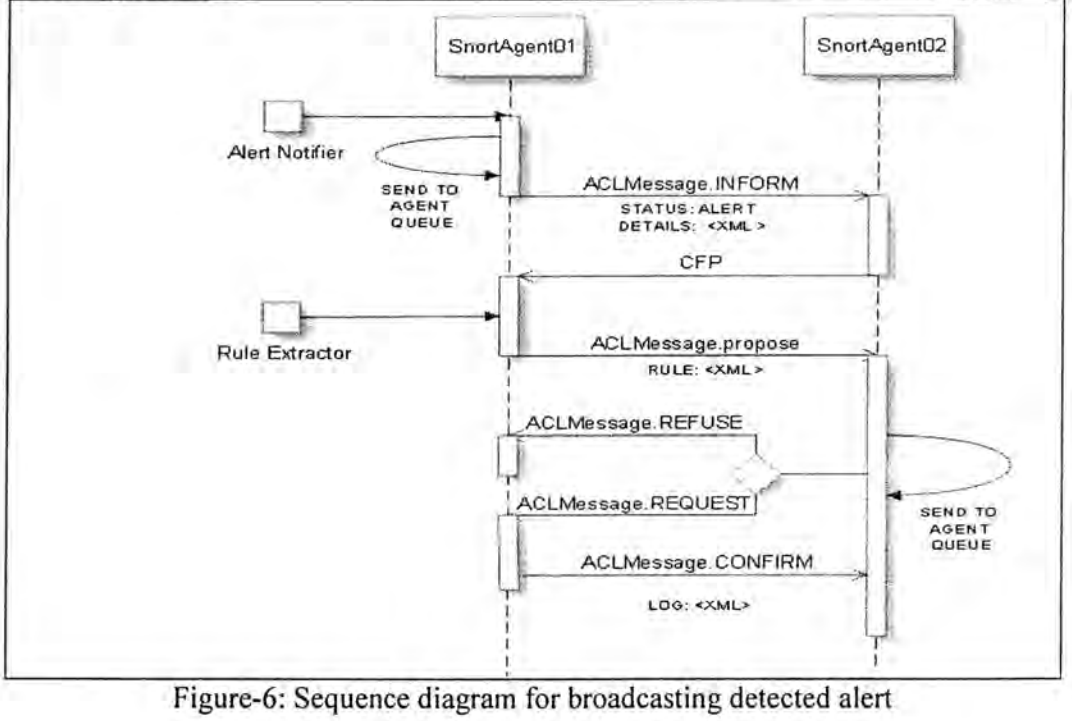

Figure-6: Sequence diagram for broadcasting detected alert

Figure (7) presents the RMA (Remote Agent Management) graphic interface, this figure shows that four firewall Agents have joined the platform and they are active and online

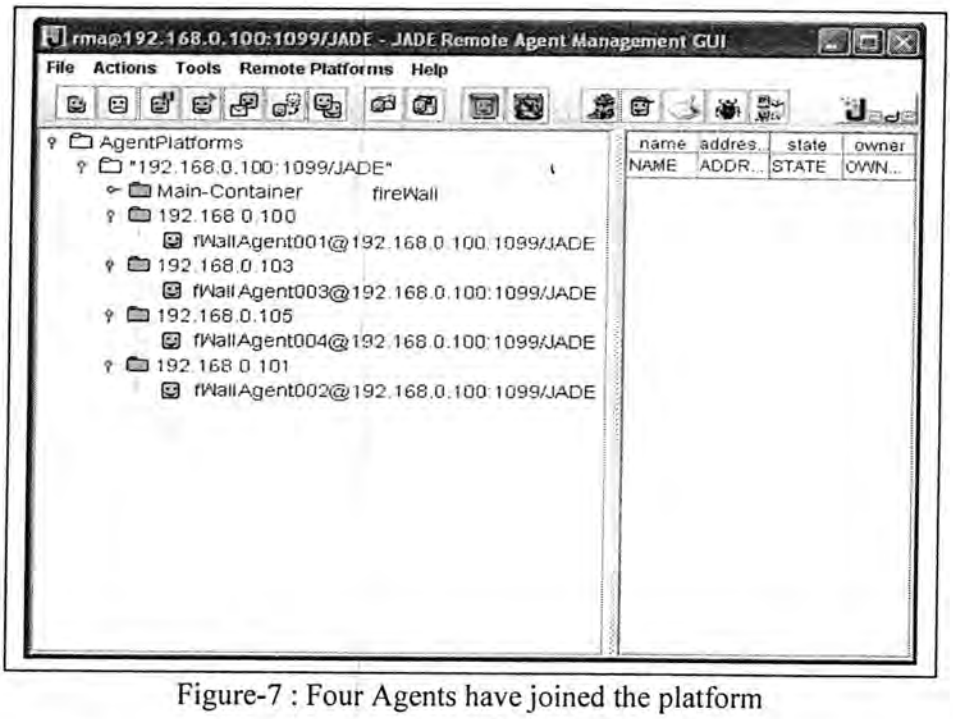

Figure-7 : Four Agents have joined the platform

Figure (8) presents Agent propagates the alert he got from Snort rule and configuration file. Agent communication session can be conducted in many scenarios (i.e., ont-to-one and one-to-many).

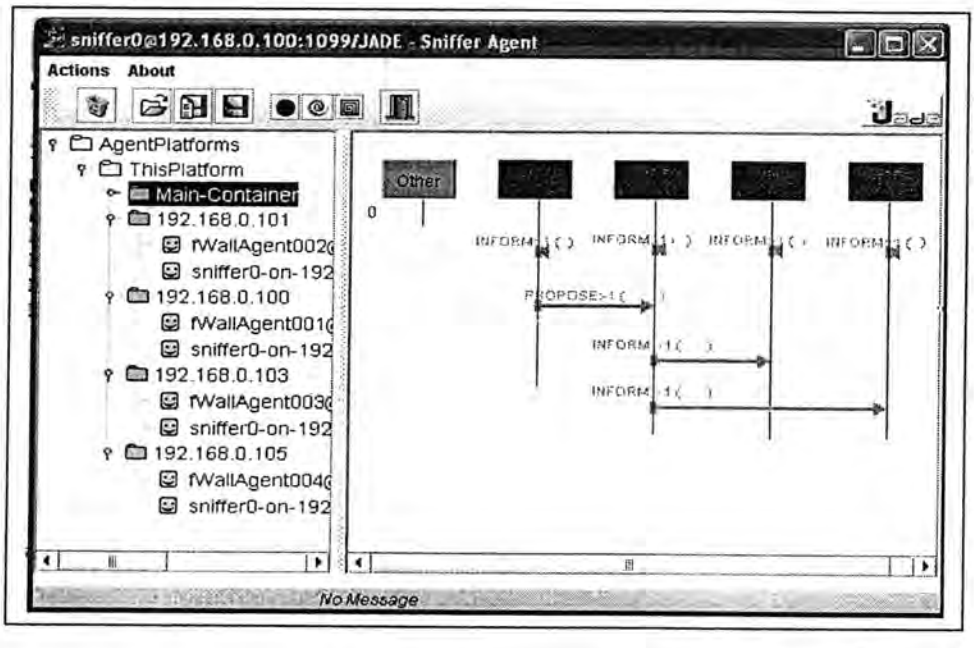

Figure-8 : Agent firewall is propagating received alert

the Agent who received the alert will not respond to fake ARP-session based on the information he got within the message from other Agents or in other occasions confirm ARP table of the system as in figure (9).

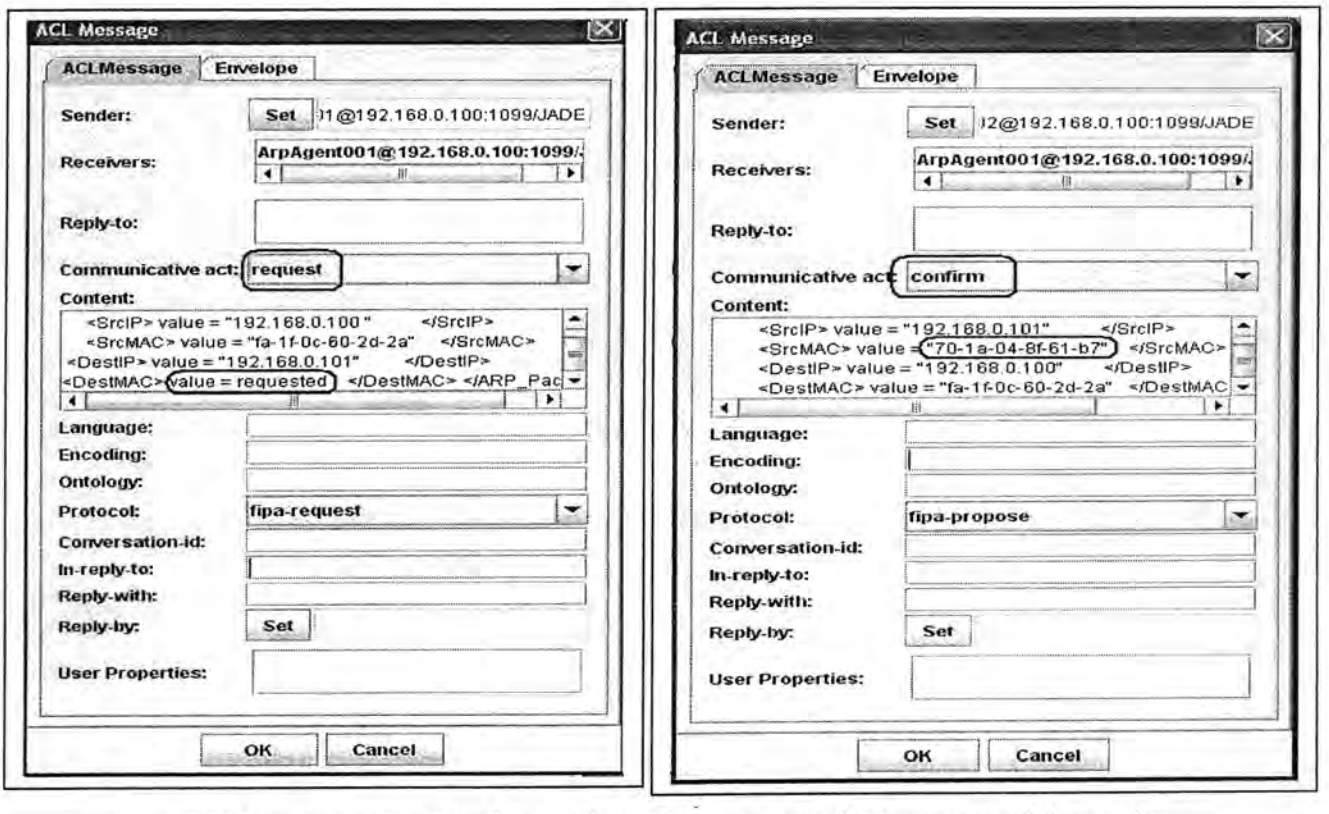

Figure-9: Agents can confirm the validity of ARP cache table to prevent ARP-spoof

7. Conclusions

1- Agent software module can be embedded in perceivable domains to add the ability to make decisions where sensor and raising alerts can be the assignments of agents. Agent platform can be built to assist sustaining events occurred at low level abstraction of any information system

2- Counter network threats can be implemented as a social activity rather than personal inspection for the threat. all network threats have their signature through which security software can identify and neutralize these threats, thus, if for some reason certain threat's signature is not recognized in some network segment; it could be recognized somewhere else.

3- Application level proxies can make a great use of intelligent agent is the domain of the application is abstracted in its essential concepts

4- Network protocols are easy to be conceptualized due to its design principles in maintaining the simplicity and lower network traffic, and ethical hacking methodologies are producing many concepts to identify threat signature and footprint. Powerful network ontology will grant

security products to conceptualize network events and eventually identify not only known threats' signature but even the anomalous behaviors.

8. References

1- Martin Roesch, " Snort – Lightweight Intrusion Detection for Network", Stanford Telecommunication Inc. 1999.
2- Brian Caswell and Jay Beale, " Snort 2.1 Intrusion Detection", second edition, Syngress publishing, Inc. 2004.
3- Carl Endorf, Eugene Schultz, and Jim Mellander,"Intrusion Detection and Prevention", USA, McGraw-Hill, 2004.
4- Kerry J. Cox and Christopher Gerg, "Managing Security with Snort and IDS tools", O'Reilly, 2004.
5- Coral Calero, Francisco Ruiz, Mario iattini, "Ontologies for Software Engineering and Software Technology", Springer-Verlag Berlin Heidelberg 2006.
6- Steve McConnell, "Professional Software Development, Shorter Schedules, Higher Quality Products", Pearson Education, 2004
7- Matthias Klusch, Rainer Unland Calisti, "Software Agent-Based applications, platforms and development kits ", springer science, Germany, 2005.
8- Fabio Bellifemine, Giovanni Caire and Dminic Greenwood, "Developing Multi-Agent Systems with JADE", John Wiley & Sons, ltd, 2007.

Vol. 23
No. 7
2012

مجلة علوم المستنصرية

تصدر عن كلية العلوم الجامعة المستنصرية

Mobile: 07711184399
e-mail: mustjsci@yahoo.com

مجلة علوم المستنصرية

هي مجلة علمية رصينة تصدر عن عمادة كلية العلوم في الجامعة المستنصرية في تخصصات الكيمياء والفيزياء وعلوم الحياة وعلوم الحاسبات وعلوم الجو. تقوم المجلة بنشر البحوث العلمية التي لم يسبق نشرها في مكان آخر بعد إخضاعها للتقويم العلمي من قبل مختصين وباللغتين العربية او الانكليزية وتُصدر المجلة عددين سنوياً بكلا اللغتين.

تعليمات النشر في المجلة

1. يقدم الباحث طلبا تحريريا لنشر البحث في المجلة ويكون مرفقا بأربع نسخ من البحث مطبوعة على ورق ابيض قياس (A4, 21.6×27.9 cm) مع ترك حاشية بمسافة انج واحد لكل اطراف الصفحة ومطبوعة بأستخدام برنامج (Microsoft Word, 97-2003) بصيغة (doc.).
2. يرفق مع البحث ملخص باللغة العربية وآخر باللغة الإنجليزية على ان لاتزيد كلمات الملخص عن (150) كلمة.
3. عدد صفحات البحث لاتتجاوز 10 صفحة بضمنها الاشكال والجداول على ان تكون الاحرف بقياس 14 نوع (Time New Roman) وبمسافة مزدوجة بين الاسطر. وينبغي ترتيب اجزاء البحث دون ترقيم وبالخط العريض (Bold) كالاتي: صفحة **العنوان، الخلاصة باللغة العربية، الخلاصة باللغة الإنجليزية، مقدمة، المواد وطرائق العمل (الجزء العملي)، النتائج والمناقشة، الاستنتاجات وقائمة المراجع.**
4. يطبع عنوان البحث واسماء الباحثين (كاملة) وعناوينهم باللغتين العربية والانكليزية على ورقة منفصلة شرط ان لاتكتب اسماء الباحثين وعناوينهم في أي مكان اخر من البحث ، وتعاد كتابة عنوان البحث فقط على الصفحة الاولى من البحث.
5. ترقم الجداول والأشكال على التوالي حسب ورودها في المخطوط، وتزود بعناوين، ويشار إلى كل منها بالتسلسل نفسه في متن البحث.
6. يشار الى المصدر برقم يوضع بين قوسين بمستوى السطر نفسه بعد الجملة مباشرة [1]، [2]، [3] وهكذا. تطبع المصادر على ورقة منفصلة ، ويستخدم الاسلوب الدولي المتعارف عليه عند ذكر مختصرات اسماء المجلات.
7. يتبع الاسلوب الاتي عند كتابة قائمة المصادر على الصفحة الاخيرة كالاتي: ترقيم المصادر حسب تسلسل ورودها في البحث ، يكتب الاسم الاخير (اللقب) للباحث او الباحثين ثم مختصر الاسمين الاولين فعنوان البحث ، مختصر اسم المجلة ، المجلد ، العدد ، الصفحات الاولى والاخيرة ، سنة نشر البحث. وفي حالة كون المصدر كتابا يكتب بعد اسم المؤلف او المؤلفين عنوان الكتاب ، الطبعة ، الصفحات ، سنة النشر ، المؤسسة الناشرة، الدولة مكان الطبع.

بخصوص اجور النشر يتم دفع مبلغ (50000) خمسون الف دينار عند تقديم البحث للنشر وهي غير قابلة للرد ومن ثم يدفع الباحث (25000) عشرون الف دينار اخرى عند قبول البحث للنشر.

جميع البحوث ترسل الى:
رئيس تحرير المجلة
أ. د. رضا ابراهيم البياتي
كلية العلوم- الجامعة المستنصرية
البريد الاليكتروني: mustjsci@yahoo.com

المـــحتـــويـات

تأثير حامض الجاسمونك في إنتاج بعض مركبات الأيض الثانوي في كالس نبات الحلبة *Trigonella foenum- graecum* L. خارج الجسم الحي

إستبرق سامي عباس[1]، سعدية حسن محمود[2]، كاظم محمد إبراهيم[3]
[2,1]كلية العلوم، الجامعة المستنصرية، بغداد- العراق.
[3]كلية العلوم، جامعة النهرين، بغداد- العراق.

تاريخ تقديم البحث 2012/4/25 - تاريخ قبول البحث 2012/6/20

ABSTRACT

The effect of adding different concentrations of jasmonic acid (0, 2, 4, 6 or 8 mg/l) on the production of some secondary metabolites in callus of *Trigonella foenum-graecum* L. plant was studied. The quality and quantity of phytochemicals were investigated using methanol extracts of hypocotyl seedlings *in vivo* and *in vitro.* Callus cultures were analyzed using high performance liquid chromatography (HPLC). Callus was initiated on dissected hypocotyls explants using Murashige and Skoog (1962) (MS) medium supplemented with Benzyl adenine (BA) at 1.5 mg/l with 0.5 2,4-Dichlorophenoxy acetic acid (2,4-D). The same combination was used for callus maintenance. Results showed an increase in alkaloids and steroidal sapinogen glycosides in methanol extracts of callus cultures. Results also showed that above concentrations caused a reduction in callus fresh weight and a significant increase in the contents of alkaloids and steroidal sapinogen glycosides derived from callus. The best concentration of jasmonic acid stimulated the production was 4 mg/l for alkaloids reached 0.2526, 0.1515, 0.8199, 0.5138 and 0.2961 mg/g for Scopaletine, Choline, Trigonelline, Carpaine and Gentianine respectively, and steroidal sapinogens glycosides reached 0.2218, 1.3529 and 0.6479 mg/g for each Yamogenin, Diosgenin and Tigogenin respectively.

Keywords: Plant tissue cultures, Fenugreek, *Trigonella foenum- graecum* L., Secondary metabolites, Jasmonic a cid,

الخلاصة

أجري البحث لدراسة تأثير إضافة تراكيز مختلفة من حامض الجاسمونك (0، 2، 4، 6 و 8 ملغم/لتر) في إنتاج مركبات الأيض الثانوي في كالس نبات الحلبة *Trigonella foenum- graecum* L. . قدرت مركبات الأيض الثانوي بالتحليل الكمي والنوعي بإستعمال جهاز High Performance Liquid Chromatography (HPLC) لعينات المستخلص الميثانولي للسويقة الجنينية السفلى المفصولة من البادرات النامية تحت ظروف الحقل والبادرات النامية خارج الجسم الحي المجففتين . حفز الكالس على النشوء من زراعة السويقة الجنينية السفلى على وسط Murashige و Skoog (1962) (MS) المدعم بإضافة 1.5 ملغم/لتر من Benzyl adenine (BA) و0.5 ملغم/لتر من 2,4-Dichlorophenoxy acetic acid (2,4-D). وقد أستعملت التوليفة نفسها أعلاه لإدامة الكالس المستحث. تميز المستخلص الميثانولي للكالس بارتفاع المحتوى الكلي للقلويدات والكلايكوسيدات الصابونينية الأستيرويدية مقارنة بالمحتوى الكلي للبادرات النامية تحت ظروف الحقل والبادرات النامية خارج الجسم الحي. أدت إضافة حامض الجاسمونك بالتراكيز اعلاه الى حدوث إنخفاض في الوزن الطري للكالس. وأظهرت النتائج وجود فروقات معنوية بين التراكيز المختلفة من حامض الجاسمونك في محتوى الكالس من القلويدات والكلايكوسيدات الصابونينية الأستيرويدية، فقد إرتفعت تراكيز القلويدات عند إضافة 4 ملغم/لتر من حامض الجاسمونك إذ وصلت الى 0.2526، 0.1515، 0.8199، 0.5138 و 0.2961 ملغم/غم وزن كالس جاف لكل من السكوباليتين (Scopaletin), الكولين (Choline)، الترايكونيلين (Trigonelline), الكاربيـــن (Carpaine) و الجنتيانين (Gentianine) على التوالي. ووصلت تراكيز الكلايكوسيدات الصابونينية الأستيرويدية الى 0.2218، 1.3526 و 0.6479 ملغم/غم لكل من الياموجنين (Yamogenin)، الدايوسجنين (Diosagenin) و التايجوجنين (Tigogenin) على التوالي.

الكلمات المفتاحية: زراعة الأنسجة النباتية، نبات الحلبة، *Trigonella foenum- graecum* L.، مركبات الأيض الثانوي، حامض الجاسمونك، HPLC

المقدمة

تعد النباتات مصدراً مهماً للمواد الغذائية ومجهزاً لعدد كبير من المواد الكيميائية التي تشتمل المواد الصيدلانية، المبيدات الحشرية، المطعمات، العطور والألوان. وعلى الرغم من التقدم في طرائق الأنتاج، لاتزال مصدراً لمركبات معقدة جداً اوباهظة الثمن عند انتاجها بالطرائق الأخرى [1]. وفرت التطبيقات المختلفة لزراعة الأنسجة إمكانية الحصول على مركبات مهمة أقتصادياً و من ضمنها المركبات الدوائية التي يصعب تحضيرها مختبرياً فضلاً عن كلفتها العالية عند تصنيعها [2]. وهناك الكثير من الفوائد التي تقترنُ بإنتاج هذه المركبات بهذه الطريقة إذا ماقورنت باستخلاصها من النبات الكامل. يمكن الحصول على هذه المركبات بدرجة نقاوة عالية من المزارع النسيجية تفوق تلك المستخلصة من النبات الكامل، وإنتاجها يكونُ سريع وغير معتمد على الموسم ولاحاجة لمساحات اراضي واسعة [3]. الحلبة *Trigonella foenum- graecum* L. نبات عشبي حولي يعود الى العائلة البقولية (Fabaceae = Leguminosae). ويتراوح ارتفاع النبات عند النضج 20-60 سم، ويمتاز بسيقان جوفاء، واوراق ريشية مركبة ثلاثية الوريقات، أزهاره بيضاء مائلة الى الاصفرار و ثمارها من نوع البقلة [4]. تعد الحلبة أحد النباتات المهمة والشائعة الأستعمال منذ القدم وتستعمل اليوم على نطاق واسع في معظم دول العالم بوصفها غذاءً ودواءً، وكونها مصدراً غنياً بمجموعة من المكونات الغذائية مثل البروتينات، الدهون، الكربوهيدرات، المعادن، الفيتامينات وغيرها من المكونات. كما تحتوي بذورها على العديد من المركبات الصيدلانية، منها مجموعة من الكلايكوسيدات المتنوعة التي يعد الدايوسجنين أهمها لكونهِ يدخلُ في تحضير هرمونات صناعية مختلفة وقلويدي الترايكونيلين والكولين، ومواد هلامية تزيد نسبتها عن 25% من وزن البذور الجافة [5 و6]. للحلبةِ أستعمالات طبية عديدة منها زيادة أدرار الحليب بعد الولادة عن طريق تنشيط الغدد اللبنية، خفض نسبة السكر والكوليسترول في الدم وتثبيط نمو الخلايا السرطانية، وتستعمل مادة الدايوسجنين الموجودة في الحلبة بوصفها مادة خام في تحضير الهرمونات الجنسية صناعياً التي تدخلُ في عمل المواد الطبية المستعملة في تحضير مادة الكورتيزون ومشتقاتها المختلفة التي تُفيد في علاج الأمراض الصدرية والروماتزمية [7 و 8]. وبناءاً على ماسبق من أهمية النبات طبياً واحتوائه على مركبات ثانوية مهمة تدخل في الصناعات الصيدلانية ولكن إنتاجها قليل مقارنة بالحاجة الفعلية لهذه المركبات. فقد أجريت هذه الدراسة التي تهدف الى حث إنسجة النبات على زيادة إنتاج مركبات الأيض الثانوي وذلك عن طريق تجهيز الوسط الحاوي على الكالس بتراكيز مختلفة من حامض الجاسمونك. والكشف كماً ونوعاً عن المركبات المنتجة عن طريق التحليل الكروماتوغرافي بإستعمال جهاز HPLC لمستخلصات السويقة الجنينية السفلى المفصولة من البادرات النامية تحت ظروف الحقل والبادرات النامية خارج الجسم الحي والكالس المجفف.

المواد وطرائق العمل

تم الحصول على بذور نبات الحلبة من محلات العطارة في بغداد. عقمت البذور بهايبوكلورات الصوديوم تركيز 3% لمدة 10دقائق ثم غسلت البذور بالماء المقطر المعقم ثلاث مرات متتالية و زرعت على وسط Murashige و Skoog [9] (MS) بنصف قوة الأملاح. حضنت الزروعات على درجة حرارة 25±1°م وإضاءة 1000 لوكس مدة 16ساعة يومياً. بعد 10 أيام من إنبات البذور، أختبرت أجزاء نباتية مختلفة (اجزاء الأوراق، السويقة الجنينية العليا و السويقة الجنينية السفلى) وعلى توليفات مختلفة من منظمات النمو النباتية وباستعمال وسط MS. ولم تستجب اجزاء الأوراق والسويقة الجنينية العليا ولذا استبعدت من التجارب. وقد أستجابة الأجزاء المفصولة من السويقة الجنينية السفلى على وسط MS المجهز بالتوليفة 0.5 ملغم/لتر من 2,4-D و 1.5 ملغم/لتر من BA فقط، لذا أعتمدت هذه التوليفة في هذه التجارب. حضنت الزروعات تحت الظروف المشار لها في زراعة البذور ولمدة ثلاثة أسابيع. وقد إستعملت التوليفة نفسها أعلاه لإدامة الكالس المستحث لحين الحصول على كمية كافية من الكالس. بعد الحصول على

الكمية المطلوبة من الكالس أخذ 250 ملغم من الكالس ووزرع في وسط إدامة الكالس مضافاً أليه حامض الجاسمونك بالتراكيز 0، 2، 4، 6 و 8 ملغم/لتر. حضنت الزروعات تحت نفس الظروف اعلاه وبعشرة مكررات لكل تركيز. حسب الوزن الطري للكالس بعد ثلاثة أسابيع من الزراعة.

ولغرض إستخلاص القلويدات تم أتباع طريقة Zaho وآخرون[10] وزن 10 ملغم من العينات (السويقة الجنينية السفلى النامية تحت ظروف الحقل والبادرات النامية خارج الجسم الحي والكالس الجاف) واضيف لكل عينة 10 مل من الميثانول النقي 95% نوع HPLC grade (لايحتوي على مواد ممتصة من قبلUV و`ذات درجة عالية من النقاوة). حرك النموذج بوساطة جهاز الأمواج فوق الصوتية لمدة 10 دقائق. ركز المذيب الحاوي على المواد الفعالة بوساطة تيار من النيتروجين (N2) للوصول بالحجم إلى 0.5 مل (زيادة تركيز المذيب بطريقة التبخير). تمت زيادة حجم المذيب بإضافة كمية من محتوى الطور المتحرك 0.01M phosphate buffer pH8.2 : acetonitrile (60:40 v\v) للوصول بالحجم الى 1 مل. رشح الحجم الأخير بأستعمال ورق ترشيح قياس 0.25 مايكروميتر. حقن 20 مايكروليتر في جهاز HPLC تحت ظروف الفصل المثلى. أما بالنسبة لأستخلاص الكلايكوسيدات الصابونينية الأستيرويدية فقد أجريت وفق طريقة Yang وآخرون [11] وتمت تحت نفس الظروف المشار لها في أستخلاص القلويدات، عدا أن زيادة حجم المذيب تمت بإضافة كمية من محتوى الطور المتحرك acetonitrile: Water 8:92 v\v للوصول بالحجم الى 1 مل.

استعمل جهاز كروموتوغرافيا السائل ذو الأداء العالي HPLC نوع Spectrophysic\UV-Visible detector في تقدير كمية ونوعية النواتج الثانوية في مستخلصات الكالس. قدرت القلويدات بحقن العينة في عمود نوع Reversed phase chiral column ذي ابعاد 4.6mm I.D× 50 وحجم الدقائق 3µm ودرجة حرارة 30°م. و قدرت النواتج الثانوية لمستخلص العينات بحقن 25 مايكروليتر في العمود وتحت الظروف الأتية:

- الطور المتحرك :0.01M Phosphate buffer pH8.2 : Acetonitrile (60:40 v\v).
- سرعة الجريان: 0.9 مل \دقيقة.
- الطول الموجي : 220 نانوميتر Zaho وآخرون[10].

قدرت الكلايكوسيدات الصابونينية الأستيرويدية بحقن العينة في عمود نوع Lichrospher C18 ذي ابعاد 4.6×50 mm I.D وبنفس حجم الدقائق ودرجةالحرارة المستخدمة في القلويدات.

قدرت النواتج الثانوية لمستخلص العينات بحقن 25 مايكروليتر في العمود وتحت الظروف الأتية :

- الطور المتحرك: Acetonitrile: Water 8:92 v\v.
- سرعة الجريان: 1.2 مل/دقيقة.
- الطول الموجي: 203 نانوميتر Yang وآخرون [11].

سجلت القراءات على الأطوال الموجية وحسب زمن الاحتجاز Retention Time (RT) للمحاليل القياسية والعينات المدروسة. قدرت تراكيز المواد الفعالة كمياً بمقارنة مساحة حزمة المادة القياسية مع مساحة حزمة النموذج تحت نفس الظروف أعتمادا على القانون التالي : تركيز المادة المجهولة = مساحة حزمة النموذج/ مساحة حزمة القياسي × تركيز القياسي ×عدد مرات التخفيف. اخضعت جميع البيانات الى التحليل الأحصائي كتجارب عاملية باستعمال التصميم العشوائي الكامل (CRD)، وتم حساب قيمة اقل فرق معنوي على مستوى احتمال0.05 [12].

النتائج والمناقشة

مزارع الكالس

أظهرت النتائج تكوين كالس هش ذي لون أخضر من قطع السويقة الجنينية السفلى المفصولة من بادرات الحلبة المعقمة في وسط MS المدعم بإضافة 1.5 و 0.5 ملغم/لترمن BAو 2,4-D على التوالي بعد ثلاثة أسابيع من الزراعة. بينما لم تستجب اجزاء الأوراق والسويقة الجنينية العليا لأستحثاث الكالس. قد يعود ذلك الى كون خلاياها متمايزة وبطيئة الأنقسام وأحتياجها لمدة زمنية أطول لكي تنقسم وتنمو [13].

تأثير حامض الجاسمونك في الوزن الطري للكالس

يلاحظ من الجدول 1 أن أضافة تراكيز مختلفة من حامض الجاسمونك أدى إلى تناقص معنوي في الوزن الطري للكالس وصلت أدنى قيمه (112 ملغم) عند تجهيز الوسط بـ 8 ملغم/لترمن حامض الجاسمونك. قد تؤدي إضافة حامض الجاسمونك للوسط الزرعي الى تثبيط نمو خلايا الكالس كما حصل في نبات*Eleutherococcus senticosus* [14]. كذلك ذكر القدسي [15] ان الوزن الطري للكالس المستحث من نبات عنب الذيب *Solanum nigrum* يقل كلما زاد تركيز حامض الجاسمونك وذكر بأن أقل وزن طري للكالس حصل عند التركيز 8 ملغم/لتر من حامض الجاسمونك وهذا يتفق مع النتائج الحالية.

جدول-1: تأثير تراكيز حامض الجاسمونك المضاف الى الوسط الغذائي في الوزن الطري للكالس بعد ثلاثة اسابيع من الزراعة، n=10.

تركيز حامض الجاسمونك (ملغم/لتر)	وزن الكالس (ملغم)
0	250
2	230
4	150
6	135
8	112
أ. ف.م $P\leq0.05$	*34.09

التقدير الكمي والنوعي للقلويدات في مستخلصات السويقة الجنينية السفلى المفصولة من البادرات النامية تحت ظروف الحقل والبادرات النامية خارج الجسم الحي المجففتين و الكالس الجاف

عند حساب تراكيز القلويدات وكما مبين في الجدولين 2 و3 وجد هنالك فروقاً معنوية ($P\leq0.05$) بين تراكيز المركب الواحد وبأختلاف الأجزاء النباتية. حقق قلويد Scopaletin اعلى تركيز له في البادرات النامية خارج الجسم الحي وبلغ 0.0916 ملغم/غم وزن جاف يليه في البادرات النامية تحت ظروف الحقل وبلغ 0.0776 ملغم/غم وأقل تركيز له كان في الكالس وبلغ 39 0.0 ملغم/غم. قلويد Choline سجل أعلى تركيز له في البادرات النامية تحت ظروف الحقل وبلغ 0.0853 ملغم/غم يليه في البادرات النامية خارج الجسم الحي وبلغ 0.0413 ملغم/غم واقل تركيز له كان في الكالس وبلغ 0.0400 ملغم/غم. قلويد Trigonelline سجل أعلى تركيز له في الكالس وبلغ 0.4832 ملغم/غم يليه في البادرات النامية خارج الجسم الحي وبلغ 0.0913 ملغم/غم واقل تركيز له كان في البادرات النامية تحت ظروف الحقل وبلغ 0.0860 ملغم/غم.اما قلويدي Carpaine و Gentianine فقد سجلا أعلى تركيز لهما في الكالس وبلغا 0.288 و 0.1082 ملغم/غم على التوالي ثم في البادرات النامية في ظروف الحقل وبلغا 0.1478 و 0.0876 ملغم/غم على التوالي وأقل تركيز لهما كان في البادرات النامية خارج الجسم الحي وبلغا 0.1435 و 0.0468 ملغم/غم على التوالي. يتبين من النتائج أعلاه أن الكالس حقق أعلى زيادة في المحتوى الكلي للقلويدات وبلغ 0.1916 ملغم/غم يليه البادرات

النامية تحت ظروف الحقل وبلغ 0.0977 ملغم/غم وأقل محتوى للقلويدات سجل عند البادرات النامية خارج الجسم الحي وبلغ 0.0829 ملغم/غم. لذلك يختلف محتوى الأجزاء الثلاث حسب نوع المركبات وحسب الجزء النباتي المفصولة منه. أن الأختلاف في تراكيز المركبات قد يرجع الى عوامل بيئية (الضوء، الرطوبة، نوع الجزء النباتي، مرحلة نمو النبات والعوامل الوراثية) [16]، بالأضافة الى عوامل اخرى مثل مكان تواجد النبات وحالة النبات الفسلجية قبل الأستخلاص [17]. ويمكن أيعاز سبب زيادة المركبات في الكالس إلى ان منظمات النمو المضافة الى وسطي إستحثاث وإدامة الكالس أدت الى تحفيز وزيادة إنتاج المركبات الثانوية في الكالس ويمكن أيضاً ان يكون اعادة الزراعة (Sub Culture) المستمر أدى الى نشوء تغاير جسماني (Somaclonal Variation) في الخلايا مما أدى الى زيادة إنتاجها للمركبات الثانوية في الكالس [18]. تتفق هذه النتائج مع ماذكره Radwan و Kokate [19] اللذان وجدا إن أضافة حامض النيكوتنك الى الوسط الغذائي قد أثر معنوياً في زيادة إنتاج Trigonelline.

جدول -2: زمن الأحتجاز، المساحة، تراكيز القلويدات القياسية المدروسة بإستعمال جهاز HPLC

ت	القلويدات المدروسة	زمن الأحتجاز (دقيقة)	مساحة القلويدات القياسية	تركيز المحلول (مايكروغرام/مل)
1	Scopletin	1.38	12962	25
2	Choline	2.36	9979	25
3	Trigonelline	3.55	16998	25
4	Carpaine	4.20	11020	25
5	Gentianine	5.00	13975	25

جدول -3: القلويدات (ملغم/غم) في مستخلصات السويقة الجنينية السفلى المفصولة من البادرات النامية تحت ظروف الحقل والبادرات النامية خارج الجسم الحي المجففتين والكالس الجاف بأستعمال جهاز HPLC، n=3.

ت	القلويدات	النامية تحت ظروف الحقل	البادرات النامية خارج الجسم الحي	الكالس	أ.ف.م P≤0.05
1	Scopletin	0.0776	0.0916	0.039	*0.0144
2	Choline	0.0853	0.0413	0.0400	*0.0216
3	Trigonelline	0.0860	0.0913	0.4832	*0.0339
4	Carpaine	0.1478	0.1435	0.288	*0.091
5	Gentianine	0.0876	0.0468	0.1082	*0.0381
متوسط تراكيز القلويدات		0.0977	0.0829	0.1916	-----

التقدير الكمي والنوعي للكلايكوسيدات الصابونينية الأستيرويدية في مستخلصات السويقة الجنينية السفلى المفصولة من البادرات النامية تحت ظروف الحقل والبادرات النامية خارج الجسم الحي المجففتين والكالس الجاف بأستعمال جهاز HPLC

عند حساب تراكيز الكلايكوسيدات و كما مبين في الجدولين 4 و 5 وجد هنالك فروقاً معنوية (P≤0.05) بين تراكيز المركب الواحد باختلاف الأجزاء النباتية. حقق كلايكوسيدYamogenin أعلى تركيز له في البادرات النامية خارج الجسم الحي وبلغ 0.2396 ملغم/غم وزن جاف يليه في البادرات النامية تحت ظروف الحقل وبلغ 0.1035 ملغم/غم وأقل تركيز لهذا المركب كان في الكالس وبلغ 0.0451 ملغم/غم. حقق Diosagenin و Tigogenin أعلى تركيز لهما في الكالس وبلغا 1.009 و 0.4179 ملغم/غم على التوالي يليه في البادرات النامية خارج الجسم الحي وبلغا 0.2184 و 0.3842 ملغم/غم على التوالي وأقل

تركيز لهما كان في البادرات النامية تحت ظروف الحقل وبلغا 0.1037 و0.092 ملغم/غم على التوالي. يتبين من النتائج أعلاه أن الكالس حقق أعلى زيادة في المحتوى الكلي للكلايكوسيدات بلغ 0.4906 ملغم/غم يليه في البادرات النامية خارج الجسم الحي بلغ 0.2807 ملغم/غم وأقل محتوى كلي للكلايكوسيدات كان في البادرات النامية تحت ظروف الحقل وبلغ 0.0997 ملغم/غم. تتفق هذه النتائج مع ماذكره Oncina وآخرون [20] و Rezaeian, [21] اللذان أكدو بان منظمات النمو المضافة الى الوسط الغذائي لها دور كبير في تنظيم عمليات بناء وتراكم مركب Diosgenin في كالس نبات الحلبة. ويفسر هذا التأثير دور هذه المنظمات في تحفيز نمو الكالس مما يترتب عليه زيادة البناء الحيوي لهذا المركب، خاصة وأن خلاياها من النوع البرنكيمي وإحدى وظائفها هي الخزن. إما بالنسبة للمركب Triqocoumarine فقد أختفى تركيزه من منحنيات تحليل كلايكوسيدات المستخلصات (السويقة النامية تحت ظروف الحقل، البادرات النامية خارج الجسم الحي والكالس) قد يعزى سبب ذلك الى نوع الجزء النباتي الداخل في التحليل، في الوقت الذي تمكن Parmar وآخرون [22] من عزل هذا المركب من مستخلص النبات الكامل.

جدول -4: زمن الأحتجاز، المساحة و تراكيز الكلايكوسيدات الصابونينية الأستيرويدية القياسية المدروسة بأستعمال جهاز HPLC.

ت	الكلايكوسيدات الصابونينية الأستيرويدية المدروسة	زمن الأحتجاز (دقيقة)	مساحة الكلايكوسيدات الصابونينية الأستيرويدية القياسية	تركيز المحلول (مايكروغرام/مل)
1	Yamogenin	1.09	29931	25
2	Diosgenin	2.27	30885	25
3	Triqocoumarin	2.91	17796	25
4	Tigogenin	3.92	27745	25

جدول -5: الكلايكوسيدات الصابونينية الأستيرويدية (ملغم/غم) في مستخلصات السويقة الجنينية السفلى المفصولة من البادرات النامية تحت ظروف الحقل والبادرات النامية خارج الجسم الحي المجففتين والكالس الجاف بأستعمال تقنية HPLC، n=3

ت	الكلايكوسيدات الصابونينية الأستيرويدية	النامية تحت ظروف الحقل	البادرات النامية خارج الجسم الحي	الكالس	أ.ف.م P≤0.05
1	Yamogenin	0.1035	0.2396	0.0451	*0.108
2	Diosgenin	0.1037	0.2184	1.009	*0.241
3	Tigogenin	0.092	0.3842	0.4179	*0.152
	متوسط تراكيز الكلايكوسيدات	0.0997	0.2807	0.4906	----

تأثير تراكيز حامض الجاسمونك في إنتاج القلويدات من الكالس والتقدير الكمي والنوعي لهذه المركبات بأستعمال جهاز HPLC

توضح نتائج جدول 6 حصول أختلافات في تراكيز القلويدات أعتماداً على تراكيز حامض الجاسمونك المضافة الى وسط الإدامة، إذ حصلت فروقات معنوية بين تراكيز المركب الواحد مقارنة مع السيطرة. إرتفعت تراكيز المركبات عند إضافة 4 ملغم/لتر من حامض الجاسمونك إذ وصلت الى 0.2526، 0.1515، 0.8199، 0.5138 و 0.2961 ملغم/غم وزن كالس جاف لكل من المركبات Scopletin، Choline, Trigonellin، Carpaine و Gentianine على التوالي. وإنخفضت أغلب تراكيز المركبات عند إضافة 8 ملغم/لتر من الحامض مسجلة 0.2126، 0.1370، 0.6329، 0.3557 و 0.2015 ملغم/غم لكل من المركبات Scopletin، Choline, Trigonellin، Carpaine و Gentianine على التوالي مقارنة بمعاملة 4 ملغم/لتر من حامض الجاسمونك. تبين النتائج إن زيادة تراكيز حامض

الجاسمونك لم تؤدي ألى نقصان تراكيز القلويدات مقارنة بمعاملة السيطرة. ويلاحظ بإن أفضل تركيز لحامض الجاسمونك والذي أدى ألى زيادة تحفيز وإنتاج القلويدات في كالس النبات كان عند التركيز 4 ملغم/لتر تحت ظروف التجربة الحالية. وقد وجد القدسي [15] إن أضافة تراكيز مختلفة من حامض الجاسمونك الى كالس نبات عنب الذيب *Solanum nigrum* أدى إلى زيادة معنوية في تراكم القلويدات وكان أفضل تركيز 6 ملغم/لتر مقارنة بالسيطرة. كما أكد Sharma وآخرون [23] إن حامض الجاسمونك يعمل على تفعيل البناء الحيوي لمواد الأيض الثانوي، لذلك فإن أستعماله كمحفز يعد مفضلاً في زيادة إنتاج المركبات الفعالة صيدلانياً في وقتٍ قصير وبتكلفة أقل. كذلك ذكر Mizukami وآخرون [24] أن حامض الجاسمونك يشارك في مسار نقل الأشارة Signal Transduction Pathway الذي يحفزالأنزيمات اللازمة للتحولات البايوكيميائية الخاصة لبناء مركبات الأيض الثانوي.

جدول-5: تأثير تراكيز مختلفة من حامض الجاسمونك في إنتاج الكلايكوسيدات الصابونينية الأستيرويدية المضافة الى وسط إدامة الكالس المستحث من السويقة الجنينية السفلى وبعد ثلاثة أسابيع من الزراعة، n=3.

تركيز حامض الجاسمونك (ملغم/لتر)	الكلايكوسيدات الصابونينية الأستيرويدية (ملغم/غم)		
	Yamogenin	Diosgenin	Tigogenin
السيطرة	0.0451	1.0090	0.4179
2	0.0963	1.1942	0.4108
4	0.2218	1.3526	0.6479
6	0.1509	0.6848	0.5770
8	0.1367	0.5966	0.3700
أ.ف.م $P\leq0.05$	*0.052	*0.083	*0.092

جدول-6: تأثير تراكيز مختلفة من حامض الجاسمونك في إنتاج القلويدات المضافة الى وسط إدامة الكالس المستحث من السويقة الجنينية السفلى وبعد ثلاثة أسابيع من الزراعة، n=3

تركيز حامض الجاسمونك (ملغم/لتر)	القلويدات (ملغم/غم)			
	Scopletin	Choline	Trigonelline	Carpaine	Gentianine
السيطرة	0.039	0.040	0.4832	0.288	0.1082
2	0.101	0.0842	0.5586	0.3001	0.1868
4	0.2526	0.1515	0.8199	0.5138	0.2961
6	0.1220	0.1131	0.6560	0.3682	0.2015
8	0.2124	0.1370	0.6329	0.3557	0.2015
أ. ف. م $P\leq0.05$	*0.076	*0.063	*0.144	*0.127	*0.114

تأثير تراكيز حامض الجاسمونك في إنتاج الكلايكوسيدات الصابونينية الأستيرويدية من الكالس والتقدير الكمي والنوعي لهذه المركبات بأستعمال جهاز HPLC

توضح نتائج جدول 7 حصول أختلافات في تراكيز الكلايكوسيدات الصابونينية الأستيرويدية أعتماداً على تراكيز حامض الجاسمونك المضافة الى وسط الإدامة، إذ حصلت فروقات معنوية بين تراكيز المركب الواحد مقارنة مع السيطرة. إرتفعت تراكيز المركبات عند إضافة 4 ملغم/لتر من حامض الجاسمونك إذ وصلت الى 0.2218، 1.3526 و 0.6479 ملغم/غم وزن كالس جاف لكل من Yamogenin، Diosagenin و Tigogenin على التوالي. وإنخفض تركيز المركب Diosgenin عند إضافة 6 ملغم/لتر من حامض الجاسمونك، بلغ 0.6848 ملغم/غم مقارنة بمعاملة السيطرة، كذلك إنخفض تركيزي المركبين Diosgenin و Tigogenin عند إضافة 8 ملغم/لتر من حامض الجاسمونك وبلغتا 0.5966 و 0.3700

ملغم/غم على التوالي، مقارنة بالسيطرة. يلاحظ إن أفضل تركيز لحامض الجاسمونك ساهم في تحفيز وإنتاج الكلايكوسيدات كان 4 ملغم/لتر. كما أكد Debjani و Bratati [25] أن التحفيز بتراكيزمختلفة من حامض الجاسمونك في المزارع النسيجية أدى الى زيادة معنوية في أنتاج الدايوسجنين عند المعاملة بـ 100مايكروليترمن الحامض مقارنة بمعاملة السيطرة.

يستنتج من البحث أن الكالس الجاف حقق أعلى زيادة في أنتاج مركبات الأيض الثانوي (القلويدات والكلايكوسيدات الصابونينية الأستيرويدية) مقارنة بأنتاج المركبات في السويقة الجنينية السفلى المفصولة من البادرات النامية تحت ظروف الحقل والبادرات النامية خارج الجسم الحي المجففتين. أن إضافة حامض الجاسمونك بتركيز 4 ملغم/لتر الى وسط أدامة الكالس أدى الى أنخفاض وزن الكالس، ولكن أدى الى أفضل زيادة لتراكيز مركبات الأيض الثانوي (القلويدات والكلايكوسيدات الصابونينية الأستيرويدية).

المصادر

1. Taiz L. and Zeiger E. Plant Physiology, (3rd Ed.). Sinauer Associates, Inc. PP: 283-308, (2002).
2. Purohit S.S. Agriculture Biotechnology. Published by Updesh Purohit for Agrobios (India), P.833, (1999).
3. Discosmo F. and Misawa M. Plant cell and tissue culture : Alternatives for metabolite production. Biotechnology Advances, 13(3):425-453, (1995).
4. Peteropoulos G.A. Fenugreek-the genus *Trigonella*. PP: 1-127.1st Ed. Taylor and Francis group, London and New york. (2002).
5. Newall C. A.; AndersonL. A. and Phillipson J. D. Herbal Medicines: A Guide for Health- Care Professionals (2nd Ed.). London: The Pharmaceutical Press, PP: 117-118, (1998).
6. Bralles J.; Anderson L. A. and Phillipson J. D. Herbal Medicines (2nd Ed.). Pharmaceutical Press, Publication division of the Royal Pharmaceutical Society of Great Britain, PP: 209-211, (2002).
7. Devasena T. and Menon V.P. Fenugreek affects the activity of β-Glucuronidase and mucinase in the colon, Phytother. Res. 9: 1088-1091, (2003).
8. Suboh S.M.; BiltoY. Y. and Aburjiai T. A. Protective effects of selected medicinal plants against protein degradation, lipid peroxidation and deformability of oxidatively stressed human erthocytes. Phytother, Res. 18 (4): 280-284, (2004).
9. Murashige T. and Skoog F. A revised medium for rapid growth and bioassays with tobacco tissue culture. Physiol. Plant, 15:473-497, (1962).

10. Zaho H.; Wang Y.; Zhang H.; Li F. and Hattar M. Determination of trigonelline in *Trigonella foenum- grarcum* L. by HPLC. Yao Xue Xue Bao. 27 (3):194-196, (2003).
11. Yang D. J.; Lu T. J. and Hwang L.S. Stimultaneous determination of furostanol and spirostanol glycosides in Taiwanese yam (*Dioscorea* spp) cultivars by high performance liquid chromatography. J. of food and drug analysis, 11(4):271-276, (2003).
12. SAS. SAS / STAT Users Guide for Personal Computers. Release 7.0. SAS Institute Inc., Cary, NC., USA, (2004).
13. Salih S. M. and Al- Mallah M. K. Plant regeneration from *in vitro* leaf and stem tissue of *Solanum nigrum*. Dirasat Agric. Sci., 27 (1): 64-71, (2000).
14. Abdullah M. S.; Hosakatte N.M.; Eun-Joo H. and Kee-Yoeup P. Methyl jasmonate induced overproduction of eleutherosides in somatic embryos of *Eleutherococcus senticosas* cultured in bioreactors, The Plant Biotechnology J., 10 (4): 13-23. (2007).
15. القدسي عادل سلطان سلمان. إنتاج بعض المركبات الثانوية من نبات عنب الذيب *Solanum nigrum* في المزارع النسيجية، إطروحة دكتوارة، كلية الزراعة، قسم البساتين، جامعة القاهرة، جمهورية مصر العربية، (2009).
16. Briskin D. and Gawienowski M. HPLC profiling of the invasive plant species *Hypericum canariense* to assess rapid evolutionary changes in defensive chemistry. Plant Physiology Biochemist., 39: 1078-1081. (2001).
17. Kirakosyan A.; Gibson M. D. and Sirvent T. A comparative study of *Hypericum perforatum* plants as a source of hypericins and hyperforins. J. of Herbs, Spices and Medicinal Plants, 10(4): 73-89. (2003).
18. Mohy A.; Khan Z.; Ahmad M.; Kashmiri M. A.; Yasmin S. and Mazhar H.. Chemotaxonomic significance of flavonoids in *Solanum nigrum* complex. Plant Sci., 108:216-222. (2009).
19. Radwan S.S. and Kokate C.K. Production of higher levels of trigonelline by cell cultures of *Trigonella foenum-graecum* than by the differentiated plant. Biomedic. and Life Sci. J., 147 (4): 340-344. (1979) (Abstract).

20. Oncina R.; Botía J.M.; Río D. and Ortuño A.. Bioproduction of diosgenin in callus of *Trigonella foenum graecum*. Food Chem., 70 (4): 489-492. (2000) (Abstract).
21. Rezaeian S. Assessment of diosgenin production by *Trigonella foenum-graecum* L. *In vitro* condition, Amer. J. of Plant Physio., 6: 261-268. (2011).
22. Parmar V.S.; Jha H.N.; Sanduja S.K. and Sanduja R. Triqocoumarine- a New Coumarin from *Trigonella foenum-graecum* .Z. Naturforsch, 37B. 521, (1982).
23. Sharma M.; Sharma A.; Kumar A. and Basu S. K. Enhasment of secondary metabolites in cultured plant cells through stress stimulus. Am. J. Plant Physiol., 6 (2): 50-71, (2011).
24. Mizukami H.; Tabira Y. and Ellis B. E. Metyl jasmonate induced rosmarinic acid biosynthsis in *Lithospermum enthrorhizon* cell suspention cultures. Plant. Cell. Rep. 12: 706-709, (1993).
25. Debjani D. and Bratati D. Elicitation of diosagenin production in *Trigonella foenum- graecum* L. Seedlings by heavy metals and signaling molecules. Acta Physiologia Plantarum, 33(5): 1585-1590, (2011).

استخدام درنات الالمازة *Helianthus tuberosus* في تحضير اوساط زرعية جديده لتنمية البكتريا

سوسن حسن عثمان و ناصر عبد الحسين الهنداوي و ايمان ناطق ناجي
كلية العلوم / الجامعة المستنصرية / قسم علوم الحياة

تاريخ تقديم البحث 2011/11/14 - تاريخ قبول البحث 2012/6/20

ABSTRACT

Helianthus tuberosus was used in preparation of a new natural medium in comparsion with culture media which used in isolation and identification of microorganisms. The first new media (HT_1) prepared using helianthus extract fortified with glucose and sodium chloride. While the second medium prepared the same extract fortified with lactose, bile salts and neutral red stain. Both HT_1 and HT_2 were used in liquid and solid state by adding agar. The efficacy of TH1 in growth of some gram negative and positive pathogenic bacteria are not significant ($P > 0.05$) in comparsion with the other culture media . Also the identification and the growth of HT_2 efficacy by discrimination of lactose fermented and non-fermented bacteria in addition to inhibition the growth of *Staphylococcus aureus* in comparison with other culture media are not significant ($P > 0.05$). The results provide a synthesis a great enrichment inexpensive medium for different bacterial species especially helianthus enriched with a nourishment materials and mineral salts that suitable for organism without any change in the morphology or metabolisms feature.

Keywords: *Helianthus tuberosus,* culture media, bacterial growth

الخلاصة

استخدمت درنات نبات الألمازة *Helianthus tuberosus* في تحضير اوساط زرعية طبيعية لأول مرة كبدائل محلية عن الاوساط الزرعية المستوردة والمعروفة لتنمية وتشخيص الاحياء المجهرية . حضر الوسط الاول وسمي (HT1) نسبة الى الاسم العلمي للنبات ، اذ استخدم راشح الدرنات مع اضافة سكر الكلوكوز وكلوريد الصوديوم . فيما حضر الوسط الثاني (HT2) من اضافة سكر اللاكتوز واملاح الصفراء الى راشح النبات . استخدم الوسط بصورة سائلة وبصورة صلبة بأضافة الاكار ، قدرت كفاءة الاوساط المحضرة من خلال المقارنة مع الاوساط المستوردة . اظهرت النتائج كفاءة الوسط (HT1) في تنمية انواع مختلفة من البكتريا الموجبة والسالبة لصبغة كرام من خلال عدم ظهور فروق معنوية ($P>0.05$) بين الاوساط المحضرة والاوساط المستوردة . كذالك اظهر الوسط (HT2) كفاءة تشخيصية وتنموية في التمييز بين البكتريا المخمرة وغير المخمرة لسكر اللاكتوز ، فضلا عن منعها لنمو بكتريا *Staphylococcus aureus* ومقارنة بوسط MacConkey agar المستورد ، اذ لم تظهر فروق معنوية في كفاءة الوسطين ($P>0.05$) .

لقد عززت النتائج الهدف من الدراسة والمتمثل بتحضير اوساط زرعية اغنائية وتشخيصية لتنمية الانواع المختلفة من البكتريا ، ولاسيما ان درنات الألمازة غنية بالمواد المغذية التي عززت من نمو هذة الاحياء المجهرية بشكل كبير مع عدم تغيير في مظهر المستعمرات او خواصها الايضية .

مفتاح الكلمات: نمو البكتريا،الاوساط الزرعيه، *Helianthus tuberosus*.

المقدمة

يعد Theodor Escherichia اول من وصف بكتريا *Escherichia coli* عام 1885 كبكتريا قولون متعايشة (Bacterium coli commune) والتي عزلت من براز الاطفال حديثي الولادة [1] . تعود هذه البكتريا الى العائلة المعوية Enterobacteriaceae [2]، وتسبب السلالات المرضية منها التهابات حادة بالمعدة والامعاء والقناة البولية ، اذ وجد [3] Muvey ان نسبة اصابات القناة البولية ببكتريا *E.coli* بلغت 80% ، تبعتها بكتريا *klebsiella* بنسبة اقل . كذلك عزل الباحث انواعا من بكتريا *Proteus spp.* , *Enterobacter spp.* من

العينات المصابة . فيما عزلت برهان [4] بكتريا *E.coli* من االمصابين بالتهاب الزائدة الدودية بنسبة 65.7% يليها كل من *Proteus mirabilis* و *Klebsilla spp.* بنسبة (7.8 و 2.6%) وعلى التوالي . كما اكدت الحسيني [5] امكانية الاصابة بسرطان القولون والكلي عند الاصابة ببكتريا E.coli وذلك من خلال حقن سلالة مرضية من بكتريا E.coli في الفئران . تمكن الحسابي [6] من عزل (13) عزلة من بكتريا *E.coli* من ادرار المصابين بالتهاب غدة البروستات ، فيما وجدت علي [7] ان نسبة عزل بكتريا *E.coli* من المصابين بالتهاب الاذن الوسطى بلغت 4.8% يليها كل من Proteus (9.6%) ثم *klebsiella* (6.02%). قام الباحثون بتحضير انواع مختلفة من الاوساط الزرعية لتنمية وعزل الاحياء المجهرية بشكل عام والمرضية منها بشكل خاص ولا سيما ان الكائن المجهري عند نموه خارج الجسم الحي فانه يعتمد على المكونات الغذائية المتوفرة في الوسط الزرعي لاسناده بمصادر الطاقة والكربون [8]. ينتمى نبات *Helianthus tuberosus* او ما يعرف بالالمازة للعائلة المركبة (composiatae) وهي نبتة متوفرة محليا تستخدم درناتها كمادة غذائية لاحتواء هذه الدرنات على العديد من المركبات الغذائية المهمة ومنها : البروتينات والكالسيوم والفسفور والبوتاسيوم والصوديوم ، فضلا عن احتوائه على فيتامينات B_2 وniacin [9]. لذا تهدف الدراسة الحالية الى استخدام نبات الالمازة في تحضير اوساط زرعية تنموية واغنائية واخرى تفريقية لغرض تنمية وتمييز البكتريا المعوية وخاصة *E.coli* لاهمية هذه البكتريا على الصعيد الصحي ولتوفير اوساط زرعية محلية ولا سيما ان نبات الالمازة من النباتات المتوفرة محليا وزهيدة الكلفة.

المواد وطرائق العمل

الاوساط الزرعية وكيفية تحضيرها

1- الوسط الجديد (HT.1) السائل (Helianthus tuberosus broth) حضر الوسط بجمع درنات نبات الالمازة *Helianthus tuberosus* من الاسواق المحلية ، غسلت الدرنات بالماء بشكل جيد وتم تقشيرها وتقطيعها الى قطع رقيقة صغيرة . ثم جففت وبدرجة حرارة 60م ولمدة 24-48 ساعة. طحن النبات الجاف ووزن منه مقدار 100 غم من المسحوق واضيف اليه 1 لتر ماء مقطر في دورق زجاجي.
وضع الدورق الزجاجي في حمام مائي بدرجة حرارة 80 م ولمدة 15 دقيقة . بعدها رشح من خلال ورق الترشيح whatman no.1 . اكمل الحجم للراشح الى 1 لتر باستخدام الماء المقطر. اضيف الى 1 لتر من الراشح كلا من كلوريد الصوديوم 5 غم وسكر الكلوكوز 10 غم . وبعد ضبط الرقم الهيدروجيني عند PH:7.2 عقم بالموصدة (autoclave) بدرجة حرارة 121 م وضغط 15 باون / انج^2 ولمدة 15 دقيقة
2- الوسط الجديد (HT_1) الصلب : (Helianthus tuberosus agar) حضر الوسط الصلب باتباع الخطوات الواردة في الفقرة اعلاه (1-1-1) مع اضافة الاكار بنسبة 1.6% وتعريض الوسط للغليان لحين اذابة الاكار ثم ضبط الرقم الهيدروجيني pH:7.2 وتعقيمه كما سبق .
3- الوسط الجديد (HT_2) السائل : حضر راشح نبات *H. tuberosus* وكما في الفقرة السابقة (1-1-1) غير ان الراشح اضيف له المكونات التالية ليصبح الوسط تفريقيا :1 لتر راشح ، سكر اللاكتوز 10 غم ،كلوريد الصوديوم 5 غم ،املاح الصفراء bile salt no.3 5 غم،صبغة neutral red 1% يضاف منه 7 مل. وبعد ضبط الرقم الهيدروجيني عند PH:7.2 عقم الوسط بالموصدة وكما سبق
4- الوسط الجديد (HT_2) الصلب : حضر الوسط الصلب باتباع الخطوات الواردة في الفقرة السابقة (1-1-3) مع اضافة الاكار بنسبة 1.6% وتعريض الوسط للغليان لحين اذابة الاكار ثم ضبط الرقم الهيدروجيني وعقم كما سبق.
5- وسط المرق المغذي (nutrient broth) ووسطNutrient agar: حضر الوسطان وحسب تعليمات الشركة المجهزة Fluka . وعقم بالموصدة

6-وسطي ما كونكي السائل والصلب (MacConkey broth and MacConkey agar) :حضر الوسطين حسب تعليمات الشركة المجهزة Fluka وعقما بجهاز التعقيم (الموصدة) وكما سبق.

المزارع البكتيرية :تم جمع العزلات البكتيرية من المختبرات التعليمية لدائرة مدينة الطب في بغداد ومن طلبة الدراسات العليا – قسم علوم الحياة –كلية العلوم الجامعة المستنصرية . اذ تضمنت العزلات :

1. *Escherichia coli* السلالة المستوردة والمرقمة 101B
2. *Salmonella typhi*
3. *Proteus mirabilis*
4. *Klebsiella pneumoniae*
5. *Staphylococcus aureus*
6. *Pseudomonas aeruginosa*

طريقة العمل

- اختبار نمو بكتريا *E.coli* على الوسطين (HT_1) السائل ووسط المرق المغذي بقياس طيف الامتصاص.

تحضير العالق الجرثومي :

حضر العالق الجرثومي بتنميته في وسط المرق المغذي وحضن بدرجة حرارة 37 م لمدة 24 ساعة . ثم قور النمو مع انبوبة ما كفرلاند المحضرة من كلوريد الباريوم ($Bacl_2$) بنسبة 1% وحامض الكبريتيك بنسبة 1% وحسب ما جاء عن [10] . للحصول على عدد خلايا $2 \text{ X } 10^8$ خلية / مل.

تلقيح الاوساط قيد الدراسه:

حضرت دوارق الوسطين المرق المغذي ووسط HT_1 السائل وبمقدار 20 مل لكل دورق. لقحت كافة الدوارق (بثلاث مكررات) ونسبة لقاح 0.5% من العالق الجرثومي المحضر في الفقرة السابقة [1]. جرى قراءة الكثافة الضوئية بطول موجي 470 نانوميتر لكل دورق واعطي وقت الصفر لهذه القراءات. ثم حضنت كافة الدوارق هوائيا في الحاضنة بدرجة حرارة 37 م واستمر في اخذ القراءات بفترات زمنية منتظمة ولمدة 12 ساعة . نظمت بعدها جداول ومنحنيات النمو.

مقارنة نمو بكتريا ال *E.coli* على الوسطين (HT_2) السائل ووسط ماكونكي السائل بطريقة طيف الامتصاص.

اتبعت الطريقة الواردة في الفقرة (3-1) لكن استمرت القراءات لمدة 24 ساعة . بعدها نظمت جداول ومنحنيات النمو.

مقارنة نمو بكتريا الـ *E.coli* و *S.aureus* على الوسطين (HT_2) الصلب وماكونكي الصلب (MacConkey). بطريقة التعداد الحي ..(Viable count)

1. حضرت مزارع العالق الجرثومي لكل من بكتريا *E.coli* و *S.aureus* وكلا على حدة باستخدام وسط المرق المغذي وتم مقارنة نمو الخلايا لكلا المزرعتين مع انبوبة ماكفرلاند [10] وكما سبق للحصول على عدد خلايا مقاربا الى $2 \text{ X } 10^8$ خلية / مل.
2. حضرت دوارق سعة 50 مل لكل من الوسطين ماكونكي السائل و (HT_2) السائل ، ولقحت الدوارق بنسبة لقاح 0.5% من اللقاح المحضر في الخطوة السابقة . تم تعليم الدوارق حسب الوقت ووضعت بالحاضنة الهزازة بدرجة حرارة 37م وبعمل ثلاث مكررات
3. اجريت تخافيف للمزارع البكتيرية تتناسب وساعات الحضن.
4. بعد فترات زمنية منظمة تم نقل 0.1 مل من المزارع البكتيرية السائلة الى سطح اطباق الوسطين Macconkey agar و (HT_2) الصلب . وباستخدام طريقة الفرش (Spreading method) [12]. حضنت الاطباق بدرجة 37م ولمدة 24 ساعة . درست بعدها المستعمرات النامية شكلا وعددا وبالاستعانة بجهاز colony counter.

اختبار مقارنة نمو انواع البكتريا المدروسة السالبة والموجبة لصبغة كرام على الوسطين (HT_1) و (HT_2) الصلبين.(Helianthus tuberosus agar no.1 and no.2)

حضرت اطباق الوسطين (HT_1) و (HT_2) . لقحت الاطباق من المزارع السائلة المنشطة وبعمر 18 ساعة كل من بكتريا: *Proteus mirabilis , Klebsiella pneumonia , Pseudomonas spp. Salmonella typhi* . بطريقة الفرش [11]. حضنت بعدها الاطباق بظروف هوائية بدرجة حرارة 37م ولمدة 24 ساعة . كذلك تم استنبات هذه المزارع على وسطي Nutrient agar , MacConkey كمعاملة سيطرة.

التحليلات الاحصائية: اجريت التحليلات الاحصائية باستخدام اختبار t (t.test) لمقارنة معدلات نمو البكتريا *E.coli* في الاختبارات (1-3,3-3,3-3) وحسب ما ورد عن[12].

النتائج والمناقشة

تستمر المختبرات الطبية والتعليمية والبنوك الخاصة بتنمية العزلات البكتيرية بتطوير الاوساط الزرعية المستخدمة لغرض تنمية وعزل وتشخيص الجراثيم . من هنا هدفت الدراسة الى ايجاد وسط زرعي ينتج على الصعيد المحلي ليرفد هذه الحاجة بدلا من استيرادها وليعمل على تسهيل عملية تنمية وتمييز البكتريا المعوية ومنها بكتريا *E.coli* لما لها من دور في تلوث الجروح والحروق والاصابة بالالتهابات المختلفة في الجسم المعوية منها والجهازية[13].

1. نتائج اختبار نمو بكتيريا *E.coli* على الوسطين HT_1 السائل والمرق المغذي.

اظهرت النتائج والموضحة في الجدول -1 ، زيادة طفيفة لنمو بكتريا القولون *E.coli* على وسط المرق المغذي ومقارنة بوسط HT_1 عندما بلغ طيف الامتصاص للعالق الجرثومي على وسط المرق المغذي (1.22)nm مقارنة بنموه على وسط HT_1 (0.94)nm وبعد مرور 12 ساعة . في حين اظهرت التحليلات الاحصائية باختبار .t عدم وجود فروق معنوية مهمة احصائيا بين الوسطي (t= 0.841,N.S,p>0.05) و (p>0.01) مما يثبت كفاءة الوسط الجديد HT_1 التي تضاهي كفاءة الوسط المستورد ، وذلك لاحتوائه اي درنات الالمازة على المواد المغذية البروتينية (3%) والكلوكوز والعناصر المعدنية كالبوتاسيوم والكالسيوم والصوديوم والفيتامينات مما يدعم نمو البكتريا[9].

2- نتائج مقارنة نمو بكتريا *E.coli* على الوسطين HT_2 السائل وماكونكي السائل.

اظهرت النتائج زيادة طفيفة في نمو البكتريا *E.coli* على وسط ماكونكي السائل ومقارنة مع نموها على الوسط الجديد HT_2 ، عندما بلغ طيف الامتصاص 1.50 nm في وسط ماكونكي مقارنة بـ1.20 nm على الوسط الجديد HT_2. وبعد مرور 14 ساعة ثم 24 ساعة لوحظت زيادة طيف الامتصاص للعالق الجرثومي ليبلغ 1.93 nm في وسط ماكونكي و 1.88 nm في الوسط الطبيعي HT_2. ومع وجود فارق بالارقام غير ان التحليلات الاحصائية اظهرت عدم وجود فروق معنوية بين الوسطين (t= 0.469 , N.S , p<0.05)و(p>0.01) مما يثبت امكانية استخدام الوسط HT_2 السائل بديلا عن وسط MacConkey السائل ، ولا سيما ان بكتريا *E.coli* النامية في وسط HT_2 قد خمرت سكر اللاكتوز بتغير لون الوسط وكما يحصل عند نموها على وسط الماكونكي . وذلك لاحتواء الوسطين ضمن مكوناتهما على سكر اللاكتوز (10 غم) لكل لتر من الوسط . ولاحتواء الوسطين على دليل Neutral red للكشف عن التخمر بانخفاض الرقم الهيدروجيني (pH) للوسط الزرعي. وهذا يعطي للوسط ميزة استخدامه كوسط تفريقي ليميز البكتريا المخمرة لسكر اللاكتوز عن غير المخمرة له.

جدول-1 : مقارنة كفاءة الوسط الطبيعي السائل HT_1 ووسط المرق المغذي في تنمية بكتريا *E.coli*.

الزمن (ساعة)	قراءات طيف الامتصاص (nm)	
	المرق المغذي	الوسط HT_1
0	0.07	0.08
2	0.28	0.12
4	0.43	0.26
6	0.75	0.55
8	0.89	0.71
10	1.06	0.80
12	1.22	0.94

3- اختبار نمو بكتريا *E.coli* و *S.aureus* على الوسطين الزرعيين HT_2 agar و MacConkey agar .

في هذا الاختبار اختير نوعين من البكتريا *E.coli* السالبة لصبغة كرام و *S.aureus* الموجبة لصبغة كرام بغية التحري عن كفاءة الوسط TH_2 . ولتحقيق ذلك استخدمت طريقة التعداد الحي (viable count) مع عدد خلايا (10^8X0.17) خلية / مل لبكتريا *E.coli* و *S.aureus* بوصفها مزرعة اساسية (stock culture) اذ حققت النتائج الموضحة في الجدول (3) هدف التجربة عندما ازداد عدد الخلايا لبكتريا *E.coli* في الوقت (صفر) (0.17 و 0.18) X 10^7 خلية / مل على الوسطين MacConkey agar و HT_2 على التوالي ليبلغ (90.3 و 100.2) X 10^7 خلية / مل بعد مرور 24 ساعة لكلا الوسطين وعلى التوالي . فيما اكدت التحليلات الاحصائية باختبار t. عدم وجود فروق معنوية بين الوسطين (t= 0.272 , N.S, p>0.5) و (p>0.01) . وتبين ايضا ميزة الوسط HT_2 في تنمية البكتريا السالبة لصبغة كرام (*E.*coli)دون الموجبة (*S.aureus*) من خلال تثبيطه لنمو *S.aureus* فيما نمت *S.aureus* *على وسط ماكونكي* باعداد قليلة مقارنة ببكتريا *E.coli* .

ظهرت مستعمرات بكتريا *E.coli* على وسط HT_2 دائرية ومحدبة ووردية اللون لكونها مخمرة لسكر اللاكتوز في الوسط وبذلك توافقت مواصفات نمو المستعمرات على وسط TH_2 مع ماذكره[14]. يمكن القول انه لجعل الوسط اختياريا وتفريقيا فقد تم الاستعانة بوسط ماكنوكي من حيث المكونات باحتواء الوسط على املاح الصفراء التي دعمت نمو *E.coli* دون *S.aureus* [15] كما انه لا بد من اضافة اللاكتوز الى مكونات الوسط ، اذ لا يتوفر هذا السكر ضمن مكونات نبات الالمازة . فيما تتوفر سكريات اخرى لتدعم نمو الكائن المجهري [9]. اذ تاكد ذلك من خلال تجاربنا السابقة بجعل الوسط تفريقيا دون اضافة اللاكتوز.

جدول-2 : مقارنة كفاءة الوسط HT_1 ووسط MacConkey broth في تنمية بكتريا *E.coli* .

الوقت ساعة	طيف الامتصاص (nm)	
	وسط MacConkey	وسط HT_2
0	0.20	0.19
2	0.29	0.22
4	0.36	0.31
6	0.56	0.45
8	0.76	0.89
10	1.20	0.99
12	1.39	1.10
14	1.50	1.20
24	1.93	1.88

جدول-3: مقارنة نمو بكتريا *E.coli* و *S.aureus* على الوسطين MacConkey agar و HT_2 بقياس عدد الخلايا الحية .

الوقت ساعة	معدل العدد الحي $X10^7$ خلية/مل			
	بكتريا *E.coli*		بكتريا *S.aureus*	
	MacConkey agar	HT_2 agar	MacConkey agar	HT_2 agar
0	0.17	0.18	0.02	0
4	0.18	0.18	0.04	0
8	8.60	9.20	0.15	0
12	30.0	40.0	0.20	0
16	60.2	55.1	0.30	0
24	90.3	100.2	0.48	0

* النتائج تمثل معدل خمس مكررات عدم وجود فروق معنوية($p>0.05$).

4. نتائج نمو انواع مختلفة من بكتريا السالبة لصبغة كرام على الوسطين TH_1 agar و TH_2 agar

تمكنت الاجناس المختلفة من البكتريا السالبة لصبغة كرام والمتضمنة *Salmonella typhi* و *Proteus mirabilis* و *klebsiella pneumoniae* و *Pseudomonas aeruginosa* فضلا عن *E.coli* من النمو وبشكل جيد على الوسطين TH_1 و TH_2 الصلبين عندما ظهرات مستعمراتها بشكل واضح وجيد على الوسطين (جدول-4) فيما تميزت البكتريا المخمرة لسكر اللاكتوز عن غير المخمرة على وسط TH_2 ففي الوقت الذي ظهرت فيه مستعمرات بكتريا *K.pneumoniae* و *E.coli* وردية اللون (مخمرة لسكر اللاكتوز) ظهرت مستعمرات كل من P.aeruginosa و *P.mirabilis* و *S.typhi* شاحبة وهذه المواصفات تتوافق وما ذكره [2] من ان هذه الانواع فير مخمرة لسكر اللاكتوز.

جدول-4: نمو انواع مختلفة من البكتريا السالبة لصبغة كرام على الوسطين TH_1 و TH_2

انواع البكتريا	الوسط الزرعي		
	HT_1	HT_2	تخميرسكر اللاكتوز
E.coli	+	+	مخمرة
Salmonella typhi	+	+	غير مخمرة
Proteus mirabilis	+	+	غير مخمرة
Klebsiella pneumoniae	+	+	مخمرة

Pseudomonas aeruginosa	+	+	غير مخمرة

+ تعني نمو البكتريا [13]

شكر وتقدير:
نتقدم بالشكر والتقدير الى عمادة كلية العلوم ورئاسة قسم علوم الحياة لتقديمهم المساندة من خلال توفير الاجهزة والمعدات المستخدمة في انجاز البحث.

الاستنتاج:
اظهرت الدراسة الحالية امكانية استخدام خلاصة الالمازة ***Helianthus tuberosus*** في تحضير الاوساط الزرعية الخاصة بتنمية وتشخيص البكتريا وبكفاءة عالية.

المصادر

1. Toder , k.Pathogenic *E.coli*. Todrar's online Text Book Bacteriology. University of Wisconsin-Madison Department bacteriology.(2008).
2. Holt , T.G; krieg, N.R and Sneath , P.H. Berge's Manual of Determinative Bacteriology. 9th-ed. Williams and wilkins. (1994).
3. Muvey , M.V. Adhesion and entry of uropathogenic *Escherichia coli*. Cell microbial. (2002) ,4,257-271.
4. برهان ، غادة حسن . دراسة بكتريولوجية مرضية ونسيجية لحالات التهابات الزائدة الدودية – رسالة ماجستير – كلية العلوم – الجامعة المستنصرية .(2006).
5. الحسيني ، ضفاف جاسم محمد . عزل وتشخيص البكتريا المرضية المرافقة لمرض سرطان القولون والكلى . رسالة ماجستير – كلية العلوم – الجامعة المستنصرية (2004)
6. الحسابي ، اشرف سامي حسن . دراسة تاثير المستخلص المائي البارد النباتي بذور الكتان واوراق التوت الابيض ضد الانواع البكتيرية المعزولة من المصابين بالتهاب غدة البروستات. رسالة ماجستير . كلية العلوم الجامعة المستنصرية .(2008).
7. علي ، نضال عبد الامير . تاثير مستخلصات اوراق العنب والخروع والبصل في بعض عوامل استعمار انواع بكتريا التهاب الاذن الوسطى في الانسان . رسالة ماجستير- كلية العلوم – الجامعة المستنصرية (2009).
8. Banerjee , A and Namerjee , N. Fundamentals of Microbiology and Immunology. New centra book ageney (P) LTD. India (2008).
9. Pellet, P.L and Shadarevian, S. Food Composition-2-nd-ed. American university of beriut , beriut , Lebanon.(1976)
10. Macfaddin , J.F. Biochemical Tests for Identification of Medical Bactria. 3d-ed. The Williams and wilkins. Baltimore , USA.(2008)
11. Norajit. K;Iaohakunjit, N.and kerdchoe chuen , O.Antibacterial effect of five zingiberaceae essential oils molecules. (2007), 12(8), 2047-2060.
12. Zar , J.H. Biostatistical Analysis , 2nd- ed. Prentice hall inc , Englewood cliffs , N.I,(1984).
13. Difco Manual of Dehydrated Culture Media and Reagents for Microbiological and Clinical laboratory Procedures. 9th-ed. Difco laboratories incorporated, Detroit, Michigan, (1969).

14. Zegarra Montes, L.R; Sanchez Mejia , A.A; loza Munarriz ; C,A and Celis. Gutiemz , E. Semenal and urine culture in the diagnosis of chronic bacterial pro statitis . international braz.J. euro, (2008) 1(1),30-40.
15. Edwars , P.R and Ewing , W.H. Identification of Enterobacteriaceae .3d-ed. Minneapolis, burges publishing com, (1970).

تأثير المستخلص المائي لنبات السواك وغسول الفم وتداخلهما في نمو الإحياء المجهرية المسببة لالتهاب اللثة وتسوس الأسنان .

اشرف سامي حسن
الجامعة المستنصرية / كلية العلوم / قسم علوم الحياة

تاريخ تقديم البحث 2012/4/16 - تاريخ قبول البحث 2012/6/20

ABSTRACT

This study was conducted in order to identify the impact of increased concentrations (100, 200 300 400, 500) mg / ml of aqueous extract of the plant *Salvadora persica* and mouthwash and overlap in the growth of microorganisms (*Streptococcus mutans* , *Lactobacillus acidophilus* , *Candida albicans*) that cause gingivitis and dental caries, by measuring the diameters of inhibition zones by using the Agar – Well Diffusion Method. microorganisms above was isolated from the mouth of people suffering from gingivitis and dental caries, the results showed the presence of a negative impact on the growth of microorganisms above, an increase of concentration of the aqueous extract of the plant *Salvadora persica* and mouthwash , and concentrations 500 mg / ml was more effect than other concentrations, noting the presence of greater negative effect this overlap between the extracted *Salvadora persica* and mouthwash on the growth of studied microorganisms when compared with the effect of extract of *Salvadora persica* and mouthwash both in private and that by increasing the diameters inhibition for all concentrations and at all types of studied microorganisms. Results also showed that the bacteria *Lactobacillus acidophilus* were the most tolerant compared with bacteria *Streptococcus mutans* and fungus *Candida albicans*, by giving lower values of the countries of inhibition , the bacterium *Streptococcus mutans* was the most sensitive and that by giving the highest values for the inhibition at all concentrations. Hence the results suggest that the overlap between the aqueous extract of the plant *Salvadora persica* with mouthwash and specifically concentration 500 mg/ml is the most effective in inhibiting the growth of studied microorganisms , so can be of use the output of this overlap in the treatment of gingivitis and dental caries.

الخلاصة

أجريت هذه الدراسة بهدف التعرف على تأثير تراكيز متزايدة (100 ، 200 ، 300 ، 400 ، 500) ملغرام / مل من المستخلص المائي لنبات السواك وغسول الفم وتداخلهما في نمو الإحياء المجهرية (*Streptococcus mutans* , *Lactobacillus acidophilus* ,*Candida albicans*) المسببة لالتهاب اللثة وتسوس الأسنان ومن خلال قياس أقطار التثبيط وبطريقة الانتشار بالحفر . تم عزل الإحياء المجهرية أعلاه من فم أشخاص مصابين بالتهاب اللثة وتسوس الأسنان . أظهرت النتائج وجود تأثير سلبي في نمو الإحياء المجهرية أعلاه بزيادة تراكيز المستخلص المائي لنبات السواك و غسول الفم مع تفوق التركيز 500 ملغرام / مل عن بقية التراكيز الأخرى ، مع ملاحظة وجود تثيرا سلبيا اكبر للتداخل بين مستخلص السواك وغسول الفم على نمو الإحياء المجهرية المدروسة عند مقارنته بتأثير مستخلص السواك وغسول الفم كلا على انفراد وذلك من خلال زيادة أقطار التثبيط ولجميع التراكيز وعلى جميع أنواع الإحياء المجهرية المدروسة . كما أظهرت النتائج أيضا إن بكتريا *Lactobacillus acidophilus* كانت الأكثر تحملا مقارنة بالبكتريا *Streptococcus mutans* والفطر *Candida albicans* وذلك من خلال إعطائها اقل قيم من أقطار التثبيط فيما كانت بكتريا *Streptococcus mutans* هي الأكثر حساسية وذلك من خلال إعطائها اعلي قيم للتثبيط وفي جميع التراكيز ، ومن هنا تشير نتائج هذا البحث إلى إن التداخل بين المستخلص المائي لنبات السواك مع غسول الفم وبالتحديد التركيز 500 ملغرام / مل هو الأكثر تأثيرا في تثبيط نمو الإحياء المجهرية المدروسة والمسببة لالتهاب اللثة و تسوس الأسنان لذا بالإمكان استخدام ناتج هذا التداخل في علاج التهاب اللثة وتسوس الأسنان.

المقدمة

يعرف تسوس الأسنان (Dental caries) على انه مرض يصيب الأنسجة المعدنية (الصلبة) للأسنان نتيجة لنشاط البكتريا على الكاربوهيدرات القابلة للتخمر من خلال فقدان العناصر من هذه الأنسجة يرافقه تفكك الهيكل العضوي لأنسجة الأسنان ، ويلاحظ من خلال هذا التعريف أن تسوس الأسنان هو عدوى جرثومية ناتجة عن نشاط البكتريا الموجودة في الفم و التي توجد على شكل طبقة تعرف باللويحة الجرثومية (plaque) و هي الطبقة البيضاء اللزجة التي تتكون على سطح الأسنان و اللثة و يتمثل دور البكتيريا في تسوس الأسنان في أنها تقوم بالتغذي على الكاربوهيدرات الموجودة في الطعام الذي نتناوله من خلال عملية التخمر اللاهوائي مؤدية إلى أنتاج أحماض تقوم بدورها مع مرور الوقت بإذابة العناصر الموجودة في تركيب الأسنان كالكالسيوم و الفسفور ومن ثم تضعف بنية السن في هذه المنطقة و تجعل المادة العضوية المكونة للسن ضعيفة و سهلة التدمير مؤديا بذلك إلى تكون ثقوب أو فجوات في مكانها فيما يعرف بنخور الأسنان **(1)** .

تتكون اللويحة الجرثومية (plaque) من مجموعة كبيرة من أنواع البكتيريا التي تعيش بشكل طبيعي داخل فم الإنسان حيث تتراكم هذه البكتيريا و تلتصق على سطح الأسنان مع مرور الوقت خلال النهار مكونة طبقة لزجة بيضاء اللون تبدأ بالظهور على أسطح الأسنان و تزداد سماكتها و تعقيد تركيبها كلما زاد وقت بقاؤها على سطح الأسنان دون إزالتها ، حيث تعتبر الكاربوهيدرات و السكريات أفضل أنواع الغذاء لهذه البكتيريا حيث ينتج عن تحليل البكتيريا لهذه الكاربوهيدرات مواد حمضية تعمل على خفض درجة حموضة البيئة الفموية pH و تساعد هذه البيئة الحمضية إذا بقيت لفترة كافية على إذابة المركبات المعدنية المكونة للأسنان تاركة ورائها الأنسجة العضوية الضعيفة و التي يصبح من السهل تفككها و تدميرها **(2)** .

تعاني معظم شعوب العالم من تسوس الأسنان ، وبموجب تعريف منظمة الصحة العالمية (WHO) بأنه مرض تلوثي موضعي تسببه بعض أنواع الإحياء المجهرية الفموية الضارة من أهمها (*Streptococcus mutans, Lactobacillus, Actinomycus viscusus*) هذه الإحياء المجهرية تتواجد بالفم بشكل طبيعي وهي تتبع مجموعه أخرى من البكتيريا الفموية ويطلق عليه (Oral flora) ويجب توفر بيئة مناسبة حتى تتكاثر هذه البكتيريا بشكل سريع ومكثف ومن ثم مهاجمه أنسجة السن بدأ بطبقة آلمينا **(3 ، 4)** .

أما بالنسبة إلى التهاب اللثة (Gingivitis) حيث تتكون اللثة من نسيج ليفي مغطى بغشاء مخاطي يشبه في تركيبه بشرة الجلد ولكنها اخف مما هو موجود في الجلد في معظم مواقع اللثة . وتغطي اللثة العظم السنخي (Alveolar Bone) وجذور الأسنان وأعناقها، ومن أهم مناطق اللثة هو ما يسمى بالميزاب اللثوي وهو الشق الصغير الذي يوجد بين اللثة والجزء العنقي لتاج السن، وعمقه في الأحوال الطبيعية حوالي نصف إلى مليمتر واحد فقط .وبما أن اللويحة السنية تترسب في هذا الميزاب اللثوي فان هذا الشق يعتبر المصدر الأول لنمو أنواع البكتيريا المختلفة أذا لم يتم تنظيفه وإزالة اللويحة منه بشكل منتظم. تستوطن البكتيريا المرتبطة بأمراض اللثة والعظم السنخي المحيط بالأسنان في شكل تجمعات بكتيرية تحت وفوق الشق اللثوي أو الميزاب اللثوي .ولقد أثبتت الأبحاث العلمية الحديثة ارتباط بعض فئات بكتيريا اللويحة السنية بالأمراض اللثوية الفتاكة **(5 ، 6)** .

تمكنت الإحياء المجهرية المسببة للأمراض البشرية من أن تطور طرق متعددة للمقاومة نتيجة الاستخدام العشوائي للأدوية التجارية المضادة للجراثيم في علاج الأمراض المعدية ، وبما إن هذه الأدوية لها الكثير من الآثار الجانبية غير المرغوب فيها و ظهور التهابات غير مألوفة دفعت العلماء عن البحث عن مواد جديدة مضادة لهذه الإحياء المرضية من مصادر مختلفة ، ومن أهم هذه المصادر هي النباتات الطبية ومنها السواك التي أظهرت مستخلصاتها تأثيرا واضحا في كبح نمو هذه الإحياء **(7)** .

تستخدم أعواد السواك *Salvadora persica* التي تحضر من أنواع مختلفة وكثيرة من الأشجار والنباتات كعادة متبعة ومتوارثة لتنظيف الأسنان لدى الكثير من الأشخاص في مناطق مختلفة من العالم وخاصة في آسيا وأفريقيا والشرق الأوسط وجنوب أمريكا (8) . وهذه العادة ليست متبعة لكون الدين فقط يحث على ذلك ولكن لأسباب أخرى مثل سهولة الحصول على هذه الأعواد وقلة تكلفتها على المستخدمين وكذلك لبساطتها في ذاتها وتجدر الإشارة إلى ما ورد في تقرير منظمة الصحة العالمية السنوي والذي يهتم بقواعد صحة الفم العامة ونظافة الأسنان، حيث انه في عدد عام (٢٠٠٠ م) قد أقر بان أعواد السواك المختلفة تلعب دورا مهما وأساسيا في تحسين صحة ونظافة الفم، وأوصى بضرورة الإسراع في إجراء الأبحاث العلمية الخاصة لتبيان تأثير استخدام مثل هذه الأعواد على صحة الأسنان (9) .

تنتشر شجرة الأراك (السواك) جغرافيا بشكل واسع في عدة بلدان فهي شجيرة تنمو في الأماكن الحارة والاستوائية وتمتد من راسثان (الهند)، نيبال وماليزيا في الشرق وتجدها تنمو أيضا في باكستان، إيران، العراق، المملكة العربية السعودية، ومن مصر إلى موريتانيا في الغرب، ومن شمال أفريقيا خلال السودان، إثيوبيا، إفريقيا الوسطى إلى جنوب شرق أفريقيا (10 ، 11) . أثبتت الأبحاث أن أعواد السواك وأثناء استخدامها تفرز بعض المواد الكيميائية، وهذه المواد لها تأثيرات وخواص حيوية مثل المواد القاتلة للبكتيريا (12 ، 13 ، 14) . قام الباحثون باستخلاص خلاصة السواك ، حيث ثبت تأثير هذه الخلاصة على بعض الخصائص الوظيفية الفسيولوجية لعدد من أنواع البكتيريا الفموية والتي تعني بتسوسات الأسنان (15) ، وجد أن التركيب الكيميائي لهذه الأعواد احتوى على مواد قلوية مثل السلفادويوريا (Salvadourea) ، الكلورايد (Chloride) ، مادة السيستوستيرول (β-Sisto Sterol) ، تراي ميثايل امين (Trimethylamine)، حمض اليانسون (m-ansinic acid) ، السيليكا (Silica) ، الكبريت (Sulfur) ، فيتامين سي (Vitamin C) ، مادة الصابونين والعفص ، التانين (Tannin) ، الفلافويند (Flavonide) ، الكلايكوسايد (Glycoside) ، ومواد لها علاقة بالخردل مثل السنيرجين (Sinnirgin) ، مادة صمغية (Resin) (16 ، 17) .

لذا جاء البحث بهدف معرفة تأثير المستخلص المائي لنبات السواك و غسول الفم وتداخلهما في نمو الإحياء المجهرية المسببة لتسوس الأسنان والتهاب اللثة مع تحديد التركيز الأفضل في تثبيط نمو هذه الإحياء .

المواد طرائق العمل

- **غزل وتشخيص الأحياء المجهرية المسببة الالتهاب اللثة وتسوس الأسنان :**

تم عزل الإحياء المجهرية (*Streptococcus mutans* . , *Lactobacillus acidophilus* , *Candida albicans*) من فم الأشخاص المصابين بالتهاب اللثة وتسوس الأسنان والبالغ عددهم 30 شخص في الجامعة المستنصرية / كلية العلوم ، شخصت هذه الأحياء المجهرية بموجب طرق التشخيص المعروفة مختبريا (18) .

- **جمع العينات النباتية وتهيئتها للاستخلاص :**

تم جمع أعواد نبات السواك الذي يعرف بالاسم العلمي (*Salvadora persica*) ، والذي ينتمي إلى الفصيلة السلفادورية (Salvadoraceae) الجنس Salvadora ، و المستخدم في الدراسة من الأسواق المحلية لمدينة بغداد مع مراعاة إن تكون الأجزاء النباتية المستخدمة في عملية الاستخلاص خالية من الأضرار الظاهرية، ثم نقلت العينات إلى المختبر في كلية العلوم الجامعة المستنصرية.

- **تحضير المسحوق النباتي :**

غسلت أعواد النبات جيدا بماء الحنفية (Tap water) لإزالة الأتربة والأوساخ منها أن وجدت بعدها تركت لتجف في درجة حرارة الغرفة مع مراعاة تقليبها المستمر ، ثم طحنت الأعواد بمطحنة كهربائية ، وضغط المسحوق النباتي في عبوات جافة ووضعت في الثلاجة بدرجة حرارة 4° م لحين استعمالها.

- **تحضير المستخلص المائي البارد Cold water extract :**

أتبعت طريقة Ratheesh and Helen (2007) بوزن 100 غرام من المسحوق النباتي ووضع في دورق أضيف له لتر من الماء المقطر ، ووضع في الحاضنة الهزازة (Shaking incubator) لمدة 24 ساعة وبدرجة حرارة 28 م° ، ثم رشح المزيج بوساطة الشاش . نبذ الراشح بسرعة 3000 دورة\دقيقة لمدة 10 دقائق ثم رشح الرائق بوساطة أوراق الترشيح Whattman No.1 ، بخر الراشح في الحاضنة بدرجة 37 م° لمدة 48 ساعة للحصول على المسحوق الجاف للمستخلص ، ثم وضع في أنبوبة محكمة الغلق ومغلفة بورق ألمنيوم وحفظ في الثلاجة بدرجة حرارة 4- م° لحين الاستعمال (**19**) .

- **تحضير محلول غسول الفم Mouth wash :**

تم الحصول على غسول الفم (Sensodyne) والمنتج من شركات جلاكسو سميث كلاين (gsk) ذات المنشأ الألماني من الأسواق المحلية والذي احتوى وحسب ما هو مثبت على العبوة على مادة الفلورايد وبتركيز 450 جزء بالمليون (450 ppm) كمادة فعالة ضد تسوس الأسنان ، حيث اعتبر المحلول الخزين الأساس الذي حضرت منه سلسلة من التخفيف العشرية التي من خلالها حصلنا على التراكيز (100، 200، 300، 400، 500) ملغرام / مل بعد ذالك أصبحت هذه التراكيز جاهزة للاستعمال .

- **تحضير المحلول الخليط من المستخلص المائي لنبات السواك وغسول الفم**

تم تحضر هذا المحلول بخلط كميات متساوية وبنسبة 1:1 من مستخلص السواك وغسول الفم ، ثم عملت لهذا الخليط سلسلة من التخافيف العشرية والتي من خلالها للحصول على التراكيز (500 ، 400 ، 300، 200 ، 100) ملغرام/ مل

- **دراسة تأثير المستخلص المائي لنبات السواك و غسول الفم في نمو العزلات البكتيرية**

تم إتباع طريقة الانتشار في الحفر (The Agar – Well Diffusion Method) في هذه الدراسة ، حيث لقح سطح أكار مولر هنتون Muller Hinton Agar بوساطة قطيلة معقمة (Sterile Swab) من مزروع البكتريا الذي بعمر 24 ساعة و الحاوي على (1.5 × 10^8 خلية / مل) بمقارنته مع محلول ثابت العكورة القياسي ، ثم تركت الأطباق لتجف في حرارة الغرفة . عملت حفر بقطر 6 ملم في الوسط المزروع بوساطة الثاقب الفليني المعقم (Cork Borer) بواقع خمسة حفر في الطبق (**20** ، **21**).

حضرت تراكيز من المسحوق النباتي المائي البارد باستخدام الماء المقطر المعقم، بإذابة 3 غرام من المستخلص الجاف في 6 مل من الماء المقطر المعقم للحصول على تركيز 500 ملغم / مل ، وعقم بورق الترشيح قطر ثقوبه (0.22) مايكرون (Millipore filter paper) اعتبر هذا التركيز هو التركيز الخزين الأساس ومنة حضرت تراكيز متدرجة وكالاتي (100، 200، 300، 400، 500) ملغرام / مل . أضيف 0.1 مل من تراكيز المستخلص المذكور آنفا لكل حفرة على انفراد بوساطة ماصة دقيقة Micropipette وبالتسلسل وعملت حفرة السيطرة المتمثلة بإضافة ماء مقطر معقم ولكي نسمح لتراكيز المستخلص بالانتشار عبر الوسط ، وضعت الأطباق في الثلاجة بدرجة حرارة 4 م° ولمدة نصف ساعة حضنت بعدها الأطباق بدرجة حرارة 37 م° ولمدة 24 ساعة . حددت فعالية كل تركيز من المستخلصات بقياس قطر منطقة التثبيط Inhibition Zone حول كل حفرة. وطبقت هذه الطريقة أيضا للتحري عن فعالية غسول الفم على الإحياء المجهرية قيد الدراسة .

النتائج والمناقشة

أظهرت النتائج في الجدول (1) بوجود تأثير سلبي للمستخلص المائي لنبات السواك في نمو الأحياء المجهرية المسببة التهاب اللثة وتسوس الأسنان من خلال زيادة أقطار التثبيط ، حيث أعطى التركيز 500 ملغرام / مل أفضل قيمة في تثبيط نمو الإحياء المجهرية المدروسة أعلاه مقارنة بالتراكيز الأخرى فيما اظهر التركيز 100 ملغرام / مل تأثيرا سلبيا فقط على نمو بكتريا *Streptococcus mutans* حيث كان قطر التثبيط 9 ملم ، كذلك أظهرت بكتريا

Lactobacillus acidophilus مقاومة للمستخلص المائي لنبات السواك من خلال اعطائة اقل قيم الأقطار التثبيط ولجميع التراكيز المدروسة ، فيما سجلت بكتريا *Streptococcus mutans* و الفطر *Candida albicans* اقل تحملا للمستخلص على التوالي.

جدول-1: : تأثير المستخلص المائي للسواك على الإحياء المجهرية المسببة التهاب اللثة وتسوس الأسنان .

أنواع الإحياء المجهرية	أقطار التثبيط بالملم				
	التركيز (ملغرام/ مل)				
	500	400	300	200	100
Streptococcus mutans	21	17	14	11	9
Lactobacillus acidophilus	16	14	10	0	0
Candida albicans	18	16	12	9	0

فيما أظهرت نتائج الجدول (2) بوجود تأثير سلبي أيضا لغسول الفم في نمو الإحياء المجهرية المدروسة ، فقد أعطى التركيز 500 ملغرام / مل أفضل قيمة في تثبيط نمو الإحياء المجهرية المدروسة وذلك من خلال زيادة أقطار التثبيط مقارنة بالتراكيز الأخرى ، كذلك لوحظ إن التركيزين (100 و 200) ملغرام / مل لم يظهرا إي تأثير سلبي على نمو الإحياء المجهرية ، يتضح أيضا من نتائج الجدول (2) تحمل بكتريا *Lactobacillus acidophilus* لغسول الفم من خلال إعطائها اقل قيم لأقطار التثبيط ولجميع التراكيز فيما سجلت بكتريا *Streptococcus mutans* و الفطر *Candida albicans* اقل تحملا لغسول الفم على التوالي.

جدول -2 : تأثير التراكيز المختلفة من غسول الفم على الإحياء المجهرية المسببة التهاب اللثة وتسوس الأسنان .

أنواع الإحياء المجهرية	معدل أقطار التثبيط بالملم				
	التركيز (ملغرام/ مل)				
	500	400	300	200	100
Streptococcus mutans	15	13	10	0	0
Lactobacillus acidophilus	12	10	0	0	0
Candida albicans	13	11	9	0	0

ويتبين من نتائج الجدول (1 و 2) إن مستخلص السواك كان الأكثر سلبا في نمو الإحياء المجهرية من غسول الفم وذلك من خلال زيادة أقطار التثبيط لمستخلص السواك مقارنة مع غسول الفم ، ويرجع ذلك إلى المواد الفعالة التي يحتويها السواك ، فقد أوضح الباحثون أن خلاصة أعواد السواك (الأراك) تحتوي على مواد مضادة للبكتيريا ومواد مضادة للالتهاب ومواد مخفضة للسكر .وأن هذه المواد لم تكن سامة حينما حقنت في الفئران بتركيز عالي جدا . وفي دراسة أخرى تم اكتشاف وجود مادة جلوكوتر وباولين (Glucotropaeolin) وهذه المادة عضوية مركبة من عنصر الكبريت ومركب السينانيد وحلقة بترينية وهي تدعى بتريل ايزوثايوسيانيت (Benzyl isothiocyanate) ، ويعتقد بان وجودها هو سبب اللذعة النفاذة في جذور الأراك .وهذه المواد قاتلة للميكروبات الضارة الموجودة بالفم، وأكدت الأبحاث أيضا أن لهذه المادة قدرة على قتل الفيروسات والميكروبات من خلال قدرتها على تثبيط نموها ومنعها من إنتاج الأحماض القاتلة (**22** ، **23**) .

أثبتت الدراسات قدرة خلاصة أعواد السواك على قتل الميكروبات الضارة تعود إلى وجود كميات عالية من عناصر الكبريت و الكلور والكالسيوم فيها (**23**) . كما ذكر أيضا قدرة السواك على إزالة طبقات اللويحة السنية (Dental Plaque) أو بقايا الطعام الملتصقة بمينا السن بدرجة مساوية أو تفوق ما تقوم بة فرشاه ومعاجين الأسنان والسبب يعود إلى وجود مادة السليكا في تركيب السواك وبكميات غير قليلة وهي مادة زالقة تجرف تلك الطبقات ألاصقة وتزيلها (**24**) .

ولا بد من الإشارة في هذا الصدد إلى أن عود الأراك يحتوى على المواد الفعالة التالية والتي تستخدم في مكافحة التسوس والتهابات اللثة: فيتامين سي، ومادة السيتوستيرول وهما يعملان على قطع نزيف اللثة وتقويتها. مادة خردلية تسمى "sinnigirin" ذات رائحة حادة وطعم لاذع، وهي تساعد على الفتك بالجراثيم. تراى ميثيل أمين، وهي مادة تعمل على التئام جروح اللثة ونموها السليم ، حيث تحتوى مكونات مطهرة يمكنها تعديل الأس الهيدروجيني للتجويف ألفمي على نحو يؤثر بصورة غير مباشرة في النمو الميكروبي، ويحتوي السواك على نسبة 1% زيوت طيارة و فلافونيدات وقلويدات وهي مواد تعمل على تقوية مناعة الجسم (25 ، 26) .

استنادا إلى النتائج التي تم الحصول عليها لكل من مستخلص السواك وغسول الفم ، جاءت فكره خلط مستخلص السواك مع غسول الفم لمعرفة تأثير هذا التداخل على الإحياء المجهرية المدروسة . يلاحظ من النتائج الموضحة في الإشكال (1، 2 ، 3) ازدياد أقطار التثبيط لناتج هذا التداخل ضد البكتريا المدروسة .

قد يرجع هذا التأثير الأعلى في التثبيط إلى إن غسول الفم يحتوي على مادة الفلورايد وبما أن مستخلص السواك يحتوي على تركيز قليل من هذه المادة فانه بخلط مستخلص السواك وغسول الفم يزداد تركيز المادة في الخليط ، حيث أكدت أحدث الأبحاث أن عنصر الفلورايد (Fluoride) والذي يعتبر من أهم المواد المساعدة في حماية الأسنان من التسوس، يكاد يكون غير موجود في تركيب أعواد الأراك، حيث أن نسبته تعتبر نسبة مهملة لا أثر لها (<0.07 µg/ml) (27) .

ومن هذا نستنتج أن خلط مستخلص السواك مع غسول الفم كان له تأثير اكبر في تثبيط نمو الإحياء المجهرية المعزولة من التهاب اللثة وتسوس الأسنان بالمقارنة مع مستخلص السواك وغسول الفم كلا على انفراد .

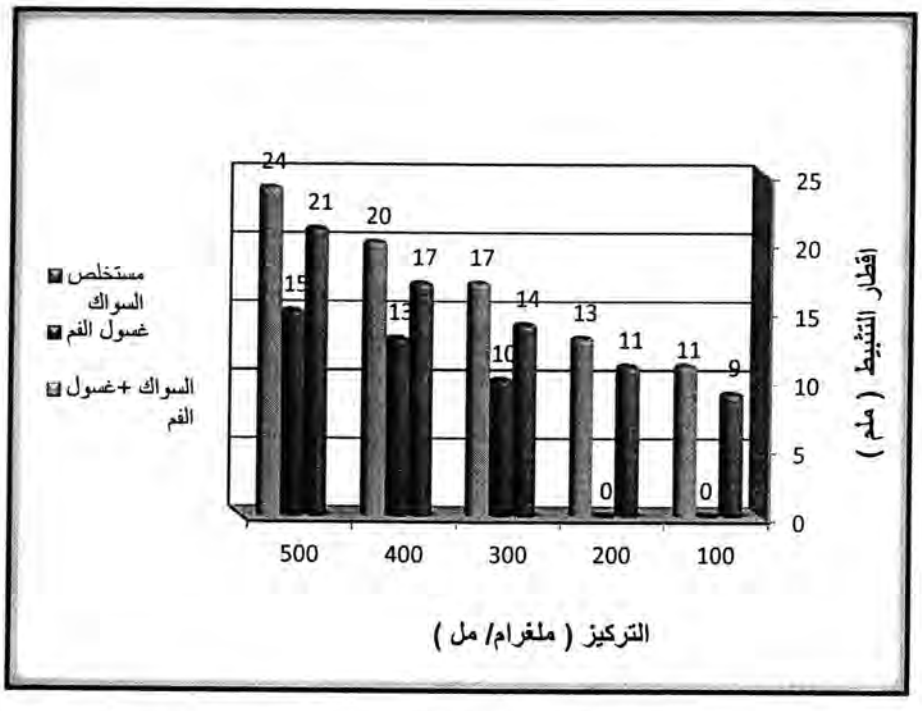

الشكل -1 : تأثير مستخلص السواك وغسول الفم وتداخلهما على بكتريا *Streptococcus mutans* المسببة التهابات اللثة تسوس للأسنان

لذا نوصي باستخدام الخليط المكون من المستخلص المائي لنبات السواك مع غسول الفم وبالتحديد التركيز 500 ملغرام/مل منة لكونه الأكثر تأثيرا في تثبيط نمو الإحياء المجهرية المدروسة والمسببة التهاب اللثة و تسوس الأسنان .

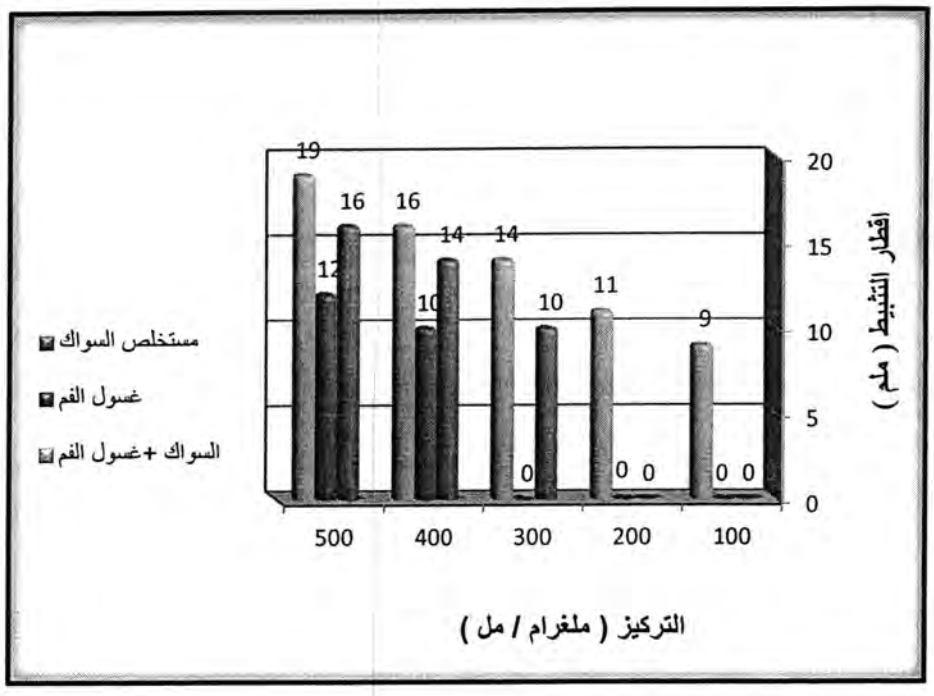

شكل -2 : تأثير مستخلص السواك وغسول الفم وتداخلهما على بكتريا *Lactobacillus acidophilus* المسببة التهابات اللثة تسوس للأسنان

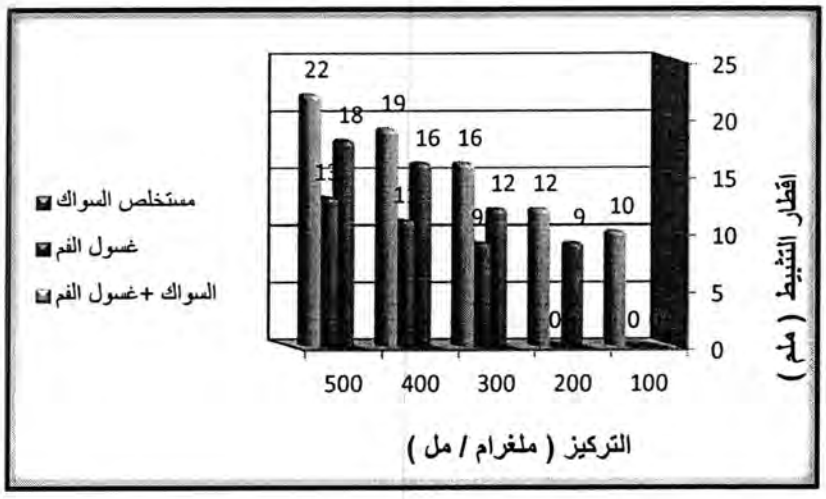

شكل-3: تأثير مستخلص السواك وغسول الفم وتداخلهما على الفطر *Candida albicans* المسببة التهابات اللثة تسوس للأسنان

المصادر

1. Barira Islam; Shahper N. Khan and Asad U. Khan . Dental caries: From infection to prevention . Interdisciplinary Biotechnology Unit, Aligarh Muslim University, Aligarh, India. Med Sci Monit; 13(11): RA196-203 (2007) .
2. Philip, D. Marsh . Dental plaque biofilm the significance of pH in health and caries . professor of oral microbiology, university of Leeds, UK. Progressive orthodontics J, 3(2):76-87(2009) .
3. Harold Marcottel and Marc C. Lavoie. Oral Microbial Ecology and the Role of Salivary Immunoglobulin A . Microbiol Mol Biol Rev. ; 62(1): 71–109 (1998) .
4. Rogers, A.H . Molecular Oral Microbiology. Caister Academic Press. ISBN 978-1-904455-24-0 (2008) .
5. Van- der Weijden G.A.; Timmerman M.F.; Reijerse E; Wolffe G.N.; Van- Winkelhoff A.J. and Van der Velden U..The prevalence of A. actinomycetemcomitans, P. gingivalis and P intermedia in selected subjects with periodontitis. J Clin Periodontol: 21(9): 583-588 (1994).
6. Socransky, S.S. and Haffajee, A.D. Dental biofilms: difficult therapeutic targets. Periodontol 2000; 28: 12-55 (2002) .
7. Firas A. AL-BAYATI and Khudir D. SULAIMAN. In Vitro Antimicrobial Activity of Salvadora persica L. Extracts Against Some Isolated Oral Pathogens in Iraq. Department of Biology, College of Education,University of Mosul, IRAQ.Turk J Biol 32 pp: 57-62(2008) .
8. Elvin-Lewis M. Plants used for teeth cleaning throughout the world. J Prev Dent; 6: 61–70 (1980).
9. World Health organization (WHO) . Concensus Statement on Oral hygiene. Int Dent J; 50: 139 (2000) .
10. Khoory, T. The use of chewing sticks in preventive oral hygiene. Clin Prev Dent; 5(4): 11-14 (1983).
11. Wu C.D.; Darout I.A. and Skaug N.. Chewing sticks: timeless natural toothbrushes for oral cleansing. J Periodontal Res; 36(5): 275-284 (2001) .
12. Elvin-Lewis M ; Hall J; Adu-Tutu M ; Afful Y; Asante-Appiah K and Lieberman D . The dental health of chewing-stick users of Southern Ghana: Preliminary findings. J Prev Dent, 6: 151-159 (1980) .

13. Eid, M.A. and Selim H.A.. A retrospective study on the relationship between miswak chewing stick and periodontal health. Egypt Dent J; 40(1): 589-592 (1994)
14. Almas, K. The antimicrobial effects of extracts of Azadirachta indica (Neem) and Salvadora persica (Arak) chewing sticks. Indian J Dent Res; 10(1): 23-26 (1999) .
15. Taiwo, O ; Xu H-X and Lee S.F. Antibacterial activities of extracts from Nigerian chewing sticks. Phytother Res; 13: 675-679 (1999) .
16. Akhtar, M.S. and Ajmal M. Significance of chewingsticks (miswaks) in oral hygiene from a pharmacological view-point. J Pak Med Assoc , 31(4):89-95 (1981)
17. Almas, K ; Skaug N and Ahmad I. An in vitro antimicrobial comparison of miswak extract with commercially available non-alcohol mouth rinses. Int J Dent Hyg , 3(1):18-24 (2005) .
18. Koneman, E.W ; Allen S.D.; Dowell U.R. *et al.* Color atlas and textbook of diagnostic microbiology. Philadelphia, J.B. Lippincott (1988).
19. Ratheesh,M. and Helen, A . anti inflammatory of Ruta graveolens .L.on carrageenan induced paw edema in wistar male rats .Africian .J.Biotechnology .6(10):1209-1211 (2007) .
20. Mahmood , M.J.;Jawad , A.Y.; Huseein , A.M.; AL – omari , M. and AL- Nabi , A. introantimicrobial activity of salsola rosanarinus and Adiantum capillus var venerisint . J. Crude Druge Res . 27 : 14- 16 (1989) .
21. Rojas,R.; Bustamante,B.; Baure,J.; Fernandez,I.; Alban,J. and Lock,O. Anti-microbial activity of selected Peruvian medical plants. J .Ethnopharmacology 88 (2-3): 199-204(2003).
22. Ezmirly S and Seif-El-Nasr M. Isolation of Glucotropaelin from Salvadora Persica. J Chem Soc Pak, 3, 9-12 (1981) .
23. Al-Bagieh N.H. and Almas, K . In vitro antibacterial effects of aqueous and alcohol extracts of miswak (chewing sticks). Cairo Dent J; 13: 221-224 (1997) .
24. Almas, K, Al-Lafi, T.R . The natural toothbrush. World Health Forum; 16(2): 206-210 (1995).
25. Darout, I.A. ; Christy, A.A. ; Skuag, N and Egeberg PK . Identification and qualification of some potentially antimicrobial

anionic components in miswak extract. Ind J Pharmacol , 32(1):11-4 (2002) .

26. Darmani, H. ; Nusayr, T and Al-Hiyasat A.S. Effects of extracts of miswak and derum on proliferation of Balb/C 3T3 fibroblasts and viability of cariogenic bacteria. Int J Dent Hyg , 4(2):62-66 (2006) .
27. Hattab, F.N . Meswak: the natural toothbrush. J Clin Dent; 8(5): 125-129 (1997) .

الوصف النسيجي والتركيب المستدق لقزحية عين الصقر (*Accipiter nisus*)

جيهان محمود رجب
قسم علوم الحياة – الجامعة المستنصرية

تاريخ تقديم البحث 2012/1/3 - تاريخ قبول البحث 2012/4/18

ABSTRACT

Iris of the eye in sparrow hawk (*Accipiter nisus*) a diurnally active bird, has been examined by light and Electron Microscopy. For this study we used (12) healthy eyes. The histological study revealed that the iris is a thin structure consists of three layers: the anterior layer is epithelium, which is composed of one row of cells. The intermediate layer is the stroma, which is characterized by containing muscle fibers within loose connective tissue. Also the stroma contains collagenous fibers, fibroblasts, mast cells, chromatophores cells and profuse blood vessels. The posterior layer of the iris is the pigmented epithelium.

The ultrastructural examination of the Iris showed that the pigmented epithelial cells have irregular shaped nuclei containing one or more nucleoli and their cytoplasm is characterized by presence of heavily spread melanosome and few mitochondria.

الخلاصة

قزحية عين الصقر (*Accipiter nisus*) طير نشط نهارياً، فحصت بواسطة المجهر الضوئي والألكتروني. أستخدمت لغرض الدراسة (12)عيناً سليمة. كشفت الدراسة النسيجية أن القزحية تركيب نحيف يتألف من ثلاث طبقات، الطبقة الأمامية هي الظهارة المؤلفة من صف واحد من الخلايا. الطبقة الوسطى هي السدى والتي تميزت باحتوائها على ألياف عضلية ضمن نسيج ضام ليفي مفكك، يحتوى السدى أيضاً على حزم من ألألياف المغراوية وأورمات ليفية وخلايا بدينة وخلايا حاملات اللون وأوعية دموية غزيرة. أما الطبقة الخلفية للقزحية فهي الظهارة الصباغية.

أظهر الفحص المستدق للقزحية أن لخلايا طبقة الظهارة الصباغية نواة غير منتظمة الشكل بداخلها نوية واحدة أو أكثر. أما الهيولي فيتميز بوجود جسيمات ملانية منتشرة بغزارة وقليل من المتقدرات.

المقدمة

تمتد قزحية عين الطيور عند المنطقة الأمامية للجسم الهدبي لتكون حاجزاً صباغياً عضلياً يقع أمام العدسة ويكون مستمراً مع الجسم الهدبي وهي تفصل الغرفة الأمامية عن الغرفة الخلفية وتساهم في تكيف فتحة البؤبؤ المستديرة الواقعة في مركز القزحية ،وتتألف القزحية من أوعية دموية متعددة وأورمات ليفية وأعصاب وألياف مغراوية وخلايا ظهارية ومكونات عضلية كثيرة تنظم معدل الضوء الداخل للعين بواسطة آلية التقلص والانبساط [1]. يعتمد لون القزحية على معدل كمية الصبغات وأنواعها ووجود الأوعية الدموية ، وتحتوي القزحية على صبغات رئيسية كصبغة البيورين purin pigment وصبغة البتريدين pteridine pigment وصبغة الكاروتينويد carotenoid pigment والأخيرة أقل إنتشاراً [4,3,2]. يتأثر لون القزحية في بعض أصناف الحمام بواسطة وجود خلايا القزحية Iridocytes الكاسرة للضوء التي تشكل البساط الصافي taptum lucidum للقزحية وهي مسؤولة عن التغيرات السريعة للألوان في القزحية، وأن التغير في حجم وشكل البؤبؤ في الطيور أكبر وأكثر سرعة مما هو موجود في اللبائن [5]. ويمكن تمييز طبقات قزحية عين الدجاج من الأمام إلى الخلف وهي على التوالي:

1- طبقة ظهارية Epithelial layer وهي طبقة مفردة لخلايا ظهارية غير صباغية مسطحة.

2- طبقة العضلات العاصرة البؤبؤية Sphincter papillae muscles وهي طبقة سميكة تتألف من عضلات ملساء مرتبة دائرياً مسؤولة عن تقلص فتحة البؤبؤ .

3- طبقة نسيج ضام Connective tissue layer وتتألف من ألياف مغراوية وأورمات ليفية وأوعية دموية دقيقة .

4- طبقة العضلات الموسعة البؤبؤية Dilator papillae muscles وهي طبقة رقيقة تتألف من عضلات ملساء مرتبة بشكل شعاعي مسؤولة عن توسع فتحة البؤبؤ.
5- الظهارة الصبغية العميقة Deep pigmented epithelium التي تكون مجاورة للعدسة وتمتلك حبيبات صبغية كروية ذات كثافة عالية ، يبلغ سمك هذه الطبقة من (3-5) خلية [6].
توجد خمس عضلات تسيطر على حجم فتحة البؤبؤ ،ثلاثة منها محيطية دائرية circumferential وعضلتان تترتب نسجياً بشكل شعاعي radial shape [3].
العضلات المحيطية الدائرية مسؤولة عن تقلص القزحية وتتألف من:
1- ظهارة عضلية حول بؤبؤية Peripupillary myoepithelium
2- حزمة حلقية لعضلات ملساء annular band of smooth muscles
3- حزمة واسعة لعضلات مخططة broader band of striated muscles
وجود العضلات الشعاعية في القزحية يسرّع من توسع القزحية السريع والمفاجئ عند أداء وظيفة الأبصار، وتتألف من:
1- ظهارة عضلية متطورة بشكلٍ جيد.
2-ألياف مخططة قليلة ومتناثرة [3,7].
توصف القزحية بأنها سميكة عند محيطها وتضيق باتجاه منطقة البؤبؤ ويتألف سدى القزحية من عضلات عاصرة وموسعة وكلاهما يتألف من خلايا عضلية هيكلية صغيرة تحتوي على فجوات دهنيةLipid vacoules ، وتكون العضلات الموسعة متناثرة وخلفية إلا أن العضلات العاصرة تكون سميكة وتقع الى الأمام و يكون السطح الأمامي المواجه للقرنية مغطى بطبقة بسيطة من خلايا ظهارية مسطحة غير صباغية أما السطح الخلفي المواجه للعدسة فيكون مغطى بطبقة من خلايا ظهارية مطبقة صباغية بسمك من (3-5) خلية [8].

المواد وطرائق العمل

أستخدمت لغرض الدراسة (12)عيناً سليمة لطير *Accipiter nisus* .حضرت (8)عيون للفحص بالمجهر الضوئي (4 يمنى+4 يسرى) بينما حضرت العيون الأربع الباقية (2يمنى+2يسرى) للفحص بالمجهر الالكتروني النافذ Transmission electron microscope.
قتلت الطيور بواسطة قطع الرأس بأستخدام سكين حادة ، أزيلت النسج العظمية والعضلية المحيطة بالمقلة بأستخدام مشرط حاد وبذلك أزيلت كل عين من حجاجها Orbit. قطعت العينات المراد دراستها ووضعت حالاً في محلول الفورمالين formalin solution (10%) لمدة (72) ساعة. غسلت العينات بالماء الجاري للتخلص من المادة المثبتة. نقلت بعدها إلى سلسلة من التراكيز التصاعدية للكحول الأثيلي (60%-70%-80%-90%-95% -100%-100%) ولمدة (2) ساعة لكل تركيز. مررت العينات في الزايلين لمدة نصف ساعة. وضعت في فرن حراري بدرجة (58) درجة مئوية لغرض إرتشاح العينة بشمع البارافين. أجريت عليها عملية الطمر في شمع نقي. تم إستخدام المشراح الدوار rotary microtome لقطع العينات بسمك (5) مايكروميتر. حملت على شرائح زجاجية باستخدام مسحة خفيفة من خليط زلال البيض مع الكليسرين [9]. لوّنت الشرائح النسجية باستخدام الملونات الآتية:
1- ملون هارس هيماتوكسلين - أيوسين Harris haematoxylin - eosin لإظهار التراكيب العامة [10,9].
2- ملون فان– كيزن Van Giesons stain لإظهار حزم الألياف المغراوية [11,9].
للحصول على مقاطع نسجية رقيقة لغرض الفحص بالمجهر الألكتروني النافذ ثبتت العينات في محلول الكلوتر الدهايد Glutrealdehyde بتركيز (2.5%)، ثم أكملت عملية التثبيت باستخدام رابع أوكسيد الأوزميوم Osmium tetroxide (1%). بعد انتهاء عملية التثبيت مررّت العينّات بسلسلة تصاعدية من الكحول الأثيلي (30%-50%-70%-80%-90%-95%-

100%-100%). وضعت العينّات في أوكسيد البروبلينPropylene oxide النقي، مررت بعدها بمزيج من أوكسيد البروبلين ومادة الطمر الأرلديت Araldite ، وضعت في محافظ لدينة Plastic capsules مملؤة بمادة الطمر[12] . قطعت العينات بوساطة جهاز المشراح المستدق Ultramicrotome من نوع Jung & Reichert للحصول على مقاطع مستدقة ultrasections بسمك يتراوح بين (60-90) نانوميتر. حملّت المقاطع على مشبك نحاسي Copper grid. لوّنت المقاطع باستعمال محلول مشبع من خلات اليورانيل Uranyl acetate وسترات الرصاص Lead citrate [12]. فحصت العينات بالمجهر الالكتروني النافذ من نوع Philips CM10 باستعمال فولتية عالية (60) كيلوفولت. التقطت الصور على فلم خاص وحمضت وطبعت في مختبرات المجهر الالكتروني في الكلية الطبية /جامعة النهرين.

النتائج والمناقشة

تشير نتائج الفحص بالمجهر الضوئي إلى أن القزحية تركيب نحيف ذو مساحة سطحية كبيرة يزداد سمكه من جهة الخلف. يغطي القزحية من جهة الأمام قرنية شفافة إما من جهة الخلف فتغطيها العدسة الكبيرة . تبدو القزحية معتمة لإحتواءها على أعداد كبيرة من جسيمات الميلانين ، كما إنها تحتوي على أوعية دموية متعددة ولوحظ بأن القزحية تحيط بفتحة دائرية كبيرة هي فتحة البؤبؤ pupil كما وتحتوي القزحية على مصرات بؤبؤية Pupillary sphincters من عضلات ملساء غزيرة مبعثرة تحيط بفتحة البؤبؤ الدائرية . تسيطر القزحية في الطيور على كمية الضوء الداخل للعين [14] عن طريق التحكم في توسيع وتضييق فتحة البؤبؤ الدائرية الواقعة في مركز القزحية في حالة تغير شدة الأضاءة عن طريق تنظيم معدل الضوء الداخل للعين بواسطة الية التقلص والأنبساط [1]. وقد أشارت دراسة أجريت على عين الدجاج الى احتواء القزحية على نوعين من العضلات هما عضلات المصرة البؤبؤية والتي تكون أليافها العضلية مرتبة دائرياً حول فتحة البؤبؤ وبتقلصها تصغر فتحة البؤبؤ، أما النوع الثاني من العضلات فهي العضلات الموسعة البؤبؤية والتي تكون أليافها العضلية مرتبة شعاعياً حول فتحة البؤبؤ وبتقلصها تكبر فتحة البؤبؤ [6] . وهذا ماأكدته نتائج الدراسة الحالية. كما أشارت نتائج دراسة أخرى لمقلة عين البوم أمتلاك القزحية مصرات مخططة وعضلات موسعة وظهارة عضلية وعضلات ملساء [15].ان تغيير شكل وحجم بؤبؤ الطيور أسرع وأوسع إلى حدما مما هو معروف في باقي اللبائن[1]. تتألف القزحية نسجياً أبتداءاً من جهة الأمام نحو الخلف (شكل 1) من الطبقات الآتية :-

1- الظهارة Epithelium

2- السدى Storma

3 -الظهارة الصباغية Pigment epithelium

تغطي الظهارة التي تتألف من صفٍ واحدٍ من الخلايا سطح القزحية المقابل للقرنية وتستمر هذه الطبقة مع الظهارة الخلفية للقرنية تليها طبقة السدى التي تتصف بأحتواءها على ألياف عضلية مرتبة باتجاهات مختلفة تقع ضمن نسيج ضام ليفي مفكك يتألف من حزم الألياف المغراوية التي تتخللها أرومات ليفية fibroblasts وخلايا بدينة وخلايا حاملات اللون Chromatophores وأوعية دموية تنتشر بغزارة.. أما في الأنسان فتتألف طبقة السدى من منطقتين: المنطقة الأمامية الواقعة تحت الظهارة تكون لاوعائية وتحتوي على خلايا حاملات الميلانين التي تعطي اللون للقزحية أما المنطقة الخلفية فتتألف من نسيج ليفي مفكك وتحتوي على العديد من الأوعية الدموية [13] . أما السطح الخلفي للقزحية فهو مبطن بظهارة صباغية مستمرة مع النسيج الظهاري المبطن للجسم الهدبي والمشيمية (شكل 2). أظهرت نتائج الفحص بالمجهر الالكتروني أن خلايا طبقة الظهارة الصباغية تحتوي على نوى غيرمنتظمة الشكل، تحتوي كل نواة على نوية واحدة أو أكثر أما الهيولي فيتصف بامتلائه بحبيبات ظهرت بأحجام متباينة وبأشكال بيضوية وبأعداد كبيرة يطلق عليها جسيمات الميلانين Melanosomes وتحتوي هذه الحبيبات

على صبغات الميلانين التي تتصف بكثافة الكترونية عالية، لوحظ وجود المتقدرات التي تتميز بقلة أعدادها وهي متناثرة بين الحبيبات أما العضيات الأخرى فقد صعب تمييزها لأمتلاء الهيولي بجسيمات الميلانين (شكل 3). أشار عدد من الباحثين إلى إن جسيمات الميلانين عضيات متخصصة محصورة داخل غشاء الخلية تساهم في تصنيع وخزن صبغات الميلانين المسؤولة عن تحديد لون القزحية [17,16]. أن غياب جسيمات الميلانين يساهم وبشكل مؤكد في حدوث حالة مرضية تعّرف بالمهقّ albinism وهي أبيضاض القزحية [19,18]. يعتمد لون القزحية على كمية الصبغات وأنواعها ووجود الأوعية الدموية ، وتحتوي القزحية على صبغات رئيسية كصبغة البيورين purin pigment وصبغة البتريدين pteridine pigment وصبغة الكاروتينويد carotenoid pigment والأخيرة أقل إنتشاراً [4,3,2].

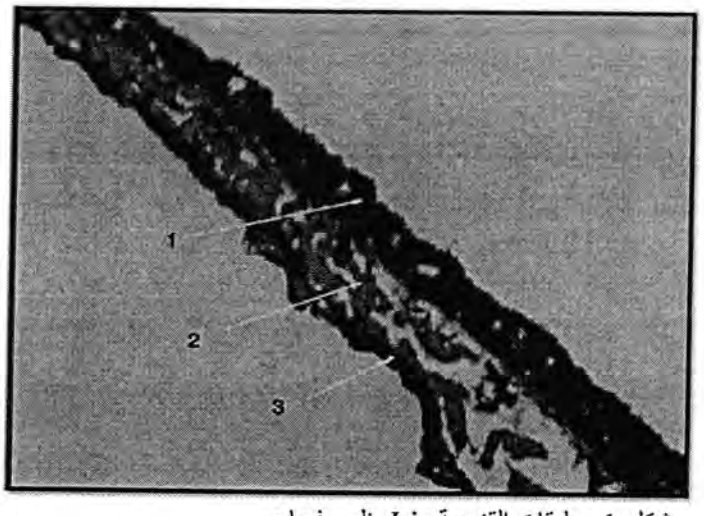

شكل-1 : طبقات القزحية Iris يظهر فيها :
1- الظهارة Epithelium، 2- السدى Stroma، 3- الظهارة الصباغية Pigmented epithelium
ملون H&E بتكبير (100X)

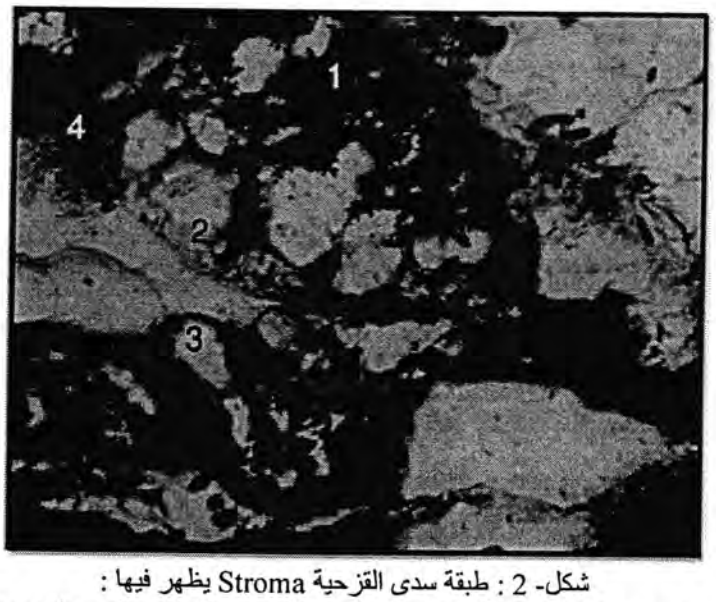

شكل- 2 : طبقة سدى القزحية Stroma يظهر فيها :
1- خلايا ميلانية Melanocytes ، 2- ألياف مغراوية Collagen fibers ، 3- وعاء دموي Blood vessel ، 4- الياف عضلية Muscle fibers
ملون Van Gieson's stain بتكبير (250X)

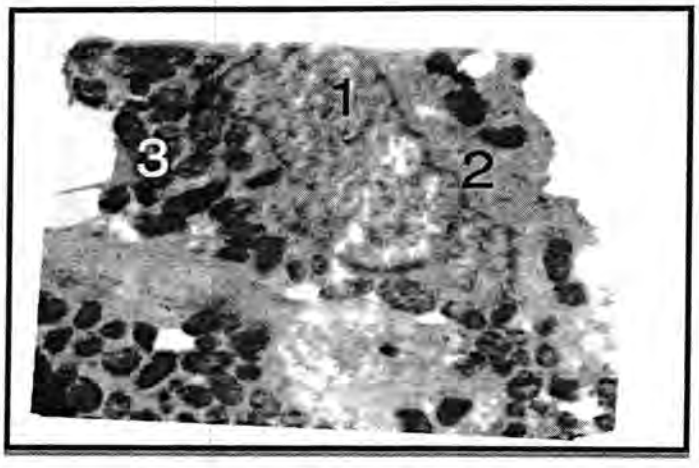

شكل-3 : الظهارة الصباغية للقزحية مكبرة بالمجهر الالكتروني يظهر فيها:
1- نواة Nucleus
2- هيولي Cytoplasm
3- جسيمات الميلانين Melanosomes
ملوّنة بخلات اليورانيل وسترات الرصاص (بتكبير13500X)

المصادر

1. Jones M P , Pierce K E and Ward D W . Avian vision: areview of form and function with special consideration to birds of prey. Journal of exotic pet medicine, Vol. 16. No 2 .Pp: 69-87 (2007).
2. Oehme H . Vergleichende Untersuchungen über die Färbung der Vogeliris . Biol. Zbl. 88, 3–35 (1969).
3. Oliphant L W, J Hudon and J T Bagnara . Pigment cell refugia in homeotherms–the unique evolutionary position of the iris . Pigment Cell Research 5:367-371 (1992).
4. Samuelson D . Ophthalmic anatomy, in Gelatt KN (ed): Veterinary Ophthalmology (ed 3). Baltimore MD, Lippincott Williams and Wilkins . Pp: 31-150 (1991).
5. King A S and McLelland J . Special sense organs, in Birds: Their Structure and Function . Arrowsmith J W press, 2nd . Ed ., Bristol, Great Britain. Pp: 284- 314 (1984).
6. Hodges R D . The histology of the fowl . Academic press . London . Great Britain .Pp: 525-560 (1974).
7. Wygnanski-Jaffe T , Murphy C J , Smith C , Kubai M P , Christopherson C R , Ethier and Levin AV. Protective ocular mechanisms in woodpeckers . Nature Publishing Group .Eye . Vol. 21. Pp: 83 – 89 (2007).

8. Bacha W J and Bacha L M . Color Atlas of Veterinary Histology. Second edition. Lippincott Williams&Wilkins. Pp : 249 (2000).
9. Luna L G . Manual of histologic staining method of Armed Forces institute of pathology . Third edition . Mc Graw – Hill book Company . New York (1968).
10. Preece A. Amanual for histologic techniques. J. and A.churchill LTD,1st.Ed., London, great Britain (1959).
11. [11]. Vacca L . Laboratory manual of histochemistry, Ravan press, 1st Ed., New York,U.S.A.(1985).
12. [12]. Hayat M A. Principles and Techniques of Electron Microscopy .Biological Application .third ed .Macmillan press. Pp: 405 (1986).
13. [13]. Arey L B. Human histology . A Text book in Outline Form .Fourth ed. WB Saunders Company Philadelphia (1974)
14. Miller P E. Uvea. In: Maggs, D J, Miller P E, Ofri, R. Slatter. Fundamentals of Veterinary Ophthalmology, 4th.ed., Saunders Elsevier, St. Louis (2008).
15. Kern T J. Exotic Animal Ophthalmology. In: Gelatt K N (ed.),Veterinary Ophthalmology, 4th e.d. Blackwell Publishing (2007).
16. Anderson M G, Haraszti T, Petersen G E, Wirick S, Jacobsen C, John S W M and Grunze M. Scanning transmission X-ray microscopic analysis of purified melanosomes of the mouse iris. Micron 37, 689-698 (2006).
17. Riley P A. Melanin. Int. J. Biochem. Cell Biol. 29, 1235-123 (1997).
18. Okulicz J F, Shah R S, Schwartz R A and Janniger C K. Oculocutaneous albinism. J. Eur. Acad. Dermatol. Venereol. 17, 251-256 (2003).
19. Scheinfeld N S. Syndromic albinism: a review of genetics and phenotypes. Dermatol. Online J. 9, 5 (2003).

فعالية أنتقال مثبط تصنيع الكايتين Novaluron على فقس البيض و تطور يرقات خنفساء اللوبيا(Fabricius) *Callosobruchus maculatus*

معن عبد العزيز شفيق
قسم علوم الحياة – كلية العلوم – جامعة المستنصرية – بغداد - العراق

تاريخ تقديم البحث 2012/4/2 - تاريخ قبول البحث 2012/6/20

ABSTRACT

The effects of the chitin synthesis inhibitor (CSI) Novaluron on egg hatch and on larval development of *Callosobruchus maculatus* (F.) concentration of 0.001, 0.0003, 0.0002 and 0.0001 ml/L of water were tested. The effect of Novaluron at low concentration dependent strongly on the exposure period. At 0.0003 ml/L, egg hatch of *C. maculatus* was totally inhibited after 28 days at 0.0002 ml/L the effect was much less but inhibition increased to 66 % in the 35 days experiment at 0.0001 ml/L Novaluron was ineffective. The viability of the larvae that hatched from the laid eggs and developed on untreated seeds of *Vigna unguiculata* (Walp.) was also dependent on concentration of Novaluron and exposure time, exposure of *C. maculates* adults to Novaluron- treated seeds at 0.0003 ml/L for 8 days or at 0.0002 ml/L for 36 days caused 100% or 97 % mortality respectively. At both 0.0003 and 0.0002 ml/L larval deaths were mainly in the first, second and third instars. Exposure of *C. maculates* adults to treated seeds may serve as a good model for evaluating the effect of CSIs on internal feeders especially *Callosobruchus maculatus* (Fab.). The present study contributes to our understanding of CSI transovarial activity against internal stored product coleopterans whose larval stage develops inside the grain without contact with the toxicants.

المستخلص

تم أختبار تأثير تراكيز مختلفة 0.001، 0.0003، 0.0002 و 0.0001 مل / لتر ماء لمثبط تصنيع الكايتين Novaluron Chitin Synthesis Inhibitor (C.S.I.) على فقس البيض وتطور يرقات خنفساء اللوبيا (F.) *Callosobruchus maculatus*. تأثير التراكيز المنخفضة للـ Novaluron يعتمد بدرجة كبيرة على فترة التعريض. عند تركيز 0.0003 مل/ لتر تم تثبيط فقس بيض *C. maculatus* كلياً بعد فترة 28 يوماً، أما عند تركيز 0.0002 مل/لتر كان التأثير تثبيط البيض منخفض بدرجة كبيرة ولكن التثبيط يزداد تدريجياً ويصل الى 66% بعد 35 يوم من الأختبار، التركيز 0.0001 مل/ لتر يكون غير مؤثر. حيوية اليرقات الناتجة من فقس البيض وتطورها على البذور غير المعاملة يعتمد أيضاً على التركيز وفترة التعريض. تعريض بالغات *C. maculatus* الى بذور اللوبيا المعاملة بـ Novaluron بتركيز 0.0003 مل / لتر لمدة 8 أيام، وبتركيز 0.0002 مل / لتر لمدة 36 يوم سبب نسبة قتل 100% و 97% على التوالي. عند التركيزين 0.0003 و0.0002 مل / لتر يؤدي الى قتل اليرقات وخاصة يرقات العمر الأول، الثاني والثالث بدرجة أكبر. تعريض بالغات *C. maculatus* الى بذور اللوبيا المعاملة ربما يفيد كنموذج جيد لتقييم تأثير مثبطات تصنيع الكايتين على الحشرات داخلية التغذية خاصة حشرة خنفساء اللوبيا *C. maculatus* (Fab.) هذه الدراسة تساهم في فهم فعالية أنتقال مثبط تصنيع الكايتين ضد المتغذيات الداخلية من الحشرات التابعة لرتبة Coleoptera التي أعمارها اليرقية تتطور داخل الحبوب بدون التماس مع السموم.

المقدمة

الأستخدام الواسع للمبيدات الحشرية التقليدية ومنها المركبات الكلورينية والفوسفاتية العضوية ينتج عنها زيادة في المقاومة عند الآفات الحشرية، وكذلك الأثار السلبية الناتجة من أستخدام هذه المبيدات على الأنسان، وهذا التقدم في أستخدام المبيدات الكيميائية يحفز بشكل كبير التأكيد على البحث عن بدائل تكون أمينة وصديقة للبائن وكذلك للبيئة [1، 2] . من أهم هذه البدائل التي تشمل منظمات النمو Insect Growth Regulators (IGRs) والتي تكون معروفة في

تأثيرها على مختلف الحشرات من ضمنها السلالات التي تكون مقاومة للمبيدات الحشرية. هذه المركبات تعوق تطور الحشرات وتقتل اليرقات ولكنها تكون غير فعالة ولاتؤثر على البالغات. بعض حشرات الحبوب المخزونة ومنها خنفساء اللوبيا *C. maculatus* (Fab.) تقضي جميع مراحل تطورها داخل الحبوب، أما حشرات الحبوب المخزونة الأخرى مثل حشرة ثاقبة الحبوب الصغرى *Rhyzopertha dominica* (Fab.) فأن العمر اليرقي الأول يتطور خارج الحبوب أما الأطوار الأخرى تقضيها داخل الحبوب. يرقات هذه الأنواع ليس لها تماس مباشر مع المادة الفعالة لمنظمات النمو Insect Growth Regulators (IGRs) وينتج عنها فعالية منخفضة لهذه المنظمات ضد المتغذيات الداخلية على الحبوب [3، 4]. أن من أهم منظمات النمو الحشرية (IGRs) ضد آفات الحبوب المخزونة هي مثبطات تصنيع الكايتين (C.S.Is) وذلك بسبب القدرة والفعالية العالية بالأنتقال عبر المبايض الى البيض ويؤدي الى تثبيط فقس البيض [5، 6]. مثبط تصنيع الكايتين Novaluron يعتبر من مثبطات تصنيع الكايتين (CSIs) التي تم تطويره بواسطة الشركة الأمريكية Makhteshim-Agan Company (U.S.A) ، يعرف Novaluron بأنه ذو فعالية قاتلة ضد اليرقات، ويستخدم حالياً في مقاومة حشرات الحقل قبل الحصاد [7، 8]. قام [9، 10] بتقيم مثبط تصنيع الكايتين Novaluron في حماية البذور والحبوب وكذلك في معاملة المخازن الفارغة ، تبين أن Novaluron له

تأثير قوي على فقس البيض لخنفساء اللوبيا *C. maculatus* (F.) حيث تعتبر من أهم آفات الحبوب المخزونة واسعة الأنتشار، وأثبتوا أن Novaluron يدخل داخل الحشرة بواسطة ملامسته للحشرة، و تم دراسة عودة فقس البيض عند منع الأتصال بين البالغات وبين Novaluron. هذه الدراسة تبحث في تأثير Novaluron بتراكيز منخفضة على فقس بيض *C. maculatus* مع تأثير التراكيز تحت القاتلة على البيض، وتأثيرها على تطور اليرقات متغذية على البذور غير المعاملة.

المواد وطرائق العمل

تم أدامة وبقاء حشرة خنفساء اللوبيا *C. maculatus* تحت ظروف المختبر بدون تعريضها الى مبيدات الحشرية لعدة أجيال. تم أكثار وعمل مستعمرة من الحشرة على حبوب اللوبيا *Vigna unguiculata* في أوعية زجاجية حجمها يتراوح 0.8-1 لتر تغطى بورق ترشيح وتم الأحتفاظ بها في الظلام على حرارة 28± 0.5 م° ورطوبة نسبية 70 ± 5%. تم الجصول على Novaluron (Rimon EC-10) من شركة Makhteshim-Agan Ltd . تم تحضير محلول بتركيز 5 % من أذابة Rimon Ec-10 في الأسيتون (أذابة 5 ملغم / مل من المحلول الأصلي لـ Novaluron)، وتم أذابة 50 مل من المحلول المحضر في 30 مل من الأسيتون ومن ثم خلط المحلول بشكل كامل مع الحبوب، الحبوب المعاملة مع الأسيتون فقط أستخدمت كمعاملة للسيطرة (مقارنة). والحبوب المعاملة تم تعريضها للهواء لمدة 24 ساعة لتبخير جميع مادة الأسيتون من النماذج. لدراسة فعالية وكفاءة أنتقال Novaluron عبر المبايض الى البيض وتأثيره على فقس البيض ومن ثم على تطور اليرقات، تم وضع 20 بالغة (10 ذكور و 10 أناث) من *C. maculatus* بعمر 10-20 يوم في وعاء حجمه 100 مل يوضع في داخله 40 غم من الحبوب التي تم معاملتها بمثبط تصنيع الكايتين Novaluron بالتراكيز 0.0001، 0.0002، 0.0003 و 0.001 مل / لتر ماء ، وكذلك وضع 20 بالغة بعمر 10-20 يوم على حبوب لم يتم معاملتها (معاملة السيطرة) لمدة 5 أسابيع (التركيز القاتل هو 0.001 مل / لتر ماء وذلك لأنخفاض الشديد في نسبة الفقس الى 0.7 % خلال 3 يوم من التعريض والتركيز تحت القاتل هو 0.0003 مل / لتر ماء لأنخفاض نسبة فقس البيض الى 28.7 % خلال نفس الفترة، مقارنة بنسب فقس البيض التي كانت مرتفعة 96.2 و 98.0 % للتركيزين 0.0002 و 0.0001 على التوالي خلال 3 يوم من التعريض). تم أحتساب نسبة فقس البيض للبيض بعمر 0-24 ساعة الموضوع من قبل البالغات بعد فترة 1، 2، 3، 7، 10، 14، 21، 28 و 35 يوم من تعريض البالغات الى Novaluron ، وجميع التجارب أنجزت بثلاث مكررات (30 بيضة لكل مكرر) و وضعت في

الحاضنة في الظلام عند درجة حرارة 28 ± 0.5 م° ورطوبة نسبية 70 ± 5 %. البيوض تم فصلها وذلك بواسطة فرشاة ناعمة جداً مع غسلها بالماء المقطر ومن ثم لصقها على بذور غير معاملة بواسطة مادة لاصقة وملاحظتها كما موضح أعلاه تم نقل بيوض معاملة السيطرة أيضاً [11، 12]. تم حساب عدد البيض الذي فقس خلال الأسبوع الأول تحت المجهر، وتم أحتساب وتسجيل عدد اليرقات أيضاً، والتجربة كانت بثلاث مكررات. الجزء الثاني من البيض بعمر 0-24 ساعة لحشرة *C. maculatus* الذي تم وضعه من قبل البالغات بعد 8، 16، 22، 30 و 36 يوم من التعريض أستخدم لأختبار تطور اليرقات. عشر يرقات من كل مكرر وضعت بشكل منفرد في طبق بتري 50 ملم مع حبوب غيرمعاملة، تم ملاحظة ومراقبة تطور اليرقات لغاية خروج البالغات أو عند موت اليرقات.

التحليل الأحصائي: جميع البيانات تم أظهارها على شكل أوساط حسابية ± SEM ، تم أستخدام أختبار Tukey-Kramer
($P < 0.05$) لتحديد الأختلافات المعنوية بين المجاميع.

النتائج والمناقشة

في (جدول 1) جميع التجارب كان عدد البيض الذي تم وضعه في جميع معاملات البالغات يكون مقارب الى عدد البيض في معاملة السيطرة، ويتراوح كمعدل من 50-120 بيضة / يوم لكل مجموعة المتكونة من 20 بالغة (50-110 بيضة للبالغات المعاملة) (60-120 بيضة لمعاملة السيطرة). بعد فترة 3 يوم من تعريض بالغات خنفساء اللوبيا الى تركيز 0.001 مل / لتر من Novaluron كانت نسبة فقس البيض 0.7 % .

عند أستخدام التركيز تحت القاتل من Novaluron وهو 0.0003 مل / لتر يتطلب فترة تعريض طويلة جداً للوصول الى مستويات عالية من تثبيط فقس البيض، بعد فترة 3 يوم، اسبوع واحد و اسبوعين من التعريض كانت نسبة فقس البيض 28.7 %، 8.4 % و 2.0 % على التوالي، والتثبيط بشكل كامل لفقس البيض تم ملاحظته بعد 28 يوم. عند التركيز المنخفض 0.0002 مل / لتر من Novaluron لغاية 5 أسابيع من التعريض كانت نسبة فقس البيض 66 % ، وعند تركيز 0.0001 مل / لتر لايوجد أي تأثير للـ Novaluron على فقس البيض بعد يوم واحد، وفي نفس الفترة كانت نسبة فقس البيض في معاملة السيطرة 91.3 %. أن تأثير Novaluron عند التراكيز المنخفضة يعتمد بشكل قوي وكبير على فترة التعريض. أن تاثير Novaluron لاينتهي عند مرحلة فقس البيض حيث التأثير القوي يمكن ملاحظته على اليرقات التي تتطور من البيض الموضوع من قبل بالغات *C. maculatus* بعد تعريضها الى حبوب معاملة ومن نقلها الى حبوب غير معاملة، حيوية اليرقات التي تتطور من البيض الفاقس يعتمد بشكل قوي وكبيرعلى تركيز Novaluron . عند تعريض بالغات *C. maculatus* الى حبوب معاملة بـ Novaluron عند تركيز 0.0003 مل / لتر لمدة 8 يوم ومن ثم نقل بشكل متتابع للبيض الى حبوب غير معاملة يسبب نسبة قتل كاملة لليرقات التي تتطور من البيض الفاقس. عند تركيز 0.0002 مل / لتر نسبة القتل لليرقات كانت عالية ومرتبطة مع فترة التعريض، وكانت نسبة القتل 97.5 % لليرقات التي تطورت من البيض الفاقس بعد 36 يوم فقط من تعريض البالغات الى الحبوب المعاملة. عند تركيز 0.0001 مل / لتر من Novaluron كانت نسبة قتل لليرقات بعد 36 يوم من تعريض البالغات 7.5% (جدول 2). عند كل من التركيزين 0.0003 و 0.0002 مل / لتر سجلت نسبة القتل لليرقات بشكل رئيسي في العمر اليرقي الأول، الثاني و الثالث أما الأعمار اليرقية التالية تكون نسبة القتل فيها مشابها الى معاملة السيطرة. في دراسات على أمتصاص 8 أنواع من مثبطات تصنيع الكايتين (CSIs) من قبل حشرة النحل الطنان *Bombus terrestris* كانت مشابهه لهذه الدراسة حيث لوحظ النسبة القتل العالية في يرقات Bumble Bee خلال أنسلاخها الى العمر اليرقي الثاني، وهذه الدراسات تبين فقط تأثير مثبطات تصنيع الكايتين على اليرقات الناتجة من بيض معامل بهذه المثبطات التي تشابه الدراسة

الحالية بغض النظر عن أختلاف النوعين للحشرتين [11]. وهذه الآفة الرئيسية لها أتصال خارجي مع الحبوب المعاملة فقط عند مرحلة البالغات حيث جميع أطوار *C. maculatus* تتطور داخل الحبوب بدون الأتصال مع السطح الخارجي المعامل للحبوب. فأن التجارب على *C. maculatus* صممت للتأكد من أن البالغات فقط ستتعرض الى الحبوب المعاملة، وهذا يخدمنا كنموذج لتقييم تأثير مثبطات تصنيع الكايتين على المتغذيات الداخلية وخاصة *C. maculatus*. [13] قام بدراسة تأثير مثبط الكايتين Chlorfluazuron على تطور أعمار حشرة *C. maculatus*، تعريض البالغات الى حبوب معاملة لمدة أسبوعين ومن ثم مراقبة وضع البيض من قبلها على الحبوب غير المعاملة وجد أن معظم نسبة القتل للأطوار غير الناضجة (البيض واليرقات) تظهر خلال 3 أسابيع، بعد هذه الفترة من التطور نسبة القتل تكون مماثلة الى نسبة القتل في معاملة السيطرة، والنتائج الحالية في تثبيط فقس البيض تبين بقوة أنتقال Novaluron الى البيض عبر المبايض بواسطة الآناث، والدراسة على البراغيث هي لبيان تأثير مثبط تصنيع الكايتين في فقس البيض من خلال أنتقاله عبرالمبايض للأنثى وليس المقارنة بين النوعين [13، 14]. دخول مثبط تصنيع الكايتين ربما يتم عن طريق الملامسة وكذلك التغذية [14، 15]، مثبط تصنيع الكايتين CSI يدخل الى البيض من خلال البالغات ومن ثم يعيق التطور الطبيعي للحشرة. هذه الدراسة على تأثيرات Novaluron على فقس البيض وكذلك على تتابع تطور اليرقات تؤكد فعالية مثبط تصنيع الكايتين ضد آفات المواد المخزونة ذات التغذية الداخلية التي تعود الى رتبة Coleoptera وأطوارها اليرقية التي تتطور داخل الحبوب بدون التماس مع المواد السامة.

جدول :1-: التأثيرات القاتلة وتحت القاتلة لمثبط تصنيع الكايتين Novaluron على فقس بيض خنفساء اللوبيا *Callosobruchus maculatus*(50 بيضة بعمر 0-24 ساعة وضعت على الحبوب، لكل مكرر من المعاملة)

	نسبة فقس البيض % ± SEM للبالغات المعرضة الى غذاء معامل لمدة أكثر من 35 يوم								
التركيز ملغم/لتر	يوم واحد	2 يوم	3 يوم	7 يوم	10 يوم	14 يوم	21 يوم	28 يوم	35 يوم
0.001	7.9 ± 75.1 bcd	1.8 ± 15.3 Gh	0.7 ± 0.7 h	0.7 ± 0.7 h	0 h	0 h	—	—	—
0.0003	9.2 ± 72.6 de	7.5 ± 67.1 f	5.1 ± 28.7 g	3.4 ± 8.4 h	4.4 ± 10.4 h	1.3 ± 2.0 h	1.2 ± 1.2 h	0 h	—
0.0002	—	2.9 ± 92.5 abd	1.5 ± 96.2 ab	2.2 ± 90.0 abc	3.2 ± 85.2 abc	3.0 ± 84.2 abc	5.7 ± 72.9 cd	2.1 ± 70.5 ef	2.6 ± 66.4 f
0.0001	—	1.7 ± 96.5 a	0 ± 98.0 a	0.6 ± 99.0 a	0.8 ± 98.0 a	1.7 ± 95.0 ab	1.7 ± 96.7 a	1.0 ± 95.5 ab	1.2 ± 96.0 ab
معاملة السيطرة	3.7 ± 91.3 ab	2.0 ± 94.0 ab	1.8 ± 94.7 ab	0.7 ± 96.7 ab	0.6 ± 98.0 a	1.2 ± 96.4 a	1.7 ± 93.6 ab	1.2 ± 96.4 a	1.3 ± 92.5 abc

* المتوسطات لها أحرف متشابه لاتختلف معنوياً ($P > 0.05$)

جدول 2-: التأثير المتأخر لمثبط تصنيع الكايتين Novaluron على يرقات خنفساء اللوبيا *Callosobruchus maculatus* التي تطورت من البيض بعمر 0-24 ساعه بعد تعريض البالغات الى حبوب معاملة

التركيز مل / لتر	نسبة القتل لليرقات (% ± SEM) بعد تعريض البالغات لفترة أكثر من 36 يوم الى غذاء معامل				
	8 يوم عمر اليرقي الأول	16 يوم عمر اليرقي الثاني	22 يوم عمر اليرقي الثاني	30 يوم عمر اليرقي الثالث	36 يوم عمر اليرقي الثالث
0.0003	100 a	100 a	———	———	———
0.0002	10.8 ± 70.0 a	5.0 ± 75.0 a	19.3 ± 77.5 a	10.0 ± 90.0 a	2.5 ± 97.5 a
0.0001	2.6 ± 7.8 b	4.1 ± 10.3 b	2.9 ± 15.0 b	5.0 ± 15.0 b	2.5 ± 7.5 b
معاملة السيطرة	3.1 ± 8.9 b	3.3 ± 6.7 b	5.0 ± 5.0 b	10.0 ± 10.0 b	9.6 ± 15.0 b

* المتوسطات لها أحرف متماثلة لاتختلف معنوياً ($P > 0.05$)

REFERENCES

1. Ishaaya I. and Horowitz A.R. Insecticides with novel modes of action: an overview in: Ishaaya I. and Degheele D. [Eds.] Insecticides with Novel Modes of Action: Mechanisms and Application. Springer, Berlin, Germany: 1-24. 1998.
2. Oberlander H., Silhacek D.L., Shaaya E. and Ishaaya I. J. Stored Prod. Res. Current status and future perspectives of the use of insect growth regulators for the control of stored product insects. 33: 1-6. 1997.
3. Dales M.J., Harding S., Freeman N. and Gaffney H. Insect growth regulators for the control of Stored-grain insect pest. Proc. Sixth International Working Conf. on Stored Product Protection (Canberra, Australia): 765-769. 1994.
4. Kostyyukovsky M., Chen B., Atsmi S. and Shaaya E. Insect Biochem. Mol. Biol. Biological activity of two juvenoids and two ecdysteroids against three stored product insects. 30: 891-897. 2000.
5. Deglish G.J. and Wallbank B.E. Efficacy of diflubenzuron plus methoprene against *Sitophilus oryzae* and *Rhyzopertha dominica* in stored sorghum. J. Stored Prod. Res. 41:353-360. 2005.
6. Desmarchelier J.M. and Allen S.E. Diflubenzuron as a grain protectant for control of *Sitophilus Species*. J. Stored Prod. Res. 28: 283-287. 1992.
7. Ishaaya I., Horowitz A.R., Tirry L. and Barazani A.R. Novaluron (Rimon), a novel IGR mechanism, selectivity and important in IPM programs. Meded. Fac. Landboww. Univ. Gent. 67: 617-626. 2002.

8. Ishaaya I., Kontsedalov S. and Horowitz A.R. Novaluron (Rimon), a novel IGR: potency and cross- resistance. Arch. Insect Biochem. Physiol. 53: 157-163. 2003.
9. Kostyukovsky M. and Trostanetsky A. The effect of a new chitin synthesis inhibitor, Novaluron, on various developmental stages of *Callosobruchus maculatus*. J. Stored Prod. Res. 42: 136-148. 2006.
10. Kostyukovsky M., Trostanetsky A., Carmi Y., Frandji H. and Schneider R. Activity of novaluron on the main stored product insects. Proc. Eighth International Working Conf. on Stored product Protection(York, UK) : 583-587. 2003.
11. Elek J.A. Treatment of adult Coleopteran with a chitin synthesis inhibitor affects mortality and development time of their progeny. Entomol. Exp. Appl. 89: 31-39. 1998.
12. Mummigatti S. G., and Krishnaiah H. E. Technique to isolate *Callosobruchus chinensis* (L.) (Coleoptera:Bruchus) eggs. J. Stored Prod. Res. 43(4): 402-403. 2007.
13. Mommaerts V., Sterk G. and Smagghe G. Hazards and uptake of chitin synthesis inhibitor in Bumble bees *Bombus terrestris*. Pest Manag. sci. 62: 752-758. 2006.
14. Dean S.R., Meola R.W., Meola S.M., Sittertz-Bhatkar H. and Schenker R. Mode of action of lufenuron on larval cat fleas (Siphonaptera: Pulicidae). J. Med. Entomol. 35: 720-724. 1998.
15. Bull D.L. and Ivie G.W. Activity and fate of diflubenzuron and certain derivatives in the boll Weevil. Pestic. Biochem. Physiol. 13: 41-52. 1980.